The preclinical evaluation of simvastatin and pitavastatin for the treatment of ovarian cancer

Elizabeth Robinson

Institute for Science and Technology in Medicine

Keele University

Thesis submitted to Keele University for the degree of

Doctor of Philosophy

June 2015

SUBMISSION OF THESIS FOR A RESEARCH DEGREE

Part I. DECLARATION by the candidate for a research degree. To be bound in the thesis

Degree for which thesis being submitted: **Doctor of Philosophy**

Title of thesis: **The preclinical evaluation of simvastatin and pitavastatin for the treatment of ovarian cancer**

This thesis contains confidential information and is subject to the protocol set down for the submission and examination of such a thesis: NO

Date of submission: Original registration date: **05/09/2011**
(Date of submission must comply with Regulation 2D)

Name of candidate: **Elizabeth Robinson**

Research Institute: **Institute for Science and Technology in Medicine (ISTM)**

Name of Lead Supervisor: **Dr Alan Richardson**

I certify that:

(a) The thesis being submitted for examination is my own account of my own research
(b) My research has been conducted ethically. Where relevant a letter from the approving body confirming that ethical approval has been given has been bound in the thesis as an Annex
(c) The data and results presented are the genuine data and results actually obtained by me during the conduct of the research
(d) Where I have drawn on the work, ideas and results of others this has been appropriately acknowledged in the thesis
(e) Where any collaboration has taken place with one or more other researchers, I have included within an 'Acknowledgments' section in the thesis a clear statement of their contributions, in line with the relevant statement in the Code of Practice (see Note overleaf).
(f) The greater portion of the work described in the thesis has been undertaken subsequent to my registration for the higher degree for which I am submitting for examination
(g) Where part of the work described in the thesis has previously been incorporated in another thesis submitted by me for a higher degree (if any), this has been identified and acknowledged in the thesis
(h) The thesis submitted is within the required word limit as specified in the Regulations

Total words in submitted thesis (including text and footnotes, but excluding references and appendices): **50980**

Signature of candidate: Date:

Extract from Code of Practice: If the research degree is set within a broader programme of work involving a group of investigators – particularly if this programme of work predates the candidate's registration – the candidate should provide an explicit statement (in an 'Acknowledgments' section) of the respective roles of the candidate and these other individuals in relevant aspects of the work reported in the thesis. For example, it should make clear, where relevant, the candidate's role in designing the study, developing data collection instruments, collecting primary data, analysing such data, and formulating conclusions from the analysis. Others involved in these aspects of the research should be named, and their contributions relative to that of the candidate should be specified (this does not apply to the ordinary supervision, only if the supervisor or supervisory team has had greater than usual involvement).

ABSTRACT

Ovarian cancer is the fifth most common cancer which affects women in the United Kingdom. The 5-year survival rate is less than 45% despite improvements in chemotherapeutic regimens. Platinum-based therapy in combination with other chemotherapy including paclitaxel is currently the best standard of care for ovarian cancer. However, many women relapse with drug-resistant disease and this has led to the development of alternative drug therapies. This research evaluated two statins, simvastatin and pitavastatin, in several ovarian cancer models. Statins competitively inhibit 3-hydroxy-3-methylglutaryl coenzyme A reductase (HMGCR) in the mevalonate pathway, resulting in the cellular depletion of the isoprenoid, geranylgeranyl diphosphate, and a reduction in the prenylation and localisation of many proteins including Ras, Rho and Rab involved in cell signalling. This is likely to have contributed to the decrease in cell proliferation, induction of apoptosis, and simultaneous induction and inhibition of autophagy observed when ovarian cancer cells were exposed to statins, although the mechanisms remain poorly defined. The concentration of statins required to cause cell death in ovarian cancer cells was significantly higher than that achieved in patients receiving a standard 40 mg dose for hypercholesterolaemia. Continual inhibition of HMGCR for several days was necessary to induce cell death. Lipids consumed in the diet may reverse the cytotoxic effects of the statins, suggesting that patients receiving statins for cancer therapy may require dietary modification. Studies evaluating statins in combination with carboplatin or targeted therapeutics demonstrated limited synergy, and in some cases, profound antagonism, and therefore, statins may be best evaluated as single agents. Statins retained cytotoxic activity in ovarian cancer cells resistant to chemotherapy, supporting the use of statins in chemoresistant disease. These observations will help to inform the design of future clinical trials evaluating statins in ovarian cancer.

CONTENTS

FIGURES

TABLES

ABBREVIATIONS

ΔΔCT	Delta delta cycle threshold
AMPK	AMP-activated protein kinase
ATCC	American Type Culture Collection
Atg	Autophagy-related gene
ATP	Adenosine triphosphate
Bak	BCL2 antagonist killer 1
Bax	BCL2 associated X protein
Bcl-2	B-cell lymphoma protein 2
Bcl-X_L	BCL2 related protein, long isoform
Bid	BH3 interacting domain death agonist
Bim	BCL2 interacting protein BIM
BSA	Bovine serum albumin
Caspase	Cysteinyl aspartic acid-protease
ccCK18	Caspase-cleaved cytokeratin 18
Cdc42	Cell division cycle 42
CI	Combination Index
CK18	Cytokeratin 18
CT	Cycle threshold
DAPI	4',6-Diamidino-2-phenylindole
ddH_2O	Double-distilled water
DMSO	Dimethyl sulfoxide
DNA	Deoxyribonucleic acid
ECM	Extracellular matrix
ELISA	Enzyme-linked immunosorbent assay

F	Farnesol
FBS	Fetal bovine serum
FLIP	FLICE-like inhibitory protein
FPP	Farnesyl diphosphate
FT	Farnesyltransferase
G	Geranylgeraniol
GAPDH	Glyceraldehyde-3-phosphate dehydrogenase
GGPP	Geranylgeranyl diphosphate
GGT	Geranylgeranyltransferase
GTPase	Guanosine triphosphate hydrolase
H-Ras	Harvey rat sarcoma viral oncogene homolog
HFF	Human foreskin fibroblast
HGSC	High-grade serous ovarian carcinoma
HMG-CoA	3-Hydroxy-3-methyl-glutaryl coenzyme A
HMGCR	3-Hydroxy-3-methylglutaryl coenzyme A reductase
HOE	Human ovarian epithelial
HPLC	High-performance liquid chromatography
HRP	Horseradish peroxidase
IC_{50}	Half maximal inhibitory concentration
JNK	c-Jun N-terminal Kinase
K-Ras	Kirsten rat sarcoma viral oncogene homolog
LC3	Microtubule-associated protein light chain 3
M	Mevalonate
Mcl-1	Induced myeloid leukemia cell differentiation protein
mTOR	Mammalian target of rapamycin
N-Ras	Neuroblastoma Ras viral oncogene homolog

NAc	N-acetylcysteine
NL20	Human bronchial epithelial
Noxa	Phorbol-12-myristate-13-acetate-induced protein 1
OS	Overall survival
PARP	Poly (ADP) ribose polymerase
PBS	Phosphate buffered saline
PCR	Polymerase chain reaction
PFS	Progression-free survival
PI3K	Phosphatidylinositol 3-kinase
Pit	Pitavastatin
qPCR	Quantitative polymerase chain reaction
Rab	Rab, member RAS oncogene family
Rac1	Ras-related C3 botulinum toxin substrate 1
Ral	V-ral simian leukemia viral oncogene homolog
Rb	Retinoblastoma protein
Rheb	Ras homolog enriched in brain
Rho	Ras homolog family member
RIPA	Radio-immunoprecipitation assay
RNA	Ribonucleic acid
RNAi	RNA interference
ROS	Reactive oxygen species
S.D.	Standard deviation
S.E.M.	Standard error of the mean
SDS	Sodium dodecyl sulphate
siRNA	Small interfering ribonucleic acid
SPE	Solid phase extraction

SREBP	Sterol regulatory element binding protein
TBHP	Tert-butyl hydroperoxide
TCGA	The Cancer Genome Atlas
VEGF	Vascular endothelium growth factor
VEGFR	Vascular endothelium growth factor receptor

PUBLICATIONS

Robinson E., Leung E., Matuszek A. M., Krogsgaard-Larsen N., Furkert D. P., Brimble M. A., Richardson A. and Reynisson J. Virtual screening for novel Atg5-Atg16 complex inhibitors for autophagy modulation. Medicinal Chemistry Communications (2015) 6: 239-246.

Robinson E., Fisher N., Stamelos V. A., Redman C. W. and Richardson A. New strategies for the treatment of ovarian cancer. Biochemical Society Transactions (2014) 42 (1): 125-129.

Robinson E., Nandi M., Wilkinson L. L., Arrowsmith D. M., Curtis A. D. and Richardson A. Preclinical evaluation of statins as a treatment for ovarian cancer. Gynecologic Oncology (2013) 129 (2): 417-424.

Stamelos V. A., **Robinson E**., Redman C. W. and Richardson A. Navitoclax augments the activity of carboplatin and paclitaxel combinations in ovarian cancer cells. Gynecologic Oncology (2013) 128 (2): 377-382.

ACKNOWLEDGEMENTS

First and foremost, I would like to thank Keele University for providing the funding for this research. I offer my sincerest gratitude to my supervisor, Dr Alan Richardson, who has provided infinite guidance, resources and intellect over the course of this research. Thank you for your friendship and encouragement and, despite your busy workload, always making time for a chat. With this is mind, thanks to Professor William E. Farrell next door for all the light-hearted discussions, and for your helpful advice throughout my PhD. I would also like to acknowledge Dr Sarah Hart and Dr Elzbieta Piatkowska for mass spectrometry analysis, Dr Clare Hoskins for high-performance liquid chromatography analysis, Karen Menezes and Dr Euan Stronach at Imperial College London for cell proliferation assays in paired ovarian cancer cell lines, Dr Nicholas Forsyth for obtaining primary fibroblasts used in this research and support with the analysis of mitochondria, Dr Paul Roach for technical expertise on microscopy, and Charles River Discovery Research Services in the USA for conducting the xenograft study. Many thanks to Dr Vasileios Stamelos for all his help in the laboratory at the start of my PhD, and for repeatedly shouting “Fire!” when I was trying to develop my western blots in the darkroom (NB: no film was ruined during the making of this PhD!). Also, thanks to the very lovely Natalie Fisher for culturing my cells when I was away and for helping me with cell migration assays. To my great friend, Dr Kim Haworth, a million thanks for providing a listening ear, teaching me all things (epi)genetic and, most importantly, grinding up the mouse chow when my arm was aching! Personally, I would like to thank my husband, Christopher de Wolf, for his everlasting love and support, and for staffing the “Western blotting technical helpline” during the first year of my PhD. Finally, I would like give a heartfelt thanks to my family, especially my parents, for their support, encouragement and confidence in me.

You have always inspired me to aim higher and I am eternally grateful for everything that you have done for me. I dedicate this thesis to Auntie Marjorie and Uncle Maurice, who would have been so proud to see me achieve this degree.

"Never regard your study as a duty, but as the enviable opportunity to learn to know the liberating influence of beauty in the realm of the spirit for your own personal joy and to the profit of the community to which your later work belongs."

Albert Einstein

CHAPTER 1

INTRODUCTION

1.1 The Female Reproductive System

The uterus (womb), ovaries and fallopian tubes make up the internal organs found in the female reproductive system (figure 1.1). The ovaries produce, store and release eggs that are required for reproduction. Up to seven million primordial follicles are produced in the foetus by the final trimester of gestation. However, less than 1% will mature and ovulate during their lifetime, as most undergo a programmed mechanism of cell death known as apoptosis (follicle atresia). A small number of recruited primordial follicles undergo cell proliferation and differentiation in order to develop into graafian follicles over a period of 1 year. Following this, the follicle either ovulates its egg into the ovarian cortex mid-way through the menstrual cycle or is removed by follicle atresia. An ovulated egg moves down the fallopian tube and through the uterus. During this time it may be fertilised by sperm, implant into the lining of the uterus and develop into a foetus. Conversely, an unfertilised egg will be expelled from the uterus during menstruation. A layer of supportive connective tissue surrounds the cortex along with an outer epithelial layer.

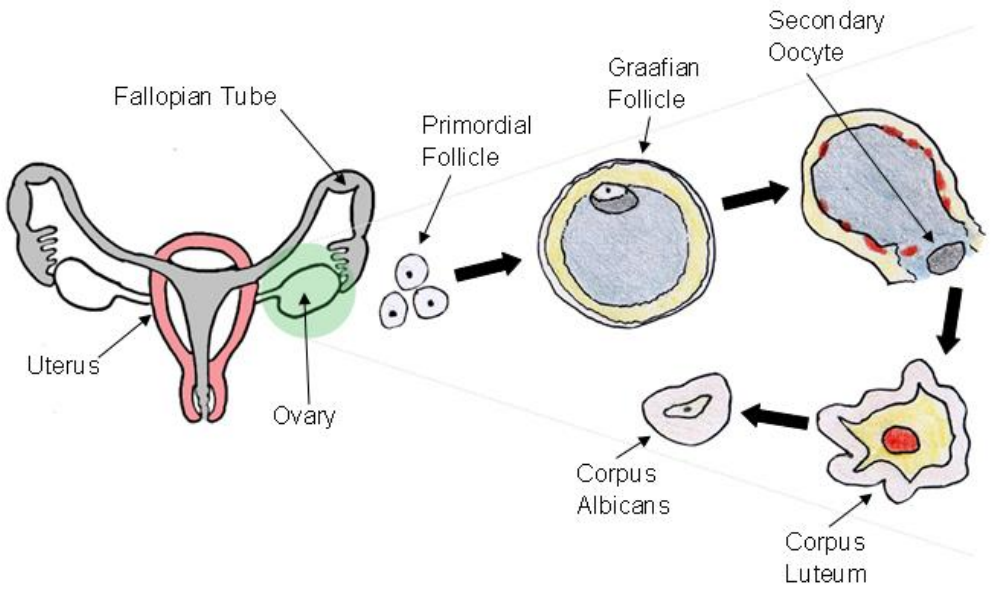

Figure 1.1: The female reproductive system and ovulation.

1.2 Introduction to Ovarian Cancer

1.2.1 Epidemiology

1.2.1.1 Incidence

Ovarian cancer is the fifth most common cancer in women with an overall 5-year survival rate of less than 45%, making it the principal cause of death from gynaecological cancer in the UK [1, 2]. A quarter of the women diagnosed with ovarian cancer between the years 2005 and 2009 died within the first year [2]. Despite this, survival rates have doubled over the last 30 years following the initiation of chemotherapy including platinum-based treatments and modifications in surgical practice [3]. Around 50-60% of cases comprise epithelial ovarian cancer occurring in women between the ages of 45 and 79 [4, 5]. Furthermore, serous carcinoma is the most common histological subtype, accounting for around one-third of all cases in 2009 [6]. A report by the National Cancer Intelligence Network indicated that the incidence of ovarian cancer is lower in Asian and Black ethnic groups compared to the White ethnic group [7]. The incidence of ovarian cancer is not affected by socioeconomic status [7]. Several risk factors have been identified which can increase the probability of developing ovarian cancer.

1.2.1.2 Age

Most ovarian cancers develop after the age of 40, with around half in women over the age of 63. The incidence continues to rise with increasing age, and reaches a peak in the 80-84 year old age group (61.8 cases of ovarian cancer per 100,000 women) [8]. Furthermore, the 5-year survival rate varies dramatically with age, as 84.2% survived in the 15-39 age group compared to only 13.7% of women over 85 years old [6]. This

may reflect differences in the tumour, as low-grade less aggressive ovarian tumours tend to occur in younger women. Other factors, including the earlier diagnosis and referral of younger women [9], and medical comorbidities in older women which can limit treatment, may also impact survival rates.

1.2.1.3 Family History

Approximately 10-15% of ovarian cancers (mostly type II) are hereditary, resulting from an inherited mutation of the breast cancer gene, *BRCA1* or *BRCA2* [10]. Whilst this predisposes women to a high risk of ovarian and breast cancer, they generally have a better prognosis than patients with sporadic ovarian cancer. Furthermore, women with either a history of breast cancer (particularly those under the age of 40) or a family history of breast or ovarian cancer were at least twice as likely to develop ovarian cancer [11]. Other inherited genetic susceptibility to ovarian cancer includes mutations in the hereditary nonpolyposis colorectal gene [12].

1.2.1.4 Reproductive Factors

An extended reproductive history can also increase the risk of ovarian cancer. Ovarian epithelial cells have a low proliferative index and generally proliferate to repair the damage caused when mature follicles rupture to release oocytes during ovulation. Ovulation can also lead to the development of epithelial cell-lined subsurface inclusion cysts. Both cellular proliferation and the growth of cysts can increase the likelihood of spontaneous genetic mutations and development of ovarian cancer. Ovulation has also been demonstrated to cause DNA damage in fallopian tube epithelial cells, possibly due to an increase in activated macrophages and release of inflammatory factors during ovulation [13], and this may contribute to the development of ovarian cancer in the fallopian tube. Increasing parity was shown to reduce ovarian cancer

risk, even when taking into account pregnancies which were terminated early [14]. Furthermore, breastfeeding appeared to have a slight protective effect [14]. Despite this, other factors which increase the number of ovulatory cycles including early menarche (before age 12) or late menopause (after age 50) had no significant effect on the risk of ovarian cancer [14, 15]. Increased levels of follicle-stimulating hormone, luteinising hormone, oestrone and androgen following menopause can also increase the proliferation of ovarian epithelial cells and thus contribute to the development of cancer. Thus unsurprisingly, the use of contraceptives which prevent ovulation can significantly decrease the risk of ovarian cancer, including in women with a BRCA mutation [16-19].

1.2.1.5 Hormone Replacement Therapy

The use of oestrogen replacement therapy following the menopause has also been linked to a slightly increased risk of ovarian cancer, particularly in women who are treated for more than 10 years [20, 21]. This treatment has been superseded by combined hormone replacement therapy (oestrogen and progesterone), which is believed to have little impact on the likelihood of developing ovarian cancer.

1.2.1.6 Chemical Agents

Whilst chemical carcinogens have not been directly linked to ovarian cancer, several studies have indicated that exposure to talc may increase the risk of developing ovarian cancer [22, 23]. Despite this, a recent meta-analysis of epidemiological studies failed to endorse an association between the use of talc powders on the female perineum and ovarian cancer [24].

1.2.1.7 Medical Conditions

Endometriosis increases the risk of developing ovarian cancer, particularly with endometrioid and clear cell morphology [25-27]. The use of oral contraceptives for more than 10 years in women with endometriosis substantially reduced this risk [25], suggesting that long-term oral contraceptive use may protect this high-risk population.

1.2.2 Origin

Cancer arises from a series of genetic mutations in a cell resulting in reregulated proliferation and apoptosis. Genetic changes can lead to the activation of oncogenes which, in the absence of normal external factors, can cause cell division. The suppression or deletion of many tumour suppressor genes prevents both the inhibition of this cell division and the programmed cell death that would normally follow. Cancer cells secrete growth factors which promote angiogenesis, thereby increasing blood supply and nutrient provision to the tumour. Together with other factors which inhibit the immune response to the cancer cells, this results in the progression of the tumour, leading to invasive and metastatic disease.

Ovarian carcinomas were originally thought to arise from the epithelium which covers the ovarian surface. Early studies reported high rates of ovarian cancer in hens forced to produce large numbers of eggs without interruption in ovulation [28]. From this, it was hypothesised that epithelial cells on the surface of the ovary were damaged during ovulation, leading to the formation of cortical inclusion cysts and subsequent development of ovarian cancer [28, 29]. However, whilst ovarian cystadenomas can

progress into low-grade ovarian cancer, transformation into high-grade serous ovarian carcinoma (HGSC) is rare [29].

A breakthrough came during the start of the 21st century, when fallopian tubes and ovaries removed from women with a high risk of developing ovarian cancer were sectioned to reveal both non-invasive and invasive carcinomas primarily in the fallopian tube fimbria [30-33]. It was then proposed that malignant cells from these tubal carcinomas may metastasise to the ovary, resulting in ovarian cancer [34]. A number of studies have since supported the theory that the fallopian tube is the origin of serous ovarian carcinoma. Gene expression analysis demonstrated that there was a high degree of similarity between HGSC and tubal carcinoma gene expression profiles [35]. Tubal carcinomas have been reported in 50-60% of women with pelvic HGSC, however the possibility that the tubal carcinomas developed from a primary ovarian cancer cannot be excluded [36, 37]. Furthermore, a mouse model was used to demonstrate that removal of the fallopian tubes at an early age prevented the formation of ovarian cancer [38].

Despite the compelling evidence indicating the importance of tubal carcinomas as precursors to ovarian cancer, there are still a significant proportion of HGSC which appear to have no fallopian tube involvement. Some tubal carcinomas may be obscured by the growth of a secondary high-grade invasive cancer [39]. Alternatively, ovarian cancer may develop suddenly from a normal-appearing ovary. Data from 35 patients with epithelial ovarian cancer were retrospectively analysed to determine abnormalities in the adnexal regions (the space containing the ovaries, fallopian tubes and uterus) [40]. In 8 patients with no apparent abnormalities 2-12 months prior to the diagnosis, stage III tumours were identified and following surgery, no malignancies in

adjacent tissue were identified [40]. Therefore, it is possible that some serous carcinomas may develop within the ovary and progress rapidly.

1.2.3 Histological Subtypes and Molecular Features

Epithelial ovarian cancer comprises more than 80% of all ovarian cancers and includes serous, endometrioid, clear cell and mucinous histotypes [41]. Serous epithelial ovarian carcinoma accounts for more than 70% of epithelial ovarian cancers and the majority (90%) are HGSC [42]. Endometrioid and clear cell types represent 20%, and mucinous type accounts for 3% [43]. Germ cell tumours begin in the egg and are a rare type of ovarian cancer which generally affects younger women.

There are four main histotypes that resemble differentiated cells found in the fallopian tube (serous), endometrium (endometrioid), endocervix (mucinous) and vagina (clear cell) (figure 1.2).

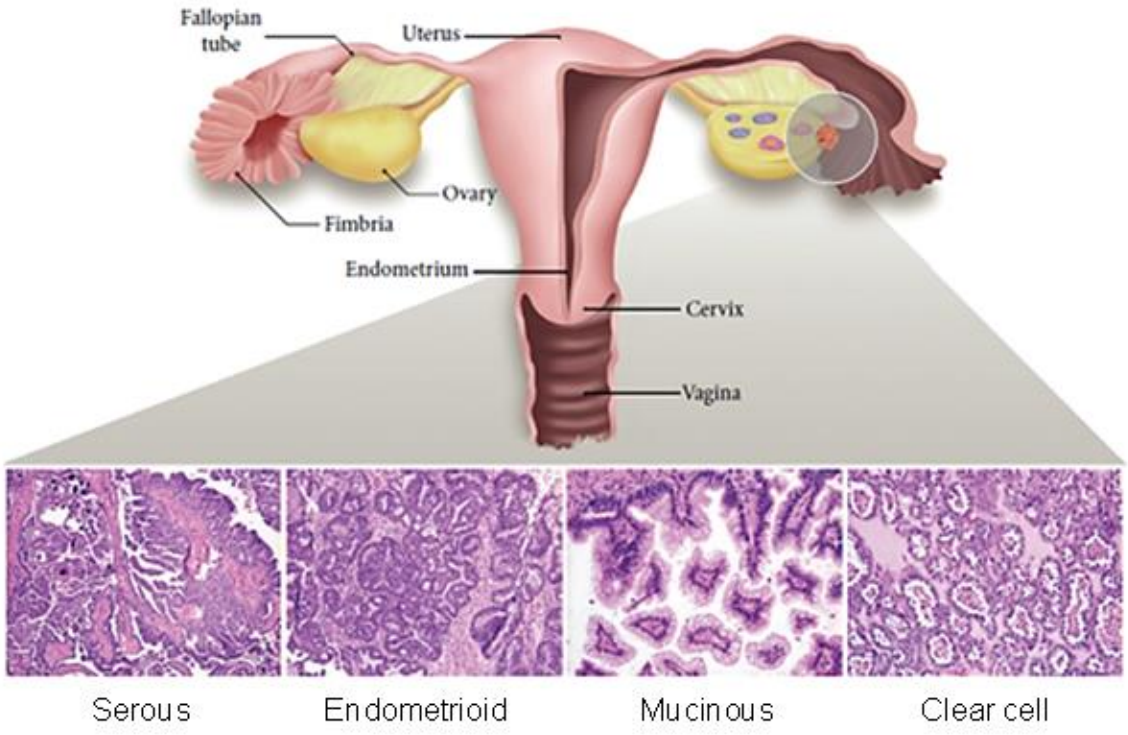

Figure 1.2: The four major types of ovarian cancer: serous, endometrioid, mucinous and clear cell. Tumour sections have been stained with hematoxylin and eosin and represent maturing ovarian follicles [44].

These four subtypes of ovarian cancer can be divided into two broad categories. Type I tumours include low-grade serous, mucinous, endometrioid and clear cell cancers and are believed to originate from precursor lesions in the ovary. Type II tumours may be derived from tubal or ovarian surface epithelium and encompass HGSC, undifferentiated cancers and carcinosarcomas.

1.2.3.1 Type I Tumours

Endometrioid and clear cell ovarian cancers

Endometrioid and clear cell ovarian cancers have both been linked to endometriosis. The inflammatory processes occurring during endometriosis may play a role in the growth and malignant transformation of ovarian surface epithelium. This is demonstrated by an induction of tumour necrosis factor-alpha (TNF-α) and growth factors such as insulin-like growth factor (IGF), which promote cellular growth and proliferation [45]. A corresponding increase in DNA repair can lead to more mutations which support the development of cancer. Mutations in the *phosphatase and tensin homolog* (*PTEN)* tumour suppressor and the *phosphatidylinositol-4,5-bisphosphate 3-kinase, catalytic subunit alpha (PI3KCA)* oncogene are common and likely to be early events in the development of endometrioid cancer. Furthermore, mutations in the beta-catenin gene (*CTNNB1*) are present in up to 30% of endometrioid cancers [46]. *CTNNB1* is involved in cell proliferation and the Wnt pathway, suggesting that dysregulation of this pathway may be implicated in the growth of endometrioid cancer [46, 47]. Clear cell ovarian cancer is relatively rare in Europe (4%) and tumours are generally resistant to chemotherapeutic agents [48]. Like endometrioid ovarian cancer, clear cell ovarian cancer is characterised by mutations in *PTEN* and *PI3KCA* [41]. A genetic signature was recently identified for clear cell cancer using microarrays and most of the 437 genes identified were related to oxidative stress [49].

Mucinous ovarian cancer

Mucinous cancers have also been linked to endometriosis, however this is relatively uncommon. They have been associated with other cancers including ovarian teratomas (germ cell tumours) and Brenner tumours, or may develop from surface

epithelial inclusions [50, 51]. Smoking has previously been identified as a risk factor linked to mucinous cancer [52, 53]. Mutations in the *kirsten rat sarcoma viral oncogene homolog (K-Ras)* gene occur in the early stages of mucinous cancer development. Furthermore, *tumor protein p53 (TP53)* mutations are associated with the transition from borderline tumours to carcinomas [41].

Serous ovarian cancer

Low-grade serous cancer is believed to develop gradually from serous cystadenomas and serous borderline tumours (figure 1.3). This subtype is characterised by a small number of mutations, of which activated *K-Ras*, *v-raf murine sarcoma viral oncogene homolog B (BRAF)* and *v-erb-b2 avian erythroblastic leukemia viral oncogene homolog 2 (ERBB2)* oncogenes are located upstream of the mitogen-activated protein kinase (MAPK) pathway, leading to uncontrolled cell proliferation [54].

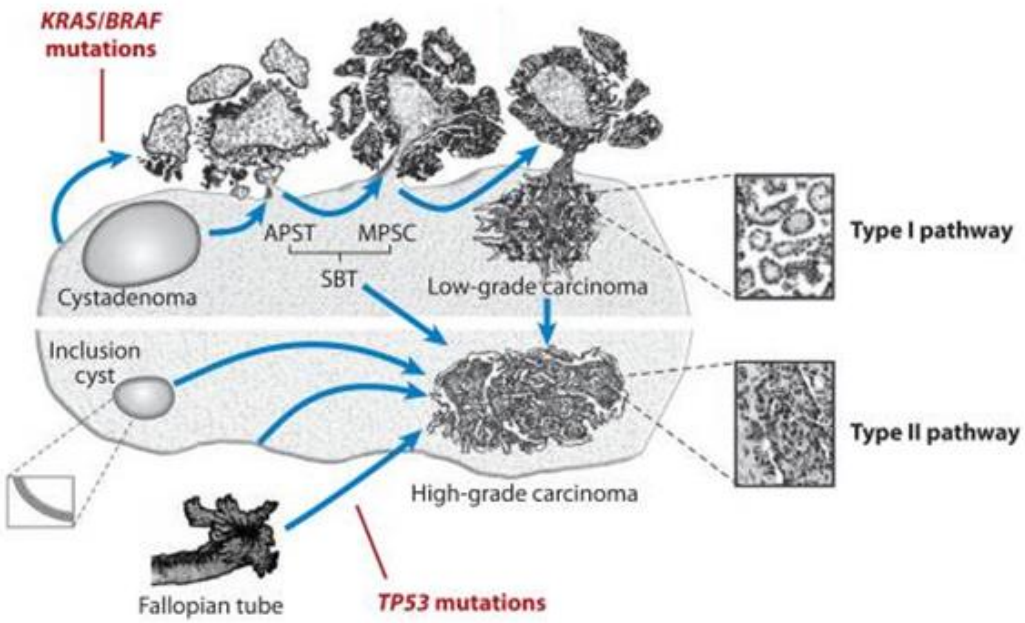

Figure 1.3: The origins of serous ovarian cancers in type I and type II pathways. APST, atypical proliferative serous tumour; MPSC, micropapillary serous carcinomas; SBT, serous borderline tumour [54].

1.2.3.2 Type II Tumours

Type II cancers include HGSC, undifferentiated cancers and carcinosarcomas [55]. These aggressive tumours are often detected at advanced stages following rapid spread to the surrounding tissues. HGSC frequently metastasise over the peritoneal surface forming many small nodules on the visceral and parietal peritoneum.

A summary of the genetic mutations recently found in HGSC is shown in table 1.1. More than 90% of type II tumours have *TP53* mutations and substantial genomic instability [41, 56]. The wild-type form of p53 functions as a tumour suppressor, which is critical to protect against cancer. In many tumours, *TP53* missense mutations result in the production of the full-length p53 protein with only a single amino acid substitution [57]. This mutant p53 protein may accumulate in cancer cells because of a prolonged half-life, and more importantly, possess activities which may contribute to tumour progression [58]. This oncogenic activity is described as “gain-of-function” mutant p53 [59]. Approximately 100 of the 301 tumour samples with *TP53* mutations in the Cancer Genome Atlas analysis of HGSC were considered to have “gain-of-function” mutant p53 [58]. Interestingly, “gain-of-function” mutant p53 was correlated with ovarian tumours with greater metastatic potential and resistance to platinum-based chemotherapy, although there was no difference in patient survival between tumours with or without “gain-of-function” mutant p53 [58].

Gene	Chromosome	Percentage of cancers mutated	Function
Tumor protein p53 (TP53)	17p13.1	96%	Tumour suppressor, cell cycle regulation
Breast cancer 1, early onset (BRCA1)	17q21.31	9%	Tumour suppressor, DNA damage repair, transcriptional regulation
Breast cancer 2, early onset (BRCA2)	13q13.1	8%	Tumour suppressor, DNA damage repair, transcriptional regulation
CUB and Sushi multiple domains 3 (CSMD3)	8q23.3	6%	Possible tumour suppressor
FAT tumor suppressor homolog 3 (FAT3)	9x	6%	Tumour suppressor, planar polarity, neuronal development
Neurofibromin 1 (NF1)	17q11.2	4%	Negative regulation of Ras signalling pathway
Cyclin-dependent kinase 12 (CDK12)	17q12	3%	Transcriptional regulation
Retinoblastoma 1 (RB1)	13q14.2	3%	Tumour suppressor, cell cycle regulation
Gamma-aminobutyric acid (GABA) A receptor, alpha 6 (GABRA6)	5q34	2%	Inhibitory neurotransmitter

Table 1.1: Genes significantly mutated in high-grade serous ovarian carcinoma (HGSC) (Modified from [56]).

In addition to the three well documented tumour suppressor genes, *TP53*, *BRCA1* and *BRCA2*, a further six mutated genes were identified in 2-6% of HGSC [56]. *CDK12* mutations have been previously reported in lung adenocarcinoma [60] and in the human *GNAS1* gene [61]. In ovarian cancer, four missense mutations in *CDK12* were located in the protein kinase domain and a further five were nonsense, potentially resulting in loss of function [56]. Whilst both *FAT3* and *GABRA6* were significantly mutated in ovarian cancer, neither were expressed in the ovarian cancer tissue or fallopian tube tissue, suggesting that they may not have a significant contribution to HGSC [56]. In contrast to type I tumours, *BRAF*, *K-Ras*, *neuroblastoma Ras viral oncogene homolog* (*N-Ras)* and *PI3KCA* are rarely mutated in type II tumours, but may still be significant drivers in the transformation to HGSC [56].

Molecular pathways altered in HGSC

Pathway analyses in 316 high-grade serous ovarian tumours revealed that the retinoblastoma (Rb) and phosphatidylinositol 3-kinase (PI3K) / Ras pathways were deregulated in 67% and 45% of cases respectively, and this is likely to contribute to cancer cell survival and cell cycle progression [56]. Furthermore, NOTCH signalling was altered in 22% of cases, genes in the homologous recombination (HR) pathway including *BRCA1* and *BRCA2* were mutated or hypermethylated in around 51% of cases, and the FOXM1 transcription factor network was activated in 84% of cases, most likely as a result of the high rate of *TP53* mutations [56]. These pathways also contribute to cell cycle progression and DNA repair in cancer cells. Taken together, these observations may provide further opportunities for the treatment of HGSC.

1.2.4 Clinical Features

Symptoms of ovarian cancer are vague and can be the result of other less serious conditions. They include abdominal swelling, unusual vaginal bleeding, pelvic pressure, increased urinary urgency or frequency, back or leg discomfort and gastrointestinal complaints such as indigestion, early satiety, stomach pain and bloating [3]. Women have often experienced symptoms for many months prior to diagnosis and consequently most present with advanced disease [62-64].

1.2.5 Screening

The probability of undiagnosed ovarian cancer in women presenting to primary care with symptoms experienced within the previous year was estimated to be approximately 1 in 25 [65]. A screening programme for ovarian cancer could aid in early detection and reduce mortality as has already been demonstrated for breast, bowel and cervical cancers [66]. Despite this, screening for ovarian cancer is not currently undertaken in the general population due to the absence of a proven reduction in mortality using current detection methods [67].

Many ovarian cancer screening trials utilise the serum biomarker CA125, a transmembrane glycoprotein that is expressed by epithelial cells in the fallopian tubes, endometrium and endocervix [68]. CA125 is released from the cell surface by proteolytic cleavage at an extracellular site, a process thought to be regulated by post-translational modifications, including glycosylation [69, 70]. Serum CA125 is elevated in around 50% of stage I ovarian cancer cases and over 90% of advanced stage

cases [68, 71]. However, CA125 levels can also be increased in benign conditions including ovarian cysts, endometriosis and fibroids, thereby complicating its use as a screening tool in the general population [72]. The Japanese Shizuoka Cohort Study of Ovarian Cancer Screening utilised a combination of CA125 and ultrasound, and the results suggested that women in the screened arm were more likely to have ovarian cancer detected in the early stages compared to the control arm [73]. Furthermore, the ongoing UK Collaborative Trial of Ovarian Cancer Screening (UKCTOS) has incorporated several arms including no intervention (control), annual screening using transvaginal ultrasound or serum CA125 interpreted using the Bayesian algorithm 'Risk of Ovarian Cancer' (ROCA) [74]. An early report indicated that there was encouraging sensitivity for detecting ovarian cancer in both screening arms [75]. The Kentucky Screening study used ultrasound to screen women. The five-year survival rate in women diagnosed with primary invasive epithelial cancer was significantly greater than the survival rate in women treated with the same surgical and chemotherapeutic interventions who were not part of the study [76, 77]. Despite these promising studies, screening by ultrasound or CA125 has been unsuccessful at detecting early stage ovarian cancer in women at an increased risk due to genetic factors or a family history of the disease [78, 79].

The continued search for cancer-specific biomarkers has resulted in some promising results. In addition to CA125, Human Epididymis protein 4 (HE4) also has a high sensitivity for the detection of ovarian cancer, however there was no advantage in detecting both HE4 and CA125 in ovarian cancer screening compared to CA125 alone [80]. Despite this, a panel of CA125, HE4 and mesothelin were increased in women three years prior to diagnosis of ovarian cancer and reached detectable levels within the final year before diagnosis [81]. In a UKCTOCS case-control study, an elevation of

putative platelet factor 4 (PF4) and connective tissue-activating peptide III (CTAPIII) was detected before the increase in CA125 and ovarian cancer diagnosis [82].

The high frequency of type-II ovarian cancers with *TP53* gene mutations has led to the use of tagged-amplicon deep sequencing (TAm-Seq) to detect *TP53* mutations in patients with high levels of circulating tumour DNA [83]. However, this technique does not currently afford the sensitivity to allow the detection of *TP53* mutations in patients with less advanced cancers. Furthermore, mutations in a panel of 12 genes were identified in cervical samples from women with ovarian cancer, advocating the use of alternative biospecimens to overcome the problems of biomarker dilution in traditional blood assays [84].

Enhanced imaging techniques have also been employed to detect cancerous tissue and angiogenesis at an earlier stage. Screening protocols may include contrast-enhanced transvaginal ultrasound with microbubbles that can be transported through capillaries and used to detect changes in tumour vascularity [85]. Furthermore, light-induced intrinsic tissue fluorescence or autofluorescence can be used to identify cancerous or precancerous epithelial tissue. Use of this technique on fallopian tubes removed during surgery can detect precursor cancerous leisons with good levels of sensitivity and specificity [86], suggesting that this technique could be introduced *in vivo*.

1.2.6 Diagnosis

The diagnosis of ovarian cancer is based upon the symptoms experienced by the patient. Clinical guidelines recommend that if symptoms are persistent, experienced more than 12 times per month or are suggestive of irritable bowel syndrome (IBS) in women aged 50 or over, further tests for ovarian cancer should be initiated [3]. The measurement of CA125 is the initial test and standard for the management of ovarian cancer. A meta-analysis reported that the sensitivity of CA125 for detecting borderline and malignant ovarian cancer was 80% [71]. However the specificity was slightly reduced at 75%, representing the elevation of CA125 levels in benign lesions in addition to ovarian cancer [71]. Therefore, the use of CA125 alone for the diagnosis of ovarian cancer is inadequate and other techniques including ultrasound and computed tomography (CT) scans are required to confirm the presence and extent of the disease. The diagnosis and histological subtype of ovarian cancer should also be confirmed by a laparotomy, where the staging (spread) of the disease can also be determined. During this surgical procedure to gain access to the abdominal cavity, peritoneal cytology should be collected and all visible tumours are removed where possible [87]. Staging the cancer (table 1.2) can inform subsequent treatment decisions and give an insight into the survival prognosis. CA125 monitoring is routinely used to indicate a response to chemotherapy and has been shown to detect recurrent ovarian cancer in 70% of patients [88]. This enables early initiation of combination chemotherapy, which can help to extend progression-free survival (PFS) and overall survival (OS). Despite this, the benefit of monitoring CA125 in patients with recurrent disease is uncertain and should be considered in each case.

Stage	Description
I	Tumour confined to ovaries or fallopian tubes
IA	Tumour confined within one ovary (capsule intact) or fallopian tube
IB	Tumour confined within both ovaries (capsules intact) or fallopian tubes
IC	Tumour confined to one or both ovaries (capsules intact) or fallopian tubes with *IC1/IC2/IC3:*
IC1	Surgical spill
IC2	Capsule ruptured prior to surgery or tumour on ovarian or fallopian tube surface
IC3	Ascites or peritoneal washings contain malignant cells
II	Tumour involves one or both ovaries or fallopian tubes with pelvic extension (below pelvic brim) or primary peritoneal cancer
IIA	Extension/implants on uterus/fallopian tubes/ovaries
IIB	Extension to other pelvic intraperitoneal tissues
III	Tumour involves one or both ovaries or fallopian tubes, or primary peritoneal cancer, with metastasis to the peritoneum or retroperitoneal lymph nodes
IIIA1	Positive retroperitoneal lymph nodes only: *IIIA1(i)* metastasis up to 10 mm or *IIIA1(ii)* metastasis greater than 10 mm
IIIA2	Microscopic extra-pelvic peritoneal involvement with or without positive retroperitoneal lymph nodes
IIIB	Macroscopic peritoneal metastasis beyond the pelvis up to 2 cm with or without retroperitoneal lymph node metastasis (includes extension to the liver or spleen)
IIIC	Macroscopic peritoneal metastasis beyond the pelvis more than 2 cm with or without retroperitoneal lymph node metastasis (includes extension to the liver or spleen)
IV	Distant metastasis excluding peritoneal metastases
IVA	Pleural effusion with positive cytology
IVB	Metastases to extra-abdominal organs, liver or spleen including inguinal lymph nodes and lymph nodes outside the abdominal cavity

Table 1.2: The FIGO staging classification for cancer of the ovary, fallopian tube and peritoneum (Modified from [5, 87]).

1.2.7 Current Treatment

Ovarian cancer treatment currently involves surgical removal of the tumour followed by chemotherapy, a regimen that has advanced over the last 50 years (figure 1.4). Platinum-based monotherapy was introduced in the late 1970's and, in combination with other chemotherapeutic agents, is currently the best standard of care. Conversely, radiotherapy has shown little success in the treatment of ovarian cancer and can have adverse effects on surrounding abdominal organs.

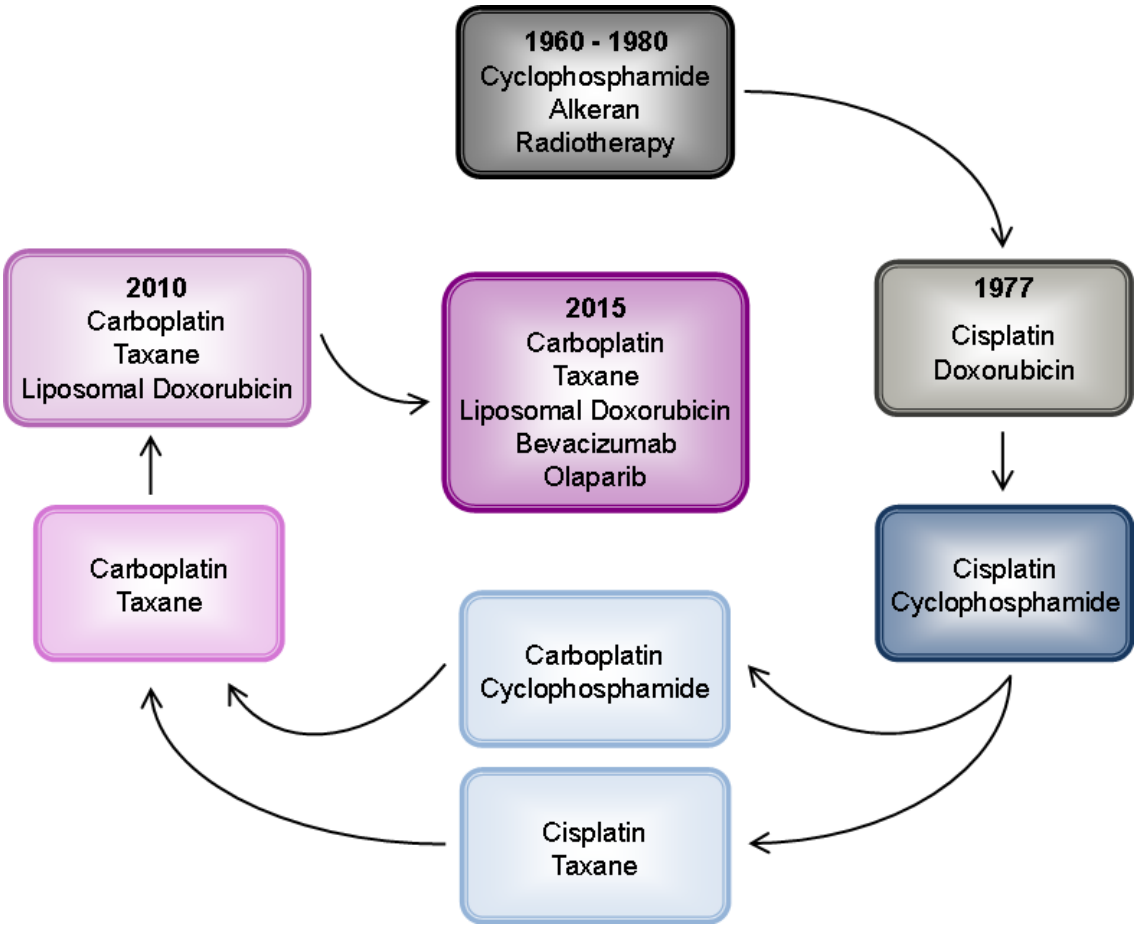

Figure 1.4: The evolution of ovarian cancer treatment over the last 50 years (Modified from [89]).

1.2.7.1 Surgery

The majority of patients are offered surgery with the aim of removing the majority of the tumour. This often results in the removal of the ovaries, fallopian tubes, womb or omentum, a fatty layer that covers the organs in the abdomen. If the tumour is limited to one ovary, consideration should be given to conserve the uterus and contralateral ovary in order to maintain fertility.

1.2.7.2 Chemotherapy

First-line chemotherapeutic agents

Chemotherapy can be used to reduce the size of the tumour before surgery or to control tumour growth in cases where surgery is not appropriate. Chemotherapy is predominantly administered to remove any remaining cancer following surgery. Current UK guidelines state that chemotherapy must be started no later than 8 weeks after surgery [3]. Adjuvant chemotherapy is not recommended for tumours that are diagnosed at an early stage (grade 1 or 2, stage Ia or Ib). Where the cancer has spread beyond the ovaries, chemotherapy comprising platinum-based therapy alone or in combination with paclitaxel is first line. Several factors including disease stage, the extent of surgical treatment required, disease-related performance status and side effect profiles should be considered when prescribing chemotherapy [90].

Platinum-containing compounds

Both cisplatin and carboplatin are platinum-based compounds which cause intrastrand linking in DNA. After entry into the cell, the compound loses a chloride ion whilst reacting with water, and subsequently, binds to DNA. Intrastrand cross-linking occurs between N7 and O6 of adjacent guanine molecules, resulting in a DNA damage

response, cell cycle arrest and apoptosis [91]. Cisplatin is highly nephrotoxic and intravenous treatment is coupled to strict hydration and diuresis regimens. Treatment also causes nausea and vomiting, tinnitus and peripheral neurotoxicity. Carboplatin is a derivative of cisplatin which has fewer toxic side effects and can be given on an outpatient basis, making it the platinum drug of choice.

Taxanes

Paclitaxel is a taxane derived from the bark of the yew tree. Taxanes function by stabilising microtubules in the polymerised state, which inhibits cell division and results in G_2/M phase cell cycle arrest and apoptosis. In addition to myelosupression and cumulative neurotoxicity, the risk of hypersensitivity requires treatment with corticosteroids and antihistamines prior to chemotherapy.

Most patients are defined as having responded to first-line chemotherapy when malignant disease is not detected for at least 4 weeks (complete response) or tumour size is reduced by at least 50% for more than 4 weeks (partial response) [90]. Despite this, 55-75% of responders relapse within two years [90].

Second-line chemotherapeutic agents

Combination treatment of carboplatin and other chemotherapeutic agents including pegylated liposomal doxorubicin (PLD), gemcitabine and topotecan can improve PFS in patients with recurrent disease. Current NICE guidelines recommend that PLD is used in patients whose disease does not respond to carboplatin, or relapses within 12 months of carboplatin treatment [90]. Topotecan is only recommended if both PLD and paclitaxel are unsuitable for the treatment of disease unresponsive to first-line therapy (platinum-refractory ovarian cancer) or disease which initially responds to

therapy but relapses within 6 months following treatment (platinum-resistant ovarian cancer) [90].

Doxorubicin

Doxorubicin is an anthracycline antibiotic that has several cytotoxic actions. The topoisomerase II enzyme nicks both DNA strands during DNA replication to enable uncoiling and subsequently reseals the breaks. Doxorubicin intercalates in the DNA and stabilises the DNA-topoisomerase complex, thereby halting DNA replication. Anthracyclines also disrupt the function of cell membranes, and generate hydrogen peroxide and hydroxyl radicals which are damaging to cells [90]. Doxorubicin can accumulate, leading to dose-related cardiotoxicity and therefore, patients must not receive more than the maximum cumulative dose. The use of liposomal formulations of doxorubicin (e.g. PLD) may reduce the incidence of cardiotoxicity and local necrosis; however, hand-foot syndrome is a common side effect.

Topotecan

Topotecan is a campothecin derived from the stem of the tree Camptotheca acuminata. Campothecins prevent DNA replication by binding to and inhibiting the topoisomerase I enzyme. They have fewer side effects compared to other chemotherapeutic agents.

1.2.7.3 Route of Chemotherapy Administration

Most chemotherapeutic agents are administered either orally or intravenously. A review of eight clinical trials reported a significant reduction in the risk of death and disease recurrence following intraperitoneal (IP) delivery [3]. The aim is to increase the concentration of drug in contact with the tumour on the peritoneal surface. IP

therapy is most appropriate for patients who have undergone surgery to remove the majority of the tumour. This allows the chemotherapy to penetrate small tumour nodules and have an enhanced cytotoxic effect. Despite this, IP drug administration is inconvenient and can be poorly tolerated by patients due to the increased incidence of adverse effects. Current guidance does not support the routine use of IP chemotherapy, except as part of a clinical trial [3].

1.2.7.4 Bevacizumab

Blood vessel formation (angiogenesis) is crucial for the progression of cancer since tumour growth is unable to proceed beyond 2mm in the absence of angiogenesis [92]. Pro-angiogenic factors including vascular endothelial growth factor (VEGF), fibroblast growth factor (FGF), platelet-derived growth factors (PDGFs), TNF-α, interleukins (IL-6, IL-8) and angiopoietins are important for cell growth and metastasis in tumour angiogenesis [92, 93]. Bevacizumab is a monoclonal antibody which recognises VEGF-A and has recently been approved for the treatment of women with recurrent platinum-resistant ovarian cancer. Initial phase II studies of bevacizumab as a single agent for the treatment of ovarian cancer demonstrated improved patient survival [94, 95]. Following this, the phase III studies GOG 218 and ICON7 both reported that bevacizumab in combination with chemotherapy in patients with stage III or stage IV ovarian cancer improved PFS compared to chemotherapy alone (GOG 218: 14.1 versus 10.3 months; $P < 0.001$; ICON7: 19.0 versus 17.3 months; $P = 0.004$) [96, 97]. Despite this, OS was only improved in high-risk women during the ICON7 trial. In the OCEANS trial, the combination of bevacizumab, gemcitabine and carboplatin for 6-10 cycles followed by bevacizumab until disease progression improved PFS compared to chemotherapy alone in women with platinum-sensitive recurrent ovarian cancer (12.4 versus 8.4 months; $P < 0.0001$) [98]. Furthermore, in platinum-resistant recurrent

disease, there was a significant improvement in PFS in patients randomised to chemotherapy (pegylated liposomal doxorubicin, paclitaxel or topotecan) with bevacizumab versus chemotherapy alone (6.7 versus 3.4 months; $P < 0.001$) [99]. Despite a trend in favour of the addition of bevacizumab to chemotherapy, there was no significant improvement in OS in the bevacizumab arm [99]. A recent study determining the effects of bevacizumab on patient-reported outcomes during the AURELIA trial found that there was a significant improvement in gastrointestinal symptoms in women with recurrent platinum-resistant ovarian cancer in the bevacizumab arm [100]. A review of the clinical efficacy and cost effectiveness of bevacizumab resulted in NICE not recommending bevacizumab in combination with paclitaxel and carboplatin for the first-line treatment of advanced ovarian cancer [101], or bevacizumab in combination with gemcitabine and carboplatin for the treatment of the first recurrence of platinum-sensitive advanced ovarian cancer (including fallopian tube or primary peritoneal cancer) that has not been previously treated with bevacizumab or other VEGF inhibitors [102].

1.2.8 Potential of Olaparib for the Treatment of Ovarian Cancer

Pathways involved in DNA damage repair mechanisms have an important role in maintaining genome integrity and the response to chemotherapy. Cancer cells have several mechanisms which function to repair this damage by removing platinum-DNA adducts from the tumour DNA [103]. The nucleotide excision repair (NER) pathway is primarily responsible for repairing platinum-induced DNA damage in ovarian cancer cells, and increased expression of NER proteins correlated with cisplatin resistance [104]. The mismatch repair (MMR) pathway is involved in the repair of post-replicative

errors and is deficient in around 10% of ovarian cancers [105]. MMR inactivation may contribute to DNA damage tolerance in cancer cells and correspondingly, several studies have linked downregulated or mutated MMR genes to platinum resistance in ovarian cancer [106, 107].

BRCA1 and BRCA2 proteins are involved in the HR pathway, which functions to repair DNA strand breaks (figure 1.5). *BRCA1/2* loss-of-function mutations can increase the risk of ovarian cancer, as cells are unable to repair damaged DNA through the defective HR pathway [108]. Poly (ADP) ribose polymerase (PARP) facilitates the addition of ADP-ribose polymers to damaged DNA, which results in the repair of DNA single-strand breaks through the base excision repair (BER) pathway [109]. The inhibition of PARP leads to an increase in DNA lesions, including double-strand breaks or collapsed replication forks that can only be repaired by HR (figure 1.5). The result, known as synthetic lethality, is the combined inhibition of two DNA repair pathways which leads to cell death [108]. However, secondary mutations may restore *BRCA1/2* and HR function and this, in combination with other mechanisms (section 1.2.9), may contribute to drug resistance [110, 111].

The Cancer Genome Atlas analysis of HGSC demonstrated that approximately 25% of cases may have disruption to the HR pathway [56], and these patients could be treated with PARP inhibitors. Tumours with *BRCA1/2* mutations were highly sensitive to PARP inhibitors, indicating that PARP inhibitors may be selective for tumour cells since normal cells retain wild-type *BRCA1/2* [112, 113]. In contrast, ongoing phase II studies have recently reported some response to PARP inhibition in patients with no *BRCA* mutations [114], suggesting that these tumours may have other mutations in genes which function in the HR pathway [115]. This provides evidence of the potential

benefit of PARP inhibitors in non-BRCA mutant ovarian cancer and highlights the need to define the population best served by PARP inhibition.

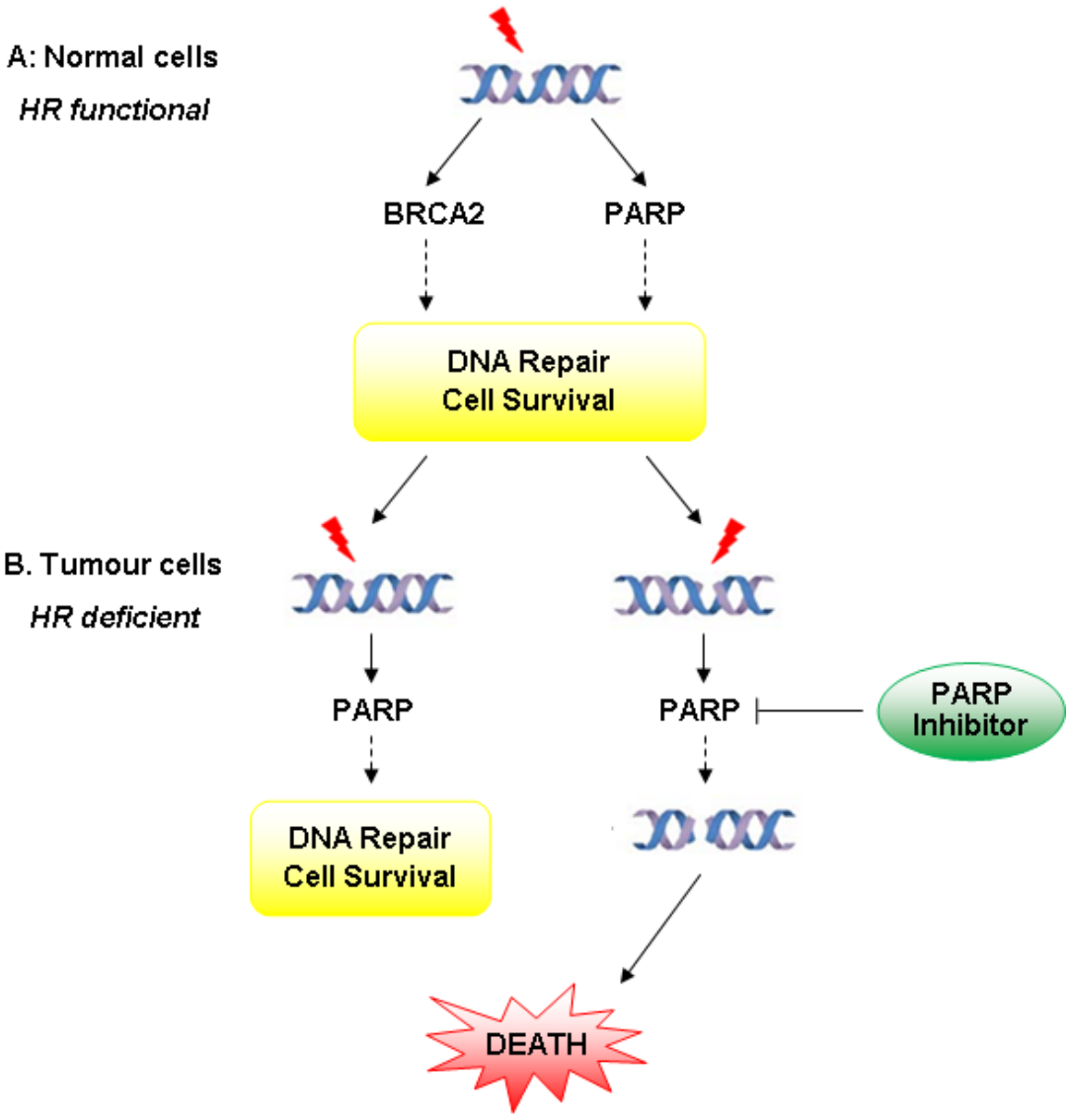

Figure 1.5: DNA repair and PARP inhibitors. Normal cells have functional HR and BER pathways which facilitate the repair of DNA strand breaks (A). Tumour cells with mutant BRCA are HR deficient and require the BER pathway to repair DNA single-strand breaks. PARP inhibitors prevent DNA repair through BER and this leads to cell death (B).

The PARP inhibitor, olaparib, demonstrated anti-tumour activity and was well tolerated in women with BRCA-mutated ovarian cancers in early phase I/II clinical trials [116, 117]. However, when olaparib was compared to liposomal doxorubicin, no significant benefit was observed [118]. Several recent clinical trials have demonstrated that PFS was significantly longer in the olaparib group compared to the placebo group (11.2 months versus 4.3 months; $P < 0.0001$), although no OS benefit was observed [114, 119]. Furthermore, the adverse effects of olaparib therapy were generally mild, including nausea, vomiting, fatigue and anaemia [114]. Taking into account these promising results, the Committee for Medicinal Products for Human Use of the European Medicines Agency have recommended the marketing authorisation of olaparib as monotherapy for the maintenance treatment of women with platinum-sensitive relapsed BRCA-mutated high-grade serous epithelial ovarian, fallopian tube or primary peritoneal cancer who are in response (complete or partial) to platinum-based chemotherapy.

Olaparib is also being evaluated in novel drug combinations in an attempt to improve clinical outcomes. A recent phase I clinical trial combining olaparib and the VEGF receptor (VEGFR) inhibitor, cediranib in patients with recurrent epithelial ovarian cancer resulted in an overall response rate of 44% [120]. A multi-institutional randomised phase II clinical trial is currently in progress [121]. Furthermore, an early study evaluating olaparib in combination with carboplatin in BRCA1/2 mutated ovarian cancer reported that this combination is well tolerated and demonstrated some promising signs of clinical activity [122].

1.2.9 Major Mechanisms of Chemotherapy Resistance

In addition to the alteration of DNA repair processes, there are several other mechanisms of drug resistance in cancer cells and these include a decrease in intracellular drug accumulation, drug metabolism and inhibition of apoptosis.

1.2.9.1 Impaired Intracellular Drug Accumulation

A decrease in the accumulation of drug in cancer cells has been documented as one of the major mechanisms contributing to drug resistance [123]. For example, copper transporter-1 (CTR1) is involved in regulating the entry of cisplatin and carboplatin into the cell. Copper can competitively inhibit the transport of cisplatin into ovarian cancer cells, resulting in a downregulation of *CTR1* expression [124]. Furthermore, copper exporters (ATP7A and ATP7B) are overexpressed in some ovarian cancers and can sequester platinum-based compounds, resulting in drug resistance [125, 126]. The multidrug resistance protein, P-glycoprotein (P-gp) is a membrane protein which functions to remove P-gp substrates from the cell. For example, P-gp has been shown to reduce the intracellular concentrations of platinum-based compounds, leading to chemoresistance [123]. Combination with P-gp inhibitors may increase the retention of chemotherapeutic agents in the cell, and subsequently improve clinical outcome. Indeed, this has been observed for combinations of doxorubicin and statins in ovarian cancer cell lines (discussed in chapter 7). However, the administration the P-gp inhibitor, valspodar with paclitaxel had limited activity in patients with paclitaxel-resistant disease and considerable toxicity [127].

1.2.9.2 Drug Inactivation

Glutathione is involved in the detoxification of platinum-based compounds, where they are converted into thiol conjugates by glutathione S-transferase and inactivated [123]. Glutathione S-transferase and enzymes involved in glutathione synthesis have been linked to cisplatin resistance in ovarian cancer cell lines [128]. The glutathione analog prodrug, canfosfamide, increased the sensitivity of ovarian cancer cells to apoptosis by reducing intracellular glutathione levels [123]. Despite this, clinical trials combining canfosfamide with chemotherapy in carboplatin-refractory or resistant ovarian cancer failed to demonstrate any clinical benefit compared to standard therapy alone [123].

1.2.9.3 Apoptosis Deregulation

Chemotherapeutic drugs can induce apoptosis in ovarian cancer cells, and therefore, inhibition of this mechanism of cell death has been associated with drug resistance. Expression of anti-apoptotic proteins (Bcl-2 and Bcl-X_L) and the caspase inhibitor, X-linked inhibitor of apoptosis protein (XIAP), have been correlated with drug resistance in ovarian cancer cells [129-131].

1.3 The Mevalonate Pathway and HMGCR Inhibitors

1.3.1 Deregulation of the Mevalonate Pathway in Cancer

Deregulation of cholesterol synthesis in mouse hepatomas was first reported around 50 years ago [132], and this observation has since been extended to other tumour types. Early studies showed that the synthesis of mevalonate had an essential function in DNA replication, and that feedback control of cholesterol synthesis was lost

in premalignant and malignant states both *in vitro* and in xenograft studies (reviewed by [133]). Following these early observations, there has been an abundance of evidence in support of increased cholesterol synthesis in cancer cells [134-138]. The increase in cellular cholesterol may be due to an increase in the activity of 3-hydroxy-3-methylglutaryl coenzyme A reductase (HMGCR) in tumours as a result of increased transcriptional regulation or deregulated feedback control of HMGCR [139-145]. HMGCR was recently described as a metabolic oncogene as ectopic expression of HMGCR increased anchorage independent growth and co-operated with other oncogenes including Ras to transform cells [137]. Furthermore, overexpression of HMGCR promoted cell growth and migration in esophageal squamous cell carcinoma cells [146] and correlated with poor prognosis and reduced survival in breast cancer patients [137]. Several cholesterol-related genes including *HMGCR* are transcriptionally regulated by the sterol regulatory element binding protein isoform 2 (SREBP-2). Correspondingly, SREBP-2 correlated with cell viability in prostate tumour cells [147]. Furthermore, *TP53* is almost ubiquitously mutated in ovarian cancer, and this can cause a “gain-of-function” association of mutant p53 with the promoters of sterol biosynthesis genes, leading to upregulation of the mevalonate pathway and tumorigenesis as demonstrated in breast cancer cells [148]. Alternatively, enhanced cholesterol synthesis may depend on the availability of other precursors in the mevalonate pathway including acetyl-CoA [149]. The Cancer Genome Atlas analysis identified gene amplification or increased mRNA expression of around 40% of the genes in the mevalonate pathway, including those involved in the synthesis of acetyl-CoA and HMG-CoA [56]. Despite this, increased HMGCR expression has been correlated with an improved clinical prognosis in breast, ovarian and colorectal cancers [150-152]. The association between cholesterol and cancer is also currently unclear, with some evidence indicating that cancer patients with high cholesterol

levels may have an improved outcome [153]. However, the levels of oxidised low density lipoprotein cholesterol (LDL) were increased in ovarian cancer patients, and were later found to stimulate cancer cell proliferation and reduce sensitivity to chemotherapeutic agents [154, 155]. Taken together, the findings regarding cholesterol are confusing, and it may be that cholesterol has no direct effect on cancer. Rather, this could be reflection of activity of the mevalonate pathway, whose real “driver” role in cancer is to make isoprenoids.

1.3.2 Introduction to HMGCR Inhibitors

HMGCR catalyses the irreversible reduction of HMG-CoA to mevalonate at the beginning of the isoprenoid biosynthetic (mevalonate) pathway (figure 1.6). This is the rate-limiting step in the pathway and the primary point of regulation of cholesterol synthesis. HMGCR is regulated both at the transcriptional level, and by phosphorylation, following an increase in intracellular cholesterol, which results in a reduction in HMGCR catalytic activity and an increase in proteolytic degradation [156]. Therefore, a decrease in HMGCR activity can regulate the output of the mevalonate pathway without accumulating unusable intermediates. Statins are a class of drug which competitively inhibit HMGCR.

The Mevalonate Pathway

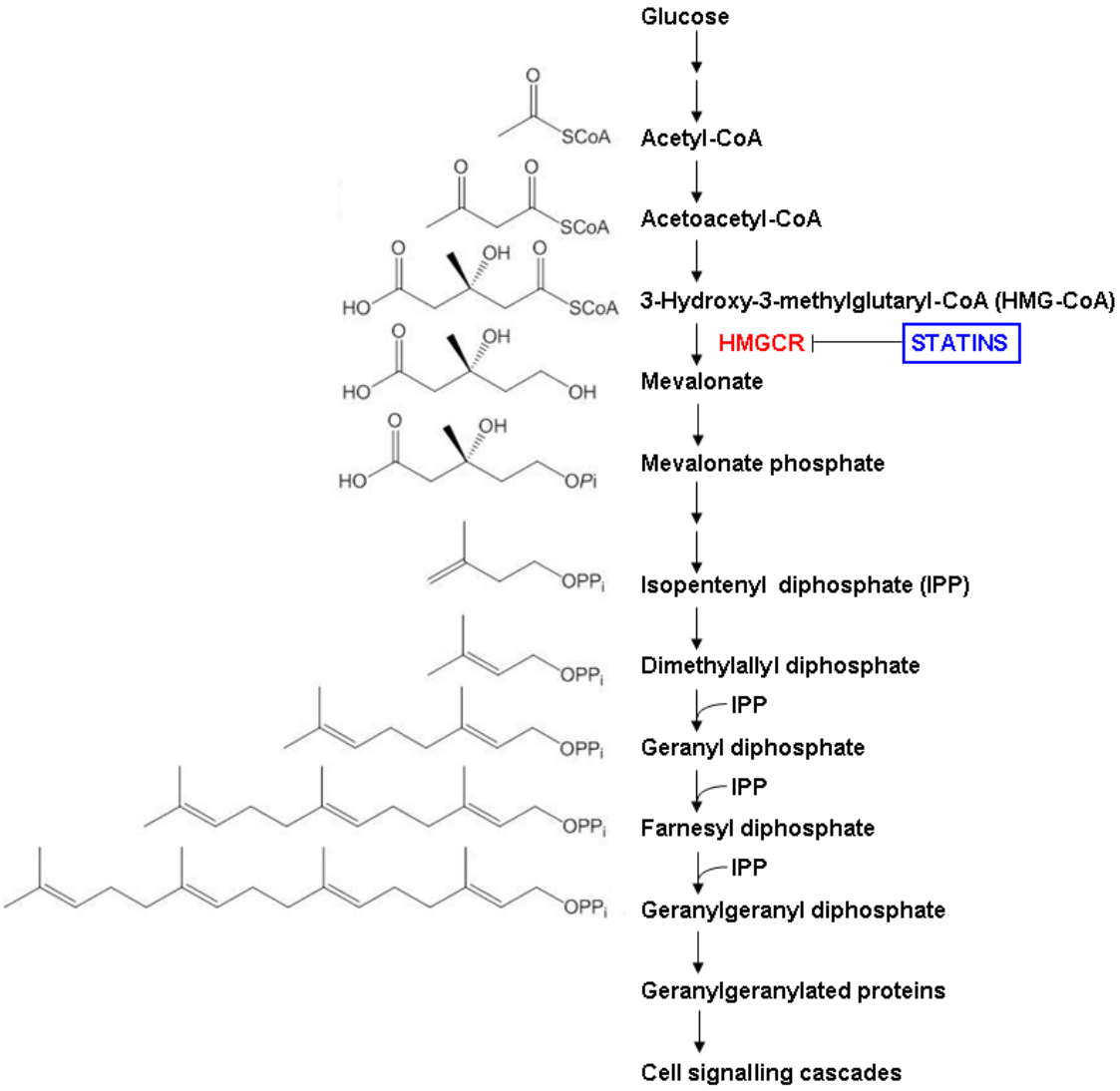

Figure 1.6: The mevalonate pathway. Statins (blue) inhibit 3-hydroxy-3-methylglutaryl coenzyme A reductase (HMGCR, red), which prevents the genanylgeranylation of proteins involved in a number of signalling pathways.

There are currently six clinically approved statins in the UK for the treatment of hypercholesterolemia (atorvastatin, fluvastatin, pitavastatin, pravastatin, rosuvastatin and simvastatin, figure 1.7). Lovastatin is an additional statin approved by the US

Food and Drug Administration (figure 1.7). Mevastatin was one of the first fungal statins isolated from *Penicillium citrinum*, although it was never marketed due to adverse effects in xenograft studies [157]. This was quickly followed by the type 1 statins, lovastatin, simvastatin and pravastatin, which are all derivatives of fungal products [158-160]. Type 2 statins include fluvastatin, cerivastatin, atorvastatin, rosuvastatin and pitavastatin, and are fully synthetic with larger, more polar groups attached to the HMG-like moiety to improve binding to HMGCR. Cerivastatin was withdrawn from the market in 2001 following an unacceptable number of deaths resulting from kidney failure attributed to statin-induced rhabdomyolysis.

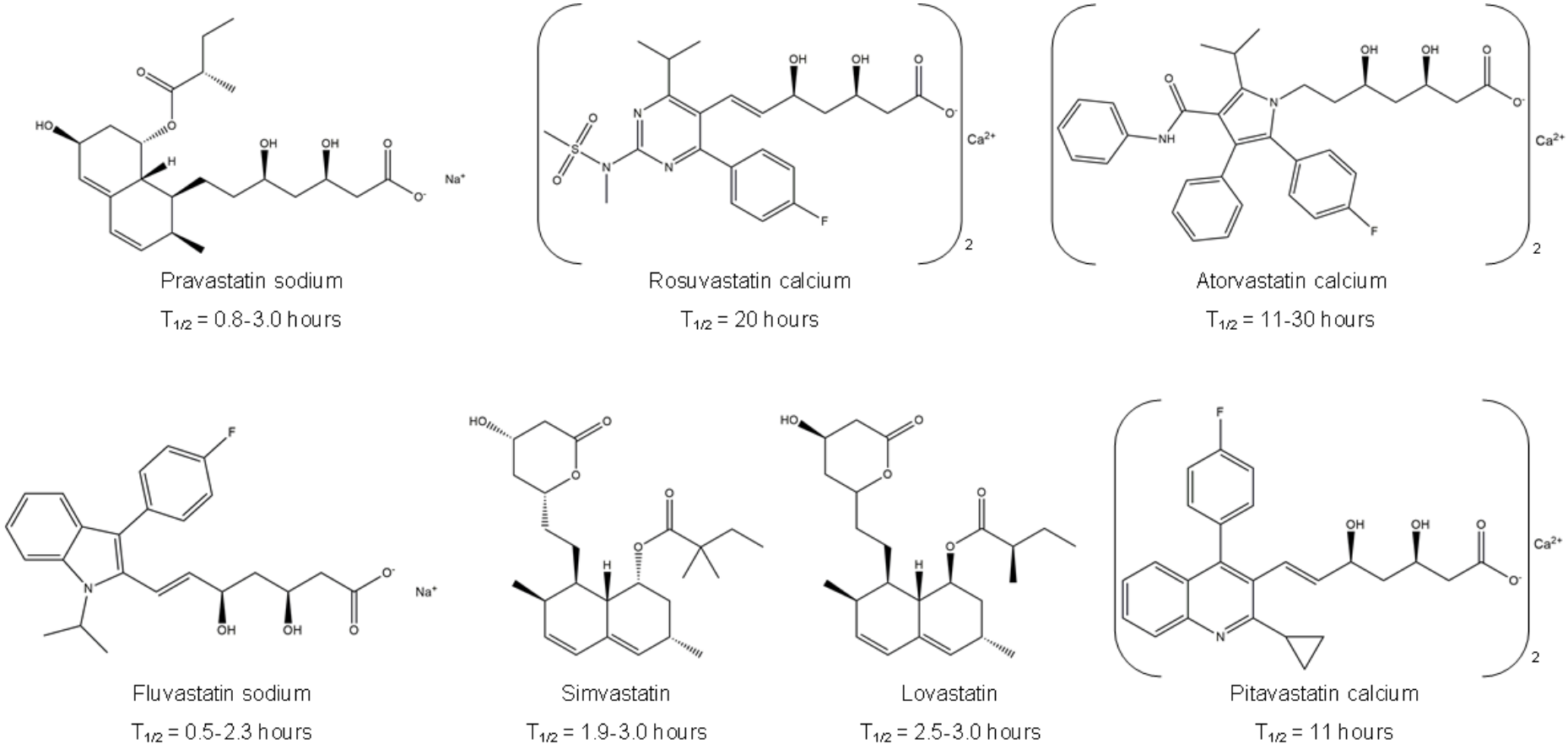

Figure 1.7: The chemical structures and half-lives ($T_{1/2}$) of the statins [161, 162].

The chemical structure of the statins can be divided into three parts: a HMG-CoA analogue, a hydrophobic ring structure involved in binding of the statin to HMGCR, and side groups which define other pharmacokinetic properties of the statins (e.g. *n*-octanol/water partition coefficient, logP). Statins occupy the enzyme active site of HMGCR where HMG-CoA is normally bound and form mostly polar interactions with residues located in the HMG-binding pocket loop (figure 1.8) including Ser^{684}, Asp^{690}, Lys^{691} and Lys^{692} [163]. A hydrogen-bonding network is formed between Lys^{691}, Glu^{559}, Asp^{767} and the statin O5-hydroxy group [163]. Additionally, the final carboxylate of the statin HMG moiety forms a salt bridge with Lys^{735}. Hydrophobic side chains in HMGCR also participate in a large number of van der Waals interactions with the statins (figure 1.8); this is likely to contribute significantly to the high affinity of statins to HMGCR [163]. The variable hydrophobic groups of the statins occupy a non-polar groove, which is accessible when the carboxy-terminal residues of HMGCR are disordered [163].

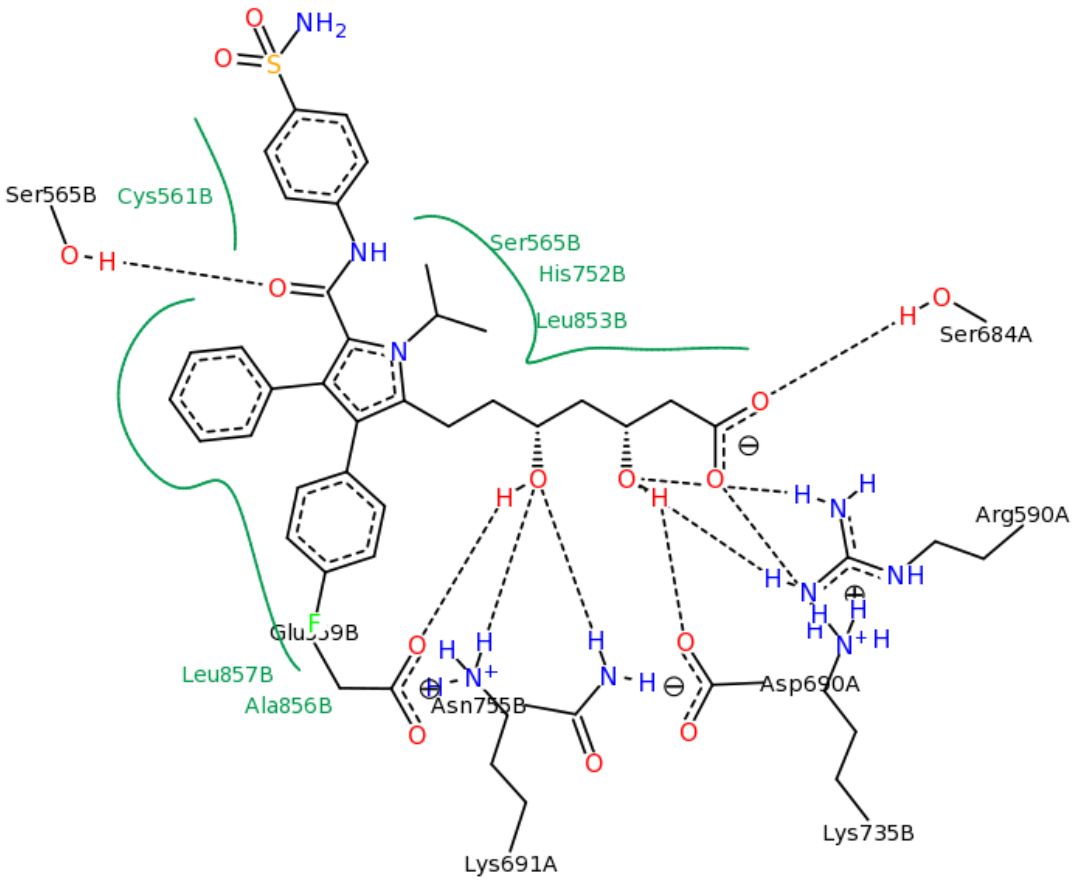

Figure 1.8: The binding interactions between HMGCR and ligand. Hydrogen bonding is indicated by the black dashed lines. Hydrophobic interactions are indicated by the green solid lines. Graphic generated using PoseView by BioSolveIT [164].

Statins were developed and licenced for the treatment of high cholesterol as they are highly efficient in lowering LDL. Rosuvastatin affords the greatest reduction in LDL (63%) following a standard daily dose of 40 mg [165]. The newest statin, pitavastatin reduced LDL by 38% after a 2 mg daily dose [166]. Statins also increase high density lipoprotein cholesterol (HDL) by up to 10% [167]. Furthermore, numerous clinical trials have shown that statins can either prevent or improve the outcome of ischemic stroke, myocardial infarction and peripheral arterial disease (Reviewed by [168-170]). Aside from these indications, statins also have cholesterol-independent or “pleiotropic”

effects arising from the inhibition of farnesyl diphosphate or geranylgeranyl diphosphate, which are substrates for the post-translational modification of proteins involved in various cell signalling pathways. This will be the focus of the remainder of this chapter.

1.3.3 Protein Prenylation and the Role in Cancer

1.3.3.1 Protein Prenylation

The anti-cancer activity of statins is thought to arise from the inhibition of several intermediate lipids, farnesyl diphosphate and geranylgeranyl diphosphate, in the mevalonate pathway, which subsequently prevents the activity of many proteins in downstream signalling pathways. It is thought that several hundred proteins undergo prenylation [171, 172]. Many of these contain a carboxy-terminal motif that is recognised as the site of isoprenylation. Farnesyltransferase (FT) or geranylgeranyltransferase-I (GGT1) recognise a CAAX motif, where ‘C’ is a cysteine moiety, followed by to two aliphatic residues, and ending in ‘X’ representing any amino acid [173]. The CAAX prenyltransferases add either a 15-carbon farnesyl or a 20-carbon geranylgeranyl group to the cysteine residue. The nature of this final amino acid ‘X’ determines if the protein is a substrate for FT or GGT1: in general, FT prefers ‘X’ to be methionine, serine, glutamine or cysteine, whereas GGT1 prefers ‘X’ to be leucine or isoleucine [174]. The prenylated protein is then further processed at the endoplasmic reticulum, where the three terminal amino acids (‘AAX’) are removed by the Ras-converting enzyme 1 (RCE1) protease, leaving the prenylcysteine at the C-terminus [175]. The protein is subsequently methylated on the carboxyl group by isoprenylcysteine carboxyl methyltransferase (ICMT) using S-adenosyl-L-methionine

as a methyl donor, and directed to the appropriate location which is often cytoplasmic surface of cell membranes [175]. Prenylcysteine methylation of the protein is believed to be important for protein-protein interactions [175], although proteolysis and methylation may not be essential for the function of some geranylgeranylated proteins [176]. Prenylated proteins which contain an additional cysteine near the C-terminus may also be further modified at the Golgi by a protein acyltransferase (PAT), which catalyses the addition of a palmitoyl group onto the cysteine [177]. Palmitoylation can provide further regulation of protein membrane localisation [178]. Many members of the Rab family lack the CAAX motif, but instead possess a CC or CXC sequence [179]. A Rab escort protein (REP) binds to the Rab protein through these motifs and presents the protein to geranylgeranyltransferase-II (Rab geranylgeranyltransferase, GGT2) [179]. This GGTase transfers two geranylgeranyl groups to the cysteine residues of the Rab protein and this dual prenylation has been shown to be essential for targeting to specific membranes [180]. Guanine nucleotide exchange factors (GEFs) and GTPase activating proteins (GAPs) are involved in cycling prenylated proteins between active and inactive states, resulting in the transduction of a signal to downstream effectors. Guanine nucleotide dissociation inhibitors (GDIs) bind to prenylated inactive proteins, and function to regulate their transport to, or extraction from, membrane compartments [181]. Once at the required destination, GDI displacement factors (GDFs) catalyse the dissociation of the prenylated proteins from GDIs, and the subsequent delivery of the protein to the membrane [181]. Many prenylated proteins are involved in tumorigenesis, including cancer cell proliferation, apoptosis, angiogenesis and metastasis [173].

1.3.3.2 Prenylated Proteins Involved in Cancer Development

Several protein families, particularly small GTPases, are known to undergo prenylation. Statins may exert their anti-cancer activity by modifying the prenylation of these proteins and consequently, their subcellular targeting.

Ras GTPases

The Ras subfamily of GTPases has 21 members, and of these, harvey rat sarcoma viral oncogene homolog (H-Ras), K-Ras and N-Ras have been found to be mutated in human cancers [182]. H-Ras is farnesylated, whereas K-Ras and N-Ras can be both farnesylated and geranylgeranylated and this is critical for localisation to the cell membrane and interactions with downstream signalling molecules (e.g. Raf-1) [183]. Both K-Ras and N-Ras have been shown to be overexpressed in ovarian cancers as previously described [54, 56]. Oncogenic Ras activates downstream signalling pathways (e.g. Raf/Mek/Erk and PI3K pathways) resulting in the uncontrolled growth, proliferation and survival of cancer cells [182].

Rho GTPases

The Rho family of GTPases belongs to the Ras superfamily and consists of around 20 GTP-binding proteins, including RhoA, RhoB, RhoC, Rac1 and Cdc42. RhoA, RhoC, Rac1 and Cdc42 are exclusively geranylgeranylated [184-186], and RhoB is either geranylgeranylated or farnesylated [186]. Rho GTPases have been shown to promote cancer cell survival in some cell types [187]. Correspondingly, RhoA, Cdc42 and Rac1 stimulate cell cycle progression and Ras-induced transformation [188, 189]. Rho GTPases have also been reported to regulate processes during angiogenesis [190] and cell migration, including the formation of membrane profusions [191], focal adhesions and stress fibres, cell contraction and rear detachment [192]. Furthermore,

increased RhoA and RhoC have been associated with the progression of ovarian cancer [193].

Rheb GTPases

The Rheb GTPase is also part of the Ras superfamily and its function has been associated with cell growth, the cell cycle, autophagy and amino acid uptake [194]. Rheb1 and Rheb2 are farnesylated and this is essential for localisation of Rheb to endomembranes [195]. Rheb is commonly overexpressed in human cancers including ovarian cancer, and may mediate cancer cell growth and cell cycle progression by binding and activating the Mammalian Target of Rapamycin (mTOR) functional complex, mTORC1 [56, 196, 197].

Rab GTPases

There are more than 60 Rab GTPases which have a range of different functions focussed on intracellular trafficking, including the regulation of protein secretion, endocytosis, recycling and degradation [198]. Most Rab GTPases are geranylgeranylated by GGT2, and this is required for Rab localisation and function [180]. Rab25 was found to be overexpressed in ovarian cancer where it correlated with poor survival [199]. Rab25 may promote cancer cell migration and invasion, thereby contributing to tumour aggressiveness and metastasis [200]. In contrast, a recent genomic analysis of almost 500 patients with HGSC reported that Rab25 was epigenetically silenced in a subset of HGSC [56]. This suggests that Rab25 may have different effects depending on the cellular context of the tumour, where it may function as an oncogene or a tumour suppressor. Rab GTPases have also been shown to contribute to tumour-stromal cell communication and cell cycle progression in other cancer types (reviewed by [198]).

Ras-like (Ral) GTPases

Ral GTPases are also members of the Ras superfamily and consist of RalA and RalB isoforms [201]. Both RalA and RalB require geranylgeranylation for membrane association and function [201, 202]. The Ral GTPases appear to have collaborative functions in tumorigenesis as RalB was shown to be critical for tumour survival and RalA was required for the anchorage-independent growth of cancer cells [203]. RalA activity was found to be increased in ovarian cancer tumours [204]. Subsequent depletion of RalA inhibited ovarian cancer cell growth and invasion [204].

Protein tyrosine phosphatases

The 4a-family of protein tyrosine phosphatases (PTPases) comprise of PR-1, PR-2 and PR-3, which are farnesylated or geranylgeranylated *in vivo* [205]. Little is known about the function of the 4a-family of PTPases, although PR-3 has recently been linked to tumour invasiveness and poor prognosis [206]. Furthermore, ovarian cancer effusions were found to express high levels of PR-1, PR-2, PR-3, although these were not associated with tumorigenesis, suggesting that these PTPases may have different cellular functions in ovarian cancer [207].

Lamins

Lamins are nuclear membrane proteins which are divided into A and B types based upon structural and protein features [208]. A-type and B-type lamins are farnesylated and localised to the nuclear envelope, however farnesylation may not be required for function, as the farnesyl group along with 18 amino acids is proteolytically removed from lamin A in the nuclear envelope [209]. Lamins have been associated with a range of nuclear functions including chromatin regulation, transcription, DNA replication and DNA repair, although their role in cancer is less clear [208]. Altered

lamin expression has been reported in a number of cancers with conflicting results (reviewed by [208]). In ovarian cancer, expression of A-type lamins was upregulated whereas expression of lamin C was reduced [210, 211]. These changes in lamin expression could control cancer cell growth, epithelial-to-mesenchymal transition and migration, although further research is required to confirm this [211, 212].

CENP-E and CENP-F

CENP-E and CENP-F are centromere proteins involved in chromosomal capture and alignment during mitosis [213]. Farnesylation of CENP-E and CENP-F is critical for their functionality in maintaining chromosomal alignment during metaphase and for G_2/M progression, thereby enabling cell cycle progression in cancer cells [214]. Inhibition of the farnesylation of CENP-E and CENP-F using the FT inhibitor, lonafarnib, resulted in mitotic chromosomal alignment defects in cell lines and human tumours [213].

1.3.4 Molecular Mechanisms of Tumorigenesis and the Cytotoxic Activity of Statins

1.3.4.1 The Cell Cycle and Cancer Progression

The cell cycle consists of four processes: cell growth, replication of DNA, transfer of duplicated chromosomes to daughter cells and cell division. Each cell cycle phase is regulated by various proto-oncogenes and tumour suppressors to allow the repair of genetic damage and to prevent tumorigenesis (figure 1.9). Cyclin dependent kinases (CDK) and cyclins form complexes which are involved in the cell cycle machinery during various stages of the cell cycle. During the first gap phase (G_1), the cell

contains two copies of each chromosome. CyclinC/CDK3, CyclinD/CDK4/6, and CyclinE/CDK2 complexes control progression through G_1 phase of the cell cycle [215]. Hypophosphorylated Rb proteins negatively regulate G_1 phase progression by binding to transcription factors including E2F and inhibiting the expression of genes which encode proteins required for cell cycle progression [215]. Furthermore, CDK inhibitors (CDKI) including p15, p16, p17, p19, p21 and p27 inhibit the phosphorylation and activation of cyclin/CDK complexes [215]. Rb is phosphorylated by CyclinD/CDK4/6 to allow the release of the transcription factors and subsequent G_1 transition [215]. The cell then enters synthesis or S-phase, where CyclinA/CDK2 controls DNA replication and maintains Rb phosphorylation. The cell then enters a second gap phase (G_2) which functions to prevent the cell from undergoing mitosis with DNA damage. Here, cyclin B interacts with CDK1, and the phosphatase Cdc25 is maintained in an inactive state, thereby allowing G_2 phase transition to mitosis (M). However, in response to DNA damage or stalled replication, Cdc25 is hyperphosphorylated which results in the ubiquitylation of Cdc25 and cell cycle arrest [216]. Aberrations in oncogenes (e.g. cyclins or CDKs) or tumour suppressor genes (e.g. *Rb1* or CDKIs) have been associated with tumorigenesis. In HGSC, the genes encoding p16 and Rb were inactivated in 32% and 10% of cases respectively [56]. Furthermore, genes encoding cyclin D1, cyclin D2 and cyclin E1 were all amplified in 4-20% of HGSC cases, likely contributing to the development of some ovarian cancers [56].

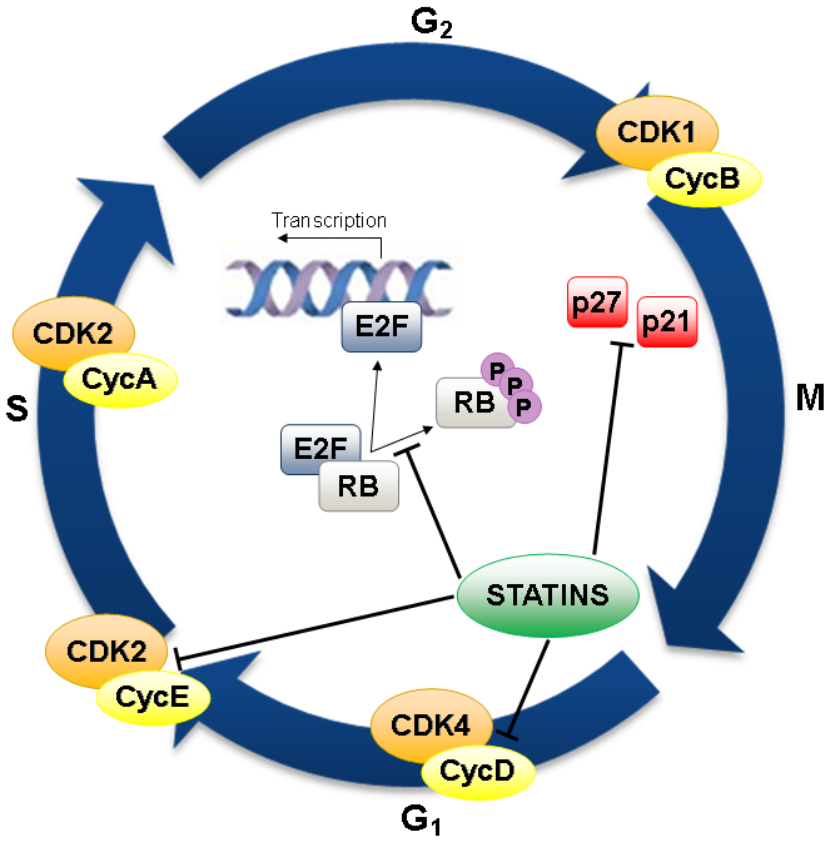

Figure 1.9: The cell cycle involving the first gap phase (G_1), DNA synthesis phase (S), second gap phase (G_2) and mitosis phase (M). Statins primarily inhibit cell cycle mediators involved in G_1 progression.

1.3.4.2 The Cell Cycle and Statins

Statins inhibit the proliferation of many cancer cell lines by causing G_0/G_1 cell cycle arrest [217-233]. Furthermore, statins have also been shown to inhibit Rb phosphorylation [220, 232], and this, in combination with a reduction in the expression of the E2F transcription factor [234], may contribute to the inhibition of G_1 progression. Others have also reported S-phase cell cycle arrest in multiple myeloma cells [235], and G_2/M cell cycle arrest in Namalwa Burkitt lymphoma cells and MCF-7 breast cancer cells [219, 236]. These effects on cell division may be mediated through the inhibition of RhoA-dependent cell signalling [226, 237, 238], resulting in the

downregulation of the cell cycle mediators cyclin D1, cyclin E, CDK1, CDK2 and CDK4, and augmentation of the CDK inhibitors, p19, p21 and p27 (figure 1.9) [220, 223, 224, 226, 229-232, 235, 236, 238-241].

1.3.4.3 Angiogenesis and Statins

During VEGF-induced angiogenesis, activation of VEGFR leads to the release of endothelial nitric oxide synthase (eNOS) from caveolae in the plasma membrane [242]. The subsequent liberation of nitric oxide (NO) promotes endothelial proliferation, migration and vascular permeability [242]. High micromolar concentrations of statins have been reported to inhibit angiogenesis in cancer cells and endothelial cells through the attenuation of pro-angiogenic factors including VEGF, urokinase plasminogen activator, IL-8, angiopoietin 2 and binding immunoglobulin protein [240, 243-249]. Statins have also contributed to the inhibition of endothelial cell proliferation [250], prevention of endothelial cell adhesion to the extracellular matrix (ECM) [243], and induction of endothelial apoptosis [250, 251]. Furthermore, these effects were mediated through inhibition of the mevalonate pathway [245]. Conversely, low nanomolar concentrations of statins have been shown to stimulate angiogenesis, possibly through the activation of Akt [252], eNOS activation [253], and the release of NO [254].

1.3.4.4 Metastasis and Statins

Cancer cell migration into the ECM is a multistep process involving Rac and Rho GTPases. Cell adhesion molecules (CAMs) including cadherins, integrins and selectins regulate cell-cell or cell-matrix adhesion [255]. Protrusion of the leading edge involves actin polymerisation which is stimulated by Rac GTPases [256]. Integrins in the extending lamellipodia then make contact with ECM ligands and collect in the cell

membrane [256]. Following attachment to the ECM, Rac GTPases regulate the formation of a focal complex assembly containing focal adhesion kinase, the actin binding compounds, vinculin, paxillin and α-actinin, and other regulatory molecules [256]. Furthermore, Rho GTPases regulate the secretion and activation of proteases (e.g. matrix metalloproteinases (MMP)) which degrade the ECM in order to enable cells to move through the matrix [256]. Contraction of the cell body requires the generation of an actomyosin contraction, which is controlled by Rho and the Rho-associated serine/threonine kinase (ROCK) [256]. Finally detachment of the trailing edge occurs after actomyosin contraction, where the protease calpain cleaves focal complex components, thereby enabling cell movement [256]. Statins have been shown to inhibit cancer cell migration and invasion, possibly through inhibition of the geranylgeranylation of Rho GTPases involved in cell motility [238, 257-260]. Statin-induced RhoA delocalisation from the cell membrane resulted in the disorganisation of actin fibres, loss of focal adhesion sites and inactivation of NF-κB, which decreased the expression of the proteases MMP2, MMP3, MMP9 and urokinase [224, 240, 258, 261, 262]. Furthermore, statins have also been demonstrated to inhibit CAMs including α-integrins, β-integrins, E-selectin, ICAM-1 and decrease the expression of CD44, thus contributing to the loss of cell adhesion [240, 258, 263-265]. Statins have also been shown to decrease ovarian clear cell cancer cell invasion by reducing the expression of osteopontin, a protein which regulates cell motility, invasiveness and growth of various cancers [266]. This was further confirmed in xenograft studies, where simvastatin decreased osteopontin expression, significantly delayed tumour growth and increased survival compared to control groups [267]. Furthermore, Wagner and colleagues reported that simvastatin inhibited ovarian cancer cell adhesion to mesothelial cells, a process involved in cancer metastasis to the surface of the peritoneum [268]. This was mediated through decreased expression of both

VCAM-1 on mesothelial cells and integrin α4β1 on ovarian cancer cells following simvastatin treatment [268]. Taken together, statins inhibit cancer cell migration, attachment to the ECM and invasion to the basement membrane, which contributes to a reduction in tumour metastasis.

1.3.4.5 The Autophagy Pathway

Autophagy is derived from two Latin words that mean “self” and “eating”. It is a highly regulated and evolutionarily conserved process amongst eukaryotic organisms, which is involved in the degradation of cellular organelles and proteins during nutrient starvation and metabolic stress (figure 1.10) [269-272]. Autophagy can be divided into six stages: omegasome formation, phagophore initiation and elongation, autophagosome formation, autophagosome-lysosome fusion and degradation as detailed below.

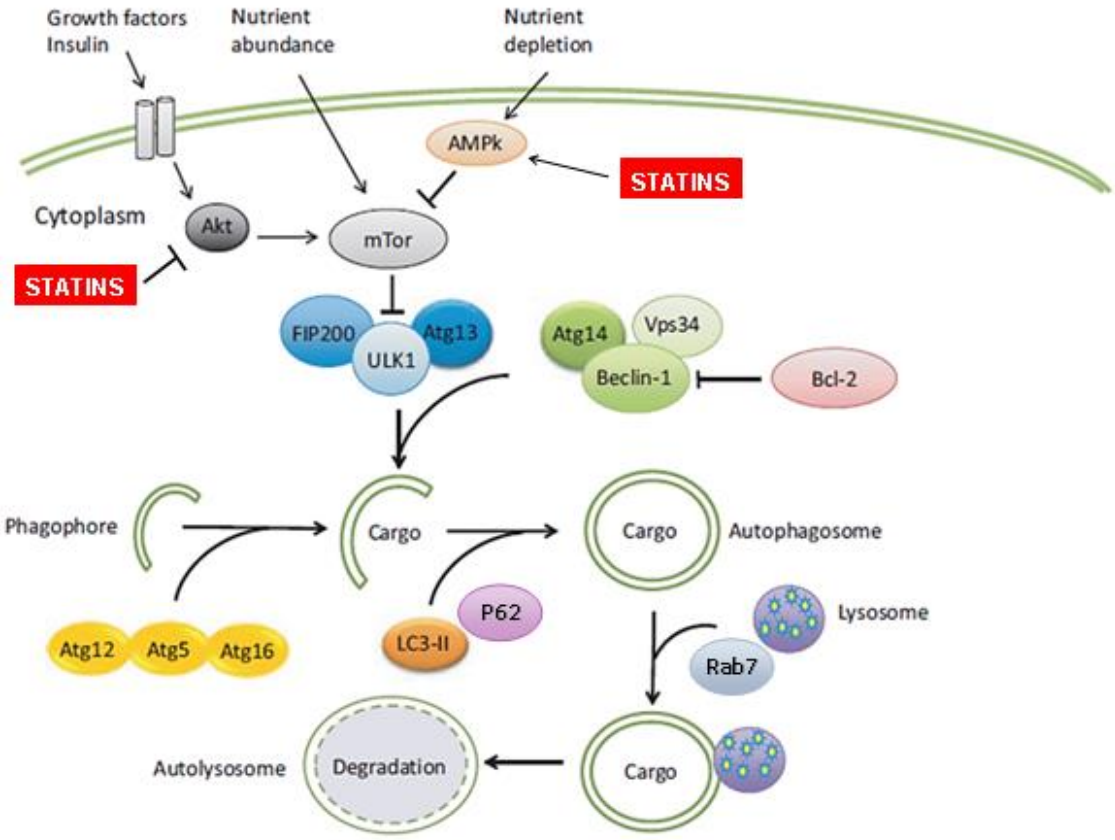

Figure 1.10: The autophagy pathway in mammalian cells. Nutrient depletion results in the activation of autophagy and subsequent formation of autophagosomes containing damaged organelles or cellular debris. Autophagosomes fuse with lysosomes, and lysosomal enzymes function to degrade damaged cargo. Statins have been reported to induce autophagy through the activation of AMP-activated protein kinase (AMPK) and the downregulation of Akt (Modified from [273]).

Omegasome formation and phagophore initiation

The autophagosomal membrane originates from cup-shaped protrusions from the endoplasmic reticulum, known as omegasomes. The Beclin1-Vps34-Atg14 PI3K complex regulates the formation of the omegasome during the initiation of autophagy [274]. Following this, an isolation membrane (phagophore) is formed on the inside of

the omegasome. The development of the initial phagophore membrane is dependent on the Beclin1-Vps34-Atg14 complex. The class III PI3K catalytic subunit Vps34 generates phosphatidylinositol 3-phosphate (PI3P) which is anchored in place by phospholipid-binding effectors (WIPI-1/2) during autophagosome formation [275]. PI3P functions to recruit other autophagy-related gene (Atg) products that are important in autophagosome formation [276].

Phagophore elongation and autophagosome formation

The Beclin1-Vps34-Atg14 complex recruits the Atg12-Atg5-Atg16 complex to the phagophore [277]. The Atg12-Atg5-Atg16 complex along with Rab32 and Rab33B causes the elongation of the isolation membrane in order to engulf damaged contents [278-280]. This complex also promotes the recruitment of cytosolic microtubule-associated protein light chain 3 (LC3-I), and AtgL1 functions to transport LC3-I to the phagophore [277]. Atg7, Atg3 and the Atg12-Atg5-Atg16 complex are involved in the lipidation of LC3-I, where the C-terminus of LC3-I is conjugated to phosphatidylethanolamine (PE) [281]. PE is a component of phospholipid bilayers, allowing the lipidated LC3-II to be localised to the autophagosomal membrane [277]. Following autophagosome formation, the Atg12-Atg5-Atg16 complex dissociates from the phagophore, Atg proteins are recycled in the cytosol and LC3-II remains bound to the inner autophagosome membrane [276, 282]. LC3-II also binds to adapter proteins including p62, neighbour of BRCA1 gene 1 (NBR1) and calcium binding and coiled-coil domain 2 (NDP52), which recruit ubiquitinated proteins to the autophagosome to enable their degradation [283]. Both p62 and NBR1 may localise to the autophagosome formation site independently of LC3 localisation and are subsequently degraded during autophagy [284, 285].

Autophagosome-lysosome fusion and degradation

The fusion of autophagosomes and lysosomes results in the formation of the autolysosome. This late stage process is positively regulated by the Beclin1-Vps34-UVRAG (UV irradiation resistance-associated gene) complex [286, 287]. UVRAG activates the GEF for Rab7, Vps34/HOPS (homotypic fusion and vacuole protein sorting) complex [288]. The GEF then promotes the activation of Rab7, which results in autophagosome tethering, docking, and fusion to lysosomes [289, 290]. Run domain protein as Beclin 1 interacting and cysteine-rich containing protein (Rubicon) negatively regulates autophagosome maturation by interacting with Vps34 via its RUN domain, which serves to inhibit PI3K activity [291]. Other proteins may also be involved in the regulation of autophagosome-lysosome fusion including the endosomal sorting complex required for transport (ESCRT III), hepatocyte growth factor-regulated tyrosine kinase substrate (Hrs), the lysosomal-associated membrane proteins: LAMP1 and LAMP2, and the soluble N-ethylmaleimide-sensitive factor attachment protein receptors: VAMP3 and VAMP7 [292, 293]. Autophagosomes move bidirectionally along microtubules, and therefore, fusion with lysosomes may also be dependent on microtubules. Two types of fusion have been proposed: one where the autophagosome and lysosome completely fuse, and a second where material is transferred from the autophagosome to the lysosome whilst keeping both vesicles intact [294]. Following autolysosomal formation, the contents of the autophagosome are degraded by lysosomal hydrolases including cathepsins, glycolytic enzymes and lipases. The vacuolar ATPases (V-ATPases) function as a source of H^+ in order to maintain a low pH for the activity of lysosomal enzymes. LC3-II localised to the inner autophagosome is also degraded by cathepsins during this process, whereas LC3-II located on the outer face of the autophagosome is converted back into LC3-I and recycled [295]. The metabolites resulting from the digestion of autophagosome

contents are released into the cytosol to enable them to be used for energy and precursors for other anabolic processes [296]. Following this, the autolysosome is elongated to form the protolysosome, which matures and reforms the lysosome [297].

1.3.4.6 Autophagy and Ovarian Cancer

Autophagy is increasingly considered to be mechanism of cancer cell survival during conditions of metabolic stress. This is supported by the fact that cancer cells can withstand a number of different stress conditions including glucose starvation, growth-factor withdrawal, hypoxia and cytotoxic agents [298, 299]. In ovarian cancer, LC3 was upregulated in some epithelial subtypes [300], whereas both aplasia ras homolog member I (ARHI) [301, 302] and several microRNAs involved in inhibiting the expression of Beclin 1 [303] were downregulated. Furthermore, lysophosphatidic acid (LPA) secreted by ovarian cancer cells was shown to increase IL-6, which induces autophagy in cancer cells and correlates with a poor prognosis [304, 305]. It is believed that autophagy can contribute to anti-cancer therapy resistance by facilitating the removal of damaged proteins and organelles for energy production and survival [298]. Indeed, when drug-induced autophagy was inhibited in ovarian cancer cells, the cytotoxic effects of the drugs were enhanced [306, 307].

Autophagy was previously proposed as a mechanism of growth inhibition and non-apoptotic cell death in cancer cells [308, 309]. It was thought that sustained autophagy may exceed the capacity of the cell, leading to the production of a large number of autophagosomes and extensive degradation of cytoplasmic proteins and organelles. The anti-cancer agent, dasatinib inhibited the growth of ovarian cancer cells through an induction in autophagy [310]. Suberoylanilide hydroxamic acid (SAHA) was demonstrated to potentiate decitabine-induced autophagy by increasing the

expression of a positive regulator of autophagy, ARHI [311]. Furthermore, a combination of two autophagy inducers, Rad001 and arsenic trioxide, synergistically inhibited the growth of ovarian cancer cells [312]. A number of studies have reported that inhibition of autophagy promotes ovarian tumour cell survival. Reductions in Beclin 1 and LC3 expression [313, 314], p53 mutations [315], and an upregulation of PI3K/Akt/mTOR signalling [316] in ovarian cancer cells can all contribute to an inhibition of autophagy and the development of advanced ovarian cancer. Collectively, these studies demonstrate that whilst autophagy has an essential role in promoting the survival of ovarian cancer cells, the precise function it fulfils may vary depending on a number of factors including the type and stage of cancer, genetic aberrations, and drug treatments.

1.3.4.7 Autophagy and Statins

Statins have been shown to induce autophagy in a range of different cancers including glioma [317], prostate [318], liver [319], rhabdomyosarcoma [320], mesothelioma cancer cells [321], and malignant peripheral nerve sheath cancer cells [322]. Furthermore, this was dependent on the inhibition of HMGCR in the mevalonate pathway [320], which resulted in the activation of AMP-activated protein kinase (AMPK), and the inhibition of Akt and the negative regulator of autophagy, mTOR (figure 1.10) [317, 319, 323]. Statins may also activate autophagy through extracellular signal-regulated kinase (Erk) and c-Jun N-terminal Kinase (JNK) signalling as a result of the production of reactive oxygen species (ROS), although the molecular mechanism is not fully understood [324]. Current evidence suggests that statin-induced autophagy is a mechanism of cell survival as inhibition of statin-induced autophagy using pharmacological agents (e.g. bafilomycin or 3-methyladenine) or siRNA against Atg5 resulted in a potentiation of apoptotic cell death [317, 319, 325,

326]. A limited number of studies have also suggested that statins may also inhibit autophagy. In human papillary thyroid cancer cells, rosuvastatin decreased the percentage of cells undergoing autophagy [227]. Furthermore, Wojkowiak and colleagues reported that dual exposure of malignant peripheral nerve sheath tumour cells to lovastatin and a FT inhibitor aborted autophagy and induced non-apoptotoic cell death [327]. Taken together, statins may induce autophagy in cancer cells as a mechanism of cell survival, although inhibition of the autophagy pathway cannot be excluded.

1.3.4.8 The Apoptosis Pathways

Apoptosis is a morphologically distinct form of programmed cell death which was first described more than 40 years ago [328]. There are currently two main apoptotic pathways recognized: the extrinsic (death receptor) pathway and the intrinsic (mitochondrial) pathway [329] (figure 1.11).

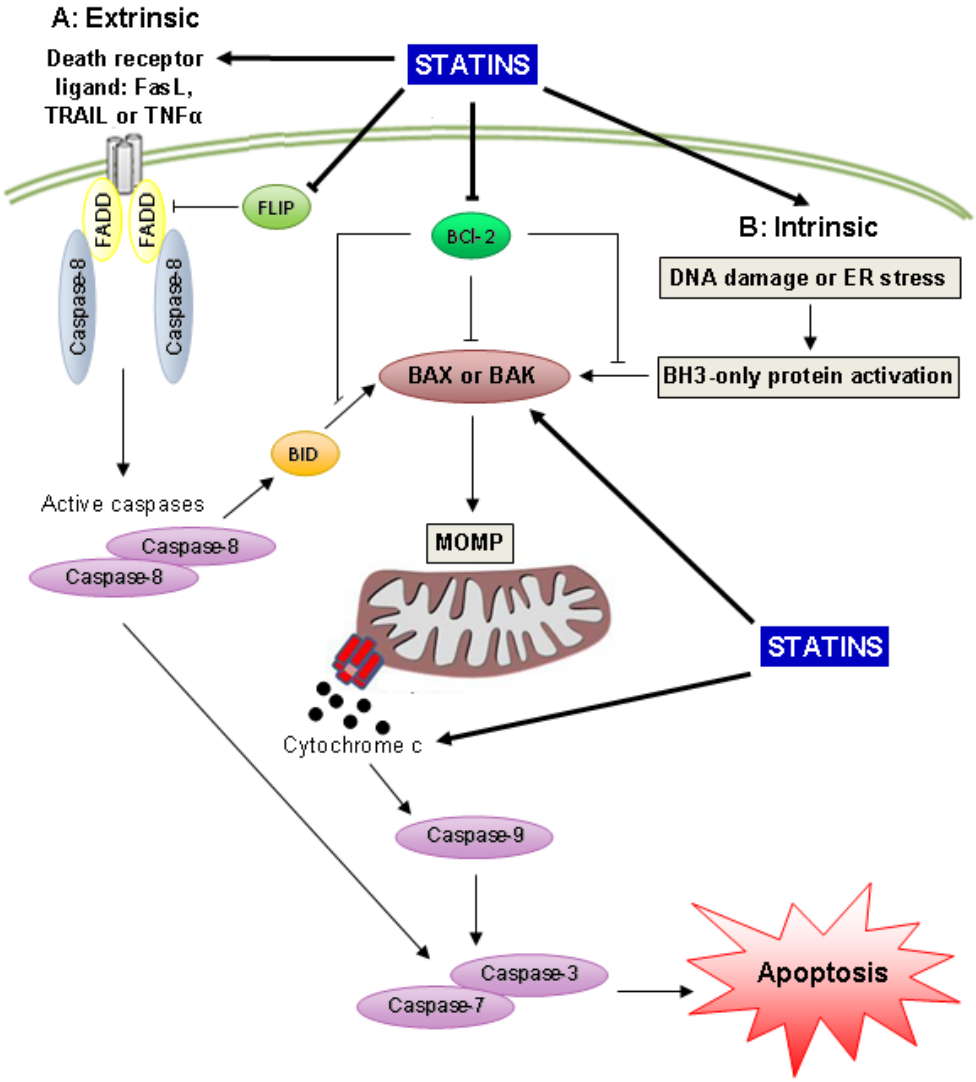

Figure 1.11: The extrinsic and intrinsic apoptotic pathways. The extrinsic pathway is initiated by ligands binding to the death receptor which results in the activation of caspase-8, and caspases 3 and 7, leading to apoptosis (A). The intrinsic pathway is stimulated by DNA damage or endoplasmic reticulum (ER) stress, resulting in the activation of Bax and Bak. Subsequent mitochondrial outer membrane permeabilization (MOMP) leads to the release of cytochrome c, activation of caspase-9, followed by caspases 3 and 7, and apoptosis (B). Statins have been reported to activate the extrinsic and intrinsic pathways.

Extrinsic apoptosis pathway

The extrinsic apoptosis pathway is activated by the binding of a ligand (e.g. fatty acid synthetase ligand (FasL), TNF-α or TNF-related apoptosis-inducing ligand (TRAIL)) to the corresponding death receptor in the cell membrane. This leads to the recruitment of a cytoplasmic adapter protein such as FAS-associated death domain protein (FADD) to the receptor death domain, which associates with procaspase-8 though dimerization of the death domain. The resulting death-inducing signalling complex (DISC) induces the auto-catalytic activation of procaspase-8. Subsequently, caspase-8 triggers the execution phase of apoptosis.

Intrinsic apoptosis pathway

The intrinsic apoptosis pathway is regulated by a range of non-receptor mediated stimuli which may activate or inhibit apoptosis. The activation of pro-apoptotic proteins including BH3-only proteins (e.g. Bid), and the effectors, Bax and Bak results in the loss of the mitochondrial transmembrane potential, mitochondrial outer membrane permeabilization (MOMP), and the release of pro-apoptotic proteins including cytochrome c. Cytochrome c binds to and activates procaspase-9, leading to the formation of an apoptosome and the activation of caspase-9.

Execution pathway

The extrinsic and intrinsic apoptosis pathways both result in the execution pathway, which involves the activation of execution caspases (caspase-3, caspase-6 and caspase-7) by the initiator caspases (caspase-8, caspase-9 and caspase-10). Execution caspases activate cytoplasmic endonuclease and proteases to degrade nuclear material, and cleave various substrates including cytokeratins and PARP. Caspase-3 activates Caspase Activated DNAse (CAD) and induces cytoskeletal

reorganisation and cellular fragmentation to form apoptotic bodies. Apoptotic cells are subsequently recognised and taken up by phagocytes for disposal.

1.3.4.9 Apoptosis and Statins

Statins have been demonstrated to induce apoptosis, primarily through the mitochondrial pathway, in many different cancers including breast [219, 222, 254, 330], lung [239, 331, 332], prostate [232, 333], liver [221, 334], colon [335, 336], ovarian [249, 337, 338], bladder [339], thyroid [227, 340, 341], glioma [342-344], lymphoma [220, 236, 345], myeloma [235], osteosarcoma [346], head and neck squamous cell [347], and medulloblastoma [225]. These pro-apoptotic effects were mediated through the depletion of geranylgeranyl diphosphate in the mevalonate pathway [337, 348-350]. Correspondingly, a number of studies have demonstrated that statins inhibit the geranylgeranylation of RhoA, Rac1 and Cdc42, and subsequent translocation to the plasma membrane [232, 341, 351]. However, instead of the loss of prenylation preventing the functions of these Rho GTPases, Zhu and colleagues have recently discovered that simvastatin decreased the binding of Rho GTPases with the RhoA GDIα, resulting in an increase in the GTP-bound forms of RhoA, Rac1 and Cdc42 [352]. Unprenylated yet activated RhoA and Rac1 maintained at least some of their functions, as nicotinamide adenine dinucleotide phosphate (NADPH) oxidase was activated, resulting in the generation of ROS following statin exposure [352]. Statin-induced ROS can lead to the activation of JNK and p38 MAPK signalling and this can contribute to apoptosis [340, 350, 352]. These results are supported by previous research where statins induced a paradoxical increase in unprenylated RhoA, Rac1 and Cdc42 together with an activation of JNK [220, 338, 353]. JNK stimulates Bak activation and inhibits Bcl-2, thereby stimulating pro-apoptotic signalling. Nevertheless, there are several examples where Rho GTPase signalling

may be impaired by statins. Rho GTPases including Rac can activate the transcription factor NF-κB following PI3K stimulation [354-356], and this results in the expression of anti-apoptotic mediators including Bcl-2, FLICE-like inhibitory protein (FLIP) and XIAP. However, statins reduced NF-κB levels and this is likely to account for the decrease in FLIP and Bcl-2 expression also observed after statin exposure [231, 240, 334, 346, 350, 357-359]. Furthermore, Rho and Rac have also been shown to interact directly with PI3K and stimulate Akt, which promotes cell survival independent of NF-κB activation [360]. Statins attenuated the activation of PI3K and Akt, possibly through the inhibition of Ras and Rho prenylation [220, 249, 335], leading to an increase in Bax phosphorylation [334, 350, 361], and an upregulation of Bim expression [338, 349]. Statin-induced cytochrome c release from the mitochondria stimulated the activation of the initiator (caspases 8 and 9) and execution (caspases 3 and 7) caspases, PARP cleavage and nuclear degradation, resulting in cell death [220-222, 239, 334, 337, 341, 345, 350, 362]. Interestingly, activation of the extrinsic pathway appears to be tumour specific. Goc and colleagues reported that simvastatin induced the activation of caspase-8 in the extrinsic pathway through upregulation of TNF-α and FasL in prostate cancer cells, whereas in myeloma cells, statin-induced caspase-8 activation acted as an amplifier of execution caspases in the intrinsic apoptosis pathway [351, 363, 364]. Furthermore, others have suggested that statins may trigger an ‘autocrine’ suicide factor, which may serve to amplify apoptotic signalling through the extrinsic apoptosis pathway [365]. Taken together, statins induce apoptosis by increasing the expression and activation of pro-apoptotic proteins (e.g. Bax and Bim) whilst inhibiting anti-apoptotic components (e.g. Bcl-2, Bcl-X_L, FLIP and survivin), resulting in the loss of the mitochondrial membrane potential [219, 221, 222, 249, 350, 351, 362], and the release of cytochrome c and smac/DIABLO [239, 333, 334, 337,

341, 345, 351], although in some cases, the extrinsic apoptosis pathway may also be activated.

1.3.5 The Potential of Statins for Cancer Prevention or Treatment

1.3.5.1 Statins and Cancer Incidence

Statins were first associated with an increased risk of cancer in animal studies, where lovastatin at high doses increased the incidence of liver and lung cancers [366]. Statin-induced carcinogenicity was restricted to pre-clinical studies which utilised much higher doses of statins than those used in the clinic [367]. In contrast, the administration of lower statin concentrations inhibited the development of various cancers including liver [368], colon [369], thyroid [370], and breast [371-373] cancers in animal studies.

Several meta-analyses have analysed the cancer risk associated with statin administration in human populations with conflicting results. Six meta-analyses found no association between statin use and the risk of any cancer (risk ratio (RR) values ranged from 0.96 – 1.00 [374-379]. Moreover, meta-analyses evaluating the effect of statins on specific cancer risk reported that statins had no significant association with breast [376, 378, 380, 381], lung [378, 382, 383], colorectal [376, 384], melanoma or non-melanoma [376, 385, 386], bladder [387], renal [388], and pancreatic [389, 390] cancers. Conversely, four analyses reported a significant decrease in the risk of hepatocellular cancer in patients treated with statins (RR: 0.58 – 0.64; [378, 391-394]. This association was observed in Asian and Western populations, and was not

affected by the type of statin (hydrophobic versus hydrophilic) or the duration of statin treatment [391-393]. Statin treatment also reduced the risk of gastric cancer (RR: 0.56 – 0.59 [378, 395]) and haematological malignancies (RR: 0.74 – 0.81 [378, 396]). In general, statin use had no effect on the risk of prostate cancer [376, 378, 397]. However, several recent meta-analyses reported that statin treatment reduced the risk of advanced prostate cancer by 20% (RR: 0.8, $P<0.001$ [398], and improved recurrence-free survival in prostate cancer patients treated with radiotherapy [399].

In ovarian cancer, several early studies including a randomised control trial and meta-analysis indicated that standard doses of statins used for the treatment of hypercholesterolemia were not associated with a reduction in the development of ovarian cancer or any gynaecological cancer [378, 400, 401]. Despite this, Elmore and colleagues reported that in patients with advanced stage or invasive epithelial ovarian cancer, statin treatment significantly improved PFS (24 months versus 16 months, $P = 0.007$) and OS compared to statin non-users (62 months versus 46 months, $P = 0.04$ [402]). This was supported by a recent case-control study, which demonstrated that statins were associated with a significantly decreased risk of ovarian cancer and an improved survival after diagnosis of ovarian cancer ($P = 0.021$ [403]). Interestingly, whilst there were no overall differences in PFS or disease-specific survival (DSS) in ovarian cancer patients taking statins compared to non-statin use, statins appeared to improve PFS and DSS specifically in the non-serous papillary subtypes [404]. Taken together, a recent meta-analysis incorporating many of these studies reported that statin treatment modestly protected against ovarian cancer (RR: 0.79), and long term statin use (>5 years) significantly reduced the risk of ovarian cancer (RR: 0.48 [405]. These recent results suggest that not only may statins reduce the risk of developing

ovarian cancer, but they may also contribute to improved survival in ovarian cancer patients.

1.3.5.2 Statins in Clinical Trials for Cancer Treatment

To date, there have been a small number of phase I/II clinical trials evaluating the use of statins for the treatment of a range of different cancers. These studies have evaluated statins both as single agents and in combinations with standard chemotherapeutic options. Furthermore, a limited number of studies have evaluated statins at the maximum tolerated dose for up to 7 days.

Several clinical trials have evaluated statins in combination with several chemotherapeutic regimens with the aim of establishing a toxicity profile to inform future studies. Simvastatin (40 mg/day) plus irinotecan, 5-fluorouracil, and leucovorin (FOLFIRI) reported a median survival of 21.8 months in metastatic colorectal patients, along with no additional adverse effects as a result of simvastatin addition [406]. This was supported by a phase I trial in acute myeloid leukemia patients where pravastatin (40-1680 mg/day) in combination with idarubicin and cytarabine did not increase the duration of neutropenia or thrombocytopenia, and the overall toxicity profile was unchanged compared to chemotherapy alone [407]. However, a recent phase I/II clinical trial combining cyclosporin A, pravastatin, etoposide and mitoxantrone in an attempt to circumvent drug resistance in acute myeloid leukemia was terminated early due to unacceptable toxicity [408]. This highlights the importance of conducting a small phase I study and carefully assessing the risk-benefit ratio when evaluating new combinations.

In non-small lung cancer (NSCLC), several studies by Han and colleagues found that the addition of a standard dose of simvastatin (40 mg/daily) to chemotherapy (irinotecan and cisplatin or gefitinib) did not significantly improve the time to progression or the one-year survival rate [409, 410]. Despite this, patients receiving gefitinib and simvastatin had a longer PFS compared to those receiving gefitinib alone (3.6 months versus 1.7 months, P = 0.027) in a subgroup of patients with wild-type epidermal growth factor receptor (EGFR) non-adenocarcinomas [409]. However, the former results were supported by a recent study in advanced pancreatic cancer patients, where simvastatin (40mg/daily) in combination with gefitinib afforded no additional clinical benefit compared to gemcitabine alone [411]. Standard doses of pravastatin (20-40 mg/daily) in patients with hepatocellular cancer significantly improved PFS in patients treated with transarterial chemoembolization (TACE) (18 months versus 9 months, P = 0.006 [412]; 20.9 months versus 12 months, P = 0.003 [413]). Conversely, pravastatin (40-80mg/daily) alone did not improve the median OS compared to patients treated with TACE [414]. Furthermore, no improvement in outcome was observed in advanced gastric cancer patients treated with pravastatin 40 mg/daily in combination with epirubicin, cisplatin and capecitabine [415].

High-dose lovastatin has been evaluated in patients with squamous cell carcinoma of the head and neck or of the cervix. This phase I study found that patients tolerated doses of up to 7.5 mg/kg/day and approximately a quarter had disease stabilisation [416]. These results were in contrast to a previous study where high lovastatin doses of 35 mg/kg/day were administered to patients with advanced gastric cancer for 7 consecutive days (repeated every 28 days) and no response was observed [417]. Furthermore, simvastatin (15 mg/kg/day) in combination with vincristine, adriamycin, and dexamethasone in patients with myeloma was discontinued due to the poor

response as only one patient achieved a partial response [418], although the high dose was well tolerated for 7 days [419]. However, a more recent study in patients with relapsed and refractory multiple myeloma found that thalidomide, dexamethasone and lovastatin (0.5 mg/kg/day) significantly improved PFS compared to patients receiving only thalidomide and dexamethasone (33 months versus 16 months, P = 0.048), with similar side effect profiles in both arms [420]. High-dose fluvastatin (80 mg/day) was shown to reduce tumour proliferation and induce apoptosis in high-grade, stage 0/1 breast cancer [421]. Furthermore, fluvastatin (8 mg/kg/day) on days 1-14 in combination with chemotherapy significantly increased survival, reduced tumour volume and increased quality of life in children with brain stem tumours [422]. However, at standard doses of fluvastatin (40 mg/day) or atorvastatin (20 mg/day) in combination with zoledronate, there was no significant improvement in time to progression compared to results from previous studies in patients with renal-cell carcinoma and bone metastasis [423].

Collectively, the clinical trials evaluating statins at standard doses used for the treatment of high cholesterol had infrequent beneficial effects and a survival benefit has only been demonstrated in two trials in patients with hepatocellular cancer. This may reflect the liver-selective uptake of pravastatin by transporters including OATP1B1, thereby potentially increasing the concentration of pravastatin in contact with the tumour [424]. Despite this poor history of success, the majority of the clinical trials ongoing are evaluating statins at these low concentrations for cancer treatment [425]. Trials utilising higher doses of statins have generated some positive results, and several clinical trials are currently evaluating high doses of statins in combination with standard chemotherapeutic agents for the treatment of leukemia, glioma and lung cancer [425].

1.4 Ovarian Cancer Experimental Models

1.4.1 Ovarian Cancer Cell Lines

Cell lines were historically the most frequently employed tumour models used to evaluate anti-cancer agents in ovarian cancer [426]. Ovarian cancer cell lines can give an insight into the molecular diversity and histology of tumours in the clinic, and cell lines that have been fully identified by molecular profiling are particularly beneficial for the evaluation of anti-cancer therapies which require specific molecular aberrations (e.g. PARP inhibitors and BRCA1/2 mutations) [426]. Furthermore, cell lines are relatively cheap, easy to manipulate and the culture conditions can be controlled. However, cell lines are less heterogeneous populations, and therefore, do not represent the whole tumour. Furthermore, cell lines that have been passaged for a number of years are likely to have undergone significant evolutionary selection, contributing to the inclusion of genomic alterations which are no longer reminiscent of the genetic and pathogenic profile of the original tumour cells [427]. Similarly, the drug resistance of the cell lines may not correspond to that observed in the parent tumour. Ovarian cancer cell lines are frequently grown as a monolayer, which is a flat layer of cells attached to the surface of culture vessels. Monolayers are advantageous for microscopy and other functional assays, however, this two-dimensional (2D) model is generally considered not to be physiologically relevant, and there may be difficulties with translation *in vivo*. This has led to the use of alternative ovarian cancer models, including spheroids and xenografts, to further evaluate anti-cancer agents.

1.4.2 Ovarian Cancer Spheroid Cultures

Ovarian cancer spheroids can be cultured *in vitro* by several methods including the suspension of ovarian cancer cells in a hanging droplet of medium [428]. Ovarian cancer spheroids more accurately represent ovarian tumours as they have been shown to exhibit similar cellular, molecular and biochemical properties compared to tumours *in vivo* [428, 429]. For example, cancer spheroids were found to be considerably less sensitive to chemotherapy compared to monolayer cultures, consistent with the chemoresistance observed in metastatic tumour spheroids [430, 431]. Cancer spheroids also exhibit oxygen/nutrient and proliferation gradients, where central regions may be poorly vascularised, resulting in limited access to essential components required for cell growth and the accumulation of catabolites [432, 433]. Therefore, ovarian cancer spheroid cultures may go some way to creating a three-dimensional (3D) microenvironment which more closely represents ovarian cancer in a clinical setting.

1.4.3 Ovarian Cancer Xenografts

Human ovarian cancer xenografts are used extensively in preclinical drug development and commonly incorporate severe combined immunodeficient (SCID) mice strains deficient in both B and T lymphocytes to prevent cancer rejection [434, 435]. Ovarian cancer cells can be implanted into xenograft models either subcutaneously, intraperitoneally or orthotopically, although accurate quantification of tumour volume can be more readily achieved following subcutaneous implantation [426]. Ovarian cancer xenograft models frequently use the Ovcar-3 cell line as many characteristics of the primary tumour are retained (e.g. ascites formation, tumour

angiogenesis and metastasis), and the histology resembles serous ovarian cancer [427, 436-438]. Ovarian cancer xenografts can be used to assess the cytotoxic activity of drugs, model biomarker responses in tissue or plasma, and determine toxicity *in vivo*. However, immunodeficient mice cannot recapitulate the effects of a functioning immune system on tumour growth, or the interaction between tumour cells and the human microenvironment [426]. Furthermore, there may be significant differences in drug pharmacokinetics in the xenograft compared to human pharmacokinetics, which must be taken into consideration when designing a xenograft study.

CHAPTER 2

AIMS AND OBJECTIVES

The identification of novel drugs which demonstrate activity in chemorefractory or chemoresistant ovarian cancer is a priority in ovarian cancer research, given the poor prognosis and low survival rates affecting many patients. Statins have previously been shown to have cytotoxic activity in many cancers including some preliminary evidence of activity in ovarian cancer. Therefore, the main aim of this research was to preclinically evaluate several potent statins in order to support clinical trials of statins in ovarian cancer. The following hypotheses were tested.

I. Simvastatin will have single agent cytotoxic activity dependent on concentration and exposure time, and may sensitise ovarian cancer cell lines to carboplatin. Pitavastatin, which offers an improved pharmacokinetic profile, will also have single agent cytotoxic activity in ovarian cancer cell lines.

II. Statins induce cell death through effects on the apoptosis and autophagy pathways.

III. Potential biomarkers of statin-induced cell death may be identified in the cell culture supernatant from cells exposed to statins.

IV. Pitavastatin may sensitise ovarian cancer cells to targeted anti-cancer therapeutics including ABT-737, obatoclax, pictilisib or metformin.

To test these hypotheses, this research utilised ovarian cancer cell lines grown both as monolayer and spheroid cultures. The results of these *in vitro* studies prompted the evaluation of pitavastatin as a single agent in an ovarian cancer xenograft model.

CHAPTER 3

MATERIALS AND METHODS

3.1 Ovarian Cancer Cell Lines

Ovarian cancer cell lines were purchased from the American Tissue Culture Collection (ATCC).

A2780 and cisA2780 cell lines were derived from a human ovarian carcinoma prior to chemotherapy treatment [439]. cisA2780 cells were rendered resistant to cisplatin by exposing A2780 cells to increasing concentrations of cisplatin [440].

The Ovcar-3 cell line was derived from the malignant ascites of a patient with progressive ovarian cancer that was resistant to cisplatin [441].

The Ovcar-4 cell line was derived from the ascites of a patient with ovarian cancer that was resistant to cisplatin [442].

The Ovcar-5 cell line was derived from the ascites of a patient with advanced ovarian cancer prior to chemotherapy treatment [442].

The Ovcar-8 cell line was derived from an ovarian carcinoma that was resistant to carboplatin [442].

The Igrov-1 cell line was derived from an ovarian carcinoma that was sensitive to chemotherapy treatment [443].

The Skov-3 cell line was derived from the ascites of a patient with ovarian cancer that was resistant to cisplatin [444, 445].

PEA1 and PEA2 cells were derived from the ascites or pleural effusion of a patient with poorly differentiated cancer. PEA1 was collected prior to treatment and PEA2 was collected on relapse following cisplatin and prednimustine treatment [446].

PEO1 and PEO4 cells were derived from the ascites of a patient with poorly differentiated serous cancer. PEO1 was collected after treatment with chemotherapy and PEO4 was collected after resistance to cisplatin, 5-fluorouracil and chlorambucil had developed [446].

3.2 Human Epithelial Cell Lines and Human Foreskin Fibroblasts

Human Ovarian Epithelial (HOE) cells were purchased from Applied Biological Materials (ABM) Inc. and were derived from normal ovarian epithelium and immortalised using SV40 large T antigen.

Human Bronchial Epithelial (NL20) cells were purchased from the ATCC and were derived from normal bronchus epithelium and immortalised using SV40 large T antigen.

Primary Human Foreskin Fibroblast (HFF) cells were provided through collaboration with Dr. Nicholas Forsyth at the Institution for Science and Technology, Guy Hilton Research Centre, Keele University, Staffordshire.

3.3 Cell Growth Conditions

Human ovarian cell lines and primary human foreskin fibroblasts were grown in Roswell Park Memorial Institute (RPMI 1640; Lonza) medium supplemented with 10% fetal bovine serum (FBS; Lonza), 50 µg/mL penicillin/streptomycin (Lonza) and 2 mM glutamine (Lonza). For Ovcar-3 cells, the medium was also supplemented with 0.01 mg/mL insulin (Lonza) and 0.11 g/L sodium pyruvate (Lonza).

The NL20 cell line was grown in Ham's F12 medium (Lonza) supplemented with 4% FBS (Lonza), 1.5 g/L sodium bicarbonate (Sigma-Aldrich), 2.7 g/L glucose (Sigma-Aldrich), 2 mM glutamine (Sigma-Aldrich), 0.1 mM non-essential amino acids (Sigma-Aldrich), 0.005 mg/mL insulin (Lonza), 10 ng/mL epidermal growth factor (Lonza), 0.001 mg/mL transferrin (Sigma-Aldrich) and 500 ng/mL hydrocortisone (Sigma-Aldrich).

Cells were incubated in a NAPCO water jacketed incubator (Precision Scientific) at 37°C and in a humidified 5% CO_2 atmosphere. cisA2780 cells were exposed to 1 µM cisplatin for 1 week every month in order to maintain chemoresistance.

3.4 Trypsinisation of Adherent Cells

All cells were routinely sub-cultured when they were more than 80% confluent as determined using an Olympus CKX41 light microscope. To detach adherent cells from the culture flask for routine passage or experimentation, cells were washed with 1 mL phosphate buffered saline (PBS; Lonza) and subsequently exposed to 1 mL 0.01%

trypsin (Lonza) in PBS. To encourage detachment, cells were incubated at 37°C and gently agitated. Following detachment, the trypsin was neutralised by the addition of 1 mL RPMI containing 10% FBS and cells were transferred into a sterile 15 mL polypropylene tube (Sarstedt). Cells were centrifuged at 150 g for 3 minutes at room temperature in a Thermo Scientific Heraeus Megafuge 8 centrifuge. The supernatant was carefully aspirated and the cell pellet was re-suspended in fresh cell culture medium. For routine passage, cells were transferred to T25 or T75 sterile tissue culture flasks (Sarstedt). For experimentation, at least 100 cells were counted using a Neubauer haemocytometer to determine cell number and an appropriate number of cells were transferred to tissue culture plates (96-well, 48-well, 12-well, 6-well; Sarstedt) as described for each experimental procedure.

3.5 Cryopreservation of Cells

Cells of a low passage number were collected by trypsinisation (section 3.4) when they had reached approximately 50% confluence in a T75 tissue culture flask, to ensure that the cells were growing in the logarithmic phase. The cell pellet was re-suspended in 1.2 mL growth medium containing 10% FBS and 8% dimethyl sulfoxide (DMSO, Sigma-Aldrich), and 0.2 mL aliquots were transferred into 2 mL cryovials (Triple Red). Cryovials were incubated overnight in a “Mr Frosty” freezing container (Nalgene) containing isopropanol (Sigma-Aldrich), at -80°C in a Nuaire -86°C Ultralow freezer, and the following day transferred into liquid nitrogen until required.

3.6 Reviving Cryopreserved Cells

Frozen cells in a cryovial obtained from the liquid nitrogen were rapidly thawed in a Grant JB Series water bath (Grant Instruments) at 37°C and then added to 5 mL pre-warmed growth medium in a 15 mL polypropylene tube. Cells were then centrifuged at 150 g for 3 minutes at room temperature and the pellet was re-suspended in 8 mL growth medium. The resulting cell suspension was transferred into a T25 tissue culture flask and incubated for 24 hours at 37°C. Subsequently, the growth medium was replaced to remove residual DMSO and dead cells, and adherent cells were grown to an appropriate density for experimentation or sub-culture (section 3.4).

3.7 Cytotoxicity Studies

3.7.1 Pharmacological Agents

Compounds were dissolved in DMSO, or PBS for carboplatin, to obtain the following concentrations: 10 mM ABT-737 (Abbot Laboratories), 13.5 mM carboplatin (Sigma-Aldrich), 20 mM doxorubicin (Tocris), 20 mM metformin (Enzo Life Sciences), 5 mM obatoclax (GeminX), 10 mM paclitaxel (Sigma-Aldrich), 20 mM pitavastatin calcium (Sequoia Research Products), 20 mM pravastatin (Enzo Life Sciences), 20 mM simvastatin (Enzo Life Sciences), 0.3 mM topotecan (Tocris), 20 mM pictilisib (LC Laboratories), 100 nM bafilomycin A1 (Tocris), 300 mM N-acetylcysteine (NAc; Sigma-Aldrich), 20 mM tert-butyl hydroperoxide solution (TBHP; Sigma-Aldrich), 20 mM farnesol (Sigma-Aldrich), 20 mM geranylgeraniol (Sigma-Aldrich) and 20 mM mevalonate (Enzo Life Sciences).

Cells were exposed to carboplatin at the IC_{50}, doxorubicin or topotecan at five times the IC_{50}, 20-50 nM paclitaxel, and simvastatin or pitavastatin at two to five times the $IC_{50,}$ in order to achieve cell death rapidly *in vitro*.

3.7.2 Cell Growth Assays

Following trypsinisation and quantification, cells (5000 cells/well except for A2780, cisA2780 and Ovcar-8, where 2000 cells/well were used) were seeded in 96-well plates in 80 µL of growth medium. After incubation for 24 hours, 20 µL of 18 different concentrations of drug or drug extract at 5 times the required concentration and a drug solvent control was added to the cells. For drug combination studies, the cells were exposed to either a range of concentrations of two drugs combined in a fixed ratio of the two drugs, or in a combination in which the concentration of one drug was held constant. (The concentrations are shown in the results section). After incubation for a further 72 hours, the growth medium was removed and the cells in each well were fixed in 100 µL 10% trichloroacetic acid (TCA, Sigma-Aldrich) on ice for 30 minutes. The TCA was then removed by washing the plates three times in water and the cells were left to air dry, before staining in 0.4% sulforhodamine B (SRB, Sigma-Aldrich) in 1% acetic acid (Sigma-Aldrich) for 30 minutes. After removing excess SRB by washing the wells three times in 1% acetic acid and drying, the dye was solubilised in 100 µL 10 mM Tris (pH 10, Sigma-Aldrich) and the absorbance at 570 nm (A_{570}) was determined using a BioTek Synergy 2 multi-mode microplate reader.

Cell growth assays, used to determine the potency of pitavastatin in PEA1, PEA2, PEO1 and PEO4 cell lines, were conducted by Karen Menezes and Dr Euan Stronach

in the Department of Surgery and Cancer at Imperial College London, using the method described above.

3.7.3 Statistical Analysis to Determine IC_{50} Value

Data obtained from cell growth assays (section 3.7.2) was analysed using the GraphPad Prism software (GraphPad Software, Inc.). Non-linear regression was used to fit a four-parameter (Hill-equation) sigmoidal dose-response curve, and subsequently, the concentration at which 50% of cell growth was inhibited (IC_{50}) was determined. Both the mean average and standard deviation were calculated using IC_{50} values from repeat experiments.

3.7.4 Drug Combinations in Cell Growth Assays

For experiments evaluating the effect of altering the schedule of administration of combinations of simvastatin with carboplatin, cells were exposed to simvastatin, carboplatin or both for 48 hours, after which the drug was washed off the cells using PBS. Following this, the cells were incubated for a further 48 hours with drug or growth medium containing solvent. Alternatively, cells were exposed to carboplatin or simvastatin for 48 hours, before fixing in TCA and staining with SRB (section 3.7.2). Scheduling experiments used a fixed ratio of carboplatin and simvastatin concentrations based on the respective IC_{50} values measured in preliminary experiments with the single agents.

Drug combinations with pitavastatin and either obatoclax or pictilisib were combined at a ratio of their IC_{50} values as determined from single agent studies. ABT-737 is insoluble at high concentrations. Therefore, fixed concentrations of ABT-737, which had been determined to inhibit cell growth by 5% (A2780, 3 µM; Ovcar-3, 1 µM; Ovcar-8, 1 µM; Igrov-1, 0.6 µM), were added to each concentration of pitavastatin. A fixed concentration of metformin (15 µM) was also added in combination with varied concentrations of pitavastatin, as this is reported to be the highest achievable plasma concentration of metformin *in vivo* [447]. Cells were incubated for 72 hours, then fixed in TCA and stained with SRB as described (section 3.7.2).

3.7.5 Calculation of Combination Indices and Bliss Independence Criterion

The Combination Index (CI) was first described by Chou and Talalay [448] to provide a quantitative estimation of the degree of synergy, additivity or antagonism between two drugs.

$$CI = \frac{(D)_1}{(D_x)_1} + \frac{(D)_2}{(D_x)_2}$$

$(D)_1$ and $(D)_2$ indicate the doses of drug 1 and drug 2 in the combination which inhibit cell growth by $x\%$. $(D_x)_1$ and $(D_x)_2$ indicate the doses of drug 1 and drug 2 alone which inhibit cell growth by $x\%$. If the sum of the two fractions is equal to 1, then the interaction between the two drugs is additive. If the CI value is smaller than 1, then the interaction is synergistic, whereas if the CI value is greater than 1, then the interaction is antagonistic [448]. Results were compared to deviation from unity with a paired *t*-test using Welch's correction.

CI values were calculated to measure the combined effect of pitavastatin with ABT-737, pictilisib, obatoclax or metformin. Dose-response curves were determined for each experiment and IC_{50} values and Hill co-efficients were calculated. CI values were quoted at a fraction affected of 0.5 or 0.75, which is the concentration of the drug combination that inhibited 50% or 75% of cell growth respectively.

The Bliss independence criterion (which does not require knowledge of the IC_{50}) was calculated to compare the observed effect of the drug combination with the expected effect.

$$E_{expected} = E_A + E_B - E_A * E_B$$

E_A and E_B indicate the effects of drug A and drug B alone and are used to calculate the expected fractional effect ($E_{expected}$) of the drug combination, which assumes that the effects of the two drugs are additive [449]. A paired *t*-test was used to compare the observed effect of the drug combination to the expected effect calculated using the Bliss independence criterion.

3.7.6 Trypan Blue Cell Viability Assay

Trypan blue is used to differentiate between viable and non-viable cells. The chromophore of Trypan blue is negatively charged, which prevents its penetration into the cell unless the cell membrane is damaged. Therefore, viable cells exclude the dye and have a clear cytoplasm when observed by microscopy, whereas dead cells are stained blue.

To assess the effect of a drug on cell viability using Trypan blue staining, 2 x 10^5 cells per well of a 12-well plate were incubated with 500 µL growth medium containing 10 µM simvastatin (Ovcar-8), pitavastatin at a concentration of 5 x IC_{50} in each cell line (1-40 µM) or solvent for 12-96 hours as indicated. In drug combination studies, Ovcar-3 and Igrov-1 cells (3 x 10^5 cells per well of a 6-well plate) were incubated with 1 mL growth medium containing pitavastatin (6 - 12 µM), ABT-737 (0.6 - 1 µM), obatoclax (2 - 3 µM), pictilisib (0.7 - 2 µM) or solvent alone or in combination with pitavastatin for 72 hours. Adherent cells were then collected by trypsinisation (section 3.4) and combined with the supernatant containing detached cells. The resulting cell suspension was centrifuged at 150 g for 3 minutes before staining with 0.2% Trypan blue (Sigma-Aldrich) and quantifying live and dead cells using a haemocytometer (section 3.4).

3.7.7 Three-Dimensional Spheroid Culture and ATP Assay

Ovarian cancer spheroids/aggregates were used to provide a 3D architecture of cancer cells that more closely resemble cancer *in vivo*. The CellTiter-Glo assay (Promega) was used to avoid the issues of reagent penetration into the spheroid during the measurement procedure. The CellTiter-Glo reagent lyses the cells in the spheroid entirely, and the ATP released results in the mono-oxygenation of luciferin and generation of a luminescent signal. The luminescence is proportional to the amount of ATP present in the cell culture, which indicates the presence of viable cells.

A2780 (2 x 10^6 cells/ml), Ovcar-3 (5 x 10^5 cells/ml), Ovcar-5 (1 x 10^6 cells/ml), Ovcar-8 (1.25 x 10^5 cells/ml) and Igrov-1 (2 x 10^6 cells/ml) cells were prepared as cell suspensions in growth medium (optimal cell concentration for spheroid formation in

each cell line was determined previously), using the hanging drop method. One 20 µL drop of cell suspension was added to each inner ring of the lids of 48-well plates. Outer rings contained a 20 µL drop of growth medium and 300 µL of sterile water was added to each well beneath the rings to maintain a humid atmosphere and minimise evaporation. The lids were inverted over the plates and incubated for 7 days. After 1 week, the spheroids were exposed to 5 µL growth medium containing simvastatin, pitavastatin or solvent and incubated for a further 72 hours. The spheroids were then collected using a wide bore pipette into opaque-walled multiwell plates containing 20 µL of PBS and an equal volume of CellTiter-Glo reagent was added in order to measure ATP. Spheroid lysis was confirmed by microscopy to ensure penetration of the reagent into the spheroid. Released cellular ATP was consumed in the luciferase reaction to produce a stable luminescence, which was measured using a BioTek Synergy 2 multi-mode microplate reader. The data was analysed as previously described by using non-linear regression to fit a four-parameter (Hill-equation) sigmoidal dose-response curve (section 3.7.3).

3.7.8 Caspase 3/7, 8 and 9 Assays

The activities of the initiator caspases, 8 and 9, and the executor caspases, 3 and 7 were measured using the Caspase-Glo Assay (Promega). The Caspase-Glo reagent initially lyses the cells and the released caspases recognise and cleave the luminogenic substrate. For example, caspases 3/7 recognise the luminogenic substrate containing the tetra peptide sequence DEVD, whereas caspase 8 and caspase 9 recognise substrates with the LETD and LEHD sequences respectively.

The cleaved substrate results in the luciferase reaction and the production of a luminescent signal, which is proportional to the caspase activity present.

Ovcar-8 (2000 cells/well), Ovcar-3 (5000 cells/well) and Igrov-1 (5000 cells/well) cells were incubated in 80 µL growth medium in a 96-well plate for 24 hours. Cells were then supplemented with 20 µL growth medium containing pitavastatin, paclitaxel or solvent. In other studies, cells were exposed to pitavastatin in combination with other compounds or extracts as stated. After 48-72 hours, 25 µL of Caspase-Glo 3/7, 8 or 9 reagent was added and cells were incubated for 30 minutes at room temperature in the dark. A BioTek Synergy 2 multi-mode microplate reader was used to measure luminescence.

3.7.9 Reactive Oxygen Species (ROS) Assay

The fluorogenic dye, 2',7'-dichlorofluorescin diacetate (DCFDA; Sigma-Aldrich), is used to measure reactive oxygen species (ROS) in cells. DCFDA diffuses into the cell and is deacetylated by intracellular esterases to the non-fluorescent compound, 2',7'-dichlorofluorescin (DCFH), which is trapped in the cell. DCFH is subsequently oxidised by a variety of ROS to the fluorescent molecule, 2',7'-dichlorofluorescein (DCF).

Ovcar-3 (5000 cells/well) and Ovcar-8 cells (2000 cells/well) were seeded in 96-well plates in 80 µL of growth medium and incubated for 24 hours. The cells were then washed with growth medium containing no FBS (FBS-free medium) and stained with 25 µM DCFDA in FBS-free medium for 45 minutes at 37°C. Several wells containing

cells were left unstained as a control to assess auto-fluorescence. After a second wash with FBS-free medium, cells were exposed to 100 µL FBS-free medium containing solvent or drug as stated, and incubated for 48 hours. After 45 hours, 50 µM TBHP was added to several wells containing stained cells and incubated for the final 3 hours. Fluorescence was measured at an excitation of 485 nm and emission of 535 nm using a BioTek Synergy 2 multi-mode microplate reader. Auto-fluorescence from the unstained cells was subtracted from the data obtained.

3.7.10 Cell Migration Scratch Assay

The “scratch assay” can be used to measure cell migration *in vitro*. A “scratch” is made in a cell monolayer and images are captured both at the beginning and at time points during cell migration. The images can be compared in order to determine the migration of the cells.

Ovcar-8 cells (1 x 10^6 cells/well) were plated in 6-well plates in 2 mL of growth medium and incubated for 24 hours. The cell monolayer was then scraped down the centre of each well using a P200 pipet tip to create a “scratch”. The debris was removed by washing the cells twice with 1 mL of PBS. The cells were then exposed to growth medium containing pitavastatin (0.1-0.2 µM) or solvent for a further 36 hours. Reference points were made on the base of each well and images of the scratch at the reference points were acquired at various time points using an Olympus CKX41 light microscope. Images were analysed using ImageJ (Wayne Rasband, National Institutes of Health, USA). The pre-migration area (before drug was added) and post-

migration area (36 hours of drug exposure) of the scratch was determined and used to calculate % closure using the equation below:

$$\%\ Closure = \left(\frac{Pre\text{-}migration\ area - Post\text{-}migration\ area}{Pre\text{-}migration\ area}\right) * 100$$

3.8 Small Interfering RNA (siRNA) Transfections

Lipofection is a widely employed technique that uses liposomes to transport genetic material into a cell. Liposomes are cationic lipids which bind to the surface of the negatively charged phospholipid bilayer and are endocytosed. The lipid-based transfection reagent, DharmaFECT 1 (Thermo Scientific), is efficient and has a low toxicity, and was used to introduce small interfering RNA (siRNA) into ovarian cancer cell lines. The optimum transfection conditions have been determined in previous studies [450], and demonstrated more than 95% transfection efficiency.

Cells were seeded in 96 well plates (2000-5000 cells/well) in 80 µL antibiotic-free growth medium and incubated overnight. After 16 hours, 1% DharmaFECT 1 was prepared in Optimum (Invitrogen) and incubated for 5 minutes at room temperature. The siRNA was also diluted in Optimum at 10 times the final concentration required and then added to the 1% DharmaFECT 1 solution. The siRNA and DharmaFECT 1 solution was incubated for 20 minutes at room temperature to enable the siRNA to form a complex with the liposomes. The growth medium on the cells was replenished with 80 µL of fresh antibiotic-free growth medium, and 20 µL of the siRNA and DharmaFECT 1 solution was added to each well containing cells (details of the siRNA

used is described in appendix 1). A non-targeting siRNA control was included in all transfections to establish any off-target effects on gene expression (off-target gene silencing). The cells were incubated for a further 24 hours at 37°C, before the growth medium was replenished with 80 µL of fresh growth medium and the cells were exposed to a range of concentrations of simvastatin or pitavastatin. Cell growth assays or caspase 3/7 assays were completed as previously described (sections 3.7.2 and 3.7.8). Knockdown of gene expression was confirmed by western blotting (section 3.9.3).

3.9 Molecular Biology Methods

3.9.1 Isolation, Purification and Quantification of Mitochondrial DNA from Cell Lines

Mitochondrial DNA was extracted and purified from cell lines using a QIAamp DNA Mini Kit (QIAGEN) and all steps were completed as per kit instructions. All reagents were incubated to room temperature before use.

Ovcar-8 cells (5 x 10^6 cells) and Ovcar-3 cells (2 x 10^6 cells) in T75 tissue culture flasks, previously exposed to pitavastatin or solvent as described, were washed in PBS and collected by trypsinisation (section 3.4), followed by centrifugation at 200 g for 5 minutes. The supernatant was discarded and the cell pellet was re-suspended in 200 µL PBS. The cell suspension was then combined with 20 µL proteinase K, and 200 µL Buffer AL was added, before vortexing for 15 seconds to ensure a homogenous solution for efficient cell lysis. The suspension was incubated at 56°C for

10 minutes, and then centrifuged briefly to collect the condensation inside the lid. Subsequently, 200 µL 99% ethanol (Sigma-Aldrich) was added to the suspension and vortexed for 15 seconds to precipitate the DNA. After a brief centrifugation, all of the suspension was transferred to a QIAamp Mini spin column in a collection tube and centrifuged at 6000 g for 1 minute in an Eppendorf 5415R centrifuge to remove the lysate. The precipitated DNA was adsorbed onto the QIAamp silica membrane during centrifugation. The bound DNA was then washed with 500 µL Buffer AW1, and centrifuged at 6000 g for 1 minute to remove residual contaminants and improve the purity of the DNA. The DNA was washed a further time with 500 µL Buffer AW2, before centrifuging at 10,000 g for 3 minutes. Purified DNA was eluted from the QIAamp Mini spin column by incubating the column at room temperature for 5 minutes with 200 µL Buffer AE, and then collecting the DNA into a clean microcentrifuge tube by centrifugation at 6000 g for 1 minute.

A NanoDrop 2000 spectrophotometer (Thermo Scientific) was used to determine the concentration and purity of the DNA in each sample. The NanoDrop 2000 uses a patented sample retention system which automatically optimises the path length depending on the DNA concentration. The absorbance of the DNA is measured at 260 nm (A_{260}) as DNA absorbs light most strongly at this wavelength. The absorbance generated is used to estimate the concentration of DNA in the sample, assuming that the A_{260} of 1.0 = 50 µg/mL pure double-stranded DNA. The A_{260} measurement is also adjusted for turbidity by deducting the absorbance measured at 320 nm. The DNA concentration is often overestimated as other molecules have absorbance values at 260-280 nm, including RNA and aromatic amino acids in proteins, and these can contribute to the total A_{260}. The purity of the DNA is calculated by taking the ratio of the absorbance at 260 nm and 280 nm (A_{280}), after correcting for turbidity. A ratio of

1.7-2.0 indicates relatively pure DNA, whereas lower ratios suggest the presence of contaminants. The NanoDrop 2000 was blanked with Buffer AE before measuring the A_{260} and A_{280} of 1 µL aliquots of each sample.

3.9.2 Quantitative Polymerase Chain Reaction

Polymerase chain reaction (PCR) is a process involved in amplifying DNA sequences of interest from small quantities of starting product. PCR involves three main stages. The reaction is started with a temperature increase to 95°C, where double-stranded DNA is denatured into single strands. The temperature is then reduced to around 60°C and two oligonucleotide primers bind to their complementary sequences on opposite ends of the desired DNA sequence. The *Taq* polymerase then binds and extends the DNA sequence between the primers. This process is repeated up to 40 times to give billions of copies of the DNA of interest. Real-time quantitative PCR (qPCR) monitors this process in 'real-time' as the amount of DNA synthesised can be detected using fluorescent dyes. SYBR green is a fluorescent dye which binds to double-stranded DNA, allowing the production of DNA to be monitored by measuring an increase in fluorescence throughout the cycles. An amplification plot can be generated from the increasing fluorescence signal and used to quantitate the amount of DNA.

Real-time qPCR reactions were carried out by first preparing the reaction mixture containing 1 X ABsolute SYBR Green ROX mix (Thermo Scientific), 167 nM forward and reverse primers (appendix 2, [451]) and double-distilled water (ddH_2O). Aliquots of 7.5 µL reaction mixture were added to individual wells of optical 8-tube strips

(Applied Biosystems), and then 5 µL of each DNA sample or a ddH_2O control was added to each well in duplicate. The reaction mixture in each strip was briefly vortexed to remove any air bubbles and collect the liquid at the bottom of the wells.

	Segment 1	**Segment 2**	**Segment 3**
	Denaturation of the two DNA strands at 95°C for 15 minutes	Denaturation at 95°C for 30 seconds	For the dissociation curve: 95°C for 1 minute, 55°C for 30 seconds and 95°C for 30 seconds
		Primer annealing at 60°C for 30 seconds	
		DNA strand elongation at 68°C for 30 seconds	
Cycle Number	1	40	1

Table 3.1: Thermal profile for qPCR

The reaction cycles (table 3.1) were carried out using a Stratagene M_x3005P thermal cycler (Agilent Technologies). The dissociation curve at the end of the reaction cycles was evaluated to confirm that only one amplicon had been detected. Contaminating DNA or primer dimers are illustrated by a peak additional to the amplicon peak.

Data was analysed by the comparative cycle threshold (CT) method which compares the CT value of one gene to the CT value of a reference gene (usually a housekeeping gene such as β-actin). The CT value is the point at which the threshold line intersects the amplification curve, and gives a relative measurement of the DNA in the reaction. The efficiencies of both the target and control gene amplifications were first confirmed by measuring the CT values of 4 serial 5-fold dilutions of DNA samples using qPCR. The standard curve produced from this data was analysed by linear

regression, and then used to calculate the efficiency of each primer using the following equation. The gradient is determined from the slope of the line of best fit.

$$Efficiency = 10^{-1/Gradient}$$

An efficiency of 100% indicates that two copies of DNA were produced in each amplification cycle. Following this, the ΔΔCT was calculated using the following equation:

$$Ratio = \frac{Efficiency\ (Target)^{CT\ (Target,Untreated)-CT(Target,Treated)}}{Efficiency\ (Control)^{CT(Control,Untreated)-CT(Control,Treated)}}$$

The target and control refer to the gene of interest and the control gene respectively. The treated and untreated refer to DNA samples extracted from cells that have been exposed to pitavastatin or solvent respectively.

3.9.3 Immunodetection of Proteins using SDS-PAGE and Western Transfer

The separation and detection of numerous intracellular proteins from ovarian cancer cells was achieved by western blotting. First the cells are lysed to release intracellular proteins and then the protein concentration of the lysate is determined. Following this, known amounts of each lysate are loaded onto a polyacrylamide gel and using gel electrophoresis, the mixture of proteins is separated based on molecular weight. The separated proteins are subsequently transferred onto a membrane, where primary antibodies can be used to bind to a specific protein. Unbound primary antibody is washed off, leaving antibody bound to the protein required. Secondary antibodies

conjugated to horseradish peroxidase (HRP) bind to the primary antibody and in the presence of chemiluminescent substrate, HRP catalyses the oxidation of luminol, with the emission of light. CCD camera imaging can be used to detect this light which corresponds to the protein band.

Cells were exposed to drugs as described, washed in PBS and lysed in 1 mL (per 100 cm^2 growth area) RIPA ("Radio-Immunoprecipitation Assay") buffer containing proteases and protease inhibitors (20 mM Hepes (CalbioChem), 150 mM sodium chloride (NaCl, Sigma-Aldrich), 2 mM ethylene-diamino-tetraacetic acid (EDTA, Sigma-Aldrich), 0.5% sodium deoxycholate (Sigma-Aldrich), 1% NP40 (Sigma-Aldrich), 120 µM leupeptin (Sigma-Aldrich), 10 µM pepstatin (Sigma-Aldrich) and 1 mM phenylmethanesulfonyl fluoride (PMSF, Sigma-Aldrich)). The cell lysate suspension was centrifuged at 10,000 g for 10 minutes at 4°C, and the supernatant containing the cellular proteins was collected. Protein lysates were stored at -80°C.

The protein concentration was determined using the Bicinchoninic acid (BCA) protein assay kit (Sigma-Aldrich). Bovine serum albumin (BSA, Sigma-Aldrich) standards were prepared at concentrations between 0.1 and 2 mg/mL. BCA reagent was prepared by adding 4% copper (II) sulphate pentahydrate solution (Sigma-Aldrich) to BCA solution (bicinchoninic acid, sodium carbonate, sodium tartate and sodium bicarbonate in 0.1 M sodium hydroxide) in the ratio of 1:50, and 100 µL of the reagent was added to either 10 µL of each BSA standard or 5 µL of each lysate diluted in 5 µL RIPA buffer. Lysates were incubated for 30 minutes at 37°C and then the A_{570} was determined using a spectrophotometer. A protein standard calibration curve was prepared from the BSA standard A_{570} values and fit using linear regression. The calibration curve was used to calculate the protein concentration in each lysate.

Prior to sodium dodecyl sulphate polyacrylamide gel electrophoresis (SDS-PAGE), 5-15 µg protein from each cell lysate was added to NuPAGE sample buffer (Invitrogen) containing 5% β-mercaptoethanol (Sigma-Aldrich), and denatured at 70°C for 15 minutes. A 4-20% NuView Tris-Glycine polyacrylamide gradient gel (Nusep) in an XCell SureLock Mini Cell (Invitrogen) with hepes running buffer (100 mM hepes, 100 mM Tris and 1% sodium dodecyl sulphate (SDS, Sigma-Aldrich)) was used to fractionate the denatured protein from each cell lysate. PageRuler Plus Prestained Protein Ladder (Thermo Scientific) was included on each gel to estimate the size of immunodetected proteins. Separated proteins were subsequently transferred onto Amersham Hybond P 0.45 µm polyvinylidene difluoride (PVDF) membrane (GE Healthcare Life Sciences) in transfer buffer (25 mM Tris, 200 mM glycine (Sigma-Aldrich), 0.075% SDS and 10% methanol (Sigma-Aldrich)) at 25 V for 1.5 hours. Following this, the membrane was incubated with Tris Buffered Saline with Tween (TBST) buffer (50 mM Tris hydrochloride (Tris HCl, pH 7.4, Sigma-Aldrich), 150 mM NaCl, 0.1% Tween 20) containing 5% skimmed milk powder for 1.5 hours with gentle rocking on a Stuart Scientific Platform Shaker STR6 at room temperature for blocking. The membrane was then incubated in primary antibody for 16 hours at 4°C overnight with gentle rocking. Following five washes in TBST, the membrane was incubated in secondary antibody for 1 hour at room temperature with gentle rocking. The antibodies and corresponding dilutions used are described in appendix 3. After a further five washes in TBST, protein bands were visualised using UptiLight HRP chemiluminescent substrate (Uptima) and a FluorChem M Imager. Bands were quantified by using AlphaView SA software (Protein Simple) to measure the total number of pixel grey levels in the selected band area and then normalised to the loading control, glyceraldehde-3-phosphate dehydrogenase (GAPDH).

3.9.4 Detection of Proteins using SDS-PAGE and Silver Staining or Coomassie Brilliant Blue

An additional method by which separated cellular proteins can be detected is by staining the polyacrylamide gel with either silver nitrate or Coomassie Brilliant Blue. Both detect total protein which enables visualisation of the protein pattern in the gel. After gel electrophoresis, proteins are fixed into the gel using an acid or alcohol wash. Exposure to the stain allows the Coomassie dye or silver ions to diffuse into the gel and bind to the proteins. Destaining removes excess stain from the gel matrix background and allows better detection of the protein bands.

The silver and Coomassie Brilliant Blue stains were used to detect proteins released from cells into the growth medium both before and after exposure to drug. Ovcar-8, Ovcar-3, HOE and HFF cells (2 x 10^5 cells/mL) were exposed to 1-8 µM pitavastatin, 2-10 µM simvastatin, 2-10 µM pravastatin, 70 µM carboplatin (1 x IC_{50} in Ovcar-8 only), 21 nM paclitaxel (3 x IC_{50} in Ovcar-8 only), 1 µM doxorubicin (5 x IC_{50} in Ovcar-8 only), 50 nM topotecan (5 x IC_{50} in Ovcar-8 only) or solvent for 48 hours at 37°C. Cells were subsequently washed three times in FBS-free growth medium, after which the experimental drugs were re-added to the cells in FBS-free growth medium. After incubation for a further 24 hours, the growth medium on the cells was collected and centrifuged at 10,000 g for 10 minutes to remove debris prior to gel electrophoresis and staining. The supernatant was collected and stored at -80°C.

For protein supernatant samples analysed by Coomassie Brilliant Blue staining or western blotting, Ovcar-8 and Ovcar-3 cells (4 x 10^6) were plated in T75 tissue culture flasks prior to drug addition in order to maximise protein concentration. The

supernatant collected after centrifugation was transferred to a Vivaspin 20 10 kDa sample concentrator (Fisher Scientific) and centrifuged at 1000 g for 1 hour. Each concentrated supernatant sample was made up to a final volume of 1 mL using FBS-free growth medium. An equal volume of each supernatant sample was resolved by Tris-Glycine SDS-PAGE, using a 4-20% polyacrylamide gradient gel (Nusep) for silver staining or an 8% polyacrylamide resolving gel (8% protogel (acrylamide and bis-acrylamide in the ratio of 37.5:1, Fisher Scientific), 2 M Tris (5% Tris HCl, 20% Tris, pH 8.8), 0.06% *N,N,N',N'*-tetramethylethylenediamine (TEMED, Sigma-Aldrich), 0.1% SDS, 0.025% ammonium persulfate (APS, Sigma-Aldrich)) for Coomassie Brilliant Blue staining, as described in section 3.9.3.

For silver staining, the polyacrylamide gel was washed in deionised water to remove running buffer from the gel matrix. The gel was then fixed (40% ethanol (Sigma-Aldrich) and 10% acetic acid) for 1.5 hours with rocking, washed (5% ethanol and 5% acetic acid) with rocking four times for 1 hour, and sensitised using 0.02% sodium thiosulphate (Fisher Scientific) for 2 minutes. Following this, the gel was washed in deionised water three times for 15 minutes, stained (0.2% silver nitrate (BDH Lab Supplies) and 0.076% formaldehyde (Sigma-Aldrich)), and washed in deionised water a further two times for 2 minutes before developing (6% sodium carbonate (BDH Lab Supplies), 0.05% formaldehyde and 0.0004% sodium thiosulphate). After the required staining intensity had been reached, the reaction was stopped by replacing the developing solution with 5% acetic acid, and the gel was imaged using a FluorChem M Imager.

For Coomassie Brilliant Blue staining, the polyacrylamide gel was fixed and stained in a solution containing 0.1% Coomassie Brilliant Blue (Sigma-Aldrich), 10% methanol

and 10% acetic acid for 16 hours with rocking at room temperature, and destained using multiple 6% acetic acid washes for a further 24 hours with rocking until protein bands were visible. The gel was imaged using a FluorChem M Imager, before excising bands for mass spectrometry analysis.

3.9.5 In-Gel Digestion of Excised Protein Bands and Protein Identification by Mass Spectrometry

Throughout the last 30 years, mass spectrometry has become the key method used to identify proteins from complex biological mixtures. Proteins separated by gel electrophoresis can be identified by mass spectrometry, following several stages of sample extraction and preparation that are critical for high-quality results.

Protein bands are first excised from the gel and destained to remove the Coomassie stain. Following this, the disulfide bonds on the cysteine residues are reduced, and the remaining free sulfhydryl groups are irreversibly alkylated to prevent disulfide reformation. The proteins are subsequently hydrolysed by trypsin on the C-terminal side of lysine and arginine. The resulting peptides are extracted from the gel matrix and prepared for mass spectrometry.

Sample preparation and mass spectrometry analysis was completed by Dr Elzbieta Piatkowska and Dr Sarah Hart at the School of Life Sciences, Keele University, Staffordshire. Excised protein bands from Coomassie Brilliant Blue stained gels were cut into small cubes and destained in 25 mM ammonium bicarbonate (Fisher Scientific) in 50% acetonitrile (Sigma-Aldrich) with occasional vortexing for 10

minutes. After discarding the supernatant, destaining was repeated a further two times, before incubating in 100% acetonitrile for 15 minutes to dehydrate the gel pieces. The resulting white gel pieces were dried in a Thermo SPD SpeedVac linked to a Savant Refrigeration Condensation Trap and High Vacuum Pump at room temperature for 30 minutes. Gel pieces were subsequently reduced in 25 mM ammonium bicarbonate and 10 mM dithiothreitol (DTT, Sigma-Aldrich) for 45 minutes at 56°C with rocking, and after discarding the supernatant, alkylated in 25 mM ammonium bicarbonate and 55 mM iodoacetamide for 1 hour at room temperature in the dark. Following this, gel pieces were washed in 25 mM ammonium bicarbonate and dried in a SpeedVac at room temperature for 20 minutes. Gel pieces were then digested in 20 µg/mL trypsin in 25 mM ammonium bicarbonate overnight at 37°C. After 16 hours, extraction buffer (50% acetonitrile and 0.1% trifluroacetic acid (TFA, Sigma-Aldrich)) was added to the gel pieces for 10 minutes to neutralise remaining trypsin activity and the supernatant was collected. The addition of extraction buffer to the gel pieces was repeated and the supernatant from both extractions was pooled, before being dried in a SpeedVac at room temperature to complete dryness.

Following digestion and extraction, peptides were added to 10 mg/mL α-Cyano-4-hydroxycinnamic acid (in 0.1% TFA and 80% acetonitrile, Sigma-Aldrich) in a 1:1 ratio (v/v) on a stainless steel Matrix Assisted Laser Desorption/Ionization (MALDI) target plate. A MALDI time-of-flight (TOF/TOF) instrument (MALDI 4800, AB Sciex, Warrington, Cheshire) was used to acquire data in a positive reflector mode in the mass range of 700-3,600 m/z, and 800-1,000 laser shots were collected during survey scan acquisition. Cal Mix 5 (a mixture of the 5 protein standards: bradykinin, angiotensin, P14R, ACTH fragment 18-39 and glufibrinopeptide, Sigma-Aldrich) was used to externally calibrate all spectra.

A 1 kV collision energy profile with air as a collision gas was used to analyse the manually generated list of precursors for tandem mass spectrometry (MS/MS). The isolation width was -1 to +2 amu around the precursor ion mass. Furthermore, 4000 laser shots were acquired for each spectrum, with a signal-to-noise ratio (S/N) of at least 20 for spectrum acceptance.

Plain text Mascot generic files (.mgf) were produced using the Macro tool in 4000 Series Explorer software (Export_to_MGF_file.ExportMascotPeakList available from Matrix Science). All product ion spectra generated for each excised gel band underwent a single Mascot search using Mascot Daemon (Matrix Science, London). The data were searched against the MSDB database with the following search parameters: enzyme trypsin; 1 miscleavage allowed; fixed modification: cysteine carbamidomethylation; variable modifications: methionine oxidation; peptide tolerance 200 ppm and MS/MS tolerance ± 0.6 Da.

3.9.6 M30 CytoDeath ELISA

During apoptosis, caspases cleave cellular proteins including the intermediate filament protein cytokeratin 18 (CK18). Caspases 3, 7 and 9 cleave CK18 after aspartic acid residue 396 and the resulting neo-epitope is recognised by the M30 antibody. The M30 CytoDeath solid phase sandwich enzyme-linked immunosorbent assay (ELISA) is used to measure the levels of soluble caspase-cleaved CK18 (ccCK18) in epithelial cells. The solid phase capture antibody, M6, binds to ccCK18 in the sample (figure 3.1). The M30 antibody then recognises and binds to the CK18Asp396 neo-epitope present only on ccCK18 (figure 3.1). Unbound conjugate is removed by washing and

subsequently, HRP linked to the M30 antibody catalyses the conversion of the chromogenic substrate, 3,3',5,5'-tetramethylbenzidine (TMB), to a measurable coloured product.

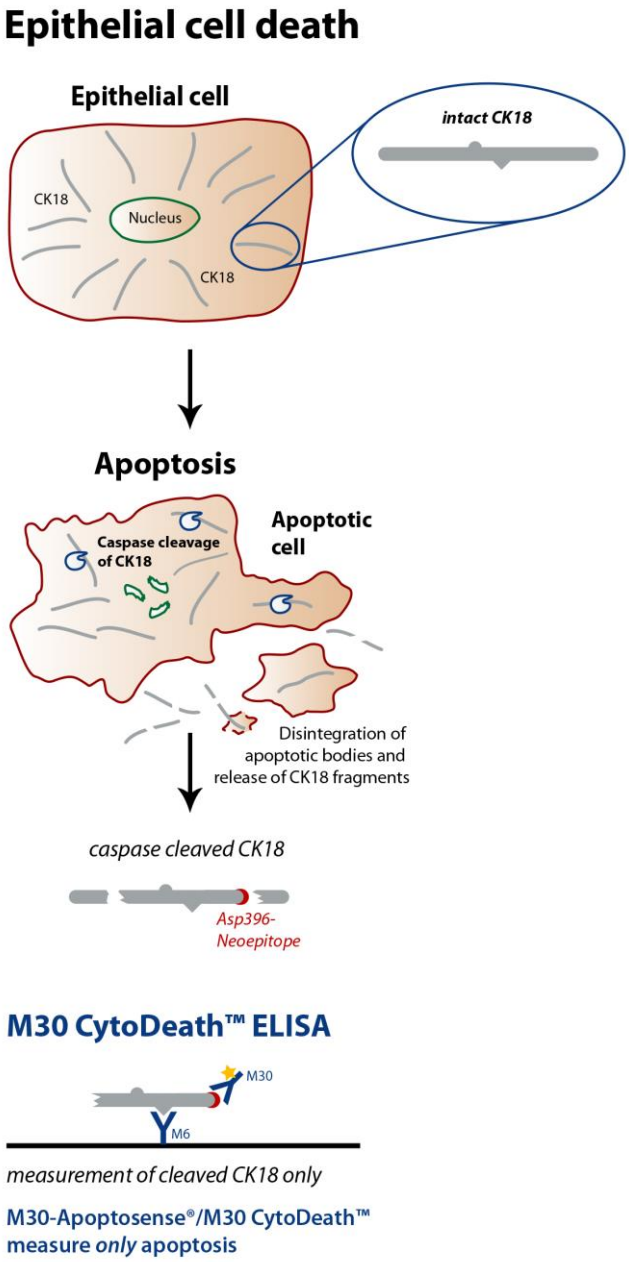

Figure 3.1: M30 CytoDeath ELISA. Cytokeratin 18 is cleaved by caspases during apoptosis to yield a CK18Asp396 neo-epitope, which is recognised by the M30 antibody in the ELISA [452].

Ovcar-8, Ovcar-3, Igrov-1 and Skov-3 cells (5000 cells/well except for Ovcar-8, 2000 cells/well) were incubated in 100 µL growth medium in a 96-well plate for 24 hours and then exposed to pitavastatin at five times the IC_{50} measured in cell growth assays (1-20 µM), carboplatin at the IC_{50} in each cell line (4-70 µM), paclitaxel (50 nM) or solvent. After 72 hours, the supernatant was collected and centrifuged at 10,000 g for 10 minutes at 4°C. The M30 CytoDeath ELISA (Peviva) was completed following the manufacturer's instructions. All reagents were incubated to room temperature before use. 25 µL of each supernatant was transferred in duplicate to the ELISA plate and 75 µL of monoclonal M30 antibody conjugated with HRP was immediately added to each well containing sample. The wells were incubated at room temperature with gentle rocking for 4 hours. The wells were then washed five times using wash solution to remove unbound conjugate. Subsequently, TMB substrate was added to each well and incubated at room temperature in the dark with gentle rocking for 20 minutes. Colour development was proportional to the amount of ccCK18 bound, and was stopped by the addition of 1 M sulphuric acid. A_{450} (nm) was measured using a BioTek Synergy 2 multi-mode microplate reader.

3.9.7 Flow Cytometry

Flow cytometry is used to analyse the characteristics of single cells in liquid suspension as they pass through a beam of light. Organelles and DNA can be labelled with fluorescent probes including MitoTracker for detecting active mitochondria and propidium iodide (PI) for labelling DNA and RNA.

MitoTracker Green probe diffuses across the plasma membrane of live cells and is sequestered in active mitochondria. Once in the lipid environment of the mitochondria, MitoTracker Green binds to the mitochondrial lipids and is converted to a fluorescent probe, which can be detected by flow cytometry or fluorescence microscopy.

PI intercalates between the nucleotide bases in both DNA and RNA. Ribonuclease (RNase) is used to enzymatically remove RNA to enable the specific staining of DNA for cell cycle analysis. Cells in G_2 and M phases of the cell cycle contain double the amount of DNA compared to cells in G_1. Apoptotic cells (subG_1) have less DNA due to DNA degradation by endogenous nucleases and diffusion out of the cell. The DNA content of cells during S phase lies between that for G_1 and G_2 phases. Fluorescence emission from PI is proportional to the cellular DNA content. Therefore, flow cytometry was used to measure progression through the cell cycle, in addition to the detection of mitochondria using MitoTracker Green.

Ovcar-8 and Ovcar-3 cells (5 x 10^5 cells/well) were seeded in 6-well plates and incubated for 24 hours at 37°C, before exposure to 1-20 µM pitavastatin or solvent for 48 hours. Adherent cells were then trypsinised and combined with the supernatant containing the detached cells, centrifuged at 150 g for 3 minutes, and re-suspended in FBS-free medium containing 100 nM MitoTracker Green FM (Invitrogen). Cells were incubated for 30 minutes at 37°C, after which the cells were centrifuged at 150 g for 3 minutes and re-suspended in 0.5 mL PBS.

For PI staining, after cell collection and centrifugation as described above, Ovcar-3 cells were re-suspended in 500 µL cold PBS and fixed by the drop wise addition of 5 mL cold 70% ethanol whilst vortexing the cell suspension. The cell suspension was

incubated at 4°C for 24 hours, and subsequently centrifuged at 200 g for 10 minutes at 4°C using an IEC Centra-8R centrifuge. The supernatant containing ethanol was removed and the cell pellet was washed in 1 mL cold PBS by centrifugation a further two times. Cells were re-suspended in 500 µL cold PBS and stained with 50 µL PI/RNase staining solution (500 µg/mL PI (Sigma-Aldrich) and 0.5 mg/mL heat treated RNase (Sigma-Aldrich)) for 30 minutes at room temperature in the dark.

A Beckman Coulter Cytomics 500 flow cytometer with CXP software was used to acquire data. The forward scatter versus side scatter plot was used to identify and gate the cell population and, after exclusion of doublets (identified using a peak pulse height versus integral fluorescence (area) plot), fluorescence data was collected in the FL1 (MitoTracker Green FM staining) and FL3 (PI staining) channels. Data acquired for unstained cells was used to eliminate auto fluorescence. Flow cytometry data was analysed using Flowing Software (Perttu Terho, Turku Centre for Biotechnology, University of Turku, Finland).

3.9.8 Fluorescence Microscopy

Immunofluorescence is commonly used to label a specific protein with an antibody, which is then conjugated to a fluorophore and detected using fluorescence microscopy. This technique can be employed to determine the abundance or cellular localisation of a protein. The development of fluorescent probes which can pass through viable cell membranes has enabled the monitoring of proteins and organelles in live cells by fluorescent microscopy.

Ovcar-8 cells (7 x 10^5 cells/well) were grown on sterile glass coverslips in 6-well plates for 24 hours, before exposure to 3-10 μM simvastatin or solvent for a further 24 hours. Cells were then exposed to growth medium or PBS supplemented with simvastatin or solvent for 2 hours, before fixing in 3% paraformaldehyde (Sigma-Aldrich) for 20 minutes at room temperature. Cells were permeabilised with 0.4% Triton X-100 (Sigma-Aldrich) in PBS for 10 minutes, and then blocked in PBS supplemented with 1% BSA for 30 minutes. Cells were subsequently incubated with anti-Rab7 and anti-LC3 antibodies diluted in PBS supplemented with 1% BSA for 1 hour at room temperature (antibody dilutions are described in appendix 3). This was followed by three washes in PBS and incubation in Alexa Fluor 568 anti-rabbit antibody or Cy2 anti-mouse antibody diluted in PBS supplemented with 1% BSA for 1 hour at room temperature in the dark (antibody dilutions are described in appendix 3). After a further three washes in PBS, Fluoro-Gel mounting medium (Interchim) containing 4',6-diamidino-2-phenylindole (DAPI) was used to mount the glass coverslips onto slides and stain the nuclei. Images were captured using a Nikon Eclipse Ti-S fluorescence microscope.

For live cell imaging, Ovcar-8 and Ovcar-3 cells in 6-well plates were exposed to drug as described in section 3.9.7 and incubated with 100 nM MitoTracker Green FM and 5 μg/mL Hoechst 33258 solution (Sigma-Aldrich) for 30 minutes at 37°C. Images were captured using a Nikon Eclipse Ti-S fluorescence microscope.

3.10 Tumour Xenograft Studies

Xenograft studies were completed by Charles River Discovery Research Services in Morrisville, North Carolina. Female CB17 severe combined immunodeficiency (SCID) mice at an age of 8-12 weeks were subcutaneously injected in the flank with 1 mm^3 Ovcar-3 tumour fragments propagated from Ovcar-3 cells (ATCC). Drug treatment was started when tumours had reached an average size of 80-120 mm^3. Pitavastatin calcium was prepared in 0.5% carboxymethyl cellulose in sterile water. Vehicle consisted of 0.5% carboxymethyl cellulose in sterile water. In a maximum tolerated dose (MTD) study, mice were treated with 26.32 mg/kg, 39.47 mg/kg, 52.63 mg/kg, 78.95 mg/kg or 157.89 mg/kg pitavastatin every 12 hours for 14 days (5 mice in each group). In the subsequent xenograft study, mice were treated with 78.95 mg/kg pitavastatin (MTD) or vehicle alone every 12 hours orally for 33 days (10 mice in each group). Mice were monitored on a daily basis, and body weight and tumour size were measured twice a week. The endpoint of the study was 33 days, after a mean tumour weight of 1000 mm^3 in the control group had been reached. At the end of the study, all mice were euthanized. Tumour samples were taken from three mice in both the control and pitavastatin-treated groups and stored at -80°C.

3.11 Detection of Proteins in Tumour Tissues

Approximately 50-100 mg of each tumour sample was cut into small pieces and homogenised in 60 µL (per 5 mg tumour tissue) RIPA buffer containing proteases and protease inhibitors (20 mM Hepes, 150 mM NaCl, 2 mM EDTA, 0.5% sodium deoxycholate, 1% NP40, 120 µM leupeptin, 10 µM pepstatin, 1 mM PMSF, 20 µg/mL

soybean trypsin inhibitor (SBTI, Sigma-Aldrich) and 0.05 TIU/mL aprotinin (Sigma-Aldrich)) using a dounce homogeniser to a liquid consistency. Tissue lysates were incubated at 4°C with rocking for a further 2 hours to allow complete cell lysis. The tissue lysate suspension was centrifuged, the supernatant collected, and the protein concentration determined as previously described in section 3.9.3. Proteins in the tissue lysate were separated and detected by western blotting (section 3.9.3).

3.12 Pitavastatin Extraction from Tumour Tissues

A sensitive method for the estimation of pitavastatin in biological samples using Solid Phase Extraction (SPE) and liquid chromatography has previously been developed [453]. SPE is a form of chromatography used to isolate an analyte from a solution. Reversed phase SPE involves a polar mobile phase and a nonpolar stationary phase. The solid phase is composed of silica packing modified with hydrophobic alkyl and aryl groups. Retention of pitavastatin from the polar lysis buffer is achieved through van der Waals or dispersion forces acting between carbon-hydrogen bonds in the analyte and the nonpolar groups on the silica surface. Furthermore, polar interactions (for example, hydrogen bonding) between residual unreacted silanols on the solid phase and hydroxyl groups of pitavastatin can also contribute to retention, and therefore, an acidic conditioning solution (0.5 M monobasic potassium phosphate) has previously been used to optimise the retention of pitavastatin [453]. A more polar solvent (methanol) is used to disrupt the hydrogen bonding and van der Waals forces to elute pitavastatin from the column. Pitavastatin can then be analysed by high-performance liquid chromatography (HPLC).

Approximately 50-200 mg of each tumour sample was cut into small pieces and homogenised in 200 µL PBS to a liquid consistency using a dounce homogeniser. The resulting suspension was centrifuged at 10,000 g for 10 minutes at 4°C and the supernatant was collected. A Supelclean LC-18 SPE tube (SupelCo) for each suspension was conditioned with 3 mL 99% methanol, followed by 3 mL deionised water, and then 3 mL 0.5 M monobasic potassium phosphate (Sigma-Aldrich), allowing each solution to pass through the matrix using positive pressure. The sample was then transferred to the tube, and once in the matrix, the tube was washed with 3 mL 0.5 M monobasic potassium phosphate, followed by 3 mL deionised water to remove weakly retained materials. Pitavastatin was then eluted from the matrix by the addition of 3 mL 99% methanol to the tube. The eluate was collected and dried in a SpeedVac at 45°C to complete dryness. The resulting residue was re-suspended in 100 µL 99% methanol for HPLC analysis or growth medium for cell growth assays (section 3.7.2).

HPLC analysis was completed by Dr Clare Hoskins at the School of Pharmacy, Keele University, Staffordshire. Pitavastatin standards were prepared in 100% acetonitrile at concentrations between 1 and 50 µg/mL. Samples were diluted 10-100 times in 100% acetonitrile and a 20 µL aliquot of standard or sample was introduced through an injector valve. Separation was achieved on a reversed-phase C18 column (Metlab Supplies) at room temperature with a mobile phase of acetonitrile:water with 0.1% formic acid (65:35) and a flow rate of 1 mL/minute. Pitavastatin was detected with an excitation of 245 nm and an emission of 420 nm using a JASCO PU-980 HPLC pump coupled to a JASCO FP-920 fluorescence detector (JASCO). Data was acquired using Azur 5.0 software (Datalysis) by measurement of the peak areas. A standard calibration curve was prepared from the pitavastatin standard peak areas and fit using

linear regression. The calibration curve was used to calculate the pitavastatin concentration in each extract sample.

Alternatively, a bioassay was performed in which a range of concentrations of the extract samples, as estimated by the HPLC method, were added to Ovcar-8 cells, and the potency of the extracts were determined by cell growth assays (section 3.7.2). The dose-response curve for authentic pitavastatin was used as a calibration curve, and an equipotent dose was used to determine the concentration of pitavastatin in each sample.

3.13 Extraction of Lipids from Foodstuffs

Eight foodstuffs were obtained for the purposes of extracting lipids. The three organisations which donated mouse chow included Lab Diet NIH 31 0045117 from Charles River in North Carolina, Special Diets Services 801960 BK001(E) from Keele University in the United Kingdom and Open Source Diets D11112201 from University of British Columbia in Canada. Four oils and food replacement drinks obtained in the United Kingdom included Tesco Pure Sunflower Oil produced in the United Kingdom, Sainsbury's Olive Oil produced in Spain, Ensure Plus Raspberry Flavour Drink produced in the European Union and Fresubin 2 kcal Vanilla Flavour Drink produced in Germany. Japonica polished rice (Kinuhikari) was obtained from Japan.

The method used for extracting lipids from foodstuffs is a modification of the "gold standard" methods by Folch [454] and Bligh and Dyer [455] for the isolation of lipids, and is described by [456].

For each foodstuff, 50 g was transferred to a mortar and manually homogenised using a pestle in 30 mL 99% methanol and extracted by further additions of 30 mL 100% chloroform (Sigma-Aldrich) and 30 mL 99% methanol. Japonica polished rice was first homogenised to a fine powder in a Tesco Jug Blender before extraction as described above. The resulting extracts were filtered through fluted filter paper to remove any solid and evaporated to dryness in a round bottom flask using an RE100 rotary evaporator (Fisher Scientific). Liquid foodstuffs were transferred to a separating funnel and extracted with 60 mL 99% methanol and 30 mL 100% chloroform. The lower lipid phase was evaporated to dryness as previously described.

Residues were dissolved in 25 mL 99% ethanol and 25 mL 5 M potassium hydroxide (Sigma-Aldrich) was added for alkaline hydrolysis. The alkaline solution was incubated with stirring at 56°C for 1 hour, and after cooling, neutralised with approximately 25 mL 5 M hydrochloric acid (Sigma-Aldrich). The resulting solution was partitioned with 120 mL 95% n-hexane (Fisher Scientific), 30 mL water and an additional 30 mL 99% ethanol, and the upper organic phase was evaporated to dryness in a pre-weighed round bottom flask using a rotary evaporator. The mass of the extract was determined using a Mettler AE 200 balance before dissolving in DMSO.

Ovcar-3 and Ovcar-8 cells were exposed to the extracts (0.15 mg/mL sunflower oil extract, 0.03 mg/mL olive oil extract, 0.55 mg/mL polished rice extract, 0.04 mg/mL Lab Diet chow extract, 0.02 mg/mL Special Diets chow extract, 0.02 mg/mL Open Source Diets chow extract, 0.03 mg/mL Ensure Plus extract or 0.03 mg/mL Fresubin extract), or 10 µM geranylgeraniol, either alone or in combination with pitavastatin in cell growth assays (section 3.7.2) or caspase 3/7 assays (section 3.7.8), as previously described.

CHAPTER 4

PRECLINICAL EVALUATION OF SIMVASTATIN AS A TREATMENT FOR OVARIAN CANCER

4.1 Introduction

Hypercholesterolemia was identified as a risk factor for the development of coronary heart disease during the middle of the last century and with this came the search for novel drugs that could be utilised to lower plasma cholesterol. Cholesterol is synthesised by the mevalonate pathway, as discussed in chapter 1, in which the enzyme, 3-hydroxy-3-methylglutaryl coenzyme A reductase (HMGCR) catalyses the synthesis of mevalonate from 3-hydroxy-3-methyl-glutaryl coenzyme A (HMG-CoA). Mevalonate is then converted into isopentenes (5 carbon atoms), which are subsequently conjugated to form farnesyl diphosphate (FPP, 15 carbon atoms) and geranylgeranyl diphosphate (GGPP, 20 carbon atoms). Cholesterol is synthesised from FPP via a series of biochemical steps [457]. HMGCR is the rate-limiting enzyme in the mevalonate pathway, and therefore, was a target for the development of inhibitors of this pathway. Lovastatin was isolated from a fermentation broth of *Aspergillus terreus* in 1978, and developed as the first clinically available inhibitor of HMGCR [457]. Simvastatin was developed in the early 1990's as a semi-synthetic derivative of lovastatin, containing an additional side chain methyl group. Simvastatin has been demonstrated to reduce total cholesterol by 19-36%, low-density lipoprotein (LDL) cholesterol by 26-47%, triglycerides by 12-24%, and increase high-density lipoprotein (HDL) cholesterol by 8-12% [458]. Furthermore, simvastatin was the first statin to show a significant reduction in cardiac-related mortality [459].

In addition to the anti-hypercholesterolemia effects, simvastatin has also been shown to inhibit the growth and proliferation of breast [460], melanoma [263], colon [358], lung [461], pancreatic [462], hepatic [229], prostate [463], renal [464], glioma [465], head and neck squamous [466], Hodgkin's lymphoma [467], myeloma [468], Barret's

adenocarcinoma [469], cervical [470], and ovarian [337] cancer cells through their additional effects on isopentenes including FPP and GPP. Both are lipid products in the mevalonate pathway that are used by prenyltransferases to post-translationally modify several proteins including the small GTPases, Ras, Rho and Rab. Prenylation increases the affinity of these proteins for cellular membranes. The membrane localisation of these proteins is essential for many biological functions, which include regulating cell cycle progression, cell signalling and membrane integrity. The inhibition of the membrane localisation and function of these GTPases by statins is thought to contribute to the anti-cancer effects of statins, including cell cycle arrest, induction of apoptosis, reduction in metastasis and inhibition of angiogenesis (discussed in chapter 1 and reviewed by [471]).

The mechanisms by which simvastatin induces cancer cell death have not been fully determined. Simvastatin induces apoptosis in myeloma [235, 351, 468], lymphoma [350], Hodgkin's lymphoma [467], glioma [342], osteosarcoma [346], breast [330, 472, 473], prostate [232, 364, 474], melanoma [230], Barrett's esophageal [475], colon [336, 358, 476], ovarian [267, 337, 477], lung [331, 461], hepatic [229, 478], cholangiocarcinoma [479], and renal [464] cancer cells through the intrinsic apoptosis pathway, and in some cases through activation of the extrinsic apoptosis pathway.

Autophagy is a process where cellular organelles and proteins are degraded and recycled during conditions of nutrient starvation and metabolic stress. The function of autophagy in cancer is currently under investigation. High levels of autophagy may promote cancer cell death and this is supported by studies demonstrating that agents which induce autophagy potentiate cancer cell death [308, 309]. However, there is increasing research that supports the hypothesis that cancer cells undergo autophagy

as a mechanism of cell survival during stress conditions such as exposure to chemotherapy. Indeed, the inhibition of cisplatin-induced autophagy using 3-methyladenine or chloroquine increased the sensitivity of ovarian cancer cells to cisplatin [307, 480]. Furthermore, inhibition of the autophagic response in glioma cells sensitised cells to simvastatin-induced apoptosis [317]. An induction in autophagy in response to simvastatin exposure has been reported in several cancer cell lines including human rhabdomyosarcoma cells [481], and glioma cells [317], but not hepatoma cells [481]. There are at least two possible explanations for this as statin-induced autophagy may contribute to either cancer cell survival or death. Further research is required to determine the effects of simvastatin on autophagy and its contribution to cell death in ovarian cancer cells.

Clinical trials evaluating simvastatin for the treatment of cancer have had varied outcomes. In non-small lung cancer, several studies by Han and colleagues found that adding standard dose simvastatin (40 mg/daily) to chemotherapy did not improve either the time to progression (TTP) or the one-year survival rate [409, 410]. More recently, the addition of simvastatin 40 mg once daily to gemcitabine in patients with advanced pancreatic cancer did not improve TTP or expected one-year survival rates [411]. Standard doses of simvastatin have previously been observed to provide plasma concentrations (C_{max} ~10 nM [424]) that are significantly below the drug concentration required for anti-cancer activity in preclinical laboratory studies. This may go some way to explaining why clinical trials utilising standard doses of simvastatin have been unsuccessful. When the pharmacokinetics of simvastatin were evaluated at the maximum tolerated dose (MTD, 7.5 mg/kg twice daily) in patients with refractory and relapsed chronic lymphocytic leukemia (CLL), the peak plasma concentrations ranged from 0.08 - 2.2 μM [482]). These concentrations are

significantly lower than those required for anti-cancer activity in CLL *in vitro*, (10 - 50 μM [483]) and may limit the success of simvastatin in clinical trials. A previous study, where the MTD of simvastatin was administered combination with chemotherapy to patients with myeloma, was discontinued due to poor response [418]. One possibility is that the short half-life of simvastatin (2-3 hours) may allow the synthesis of isoprenoids in the mevalonate pathway in between simvastatin doses, thereby overcoming the anti-cancer activity of the statin. Increasing the frequency of simvastatin dosing or use of an alternative statin with a longer half-life would be required to overcome this.

Clinical trials of novel anti-cancer agents are generally conducted using either the drug as a single agent or in combination with existing therapy. Previous studies have reported that statins are synergistic with cisplatin in ovarian cancer cell lines [337, 484]. However, tumour resistance to cisplatin is common and therefore, simvastatin should also be evaluated in combination with the first line chemotherapeutic agents, carboplatin and paclitaxel.

4.2 Aims

The research in this chapter aimed to evaluate the activity of simvastatin as a single agent in a panel of ovarian cancer cell lines, to further understand the mechanism by which simvastatin elicits anti-cancer activity including the impact on the autophagy pathway, and to determine if simvastatin should be used in combination with carboplatin.

4.3 Results

4.3.1 Statins inhibit the growth of ovarian cancer cell lines

Cell proliferation assays were used to determine the concentration of drug at which 50% of cell growth was inhibited (IC_{50}) as a measure of potency. Results obtained previously by Mandrita Nandi suggested that the lipophilic statins, fluvastatin and simvastatin, were consistently more potent than statins that were more water soluble. In seven ovarian cancer cell lines, fluvastatin and simvastatin had IC_{50} values ranging between 1 µM and 20 µM, whereas rosuvastatin and atorvastatin had slightly greater IC_{50} values of between 3 µM and 32 µM (figure 4.1, results obtained as part of an MSc project by Mandrita Nandi).

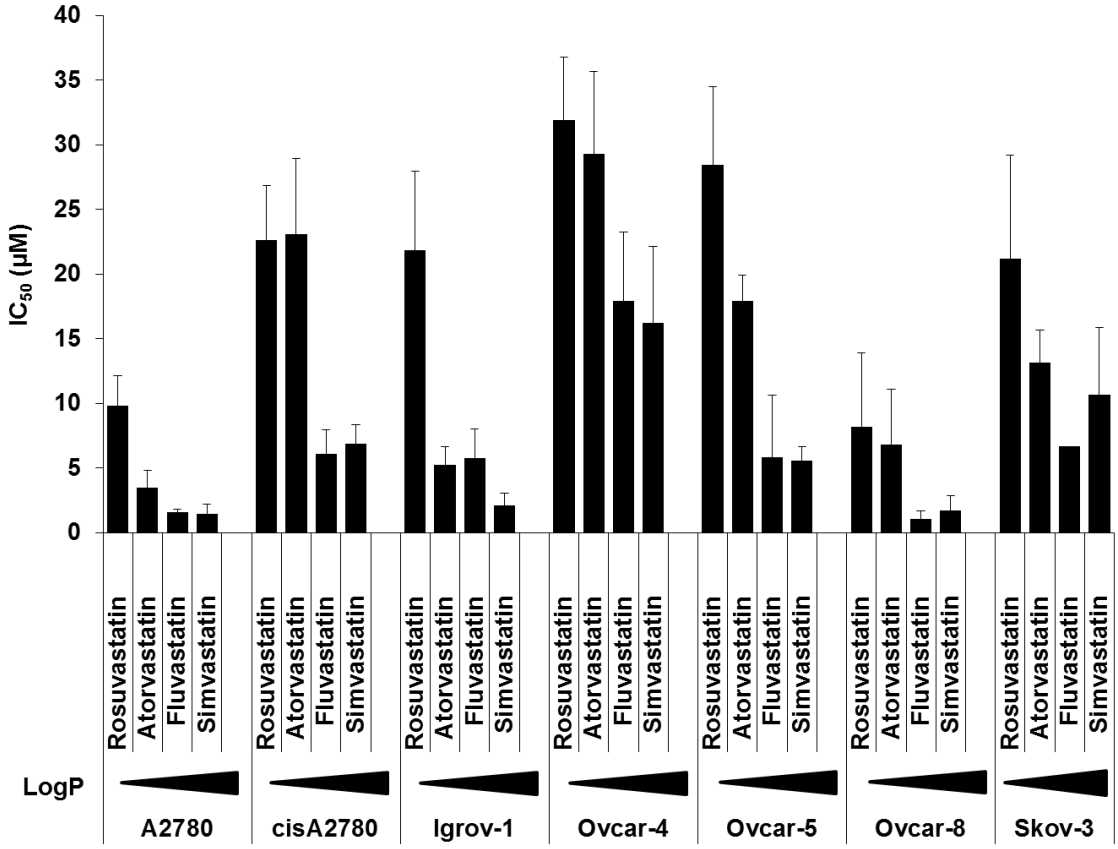

Figure 4.1: The activity of four statins in a panel of ovarian cancer cell lines. ($IC_{50,}$ mean ± S.D., n = 3-7). Increasing lipophilicity is represented by the triangle showing increasing logP. Data obtained as part of an MSc project by Mandrita Nandi.

To determine if the anti-proliferative activity of simvastatin had resulted from inhibition of HMGCR, Ovcar-8 cells exposed to simvastatin were supplemented with mevalonate, farnesol or geranylgeraniol. The addition of mevalonate to Ovcar-8 cells significantly inhibited the anti-growth effects of simvastatin (figure 4.2). Furthermore, supplementing simvastatin-treated cells with geranylgeraniol but not farnesol also prevented growth inhibition (figure 4.2). These results suggested that the anti-proliferative activity of simvastatin was mediated though the inhibition of geranylgeranylation.

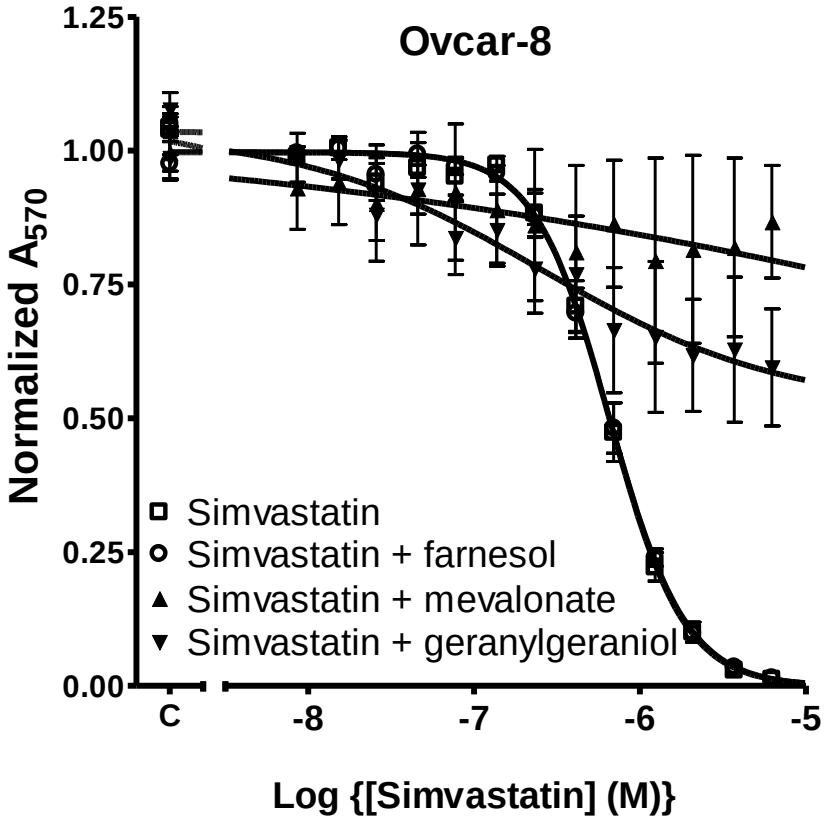

Figure 4.2: Prevention of the anti-growth effects of simvastatin. Ovcar-8 cells were exposed to different concentrations of simvastatin for 72 hours in the presence of 100 μM mevalonate, 10 μM farnesol, 10 μM geranylgeraniol or solvent. The data was represented as a fraction of the top of the curve which was identified by curve fitting (mean ± S.D., n = 3). "C" represents the control cells exposed to solvent alone.

The anti-growth effects of simvastatin have previously been evaluated in monolayer cell cultures. In order to determine the anti-cancer activity of simvastatin in a more physiologically relevant model, ovarian cancer spheroids or aggregates were produced from five ovarian cancer cell lines: A2780, Ovcar-3, Ovcar-5, Ovcar-8 and Igrov-1 (figure 4.3).

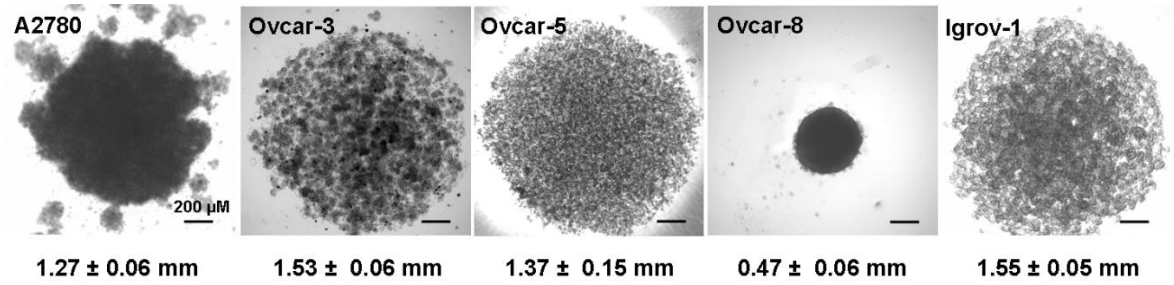

Figure 4.3: Phase contrast microscopy images of ovarian cancer spheroids grown for 7 days. The mean diameter of the spheroid/aggregate is reported below each image (mean ± S.D., n = 3).

The ability of statins to cause cell death in ovarian cancer spheroids was evaluated by measuring ATP in cells exposed to increasing concentrations of simvastatin. The dose-response curves for each ovarian cancer cell line showed a striking decrease in ATP of more than 75% at the highest simvastatin concentrations tested. This was observed in all ovarian cancer cell lines that were tested and suggested a reduction in cell viability (figure 4.4).

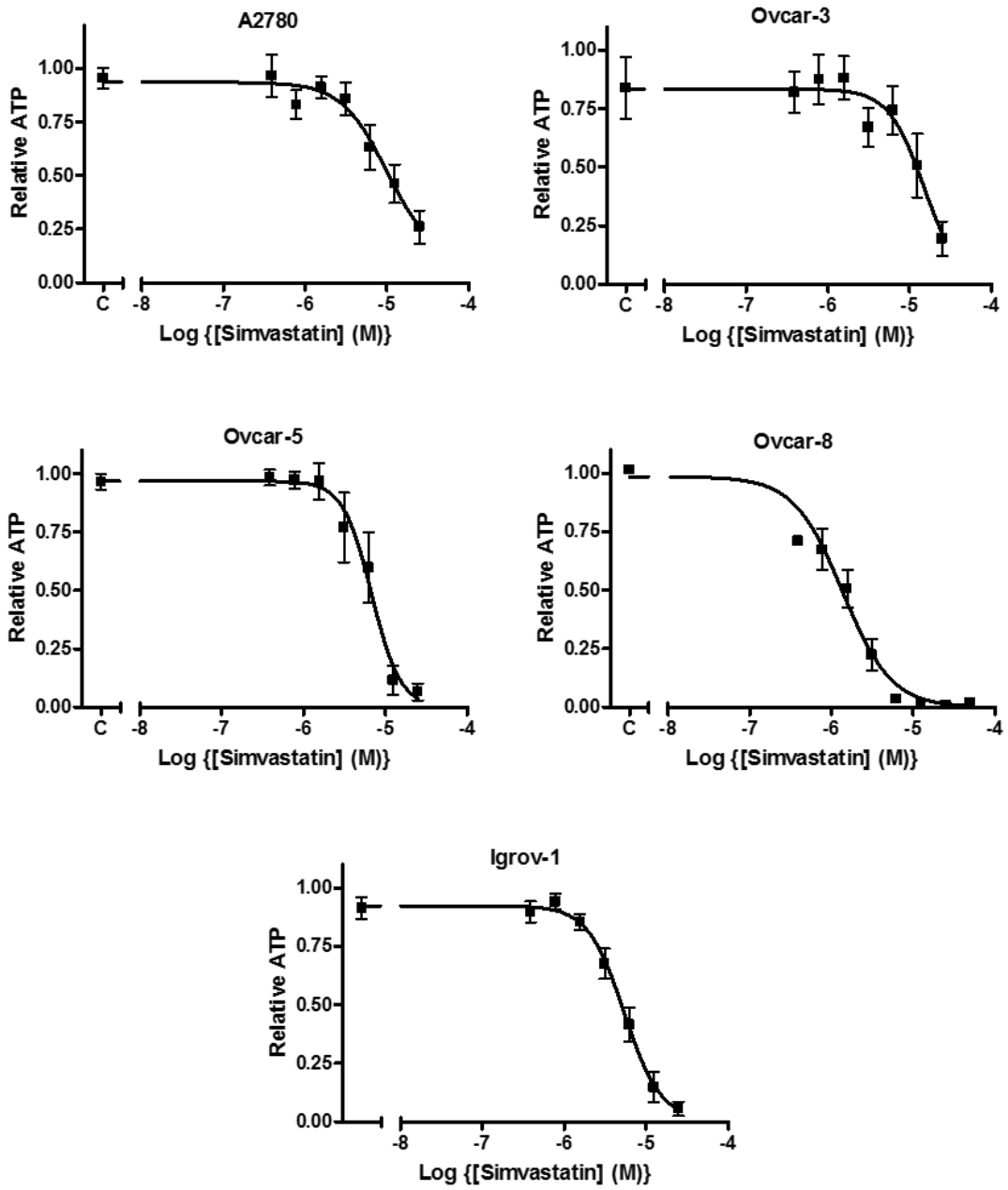

Figure 4.4: Simvastatin dose-response curves in ovarian cancer spheroids. A2780, Ovcar-3, Ovcar-5, Ovcar-8 and Igrov-1 spheroids were exposed to the indicated concentrations of simvastatin for 72 hours and total ATP was measured. The data was represented as a fraction of the top of the curve which was identified by curve fitting (mean ± S.D., n = 5). “C” represents the control samples exposed to solvent alone.

The potency (IC_{50}) of simvastatin in each cell line was compared to the potency previously measured in cell monolayers. The anti-cancer activity of simvastatin was retained in spheroid models, with IC_{50} values ranging between 1 µM and 15 µM (figure 4.5), which in most cases were comparable to the potency measured with cell monolayers. However, the IC_{50} of simvastatin measured in Igrov-1 spheroids and particularly in A2780 spheroids was significantly higher than the respective values in monolayer cultures (figure 4.5).

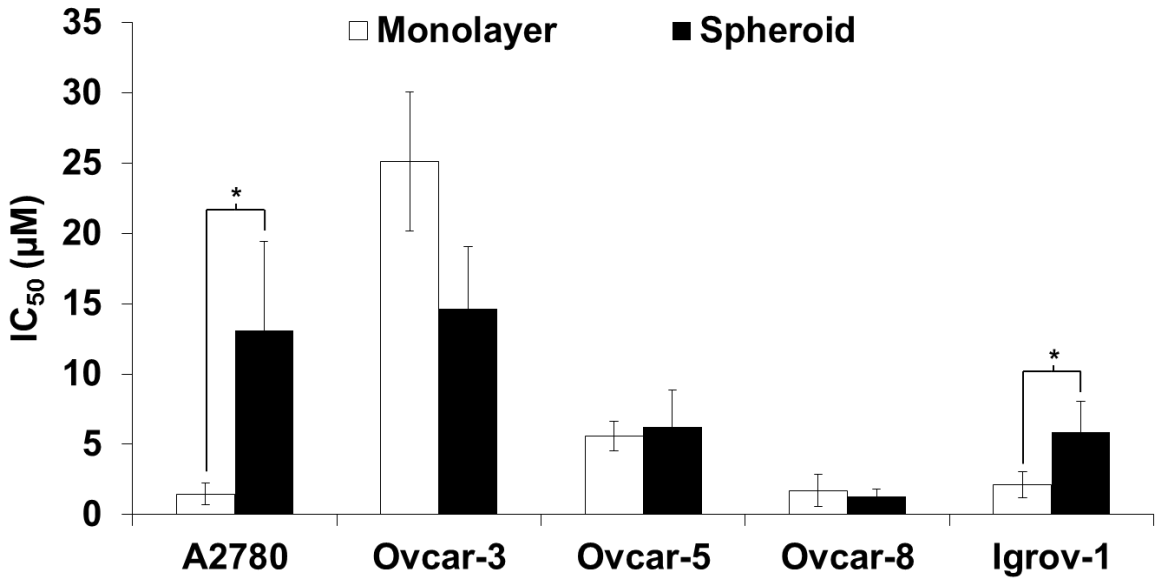

Figure 4.5: The potency of simvastatin in A2780, Ovcar-3, Ovcar-5, Ovcar-8 and Igrov-1 spheroids compared to monolayer cultures (mean IC_{50} ± S.D., n = 5). The duration of simvastatin exposure in monolayer and spheroid cultures was the same (72 hours), however the analysis methods varied (spheroids, ATP assay; monolayer, SRB assay). The IC_{50} was significantly increased in A2780 and Igrov-1 spheroids compared to monolayer cultures (*, paired *t*-test, $P<0.05$).

To determine if there was a correlation between ovarian cancer cell sensitivity to simvastatin and chemotherapeutic agents, the IC_{50} of carboplatin was also determined in ovarian cancer cell monolayers and spheroids. Simvastatin retained potency in cells that were relatively resistant to carboplatin (figure 4.6). Furthermore, there was no significant correlation between the sensitivity of ovarian cancer cells to simvastatin and carboplatin (figure 4.6). This raises the possibility that simvastatin may have activity in chemoresistant disease. This prompted the evaluation of statins in paired cell lines, which were obtained from ovarian cancer patients both before and after the development of resistance to chemotherapy (chapter 5).

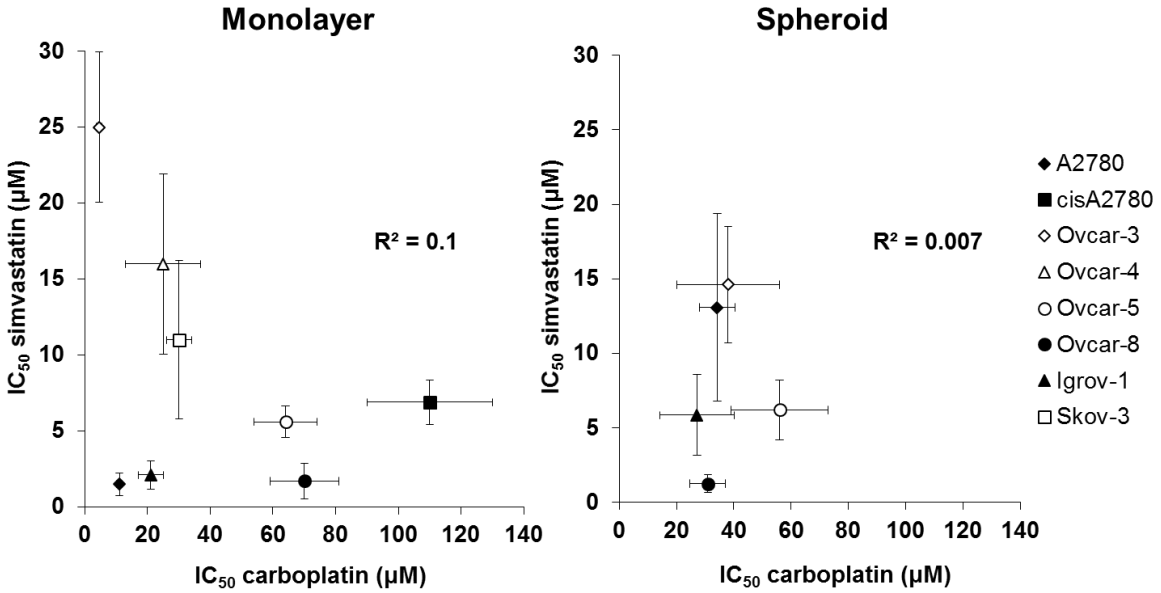

Figure 4.6: The potency of simvastatin versus carboplatin compared between cell lines in both monolayer (left) and spheroid (right) cultures. There was no significant linear correlation between simvastatin and carboplatin activity (Monolayer R^2 = 0.1, mean IC_{50} ± S.D., n = 3-7 and spheroid R^2 = 0.007, mean IC_{50} ± S.D., n = 5).

4.3.2 Kinetics of simvastatin-induced cell death

Simvastatin has a relatively short half-life of around 2-3 hours, and therefore, single daily dosing in patients may allow the plasma concentration of simvastatin to fall below that required for anti-cancer activity. These studies aimed to model the cytotoxic effects of a single daily dose of simvastatin *in vitro* and also determine how long exposure to simvastatin must be maintained in order to induce cell death. Ovcar-8 cells were exposed to simvastatin, at 5 times the IC_{50} measured in cell growth assays, for up to 96 hours. Cell death was determined every 24 hours by quantifying the number of cells that failed to exclude Trypan blue.

Cell death observed after 48 hours of simvastatin exposure was almost undetectable (figure 4.7), however morphological changes were present after 24 hours as some cells had begun to round and detach from the plate (figure 4.8). Significant cell death (figure 4.7) and detachment from the plate (figure 4.8) was observed after 72 or 96 hours of continuous exposure to simvastatin, indicating that prolonged exposure to simvastatin was required for cell death. The commitment to cell death did not occur before 48 hours exposure, because 48 hours exposure to simvastatin followed by 48 hours without simvastatin did not result in significant cell death.

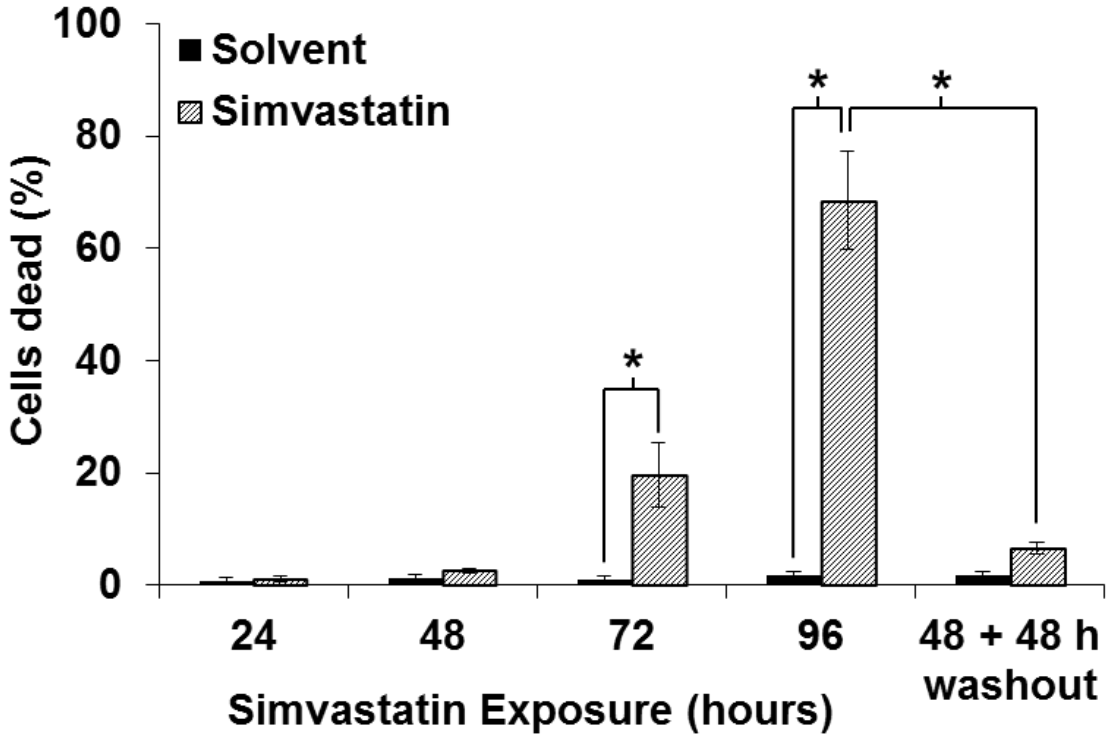

Figure 4.7: Ovarian cancer cell death induced by simvastatin. The number of dead Ovcar-8 cells was determined by Trypan blue staining, after exposure to drug solvent or 10 µM simvastatin (5 x IC_{50}) exposure for 24-96 hours. Alternatively cells were exposed to simvastatin for 48 hours, then culture medium ("washout") for a further 48 hours. The results (mean ± S.D., n = 4) are expressed as a proportion of the total cell number at each time point. After exposure to simvastatin for 72 hours or 96 hours, the number of dead cells was significantly increased compared to cells treated with solvent or to cells exposed to simvastatin for 48 hours followed by solvent for an additional 48 hours (1-Way ANOVA, $P<0.0001$; *, Tukey's Multiple Comparison Test, $P<0.001$).

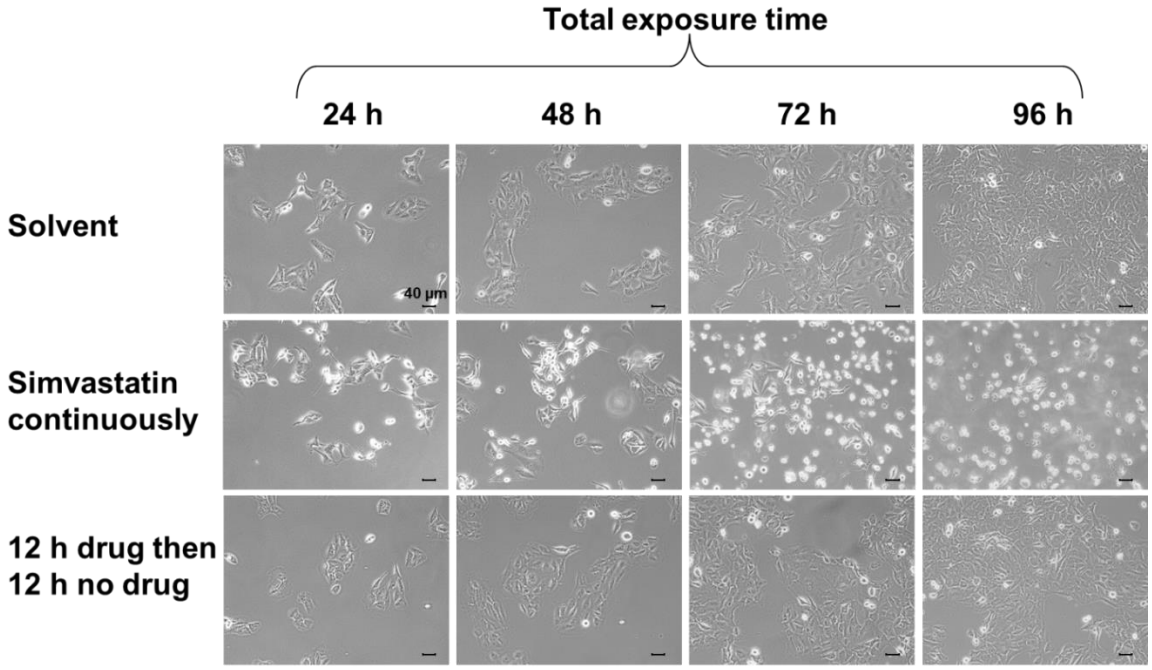

Figure 4.8: Phase contrast microscopy images of ovarian cancer cells exposed to simvastatin. Ovcar-8 cells were exposed to solvent or 10 µM simvastatin (5 x IC_{50}) either continuously for 24-96 hours (h), or pulsed daily (simvastatin for 12 hours followed by no drug for 12 hours) for 96 hours (representative of 3 experiments).

To simulate (in a somewhat crude fashion) patient exposure to simvastatin in a clinical setting, Ovcar-8 cells were exposed to 10 µM simvastatin every 12 hours followed by 12 hours of culture medium without simvastatin. This cycle was repeated for 96 hours or 192 hours.

Cell death occurred in Ovcar-8 cells continuously exposed to simvastatin for 4 days, whereas cells that had been exposed to simvastatin in a pulsatile fashion every 12 hours for a total of 4 days retained viability (figure 4.9) and continued to proliferate (figure 4.8). Ovcar-8 cells were also exposed to pulsed simvastatin for 8 days to ensure that the total exposure to pulsed statin was equivalent to 4 days of continual

exposure. No additional cell death was observed after exposing cells to simvastatin in a pulsatile fashion for 8 days (figure 4.9). These results indicate that continuous blockade of HMGCR is required to cause cell death.

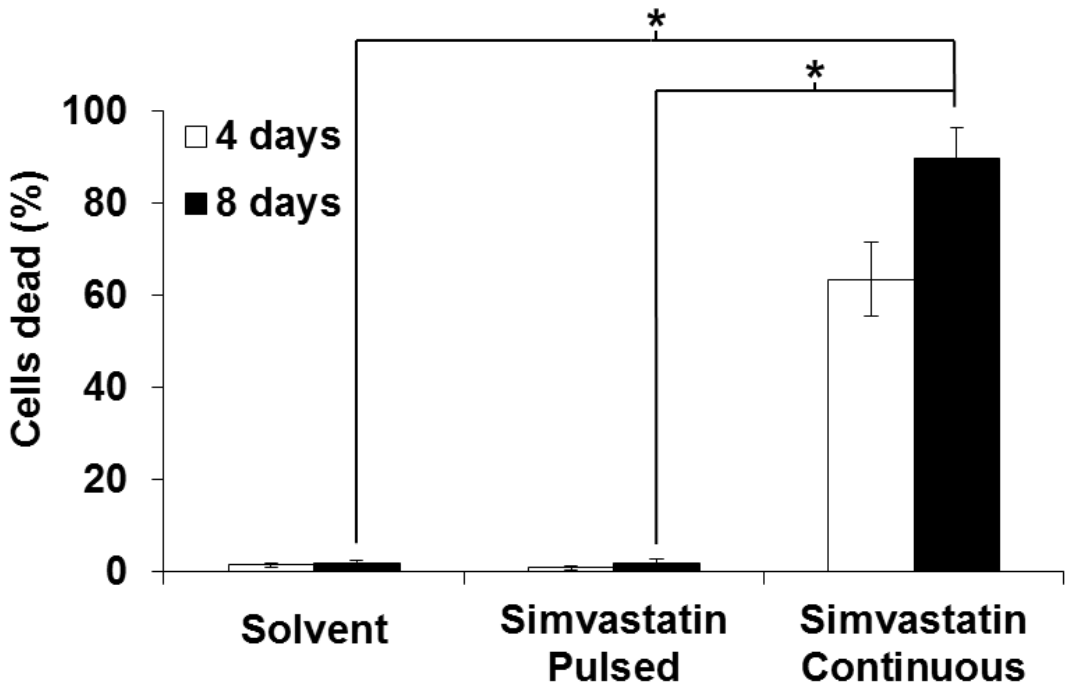

Figure 4.9: The kinetics of simvastatin-induced cell death. The number of dead Ovcar-8 cells was determined by Trypan blue staining after exposure to 10 µM simvastatin (5 x IC_{50}) either continuously or alternating between 12 hour drug exposure and 12 hour no drug ("pulsed") for 4-8 days. The number of dead cells (mean ± S.D., n = 4) was significantly increased in cells exposed to simvastatin continuously compared to cells treated with solvent or pulsed simvastatin (1-Way ANOVA, *P*<0.0001; *, Tukey's Multiple Comparison Test, *P*<0.001).

4.3.3 The contribution of autophagy to simvastatin-induced cell death

Apoptosis has previously been identified as one mechanism of simvastatin-induced cell death in ovarian cancer cell lines [337, 338, 485]. To further identify additional mechanisms by which statins may cause cell death, the autophagy pathway was investigated. Previous studies have reported either an induction or inhibition of autophagy following statin exposure, which may have resulted in cell death [317, 318, 322, 327]. These conflicting results prompted further research into the effects of simvastatin on autophagy in ovarian cancer cell lines.

Statins have been proposed to stimulate autophagy, because they cause an increase in the synthesis of LC3-II. However, LC3-II can also be increased when autophagy is inhibited because the turnover of LC3-II is prevented. To address this, p62 was also measured, as p62 accumulation is a marker of autophagy inhibition [486]. Simvastatin exposure for 8-48 hours resulted in an accumulation of both LC3-II and p62 in a panel of four ovarian cancer cell lines, suggesting an inhibition of autophagy (figure 4.10). However, after 24 hours of simvastatin treatment, a modest reduction in p62 was observed in several cell lines (Ovcar-8 and Ovcar-5), consistent with the turnover of p62 through autophagy, which may be accompanied by a reduction in p62 synthesis.

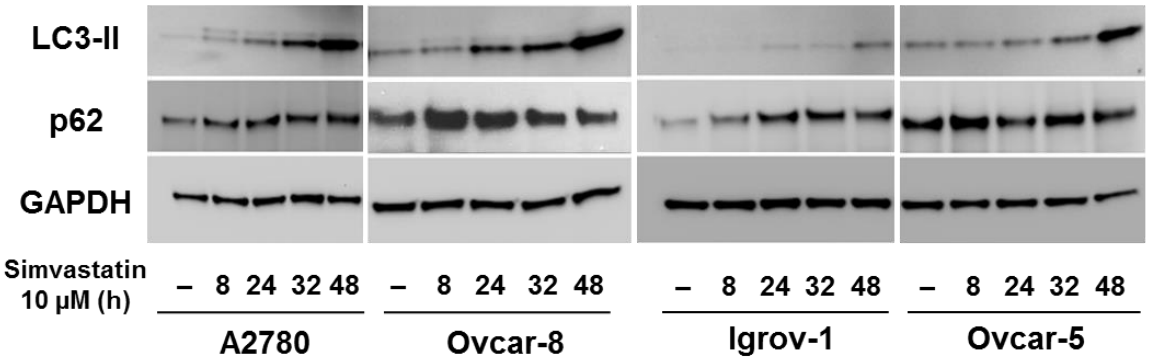

Figure 4.10: The effects of simvastatin on the autophagy pathway. A panel of four ovarian cancer cell lines were exposed to 10 μM simvastatin (5 x IC_{50}) or solvent (-) for 8–48 hours (h). The levels of LC3-II and p62 were measured by western blotting. GAPDH was used as a loading control (n = 3).

It was necessary to determine if the increase in LC3-II observed following simvastatin exposure was due to an induction or inhibition of autophagy, and therefore, a principle method involving the autophagy inhibitor, bafilomycin, was used to measure LC3-II turnover [487]. Bafilomycin inhibits lysosome acidification, which blocks the degradation of LC3-II, and leads to an accumulation of LC3-II [487]. Drugs which further increase LC3-II in the presence of bafilomycin are considered to stimulate autophagy [487]. It was important to achieve full inhibition of autophagy with bafilomycin to ensure that any additional increase in LC3-II following simvastatin exposure could be attributed to an induction in autophagy, rather than an accumulative inhibition. Therefore, the bafilomycin concentration required to completely block autophagy was first determined in a dose-response study.

Preliminary studies demonstrated that Ovcar-8 cells required 30 nM bafilomycin for 2 hours in order to achieve full blockade of the autophagy pathway. No further

accumulation of LC3-II was observed following exposure to higher concentrations of bafilomycin (figure 4.11).

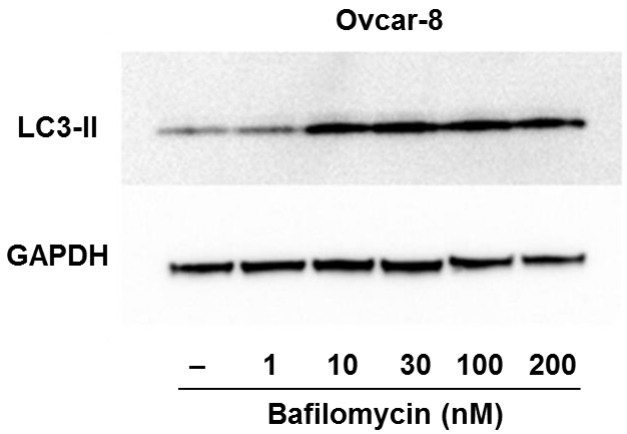

Figure 4.11: The inhibition of autophagy in ovarian cancer cells using bafilomycin. Ovcar-8 cells were exposed to increasing concentrations of bafilomycin (1-200 nM) or solvent (-) for 2 hours, before determining LC3-II levels by western blotting. GAPDH was used as a loading control (n = 2).

When autophagy was maximally inhibited with bafilomycin in Ovcar-8 cells, simvastatin caused a small but significant increase in LC3-II. This was confirmed by quantification of the immunoblot images (figure 4.12). These observations suggest that simvastatin can stimulate the autophagy pathway in Ovcar-8 cells.

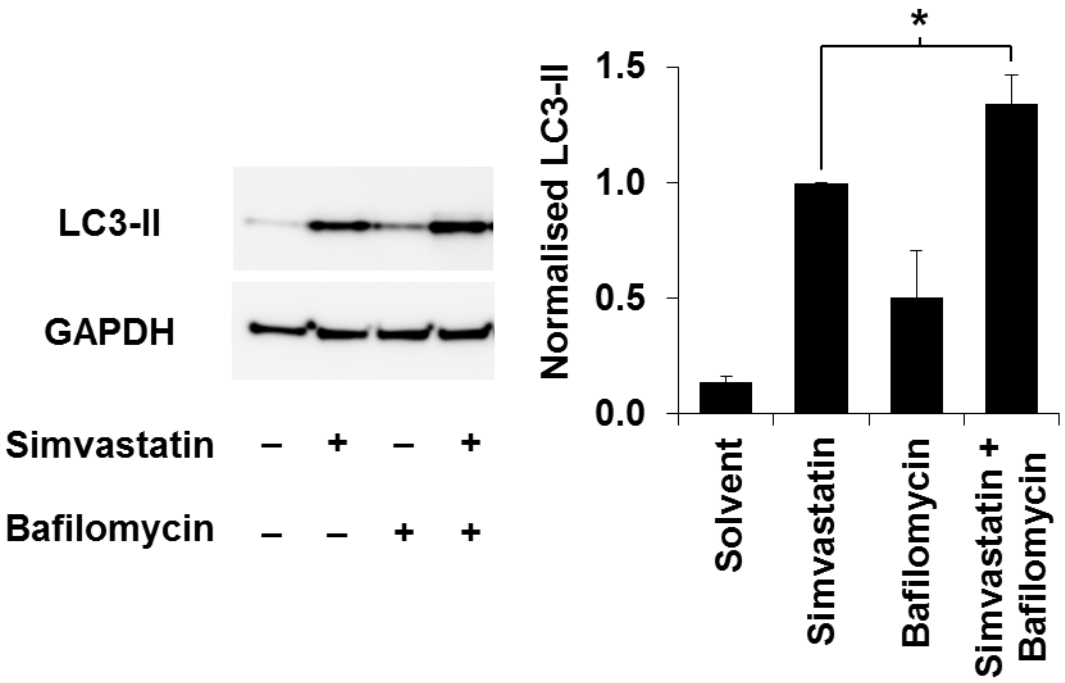

Figure 4.12: The effects of simvastatin on the autophagy pathway in the presence of bafilomycin. Ovcar-8 cells were exposed to 10 μM simvastatin (5 x IC_{50}) or solvent (-) for 48 hours, followed by solvent or 30 nM bafilomycin for 2 hours. LC3-II levels (n = 3) were significantly increased in cells exposed to both simvastatin and bafilomycin compared to cells exposed to only simvastatin (*, paired *t*-test, $P<0.005$). GAPDH was used as a loading control.

The mechanism by which simvastatin effects autophagy was further explored by supplementing statin-treated Ovcar-8 cells with mevalonate, farnesol or geranylgeraniol. The addition of either mevalonate or geranylgeraniol reversed the increase in LC3-II and p62, suggesting that effects on the autophagy pathway were mediated though inhibition of HMGCR (figure 4.13).

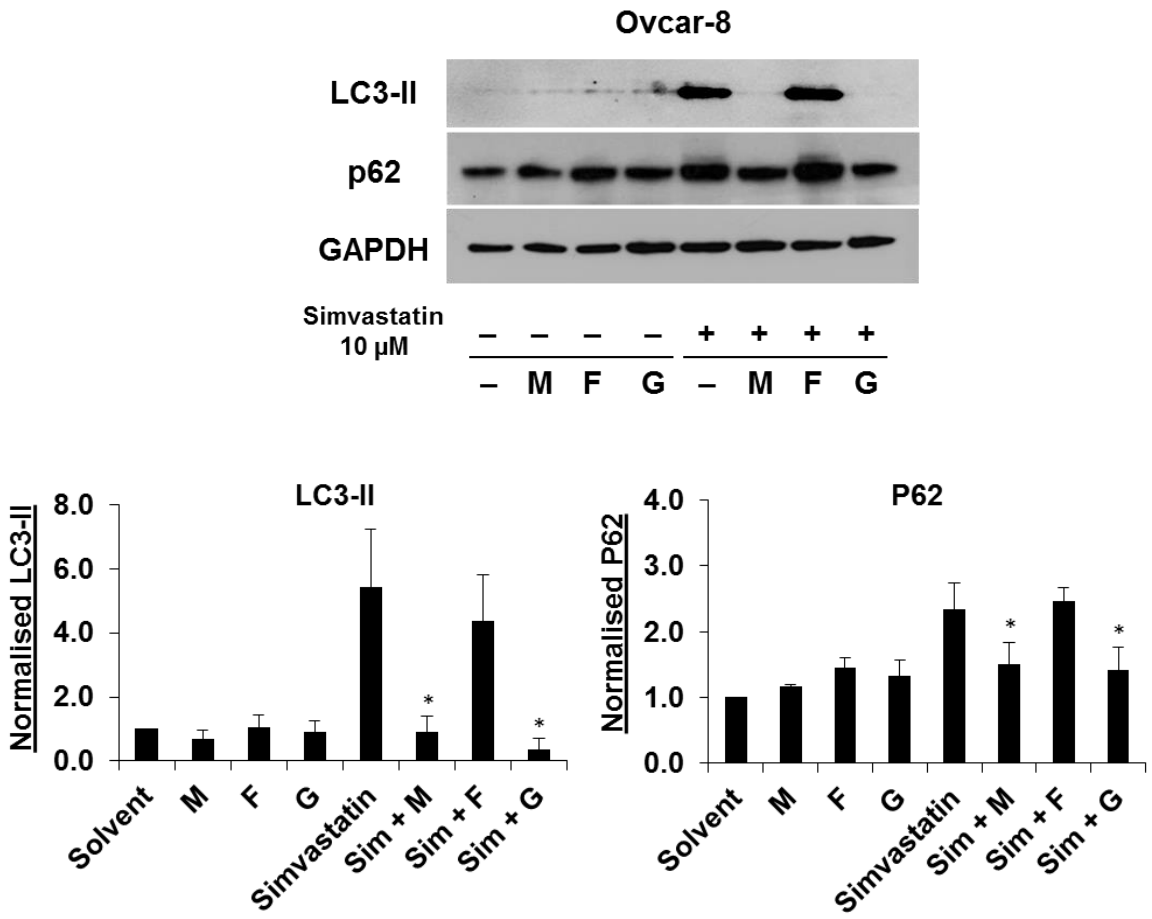

Figure 4.13: Prevention of the effects of simvastatin on the autophagy pathway. Ovcar-8 cells were exposed to 10 µM simvastatin (+, sim, 5 x IC_{50}) or solvent (-) for 48 hours either in the presence of solvent, 100 µM mevalonate (M), 10 µM farnesol (F) or 10 µM geranylgeraniol (G). The levels of LC3-II and p62 were significantly decreased in cells exposed to simvastatin and mevalonate or geranylgeraniol compared to cells exposed to simvastatin alone (1-Way ANOVA, $P<0.05$; *, Tukey's Multiple Comparison Test, $P<0.05$). GAPDH was used as a loading control (n = 3).

The Rab7 GTPase is essential for the regulation of autophagosome trafficking during autophagy, and knockdown of Rab7 resulted in impaired epidermal growth factor receptor degradation and autophagy inhibition [488]. Rab7 geranylgeranylation is required for membrane localisation to late endosomes, and subsequent regulation of autophagy [489, 490]. This raised the possibility that statins may block autophagy by inhibiting the prenylation and function of Rab7. Simvastatin decreased the total amount of Rab7 in Ovcar-5 and Ovcar-8 cells after 24-48 hours of continuous exposure (figure 4.14). Despite this, in A2780 and Igrov-1 cells, Rab7 levels were initially increased, followed by a subsequent reduction after 32-48 hours. This may reflect an initial increase in the synthesis of Rab7, possibly due to a reduction in the amount of Rab7 in the membrane [491]. Rab7 was restored in Ovcar-8 cells following the addition of mevalonate, and modestly, but nevertheless significantly, rescued by geranylgeraniol, suggesting that inhibition of prenylation may have resulted in the reduction in Rab7 (figure 4.14).

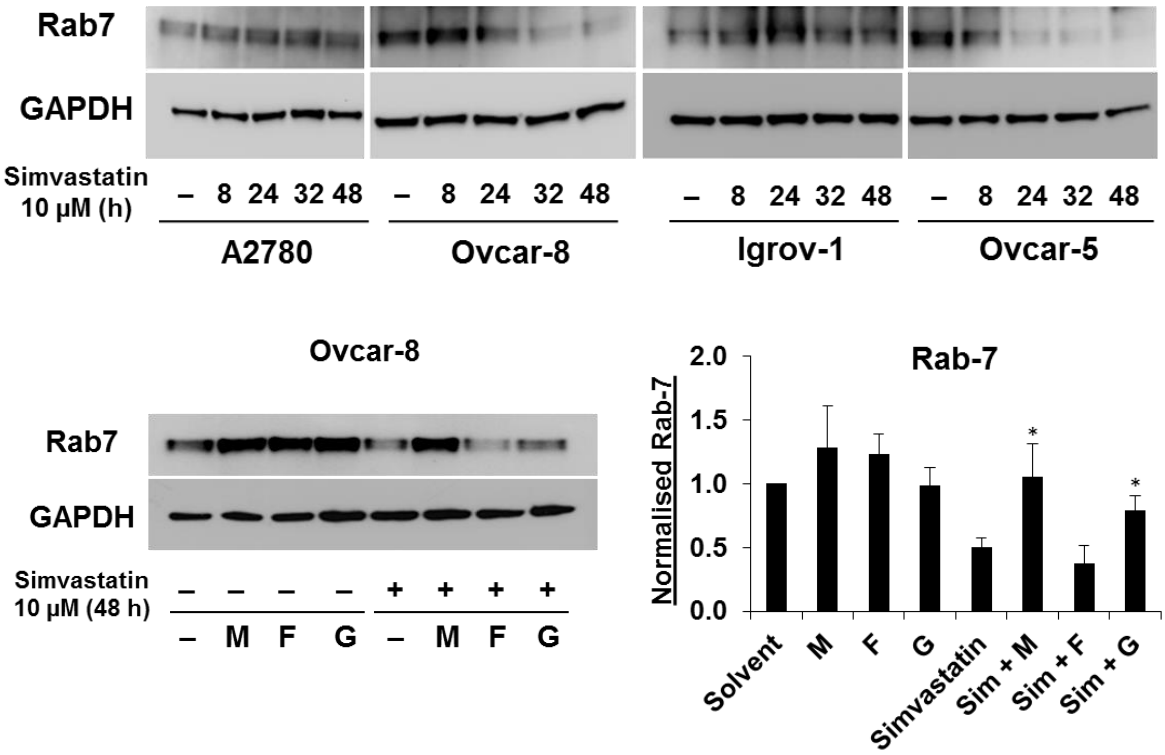

Figure 4.14: The effect of simvastatin on the level of Rab7. A panel of four ovarian cancer cell lines were exposed to 10 μM simvastatin (5 x IC_{50}) or solvent (-) for 8–48 hours (h). The level of Rab7 was measured by western blotting (n = 3). Ovcar-8 cells were also exposed to 10 μM simvastatin (+, sim) or solvent (-) for 48 hours either in the presence of solvent, 100 μM mevalonate (M), 10 μM farnesol (F) or 10 μM geranylgeraniol (G). The level of Rab7 was significantly increased in cells exposed to simvastatin and mevalonate or geranylgeraniol compared to cells exposed to simvastatin alone (1-Way ANOVA, $P<0.05$; *, Tukey's Multiple Comparison Test, $P<0.05$). GAPDH was used as a loading control (n = 3).

Immunocytochemistry confirmed the reduction in Rab7. There was a significant decrease in the number of cells with punctate Rab7 staining following simvastatin exposure (figure 4.15). Although the number of cells with punctate LC3-II staining did not significantly change, the intensity of LC3-II staining increased in cells treated with simvastatin, corresponding to the increase in LC3-II previously observed by western blotting (figure 4.15). Furthermore, induction of autophagy by nutrient deprivation for 2 hours failed to restore Rab7. These results suggested that simvastatin inhibited autophagy by preventing Rab7 activation, and subsequently, autophagosome degradation.

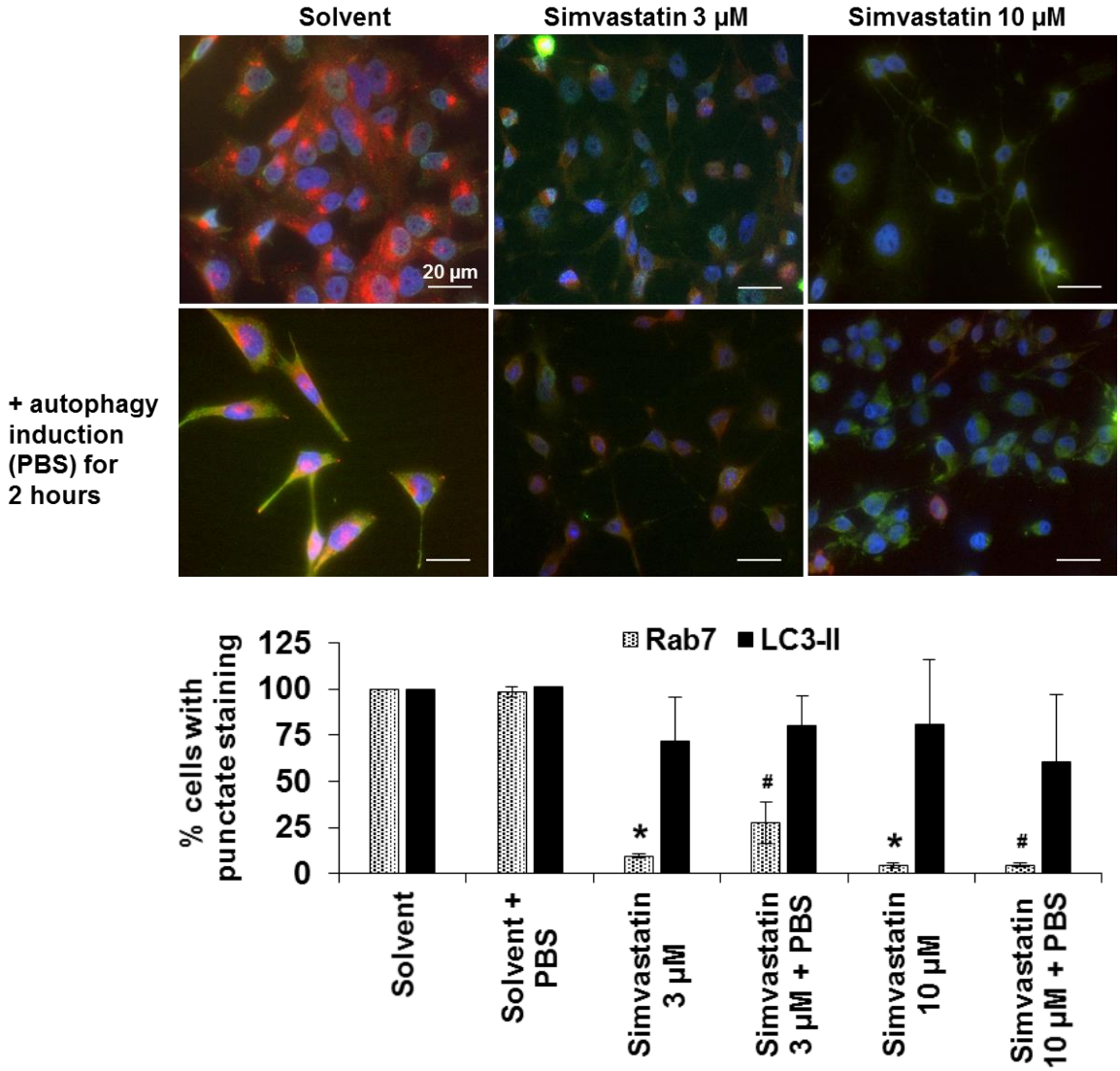

Figure 4.15: The effects of simvastatin on Rab7 and LC3-II immunofluorescence. Ovcar-8 cells were exposed to 3 µM or 10 µM simvastatin (1.5 and 5 x IC_{50}) or solvent for 24 hours (n = 3), and stained for LC3-II (green) or Rab7 (red). Nuclei were stained with DAPI (blue). Other cells were exposed to 3 µM or 10 µM simvastatin for 22 hours, then PBS supplemented with simvastatin or solvent for a further 2 hours. The number of cells with punctate LC3-II or Rab7 staining was quantified in blinded immunofluorescent images (mean ± S.D., n = 3, >100 cells counted per experiment). Rab7 punctate staining was decreased following simvastatin treatment compared to cells treated with solvent (*, paired *t*-test, $P<1\times10^{-6}$), and this was not reversed by nutrient deprivation ($^{\#}$, paired *t*-test, $P<0.01$).

The conflicting effects of statins on autophagy (apparently both stimulating and inhibiting different stages of autophagy) raised the possibility that this contributed to the cytotoxicity of statins. Atg5 is necessary for autophagy as it forms part of a complex which is involved in autophagosome elongation and LC3-II formation [277]. To assess the contribution of autophagy to the cytotoxic effects of simvastatin, Atg5 expression was inhibited by RNA interference (RNAi). Atg5 siRNA was used at a concentration which on its own did not significantly reduce cell viability alone. Knockdown of Atg5 and autophagy inhibition was confirmed by western blotting. Atg5 knockdown somewhat increased the sensitivity of Ovcar-8 cells to simvastatin at high statin concentrations (figure 4.16). Despite this, the IC_{50} of simvastatin after Atg5 knockdown was not significantly lower compared to cells exposed to non-targeting siRNA.

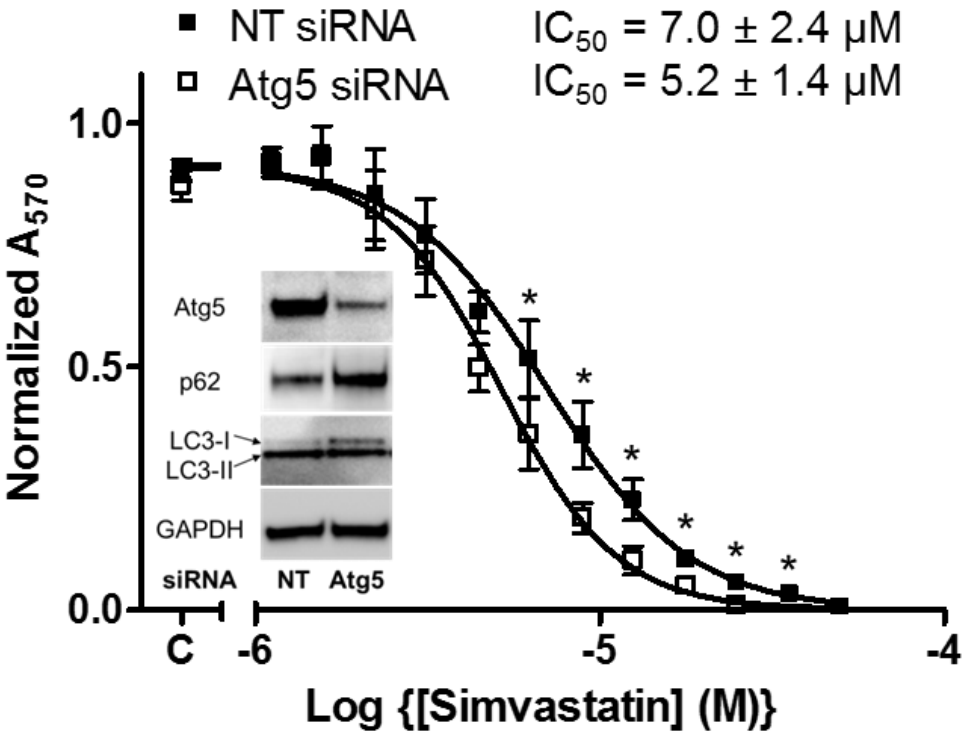

Figure 4.16: The effects of autophagy inhibition by Atg5 knockdown on the potency of simvastatin. Ovcar-8 cells were transfected with Atg5 SMARTpool (20 nM) or non-targeting (NT) SMARTpool for 24 hours, followed by exposure to simvastatin at a range of concentrations for 72 hours. The data was represented as a fraction of the top of the curve which was identified by curve fitting (mean ± S.D., n = 4). "C" represents the control cells exposed to solvent alone. Western blotting (inset) confirmed knockdown of Atg5 and inhibition of autophagy. GAPDH was used as a loading control. Atg5 knockdown increased Ovcar-8 sensitivity to simvastatin at the indicated simvastatin concentrations (*, paired *t*-test, $P<0.05$).

In contrast, inhibition of Beclin 1, an additional protein involved in the initiation of autophagy, did not sensitise Ovcar-8 cells to simvastatin (figure 4.17). There was no significant difference in the potency of simvastatin in cells exposed to Beclin 1 siRNA compared to non-targeting siRNA.

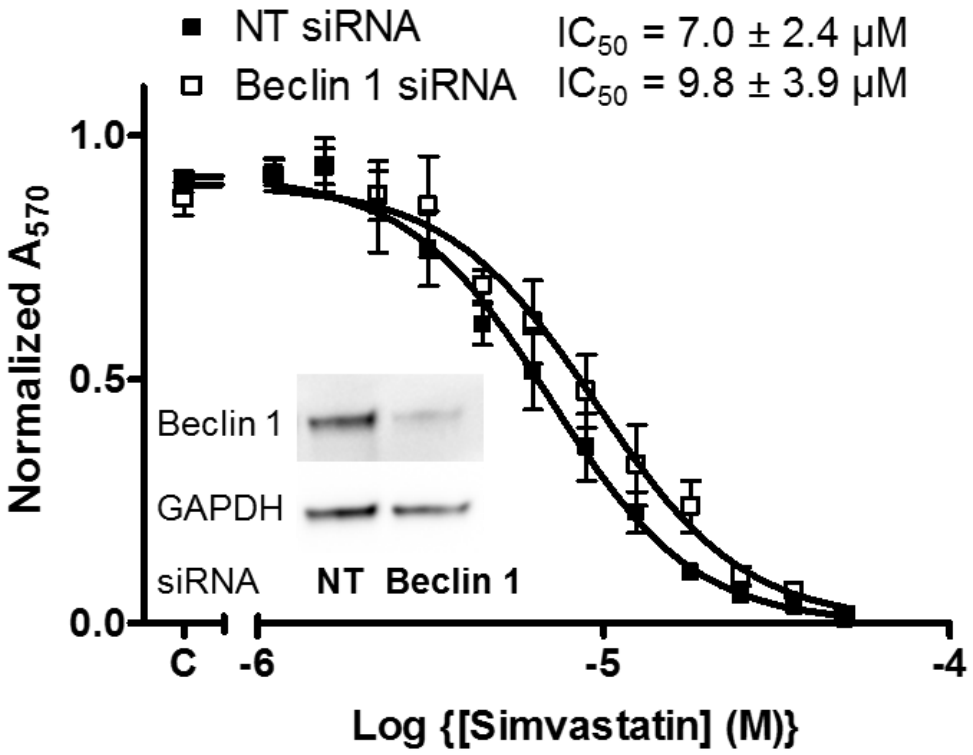

Figure 4.17: The effects of Beclin 1 knockdown on the potency of simvastatin. Ovcar-8 cells were transfected with Beclin 1 SMARTpool (20 nM) or non-targeting (NT) SMARTpool for 24 hours, followed by exposure to simvastatin at a range of concentrations for 72 hours. The data was represented as a fraction of the top of the curve which was identified by curve fitting (mean ± S.D., n = 4). “C” represents the control cells exposed to solvent alone. Western blotting (inset) confirmed knockdown of Beclin 1. GAPDH was used as a loading control.

4.3.4 Simvastatin in combination with chemotherapy

In previous studies, ovarian cancer cell lines were simultaneously exposed to simvastatin and either carboplatin or paclitaxel, combined at a ratio of their single agent IC_{50} values. The combinations were additive or mildly antagonistic (combination index >1), however the antagonism was only statistically significant in one cell line (results obtained as part of an MPharm project by Laurelle Wilkinson). Varying the schedule of drug addition may dramatically influence whether synergy is observed. Witham et al reported that ABT-737 was more effective at sensitising ovarian cancer cells to carboplatin when administered after chemotherapy [450]. Therefore, cells were sequentially exposed to simvastatin and carboplatin for 48 hours, or treated with both simvastatin and carboplatin simultaneously for 48 hours, followed by recovery for a further 48 hours. In each case, the cells were exposed to either drug at a fixed concentration ratio equal to the ratio of the IC_{50}s of the single agents.

The exposure of three ovarian cancer cell lines to simvastatin for 48 hours prior to treatment with carboplatin was profoundly antagonistic compared to treatment with either carboplatin followed by simvastatin or both drugs simultaneously (figure 4.18).

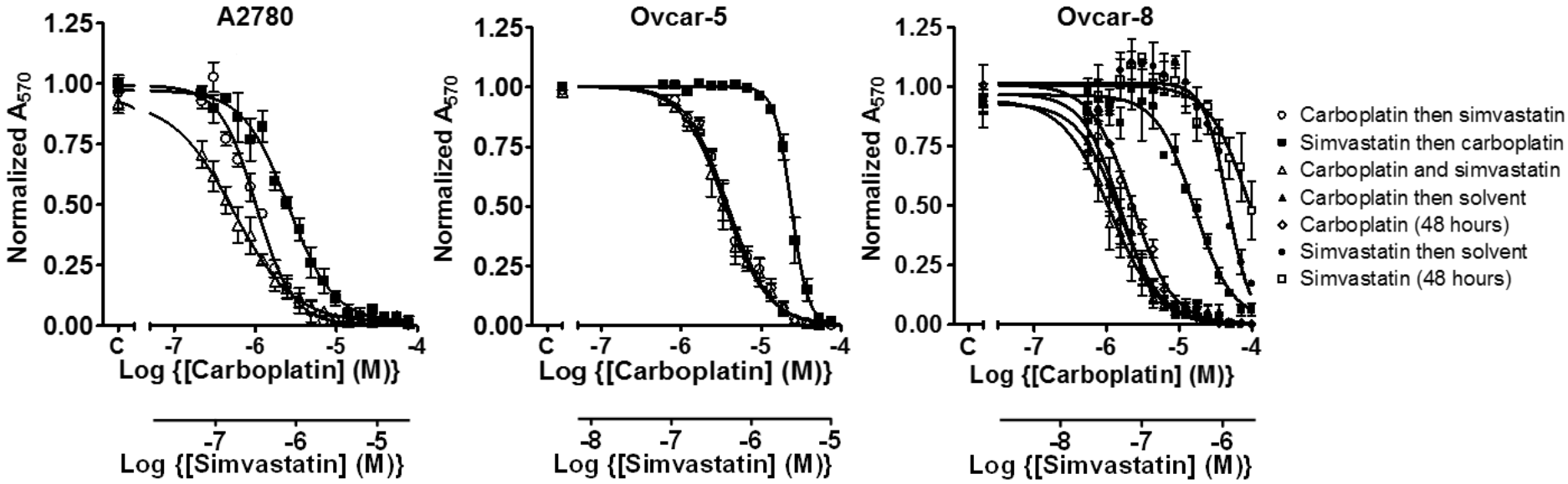

Figure 4.18: Scheduled combinations of simvastatin and carboplatin. Three ovarian cancer cell lines were exposed to a range of concentrations of carboplatin and simvastatin at a ratio of their single agent IC_{50}s. The data was represented as a fraction of the top of the curve which was identified by curve fitting (mean ± S.D., n = 3). "C" represents the control cells exposed to solvent alone. The schedule of drug exposure comprised of treatment with carboplatin for 48 hours then simvastatin for 48 hours, or simvastatin for 48 hours then carboplatin for 48 hours, or simvastatin and carboplatin for 48 hours then no drug for 48 hours. Ovcar-8 cells were also exposed to carboplatin or simvastatin for 48 hours, followed by a further 48 hours in growth medium containing solvent. Alternatively, Ovcar-8 cells were exposed to carboplatin or simvastatin for 48 hours, before fixing in trichloroacetic acid.

This made it important to understand if patients already receiving statins for the treatment of hypercholesterolemia (typical dose is 40 mg of simvastatin) had a reduced response to chemotherapy for ovarian cancer. The maximum plasma concentration achieved following a standard 40 mg dose of simvastatin or atorvastatin for the treatment of high cholesterol is approximately 10-50 nM [424]. However, in the previous experiments, a fixed ratio of carboplatin and simvastatin were used. The concentration at which antagonism was evident (>1 μM) was considerably greater than the plasma concentration obtained in patients receiving a 40 mg daily dose of statin. Therefore, the experiments were repeated with a fixed concentration of statin (100 nM) which is closer to the concentration likely to occur in patients treated for hypercholesterolemia. These studies used the two commonly prescribed statins, simvastatin and atorvastatin.

Pre-treatment of three ovarian cancer cell lines with 100 nM simvastatin or 100 nM atorvastatin for 48 hours prior to carboplatin had no effect on the sensitivity of the cells to carboplatin (figure 4.19). Furthermore, these low statin concentrations have no effect on ovarian cancer cell growth and proliferation.

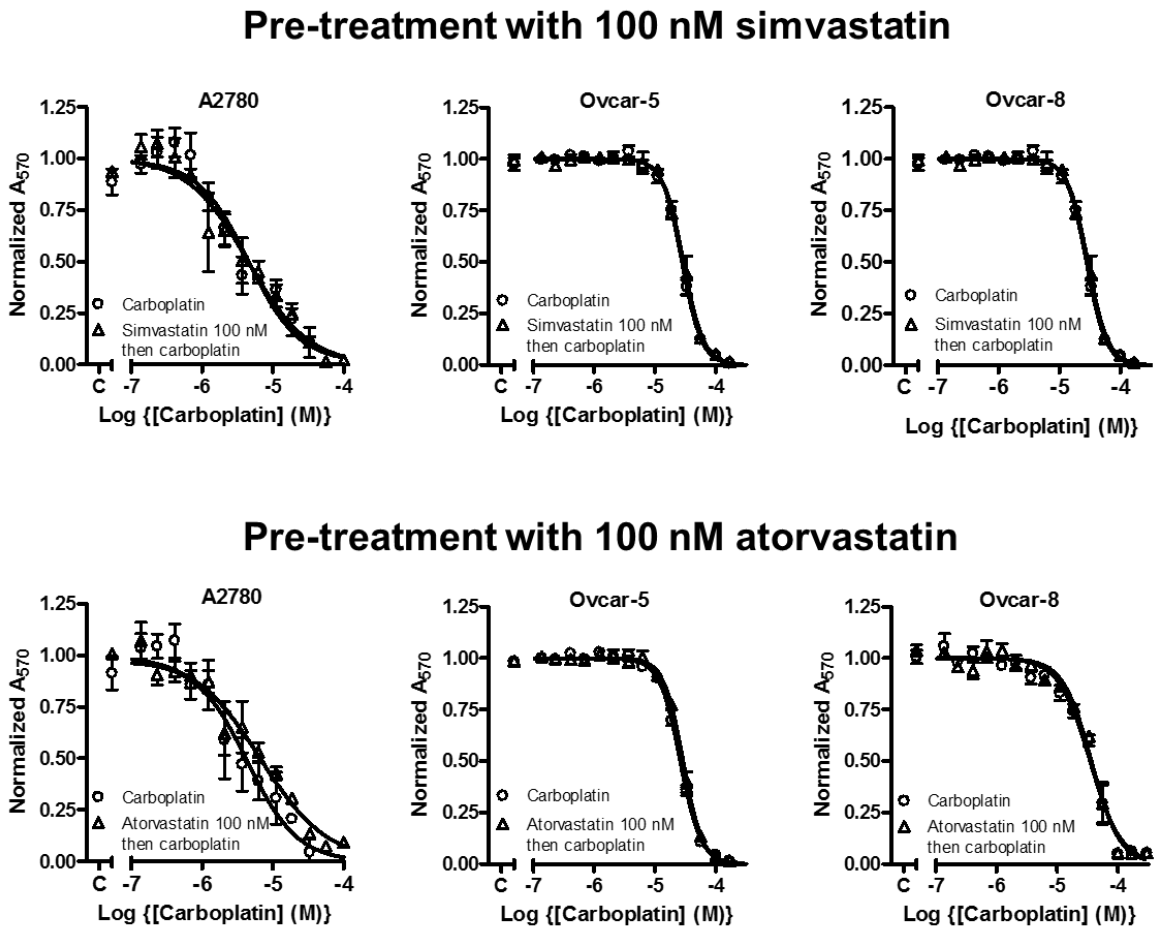

Figure 4.19: Carboplatin in combination with low concentrations of statins. Three ovarian cancer cell lines were pre-treated with 100 nM simvastatin, 100 nM atorvastatin or solvent for 48 hours, then washed, and exposed to a range of concentrations of carboplatin. The data was represented as a fraction of the top of the curve which was identified by curve fitting (mean ± S.D., n = 3). “C” represents the control cells exposed to solvent alone.

4.4 Discussion

A range of statins have previously been evaluated in a panel of ovarian cancer cell lines, demonstrating that the lipophilic statins (simvastatin and fluvastatin) were more potent than the hydrophilic alternatives (e.g. rosuvastatin). This inhibition of cell growth was reversed by the addition of mevalonate or geranylgeraniol, suggesting that these effects were mediated through inhibition of HMGCR. Simvastatin was found to be the most potent statin across most cell lines and was therefore chosen for further analysis. Simvastatin has previously been shown to inhibit the proliferation of cancer cell lines and induce apoptotic cell death (reviewed by [471]). Despite this, clinical trials evaluating both standard doses of simvastatin, used for the treatment of hypercholesterolemia, and the MTD of simvastatin have not been successful at improving patient survival. The studies presented here aimed to evaluate simvastatin as a therapy for the treatment of ovarian cancer, and determine how statins can be used more successfully in the clinic than has been achieved in clinical trials to date.

The cytotoxic activity of simvastatin was confirmed in a spheroid model. Ovarian cancer spheroids are a three-dimensional architecture of cancer cells that potentially more closely resembles cancer in a physiological setting. Simvastatin retained anti-cancer activity in this cellular model, with IC_{50} values similar to those obtained in monolayer cultures, thereby supporting the use of simvastatin *in vivo*. Modest, but nevertheless significant, increases in the IC_{50} of simvastatin in A2780 and Igrov-1 spheroid cultures compared to monolayer cultures could reflect the inability of simvastatin to affect cells contained within the spheroid core. These ovarian cancer spheroids may be more resistant to anti-cancer agents compared to monolayer cultures, which may be due to limited drug penetration into the spheroid and reduced

proliferation of cells contained within the spheroid core [430]. This leaves unanswered the question why simvastatin could (presumably) penetrate the core of the other spheroids.

Further kinetic studies on cell monolayers demonstrated that prolonged and continuous exposure to high concentrations of simvastatin for 72-96 hours was required to achieve cell death. This period may be required to allow the turnover of proteins which are already prenylated before cell death can occur. However, there was no significant cell death after cells were exposed to simvastatin for 48 hours, followed by a further 48 hours without simvastatin. This is in contrast to previous research, which reported a significant increase in caspase 3/7 activity in ovarian cancer cells exposed to simvastatin after 48 hours [492], and suggests that cells can recover from caspase-3 activation. This is supported by increasing evidence which demonstrates that upon removal of the apoptotic stimuli, cells can reverse apoptosis and survive, even after caspase activation and DNA damage [493, 494]. Furthermore, minority mitochondrial permeabilization can lead to limited caspase activation, which results in DNA damage that can promote cellular transformation, but is insufficient to trigger cell death [495]. Therefore, 3-4 days of continuous statin exposure may be required for complete mitochondrial permeabilization and commitment to cell death. This has a number of implications for the use of simvastatin in a clinical setting. Simvastatin has a considerably short half-life of approximately 2-3 hours [424], and therefore, single daily dosing with this statin may allow a period of time when the synthesis of isoprenoids could occur. This is likely to prevent the anti-cancer activities of simvastatin by enabling cancer cells to survive and proliferate. Indeed, ovarian cancer cells exposed to simvastatin in a pulsatile fashion every 12 hours for more than 1 week failed to undergo cell death. This may partially explain the lack of clinical

success that has been achieved with statins to date. Instead, patients may require either several daily doses of simvastatin or continuous infusion to ensure constant inhibition of HMGCR. Alternatively, statins with a longer half-life may be used, which allow less frequent dosing. However, the choice of statin is problematic, because data presented here suggest that lipophilic statins are notably more potent. The commonly prescribed statins that have long half-lives tend to be more hydrophilic compared to simvastatin. The recently developed statin, pitavastatin, is both lipophilic and affords a substantially improved half-life of 11 hours [496]. This may significantly improve drug exposure compared to simvastatin. Pitavastatin is evaluated in chapter 5.

The concentrations of simvastatin required to induce cell death *in vitro* (2-15 μM in ovarian cancer cell lines) are considerably greater than those achieved in the plasma following a 40 mg dose of simvastatin for the treatment of high cholesterol (7.6 - 16.5 nM [424]). Despite this, several clinical trials have evaluated simvastatin at standard doses (40 mg daily) with chemotherapy in patients with non-small lung cancer without success [409, 410]. The plasma concentration obtained in patients following administration of simvastatin at the MTD (7.5 mg/kg twice daily) was 0.08 - 2.2 μM [482], closer to the concentration required for anti-cancer activity *in vitro*. These doses were administered orally for 7 consecutive days during 21-day cycles without significant toxicity [419, 482, 497]. Several studies have reported side effects including fatigue, gastrointestinal symptoms and neutropenia following administration of high statin doses, however these were manageable or tolerable over the short treatment period [419, 497]. Several clinical trials are evaluating high doses of statins for the treatment of cancer [425], although these trials do not currently address the issue of the short half-life of simvastatin. Instead, clinical trials should evaluate simvastatin at high doses with a dosing frequency to maintain suppression of HMGCR.

Novel therapeutic agents are often evaluated in combination with existing chemotherapeutic therapies in oncology. In the case of simvastatin, a synergistic interaction with first line therapy for ovarian cancer (carboplatin and paclitaxel) could lower the concentrations of statin required to cause cell death. These concentrations may be more achievable in patients, and therefore, clinical trials using high doses of simvastatin are more likely to be successful. This may also facilitate the use of lower doses of statins, thereby minimising the adverse effects. However, previous studies have demonstrated additive or modest antagonistic interactions in ovarian cancer cells simultaneously exposed to simvastatin and carboplatin or paclitaxel [492]. In dose scheduling experiments, profound antagonism was observed when cells were exposed to high concentrations of simvastatin prior to carboplatin. One possible explanation is that inhibition of HMGCR by statins results in cell cycle arrest [229, 235], which may render ovarian cancer cells refractory to carboplatin. Chemotherapy is generally considered to be most potent in cells which are proliferating. Carboplatin causes the accumulation of ovarian cancer cells in S- and G_2/M phase of the cell cycle [498], and therefore, prolonged G_1 arrest induced by simvastastin may blunt the pro-apoptotic effect of carboplatin. Taken together, these results suggest that simvastatin (or another statin) is best evaluated in clinical trials as a single agent. Trials could be carried out as “consolidation therapy” in patients who have completed and responded to chemotherapy. Furthermore, simvastatin displayed anti-cancer activity in ovarian cancer cell lines which were relatively resistant to chemotherapy, suggesting that simvastatin could also be used in patients with chemotherapy resistant disease. It is worthwhile noting that in situations where the cancer is advanced, it may be difficult to show a therapeutic benefit following high dose simvastatin treatment.

The significant antagonism observed in cells exposed to simvastatin followed by carboplatin raised the concern that standard doses of statins for the treatment hypercholesterolemia could antagonise chemotherapy prescribed for the treatment of ovarian cancer. The potential impact of this is that patients may benefit from having their statin therapy withdrawn prior to receiving chemotherapy. However, the plasma concentration of statin achieved from a standard dose of simvastatin or atorvastatin is not sufficient to antagonise the anti-cancer effect of carboplatin *in vitro*, suggesting that existing statin therapy should not be an issue.

The mechanism by which statins inhibit growth and induce cell death has previously been explored in ovarian cancer cells. Statins induce G_1 cell cycle arrest [484], apoptosis [337, 338, 485], and more recently, autophagy in other cancer types [317, 322]. In ovarian cancer cells, simvastatin increased the level of LC3-II even when the autophagy pathway was fully blocked with bafilomycin, supporting previous reports that statins stimulate autophagy. P62 was also evaluated as a marker of autophagy, as p62 has been shown to accumulate when autophagy was inhibited [486]. Simvastatin caused an initial accumulation of p62 in all cell lines tested, consistent with autophagy inhibition and a reduction in the turnover of p62. However, this increase in p62 may also reflect an increase in the synthesis of p62. Evidence for p62 induction at the transcriptional level by oxidative stress conditions has been reported [499]. The GTPase Rab7 is essential for the late stages of autophagosome maturation as knockdown of Rab7 has been shown to inhibit autophagy [488]. Prenylation and membrane recruitment is required for the activation of Rab7 [489, 490], raising the possibility that statins may block autophagy through the inhibition of Rab7 activation. Simvastatin significantly decreased the level of Rab7 and this was moderately reversed by the addition of geranylgeraniol, suggesting that statins may block the later

stages autophagy by inhibiting the prenylation and membrane translocation of Rab7. Statin-mediated inhibition of Rab geranylgeranylation has also been demonstrated for Rab5 and Rab6 GTPases [322, 327, 500, 501]. These studies also reported that the addition of geranylgeranyl diphosphate to statin-treated cells restored prenylation and active Rab proteins in several different cancer cell lines [500, 501]. However, two groups reported an induction in autophagy following statin exposure, despite a reduction in Rab5 prenylation [322, 327]. Therefore, it is also possible that statins may only be capable of partially blocking the activity of Rab GTPases, and that remaining prenylated Rab5 or Rab7 may be sufficient to sustain autophagy. This incomplete inhibition of autophagy could account for the modest reduction in p62 levels in several cell lines after 48 hours of simvastatin exposure. Taken together, these results raise the possibility that statins may simultaneously stimulate and inhibit autophagy at different points on the autophagic pathway. Futile cycles have been linked to cell death [502], and this may contribute to the cytotoxic effects of statins. Indeed, inhibition of autophagy using siRNA against Atg5, an essential autophagy-related protein involved in the early stages of autophagosome formation, modestly sensitised cells to simvastatin. Furthermore, another study reported that co-treatment with lovastatin and a farnesyltransferase inhibitor resulted in an inhibition of autophagy and cell death [327]. Conversely, autophagy inhibition using siRNA against Beclin 1 (Atg6), a protein also involved in autophagosome formation, had no significant effects on the sensitivity of cells to simvastatin. Beclin 1 knockdown has previously been reported to inhibit drug-induced apoptosis, and this could go some way to explaining why attenuation of Beclin 1 had no overall effect on cells exposed to simvastatin [503, 504]. In conclusion, whilst the effects of statins on the autophagy pathway may contribute to cell death, it is likely that there are additional mechanisms involved in the

cytotoxicity of statins in ovarian cancer, which are also mediated through the inhibition of HMGCR.

In summary, these results suggested that simvastatin should be evaluated in clinical trials at high concentrations, with an appropriate dosing schedule, which will enable continual inhibition of HMGCR. The short half-life of simvastatin may require a frequent and inconvenient dosing schedule, and therefore, this has led to the pre-clinical evaluation of an alternative statin (pitavastatin) with a longer half-life.

CHAPTER 5

PRECLINICAL EVALUATION OF PITAVASTATIN AS A TREATMENT FOR OVARIAN CANCER

5.1 Introduction

Pitavastatin (NK-104) is a synthetic statin synthesised by Nissan Chemical Industries and developed by Kowa at the beginning of the century [505]. The structure of pitavastatin retains the dihydroxy-heptanoic acid chain, which is responsible for binding to the active site of 3-hydroxy-3-methylglutaryl coenzyme A reductase (HMGCR) [506]. Furthermore, the abundance of hydrophobic moieties in the compound allows the formation of van der Waals interactions with the enzyme [163]. The unique cyclopropyl group may also contribute to effective inhibition of HMGCR. Pitavastatin is moderately lipophilic (*n*-octanol/water partition coefficient (logP) of 1.49) compared to other statins including simvastatin (logP = 1.6) and fluvastatin (logP = 1.27) [162], and this may support passive diffusion across plasma membranes into the cellular cytosol. In addition, pitavastatin is a substrate of organic anion-transporting polypeptide 1B (OATP1B), which also mediates the translocation of pitavastatin into cells located in the liver, kidney and brain [507]. The OATP transporters play a crucial role in hepatic uptake mechanisms, and statins utilise these carriers to gain entry to the liver and inhibit cholesterol synthesis [507]. Pitavastatin has been shown to reduce low density lipoprotein cholesterol to a level comparable to that achieved by simvastatin [508], in addition to increasing high density lipoprotein cholesterol levels [509]. In conjunction with these impressive cholesterol-lowering effects, pitavastatin has also been demonstrated to exhibit cholesterol-independent or “pleiotropic” effects including anti-cancer activity.

Following the success in reducing cholesterol levels, initial studies in the oncology field focussed on the evaluation of pitavastatin in colon or liver tumorigenesis. Pitavastatin inhibited proliferation and induced apoptosis in cholangiocarcinoma cells,

as demonstrated by G_0/G_1 phase cell cycle arrest and an increase in cleaved caspase 3 levels [218]. Furthermore, pre-treatment of these cells with 20 μM pitavastatin for 48 hours prior to gemcitabine, cisplatin or 5-fluorouracil exposure resulted in a synergistic reduction in cell proliferation [218]. However, results from the combination experiments were not compared to the response to single agent pitavastatin, and therefore, the anti-proliferative effects could be attributed to pitavastatin alone. Low concentrations of pitavastatin (0.1-1 μM) decreased tumour necrosis factor-alpha (TNF-α)-induced NF-κB activation, resulting in reduced expression of the pro-inflammatory cytokine, interleukin 6 (IL-6), in breast and liver cancer cells [510, 511]. These effects also contributed to the inhibition of cancer cell growth and proliferation.

Pitavastatin has also been evaluated *in vivo* for the treatment of obesity-related cancers. Pitavastatin significantly inhibited the development of drug-induced liver or colonic preneoplastic lesions in mice [512, 513]. Pitavastatin-induced apoptosis *in vivo* was confirmed by an increase in single-stranded DNA (ssDNA)-positive nuclei [514], increased levels of the pro-apoptotic protein, Bad, and decreased expression of Bcl-2 mRNA [512]. Furthermore, a decrease in the expression of TNF-α, IL-6 and IL-8 was reported, suggesting a reduction in inflammation and an activation of AMP-activated protein kinase (AMPK), all of which can inhibit lipid accumulation [512, 513]. Pitavastatin exposure did not result in significant liver toxicity at the relatively low concentrations used (10 ppm) [512]. In a similar study, pitavastatin decreased drug-induced intestinal polyp formation in mice, possibly by decreasing the expression of *cyclooxygenase-2, IL-6, inducible nitric oxide, monocyte chemoattractant protein-1, and plasminogen activator inhibitor-1* mRNA in intestinal nonpolyp areas [515].

More recently, pitavastatin has been evaluated both *in vitro* and in xenograft studies in human breast and brain cancer [516, 517]. Pitavastatin inhibited the proliferation of cancer cells, induced G_1/S phase cell cycle arrest, and increased the autophagy protein, LC3-II, which could be attributable to an induction or inhibition of autophagy. Jiang and colleagues also reported that pitavastatin did not induce apoptosis [517], however this may reflect the short duration of exposure to pitavastatin, as cells are likely to require the turnover of prenylated proteins before cell death occurs (chapter 4). Furthermore, pitavastatin significantly inhibited the growth of glioblastoma tumours in xenograft models when administered intraperitoneally [516]. Interestingly, the growth of these tumours was not significantly inhibited by pitavastatin administered by oral gavage, suggesting that the formulation and dose may require careful optimisation. Pitavastatin also inhibited drug exclusion by the multi-drug resistant protein, MDR-1, and this may contribute to the potentiation of other chemotherapeutic agents [517].

Whilst all statins inhibit HMGCR, they have distinct pharmacokinetic properties. Most statins have short half-lives of between 0.5 and 3 hours, with the exception of atorvastatin, pitavastatin and rosuvastatin (chapter 1, [162]). Previous research demonstrated that continued inhibition of HMGCR was necessary to cause cell death, suggesting that several daily doses of simvastatin would be required in order to effectively treat cancer (chapter 4). Pitavastatin has a half-life of 11 hours [162], which may prolong exposure to statin and thereby reduce the dosing frequency required. Thus, the promising anti-cancer activity of pitavastatin in cancer cell lines and xenografts, together with an extended half-life, make pitavastatin an ideal candidate for evaluation in ovarian cancer.

To conduct clinical trials evaluating pitavastatin for the treatment of ovarian cancer, biomarkers of statin-induced cell death are required to confirm the cytotoxic effects of statins on cancer cells. Clinical trials have previously estimated HMGCR inhibition as an indicator of statin activity. This has been achieved by measuring plasma cholesterol levels, urinary mevalonate excretion, and by measuring the degree of inhibition of a standard amount of HMGCR present in a rat microsomal preparation [407, 416, 421, 518]. However, cholesterol and mevalonate markers are not always correlated to statin cytotoxicity and therefore, may not be adequate biomarkers of statin-induced cell death *in vivo*. Additional biomarkers which may be used to predict response to statin therapy include markers of apoptosis. Immunostaining tumour tissue for the cell proliferation marker, Ki-67, and the apoptosis marker, cleaved caspase-3, before and after statin treatment revealed a significant decrease in Ki-67, and an induction in apoptosis in high-grade breast tumours [421]. Furthermore, cytokeratin 18 is cleaved by caspases during apoptosis to form caspase-cleaved cytokeratin 18 (ccCK18), which is released from cells, and can be detected in the plasma of patients exposed to chemotherapy [519]. Alternatively, proteins released from cells exposed to pitavastatin can be analysed by gel electrophoresis and mass spectrometry [520], with the aim of identifying proteins which are predominantly released from cancer cells compared to normal cells.

5.2 Aims

The research in this chapter aimed to evaluate the activity of pitavastatin as a single agent in a panel of ovarian cancer cell lines, to further understand the mechanism by which pitavastatin induces cytotoxic activity, to identify biomarkers of statin-induced

death, and to evaluate pitavastatin activity in a xenograft study. The results of this research will inform clinical trials of pitavastatin in ovarian cancer, and establish novel biomarkers which could be utilised to confirm response to pitavastatin in the clinic.

5.3 Results

5.3.1 HMGCR levels in epithelial, fibroblast and ovarian cancer cell lines

HMGCR has previously been described as a metabolic oncogene, as ectopic expression of HMGCR contributed to anchorage-independent growth and cellular transformation [137]. Furthermore, overexpression of HMGCR in oesophageal squamous cell carcinoma cells increased cell growth and migration [146]. Therefore, HMGCR protein level was determined in a panel of ovarian cancer cell lines, and compared to the HMGCR level in three normal cell lines. HMGCR protein level was increased in all ovarian cancer cell lines compared to normal ovarian epithelial (HOE) cells, lung epithelial (NL20) cells and fibroblasts (HFF) (figure 5.1). Quantification of HMGCR protein level confirmed that this was significant ($P<0.05$) in A2780, cisA2780, Ovcar-3 and Ovcar-8 cell lines compared to HOE cells (figure 5.1). These results raised the possibility that an increase in HMGCR may contribute to the development of ovarian cancer, and therefore, provided a rationale for the evaluation of pitavastatin in ovarian cancer.

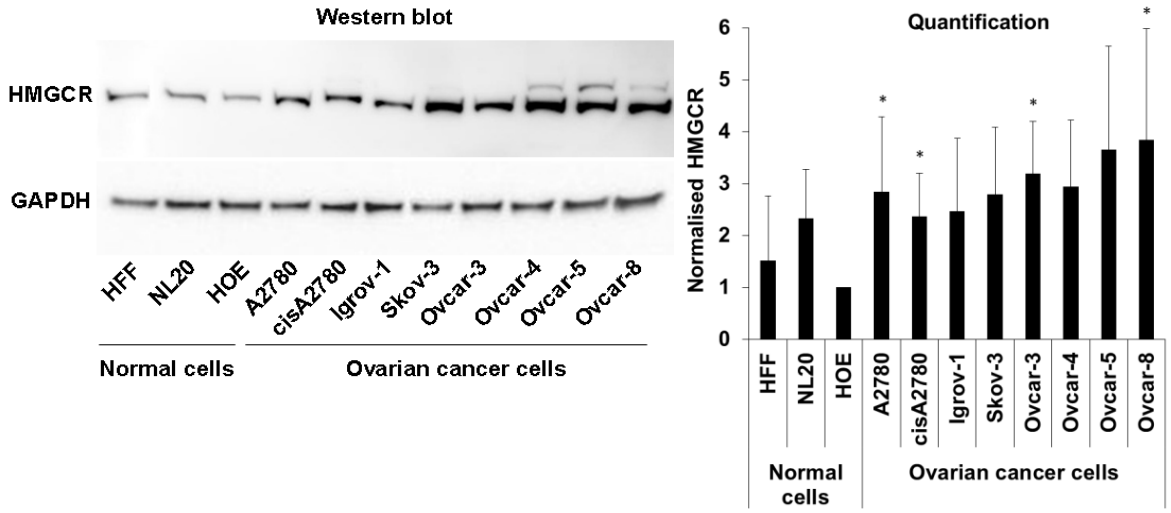

Figure 5.1: HMGCR levels in a panel of ovarian cancer cell lines and normal cells including human foreskin fibroblasts (HFF), human bronchial epithelial cells (NL20) and human ovarian epithelial cells (HOE) (n = 3-4). GAPDH was used as a loading control. HMGCR levels were normalised to GAPDH and significantly increased compared to HOE cells where indicated (*, paired *t*-test, $P<0.05$).

5.3.2 Pitavastatin inhibits the growth of ovarian cancer cell lines

The activity of pitavastatin in cell growth assays was determined in a panel of ovarian cancer cell lines, normal cells and ovarian cancer spheroids. In eight ovarian cancer cell lines grown as monolayers, pitavastatin exhibited IC_{50} values ranging between 0.2 µM and 8 µM (figure 5.2). Pitavastatin had the most potent activity in Ovcar-8 cells (IC_{50} = 0.2 ± 0.05 µM), but also demonstrated activity in normal ovarian epithelial cells and in fibroblasts (IC_{50} ~ 1 µM; figure 5.2). To evaluate the activity of pitavastatin in a 3-dimensional culture, the effect of pitavastatin on ovarian cancer spheroids was evaluated by measuring ATP in cells exposed to increasing concentrations of

pitavastatin. The activity of pitavastatin in ovarian cancer spheroids was comparable to that determined in cell monolayers with IC_{50} values ranging between 0.6 µM and 4 µM (figure 5.2). However, the IC_{50} values in A2780 spheroids and Ovcar-8 spheroids (2 µM and 0.6 µM) were notably increased compared to the IC_{50} values in respective monolayer cultures (0.7 µM and 0.2 µM).

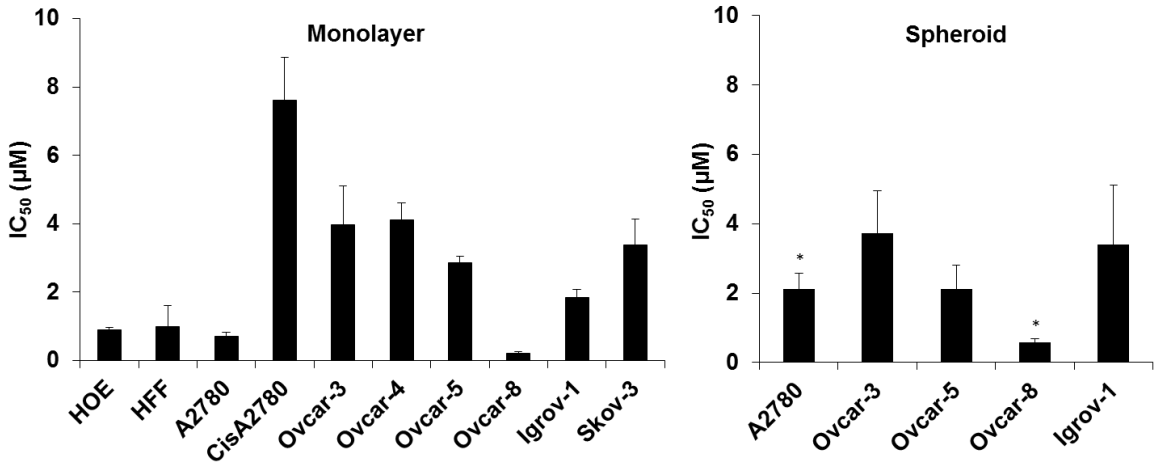

Figure 5.2: The potency of pitavastatin in normal cell monolayers (human ovarian epithelial (HOE) cells or human foreskin fibroblasts (HFF)), eight ovarian cancer cell monolayers (mean IC_{50} ± S.D., n = 3-4), and in five ovarian cancer spheroids (mean IC_{50} ± S.D., n = 4-5). IC_{50} values were significantly increased in spheroid cultures compared to monolayer cultures where indicated (*, paired *t*-test, $P<0.01$).

Simvastatin was previously found to have cytotoxic activity in ovarian cancer cells that were resistant to carboplatin, suggesting that statins may have activity in cancers resistant to chemotherapy (chapter 4). Therefore, the anti-growth activity of pitavastatin was evaluated in several paired cell lines (PEA1/PEA2 and PEO1/PEO4), which have been obtained from ovarian cancer patients both before and after the development of clinical resistance to chemotherapy. Pitavastatin IC_{50} values in the

paired cell lines (1 μM – 3.5 μM) were comparable to those obtained in ovarian cancer cell lines (figure 5.3, data obtained by Dr Euan Stronach and Karen Menezes at Imperial College, London). Interestingly, PEA2 and PEO4 cells derived from chemoresistant and relapsed tumours appeared modestly more sensitive to pitavastatin compared to their paired chemosensitive cell lines.

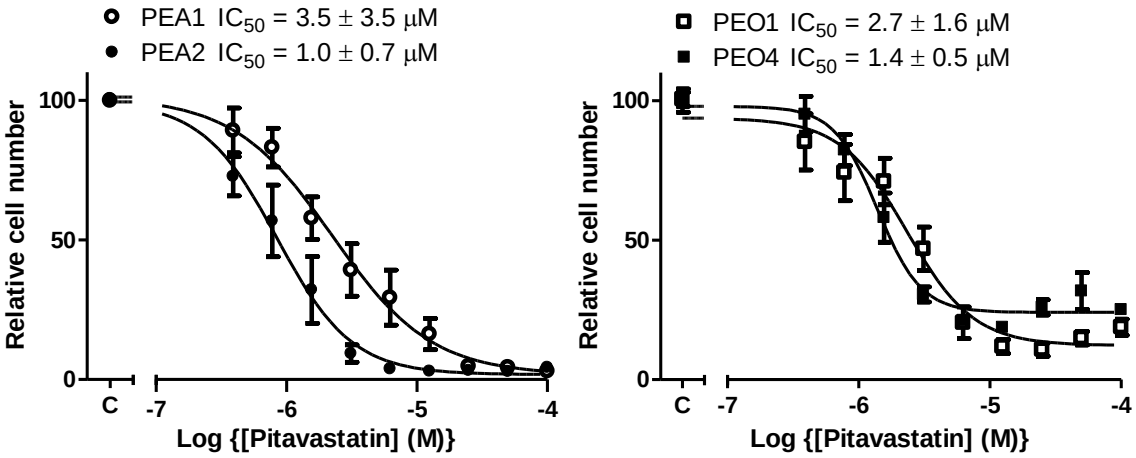

Figure 5.3: The potency of pitavastatin in paired ovarian cancer cell lines. The paired cell lines PEA1 and PEA2, and PEO1 and PEO4 were exposed to the indicated concentrations of pitavastatin for 72 hours. The data was represented as a fraction of the top of the curve which was identified by curve fitting (mean ± S.D., n = 6-9). "C" represents the control cells exposed to solvent alone. Data was obtained from Dr Euan Stronach and Karen Menezes at Imperial College, London.

To confirm the anti-growth activity of pitavastatin had resulted from inhibition of HMGCR, Ovcar-8 and Ovcar-3 cells exposed to pitavastatin were supplemented with farnesol or geranylgeraniol, or both. The addition of geranylgeraniol but not farnesol to Ovcar-8 and Ovcar-3 cells significantly suppressed the anti-growth effects of

pitavastatin (figure 5.4). Furthermore, supplementing pitavastatin-treated cells with both geranylgeraniol and farnesol also significantly suppressed the inhibition of the growth of Ovcar-8 cells, although this occurred to a lesser degree in Ovcar-3 cells (figure 5.4). These results suggested that the anti-growth activity of pitavastatin was mediated though the inhibition of geranylgeranylation.

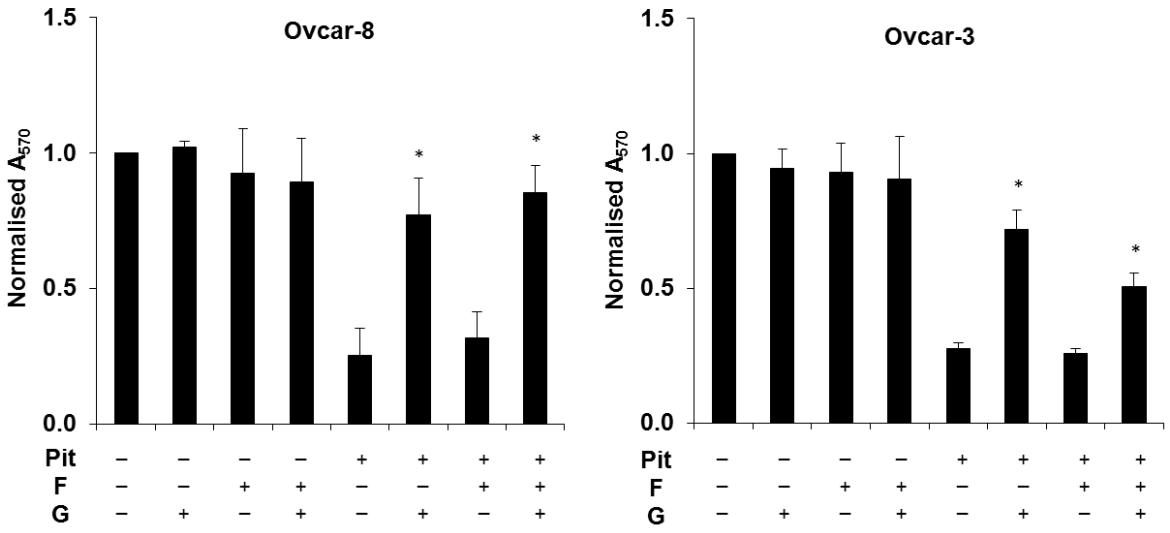

Figure 5.4: Prevention of the anti-growth effects of pitavastatin. Cells were exposed to 1 μM (Ovcar-8) and 20 μM (Ovcar-3) pitavastatin (pit, 5 x IC_{50}) for 72 hours in the presence of 10 μM farnesol (F), 10 μM geranylgeraniol (G) or solvent. The number of cells surviving (mean ± S.D., n = 3) was expressed as a fraction of those surviving in samples treated with solvent alone. The number of cells were significantly increased compared to pitavastatin where indicated (*, paired *t*-test, $P<0.01$).

5.3.3 Pitavastatin has no significant effects on cell migration

Statins have also been shown to inhibit cancer cell migration and invasion through inhibition of HMGCR (chapter 1). Therefore, the effects of pitavastatin on ovarian cancer cell migration were determined. Ovcar-8 cells were grown to confluence, the monolayer was wounded, and cell migration was measured after 36 hours in medium supplemented with pitavastatin at concentrations up to the IC_{50}. These concentrations were chosen to avoid significant cell detachment. Pitavastatin had no effect on the relative migration of Ovcar-8 cells after 36 hours (figure 5.5), suggesting that inhibition of cell migration is unlikely to contribute to the anti-cancer effects of pitavastatin on ovarian cancer cells.

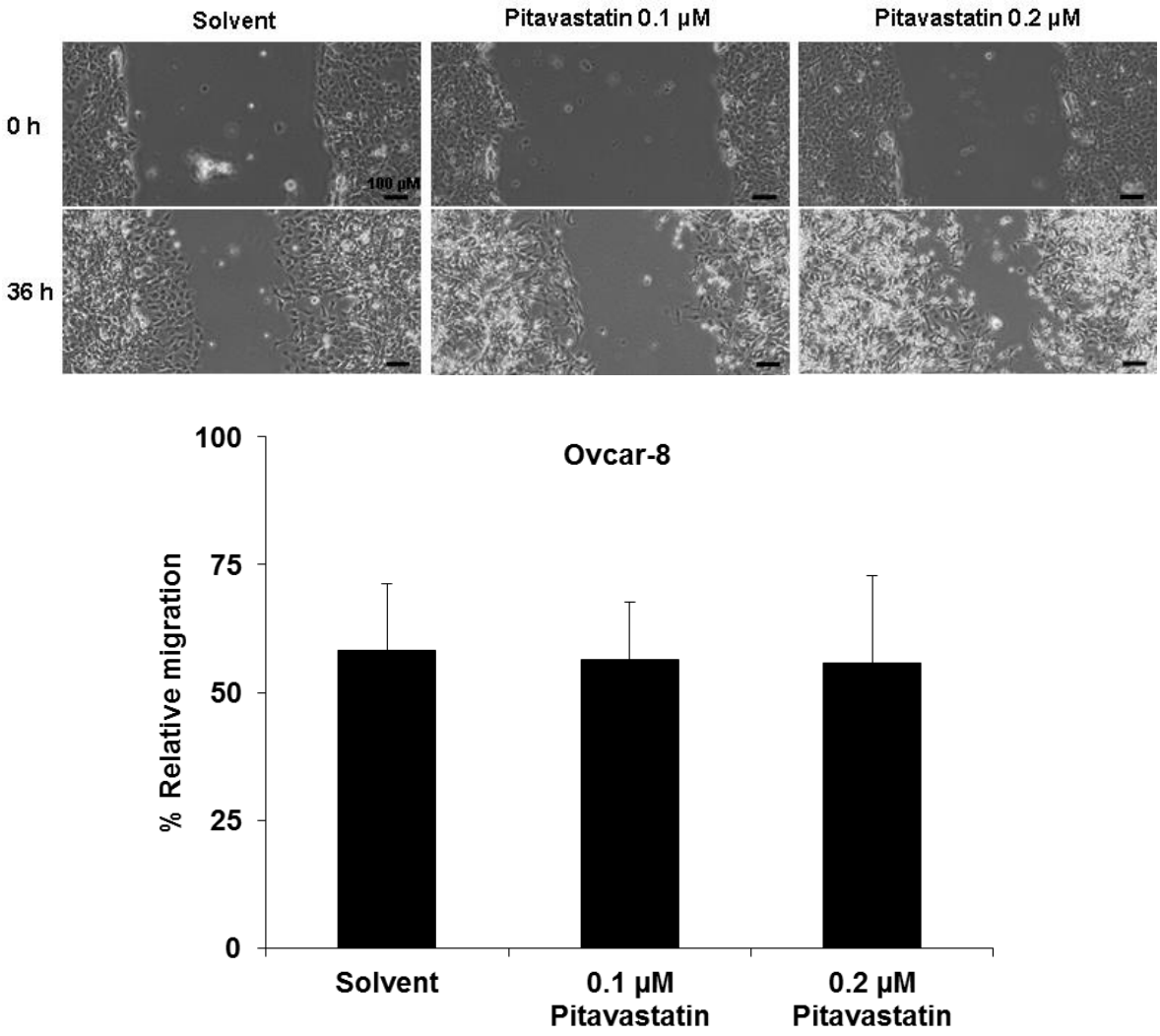

Figure 5.5: The effects of pitavastatin on cell migration. Analysis of Ovcar-8 migration after exposure to 0.1 µM or 0.2 µM pitavastatin (0.5 and 1 x IC_{50}), or solvent by phase contrast microscopy immediately after wounding or after 36 hours (h) (mean ± S.D., n = 3). Relative migration was calculated as described in chapter 3.

5.3.4 Pitavastatin induces cell cycle arrest and apoptotic cell death

Next, experiments were completed to identify the mechanisms by which pitavastatin inhibited the growth of cultures of ovarian cancer cells. Exposure of Ovcar-3 cells to pitavastatin resulted in a decrease in the fraction of cells in G_2/M phase(s) of the cell cycle and an increase in subG_1 (figure 5.6).

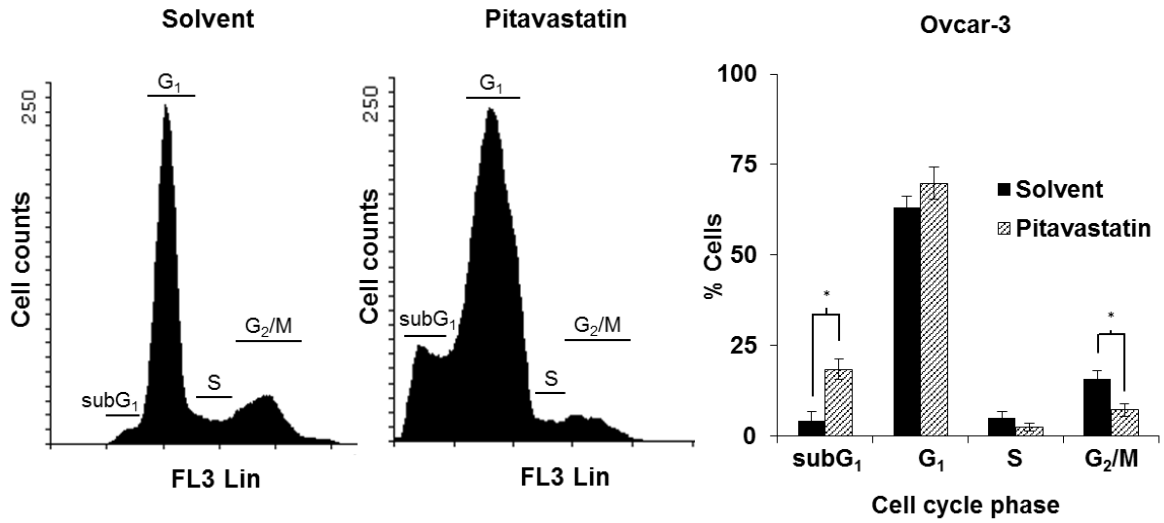

Figure 5.6: The effects of pitavastatin on the cell cycle. Flow cytometry analysis of the DNA content in Ovcar-3 cells exposed to 12 μM pitavastatin (3 x IC_{50}) or solvent for 48 hours (mean ± S.D., n = 3). The percentage of pitavastatin-treated cells in G_2/M phase(s) of the cell cycle was significantly decreased compared to cells exposed to solvent alone, together with a significant increase in subG_1 phase where indicated (*, paired *t*-test, $P<0.01$).

The increase in subG_1 phase following pitavastatin exposure may indicate an increase in apoptosis. This prompted further studies to confirm that cell death contributed to the reduced growth of monolayer cultures of ovarian cancer cells. To quantify cell death

induced by pitavastatin, a panel of eight ovarian cancer cell lines were exposed to pitavastatin at 5 times IC_{50} for 96 hours, and the number of cells that failed to exclude Trypan blue were determined. Cell death was significantly increased in every cell line exposed to pitavastatin (figure 5.7). Notably, almost all A2780, cisA2780 and Ovcar-3 cells were dead after 96 hours.

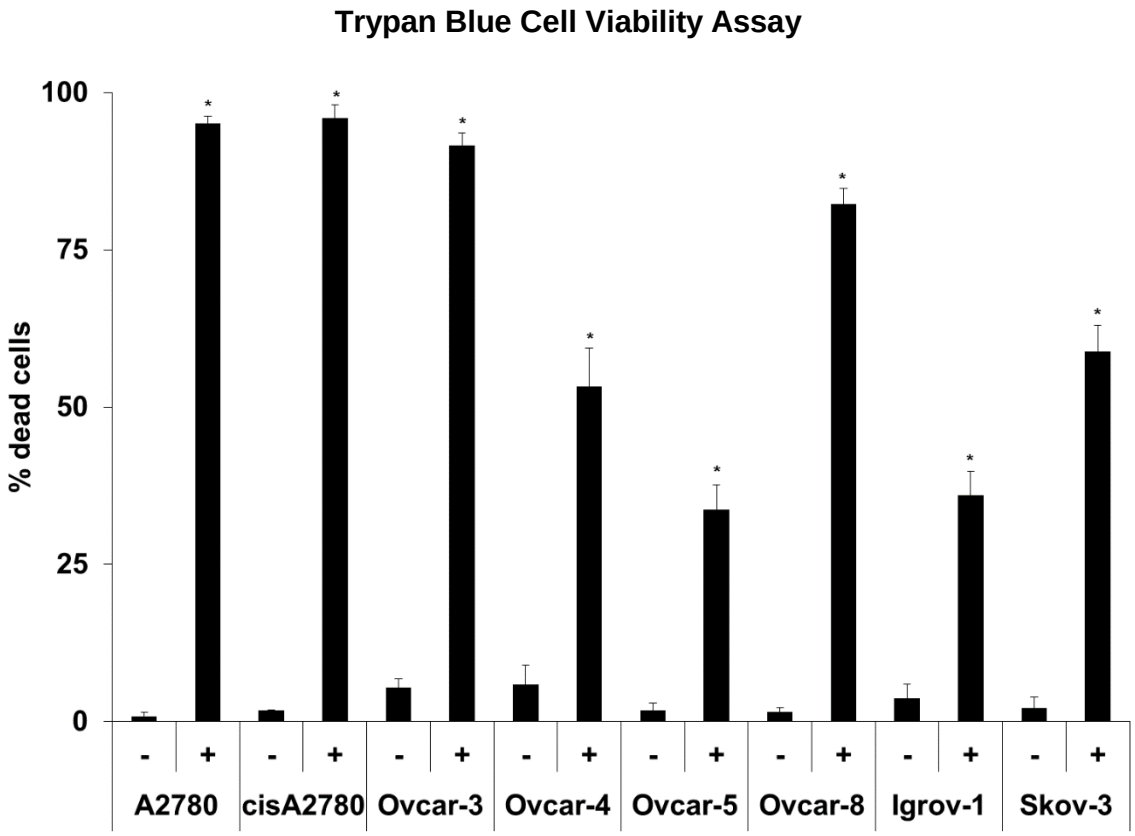

Figure 5.7: Ovarian cancer cell death induced by pitavastatin. The number of dead ovarian cancer cells was determined by Trypan blue staining after exposure to solvent (-) or pitavastatin (+) at 5 x IC_{50} for 96 hours (mean ± S.D., n = 3). The percentage of dead cells after exposure to pitavastatin was significantly increased compared to the solvent alone for all cell lines (*, paired *t*-test, $P<0.0005$).

Apoptosis has previously been identified as one mechanism of statin-induced cell death in ovarian cancer cell lines [337, 338, 485]. To confirm that pitavastatin also induced apoptosis in ovarian cancer cell lines, several markers of apoptosis including caspases 3, 7, 8, 9 and poly (ADP) ribose polymerase (PARP) cleavage were measured in cells exposed to pitavastatin. Pitavastatin significantly increased caspase 3/7 activity in all cell lines tested, indicating the induction of apoptotic cell death (figure 5.8). This was confirmed by an increase in PARP cleavage in pitavastatin-treated Ovcar-8 cells (figure 5.8). Furthermore, the cleavage of PARP was fully reversed by the addition of mevalonate or geranylgeraniol, suggesting that the pro-apoptotic activity of pitavastatin was mediated through inhibition of HMGCR.

The activation of apoptosis can occur through the extrinsic (death receptor) pathway or the intrinsic (mitochondrial) pathway (chapter 1). Statins have predominantly been shown to induce apoptosis through the mitochondrial pathway; however one study reported an increase in death receptor ligands, and subsequent activation of the extrinsic apoptotic pathway following simvastatin exposure [338, 364]. In order to further elucidate the pathway by which pitavastatin induced apoptosis in ovarian cancer cells, the activities of the initiator caspases were also determined. Caspase-8 is activated following the binding of ligands to the death receptor and activation of the death-inducing signalling complex in the extrinsic apoptosis pathway, whereas caspase-9 is activated by Bax/Bak-mediated cytochrome c release from the mitochondria in the intrinsic apoptotic pathway. Pitavastatin significantly increased the activity of both caspase-8 (extrinsic pathway) and caspase-9 (intrinsic pathway) in most cell lines tested, suggesting that both the extrinsic and intrinsic apoptosis pathways were activated during pitavastatin-induced apoptosis (figure 5.8).

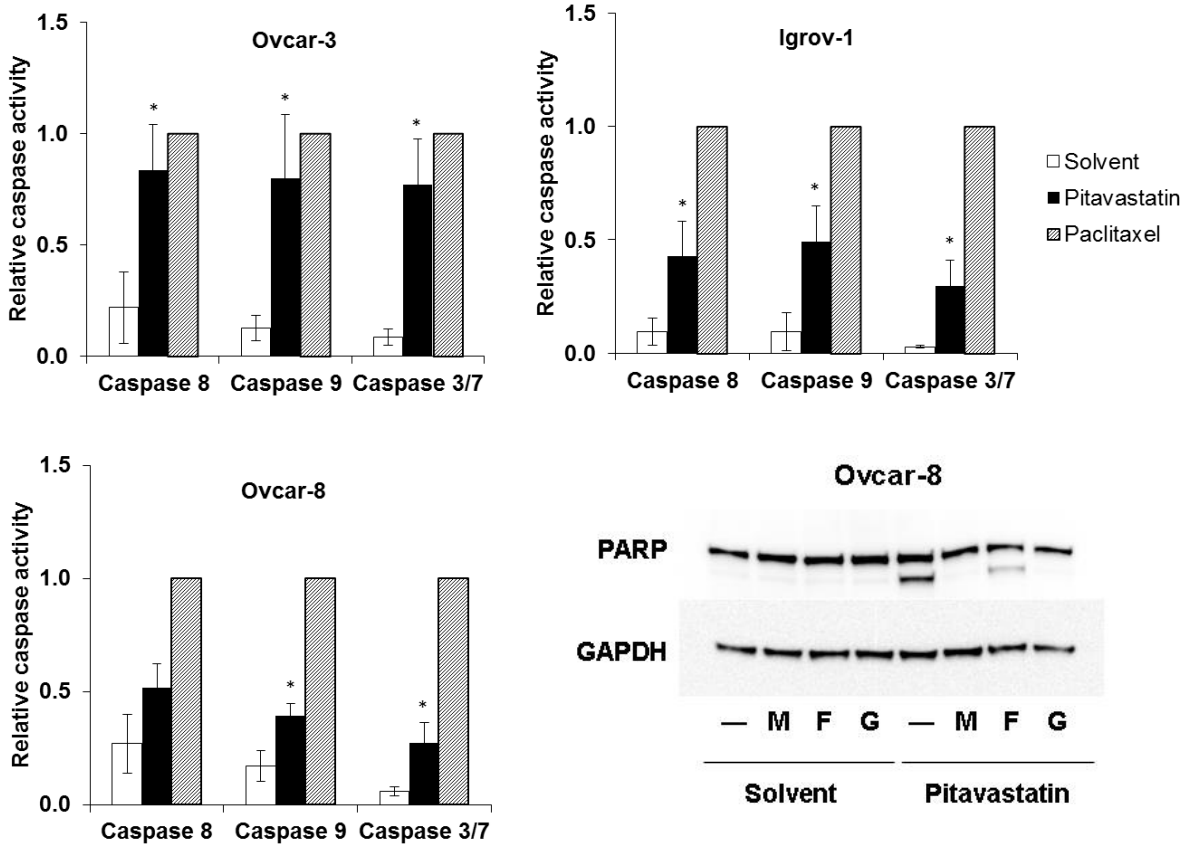

Figure 5.8: The effects of pitavastatin on the apoptosis pathway. Caspase 8, 9 and 3/7 activities were measured in Ovcar-3, Igrov-1 and Ovcar-8 cells following exposure to 20 µM (Ovcar-3), 10 µM (Igrov-1) and 1 µM (Ovcar-8) pitavastatin (5 x IC_{50}), 50 nM paclitaxel or solvent for 48 hours. Caspase activity was expressed as a fraction (mean ± S.D., n = 3) of the activity measured in cells exposed to paclitaxel. Relative caspase activity was significantly increased following pitavastatin exposure (*, paired *t*-test, $P<0.05$) compared to cells treated with solvent where indicated. Ovcar-8 cells were also exposed to 1 µM pitavastatin or solvent for 48 hours either in the presence of 100 µM mevalonate (M), 10 µM farnesol (F), 10 µM geranylgeraniol (G) or solvent, and PARP cleavage was determined by western blotting. GAPDH was used as a loading control (n = 3).

FLICE-like inhibitory protein (FLIP) negatively regulates the extrinsic apoptosis pathway by inhibiting the cytoplasmic adaptor protein and caspase-8 complex, and has previously been implicated in drug resistance in ovarian cancer [521, 522]. This raised the possibility that FLIP knockdown may sensitise ovarian cancer cells to apoptosis induced by pitavastatin. FLIP expression was inhibited by siRNA which recognised the long form of FLIP (FLIP#4), and both the long and short isoforms of FLIP (FLIP#18). FLIP siRNA was used at a concentration which did not significantly reduce cell viability alone [522].

FLIP SMARTpool and FLIP#4 siRNA did not have a significant effect on the sensitivity of Ovcar-3 cells to pitavastatin (figure 5.9). FLIP#18 siRNA modestly decreased the potency of pitavastatin in Ovcar-3 cells (IC_{50} = 5.6) compared to cells transfected with non-targeting siRNA (IC_{50} = 7.4, figure 5.9), although this was not statistically significant. Knockdown of FLIP, as evaluated by western blotting, was incomplete, and this may have contributed to the lack of any significant changes in sensitivity to pitavastatin (figure 5.9).

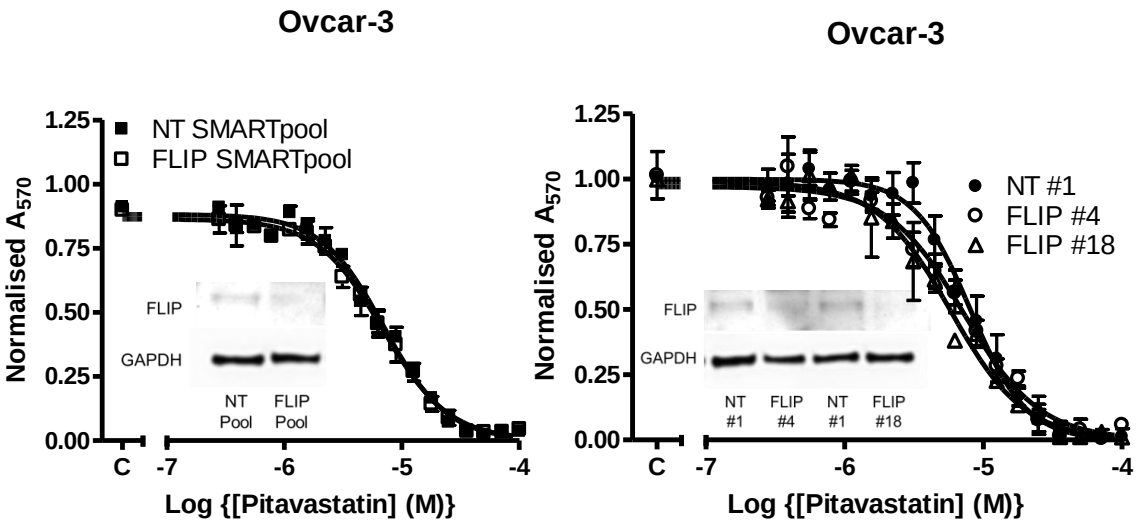

siRNA	IC_{50} (μM)
NT SMARTpool	7.0 ± 0.8
FLIP SMARTpool	6.9 ± 1.0
NT #1	7.4 ± 1.9
FLIP #4	7.3 ± 0.4
FLIP #18	5.6 ± 1.1

Figure 5.9: The effects of FLIP knockdown on the potency of pitavastatin. Ovcar-3 cells were transfected with FLIP SMARTpool (0.3 nM), FLIP #4 (25 nM) or FLIP #18 (3 nM) and the corresponding non-targeting (NT) siRNA for 24 hours, followed by exposure to pitavastatin at a range of concentrations for 72 hours. The data was represented as a fraction of the top of the curve which was identified by curve fitting (mean ± S.D., n = 3). "C" represents the control cells exposed to solvent alone. Western blotting (inset) confirmed knockdown of FLIP. GAPDH was used as a loading control. The IC_{50} values were calculated from the dose-response curves (mean ± S.D., n = 3).

5.3.5 The contribution of autophagy to pitavastatin-induced cell death

To further identify additional cellular pathways which may affect statin-induced cell death, autophagy was investigated. Previous studies demonstrated that simvastatin may simultaneously induce and inhibit the autophagy pathway at different points, and this could contribute to the cytotoxic effects of statins (chapter 4). To confirm this, the effects of pitavastatin on autophagy were also determined.

An accumulation of LC3-II can result from an induction or inhibition of autophagy, whereas an increase in p62 is often a marker of autophagy inhibition. Pitavastatin exposure resulted in an accumulation of LC3-II and p62 in Ovcar-8 cells after 48 hours, suggesting that pitavastatin inhibited autophagy (figure 5.10). However, this could also be representative of autophagy induction, as p62 synthesis can be increased in response to autophagy stimulation [486]. The geranylgeranylated GTPase Rab7 is essential for the late stages of autophagosome maturation [488]. Pitavastatin reduced the level of Rab7, raising the possibility that inhibition of the prenylation of Rab7 promotes its turnover (figure 5.10). Whatever the explanation for the pitavastatin-induced decrease in Rab7, these data suggest that pitavastatin may block the late stages of autophagy. Notably, the effects on LC3-II, p62 and Rab7 were reversed by the addition of either mevalonate or geranylgeraniol to pitavastatin-treated cells, suggesting that effects on the autophagy pathway were mediated through HMGCR inhibition (figure 5.10).

Atg5 is involved in the early stages of autophagosome formation and LC3-II production [277]. To determine if autophagy contributed to the pro-apoptotic effects of pitavastatin, Atg5 expression was inhibited using Atg5 siRNA at a concentration which

did not significantly induce apoptosis alone (figure 5.10). Knockdown of Atg5 and autophagy inhibition was confirmed by western blotting. Atg5 knockdown modestly, but significantly, increased the sensitivity of Ovcar-8 cells to apoptotic cell death induced by pitavastatin (figure 5.10).

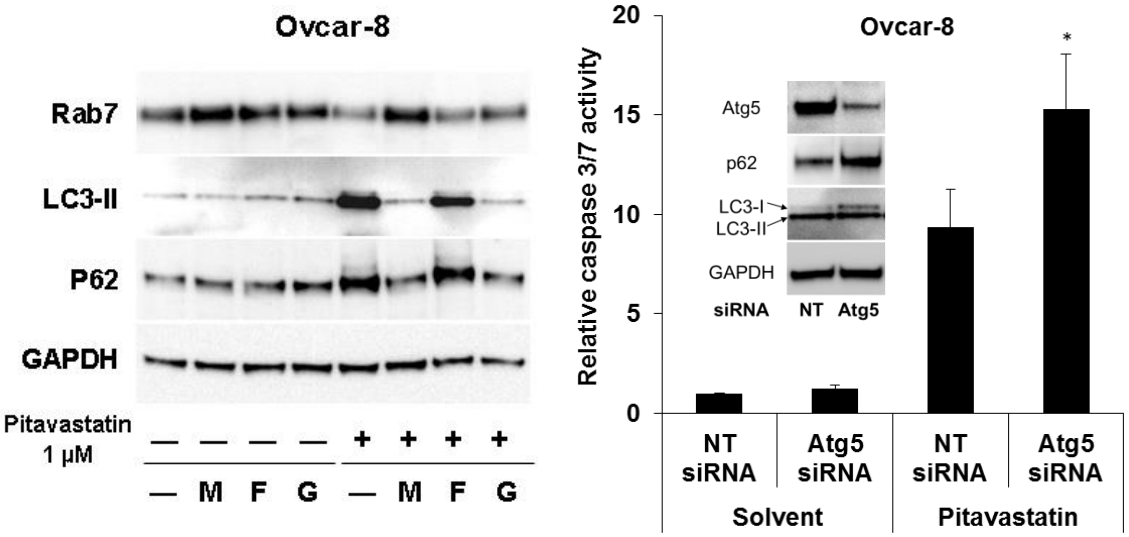

Figure 5.10: The effects of pitavastatin on the autophagy pathway. Ovcar-8 cells were exposed to 1 µM pitavastatin (5 x IC_{50}) or solvent for 48 hours either in the presence of 100 µM mevalonate (M), 10 µM farnesol (F), 10 µM geranylgeraniol (G) or solvent. The levels of LC3-II and p62 were measured by western blotting (n = 3). Ovcar-8 cells were also transfected with Atg5 SMARTpool (20 nM) or non-targeting (NT) SMARTpool for 24 hours followed by exposure to solvent or 2 µM pitavastatin (10 x IC_{50}) for 48 hours. Western blotting (inset) confirmed knockdown of Atg5 and inhibition of autophagy. GAPDH was used as a loading control. Caspase 3/7 activity (mean ± S.D., n = 3) was expressed as a fraction of the activity in cells exposed to NT siRNA and solvent. Atg5 knockdown significantly increased pitavastatin-induced apoptosis in Ovcar-8 cells (*, paired *t*-test, $P<0.05$).

5.3.6 Increased reactive oxygen species (ROS) production is not a mechanism of pitavastatin-induced cell death

Deregulation of autophagy has been correlated with increases in reactive oxygen species (ROS), and in some cases, increased mitochondrial content; mitochondria are the major cellular source of ROS (reviewed by [295]). The effects of both simvastatin (chapter 4) and pitavastatin on the autophagy pathway prompted further investigations on the effects of pitavastatin on mitochondrial content and ROS in ovarian cancer cells.

Mitochondrial turnover (mitophagy) relies on the autophagy pathway and defective autophagy can result in alterations in mitochondrial number or function [295]. Therefore, mitochondrial content was estimated in Ovcar-8 and Ovcar-3 cell lines using MitoTracker Green FM dye, which binds to mitochondrial proteins predominantly in the inner mitochondrial membrane in viable cells. Pitavastatin significantly increased the mitochondrial content in Ovcar-8 and Ovcar-3 cells, as indicated by a significant increase in mitochondrial fluorescence (figure 5.11). Furthermore, the majority of cells exposed to pitavastatin exhibited an increase in mitochondrial staining as observed by fluorescence microscopy. Collectively, these results suggest that pitavastatin may inhibit mitochondrial turnover.

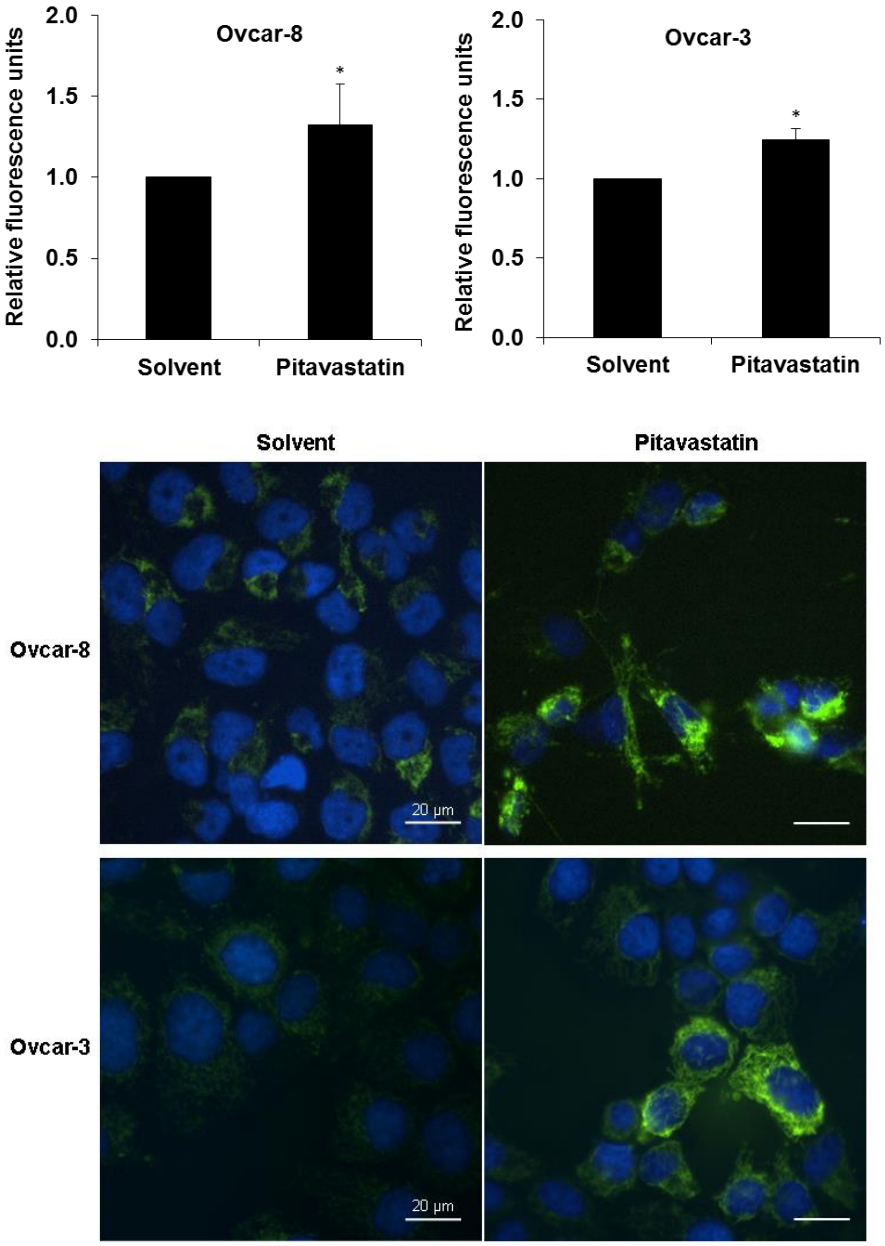

Figure 5.11: The effects of pitavastatin on mitochondrial content. Ovcar-8 and Ovcar-3 cells exposed to 1 µM and 20 µM pitavastatin (5 x IC_{50}) respectively or solvent for 48 hours. Mitochondria were stained using 100 nM MitoTracker Green FM and fluorescence was determined by flow cytometry (mean ± S.D., n = 3). Relative fluorescence was significantly increased in pitavastatin-treated cells compared to cells exposed to solvent alone (*, paired *t*-test, $P<0.05$). Mitochondria were also visualised by fluorescence microscopy (green). Nuclei were stained with Hoechst 33258 (blue).

To confirm the increase in mitochondrial content in ovarian cancer cells exposed to pitavastatin, the cellular mitochondrial DNA (mtDNA) content was measured. The mitochondrial NADH dehydrogenase 1 (ND1) gene is located exclusively in mtDNA. Therefore, ND1 and an internal reference gene, β-actin, were used to quantify the relative mtDNA content (chapter 3). There was a significant increase in relative mtDNA content in Ovcar-8 cells exposed to pitavastatin, consistent with the increase in mitochondrial content (figure 5.12). However, there was no difference in mtDNA content in Ovcar-3 cells exposed to pitavastatin compared to the solvent control (figure 5.12). This may reflect the accumulation of mitochondria containing damaged mtDNA in pitavastatin-treated Ovcar-3 cells.

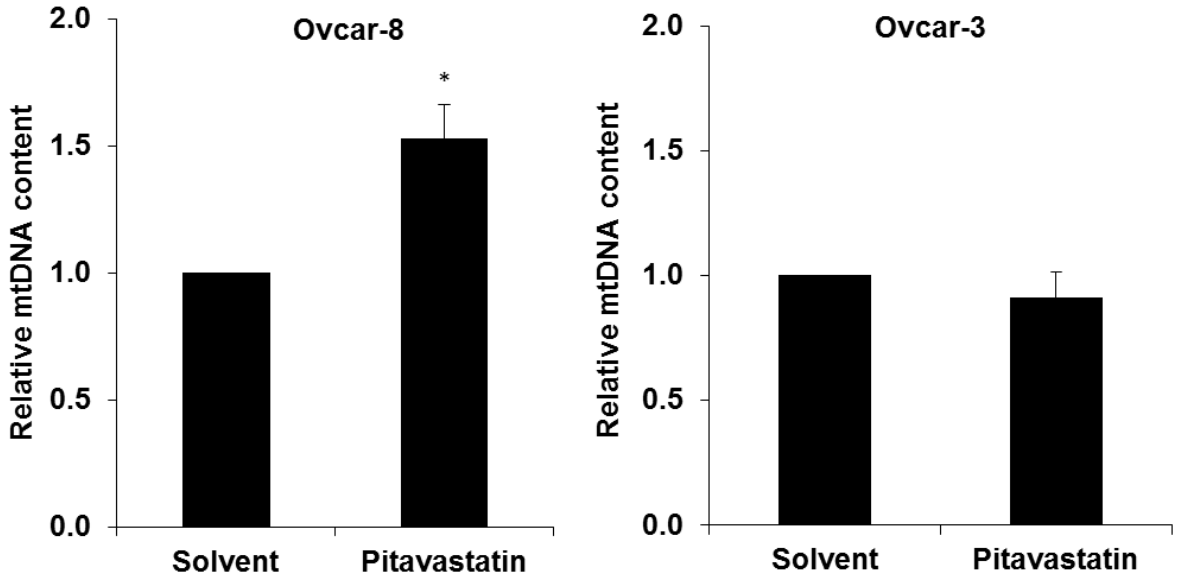

Figure 5.12: The effects of pitavastatin on mitochondrial DNA (mtDNA). Ovcar-8 and Ovcar-3 cells were exposed to 1 μM and 20 μM pitavastatin (5 x IC_{50}) respectively or solvent for 48 hours. ND1 content was determined by qPCR and normalised to β-actin content, as described in chapter 3 (mean ± S.D., n = 3). Relative mtDNA (ND1) content was significantly increased in Ovcar-8 cells exposed to pitavastatin (*, paired *t*-test, $P<0.05$).

Mitochondria are the major intracellular producers of ROS, and increased mitochondrial content has previously been linked to elevated ROS [523, 524]. Furthermore, statins have been reported to increase ROS in colon cancer cells and lymphoma cells [350, 352]. To determine if the increase in mitochondria in ovarian cancer cells was accompanied by an increase in ROS, 2',7'-dichlorofluorescin diacetate (DCFDA) was used to measure ROS in Ovcar-3 and Ovcar-8 cells exposed to pitavastatin.

A significant increase in ROS was detected in Ovcar-3 cells exposed to pitavastatin, and this was inhibited by the ROS scavenger, N-acetylcysteine (NAc) (figure 5.13). Conversely, there was no increase in ROS in Ovcar-8 cells after exposure to pitavastatin for 48 hours compared to the solvent control (figure 5.13). Tert-butyl hydroperoxide (TBHP) can decompose to alkoxyl and peroxyl radicals, resulting in the generation of hydrogen peroxide, and therefore, TBHP can be used to generate oxidative stress *in vitro*. TBHP significantly induced ROS in both Ovcar-3 and Ovcar-8 cells (figure 5.13).

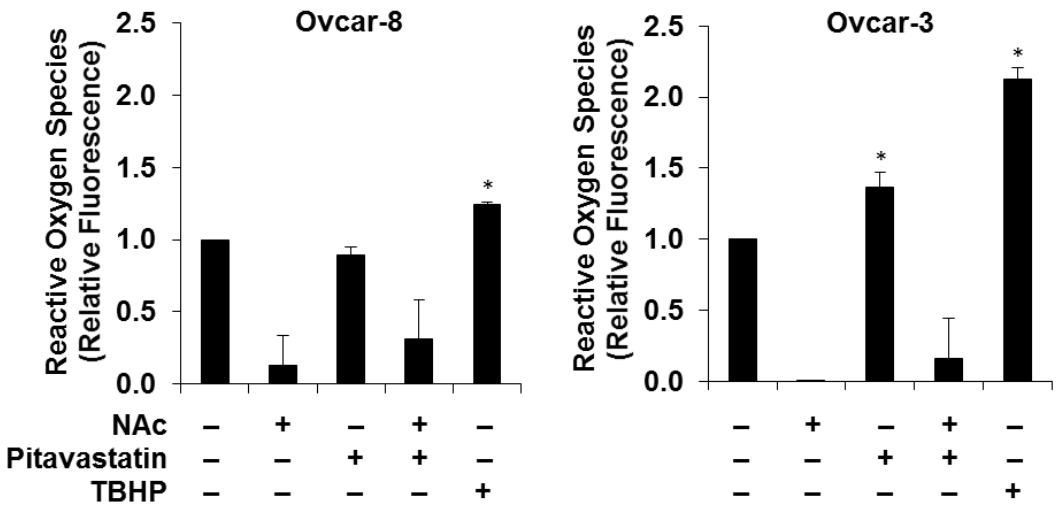

Figure 5.13: The effects of pitavastatin on reactive oxygen species (ROS) production. Ovcar-8 and Ovcar-3 cells were exposed to 1 µM and 20 µM pitavastatin (5 x IC_{50}) respectively or 50 µM tert-butyl hydroperoxide (TBHP) to generate ROS, either in the presence of solvent or 0.5 mM N-acetylcysteine (NAc) for 48 hours (3 hours for TBHP). ROS were measured using 2',7'-dichlorofluorescin diacetate (DCFDA) and expressed as a fraction of the activity in cells exposed solvent (mean ± S.D., n = 3). ROS were significantly increased in ovarian cancer cells exposed to pitavastatin or TBHP where indicated (*, paired *t*-test, $P<0.05$).

The generation of superoxide in simvastatin-treated colon cancer cells was demonstrated to induce activation of the JNK pathway, resulting in the expression of the pro-apoptotic protein Bim and subsequent apoptosis [352]. Furthermore, suppression of ROS using superoxide scavengers attenuated apoptosis, suggesting that superoxide was important for simvastatin-induced apoptosis in colon cancer cells [352]. To evaluate whether the increase in ROS in ovarian cancer cells contributed to apoptosis induced by pitavastatin, Ovcar-3 and Ovcar-8 cells were exposed to

pitavastatin alone, or in combination with the superoxide scavenger, N-acetylcysteine (NAc), and caspase 3/7 activity was determined.

Inhibition of ROS in Ovcar-3 and Ovcar-8 cells exposed to pitavastatin had no significant effect on caspase 3/7 activity, suggesting that ROS production is not likely to be a major mechanism contributing to pitavastatin-induced apoptosis in these ovarian cancer cell lines (figure 5.14). Notably, induction of ROS using TBHP modestly induced apoptosis in Ovcar-8 cells but not Ovcar-3 cells, and this was somewhat reversed by the addition of NAc, indicating that Ovcar-8 cells may be sensitive to ROS-induced cell death (figures 5.13 and 5.14).

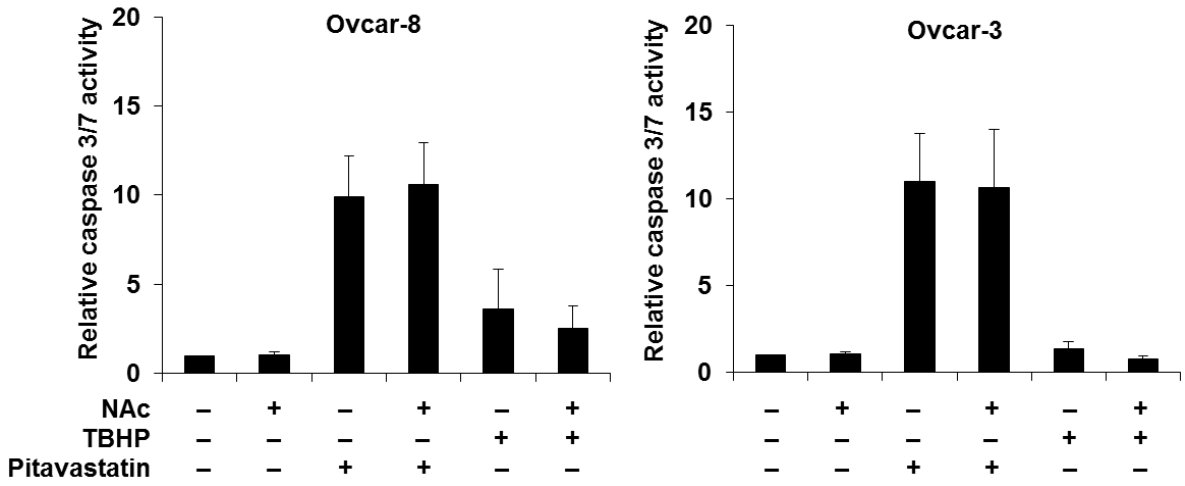

Figure 5.14: The effects of reactive oxygen species (ROS) inhibition on pitavastatin-induced apoptosis. Ovcar-8 and Ovcar-3 cells were exposed to 1 μM and 20 μM pitavastatin (5 x IC_{50}) respectively or 50 μM tert-butyl hydroperoxide (TBHP), either in the presence of solvent or 0.5 mM N-acetylcysteine (NAc) for 48 hours or 3 hours for TBHP. Caspase 3/7 activity was measured and expressed as a fraction of the activity in cells exposed solvent (mean ± S.D., n = 3).

5.3.7 Biomarkers of pitavastatin treatment

Cytokeratin 18 is cleaved by caspases during apoptosis to produce ccCK18, which is released into the extracellular environment and can be detected in the plasma of breast cancer patients treated with chemotherapy [519]. To determine if ccCK18 was elevated in response to statin treatment, ccCK18 was measured in cell culture medium taken from ovarian cancer cells which had been exposed to pitavastatin for 72 hours.

A significant amount of ccCK18 was detected in the medium taken from Ovcar-3 and Ovcar-8 cells, but not Igrov-1 or Skov-3 cells exposed to pitavastatin for 72 hours, suggesting that ccCK18 may only be useful as a biomarker of pitavastatin-induced cell death in a subset of patients (figure 5.15).

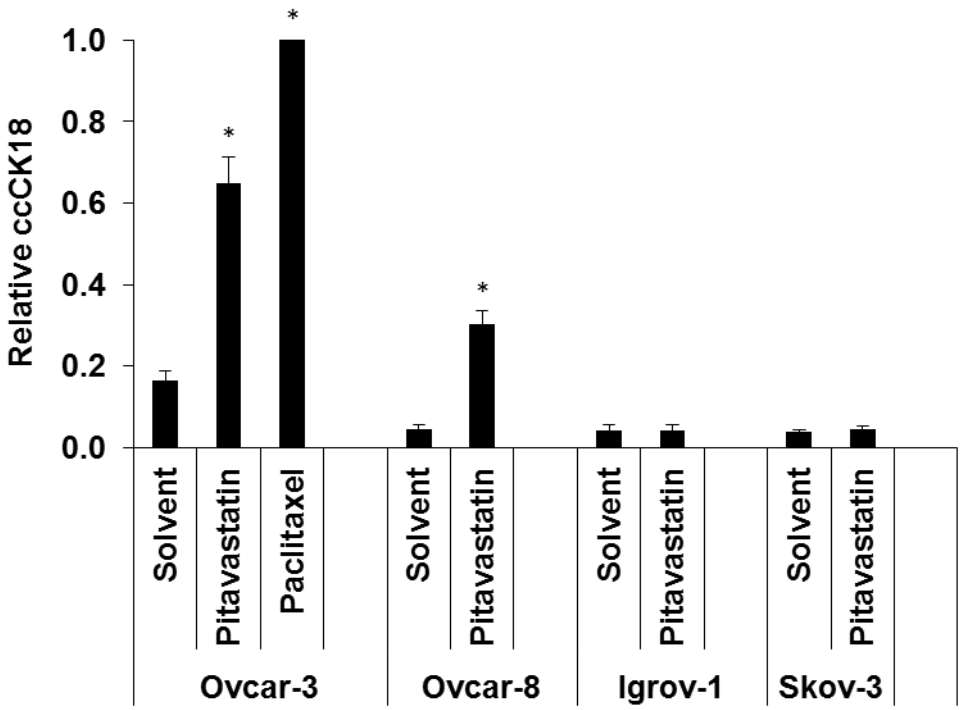

Figure 5.15: Caspase-cleaved cytokeratin 18 (ccCK18) released from ovarian cancer cells exposed to pitavastatin. Ovarian cancer cells were exposed to 1 µM (Ovcar-8), 10 µM (Igrov-1), 18 µM (Skov-3) and 20 µM (Ovcar-3) pitavastatin (5 x IC_{50}), 50 nM paclitaxel (Ovcar-3) or solvent for 72 hours. ccCK18 levels were measured in supernatant samples and expressed as a fraction of the ccCK18 from Ovcar-3 cells exposed to paclitaxel (mean ± S.D., n = 3). ccCK18 was significantly increased in Ovcar-3 and Ovcar-8 cells exposed to pitavastatin (*, paired *t*-test, $P<0.005$).

To identify additional novel biomarkers which were predominantly released from cancer cells in response to statin-induced cell death, ovarian cancer cells and normal cells were exposed to a panel of chemotherapeutic drugs or statins, and the proteins released into the cell culture medium were detected by silver staining of SDS-PAGE gels.

There were generally more proteins released into the medium from ovarian cancer cells exposed to simvastatin, pitavastatin or paclitaxel compared to cells exposed to solvent, pravastatin, carboplatin, doxorubicin or topotecan (figure 5.16). Furthermore, the profiles of proteins released from Ovcar-8 and Ovcar-3 cell lines were different compared to the protein profiles from HOE cells and fibroblasts (figure 5.16). This enabled the identification of seven protein bands, which were detected specifically in the supernatant of ovarian cancer cells exposed to pitavastatin or simvastatin, and were present at lower levels in the silver stains of normal cells or ovarian cancer cells exposed to solvent or pravastatin (marked with arrows in figures 5.16 and 5.17). These protein bands were extracted from a gel stained with Coomassie Brilliant Blue and provisionally identified by tryptic peptide sequencing using mass spectrometry in collaboration with Dr Elzbieta Piatkowska and Dr Sarah Hart at Keele University (figure 5.17; appendix 4).

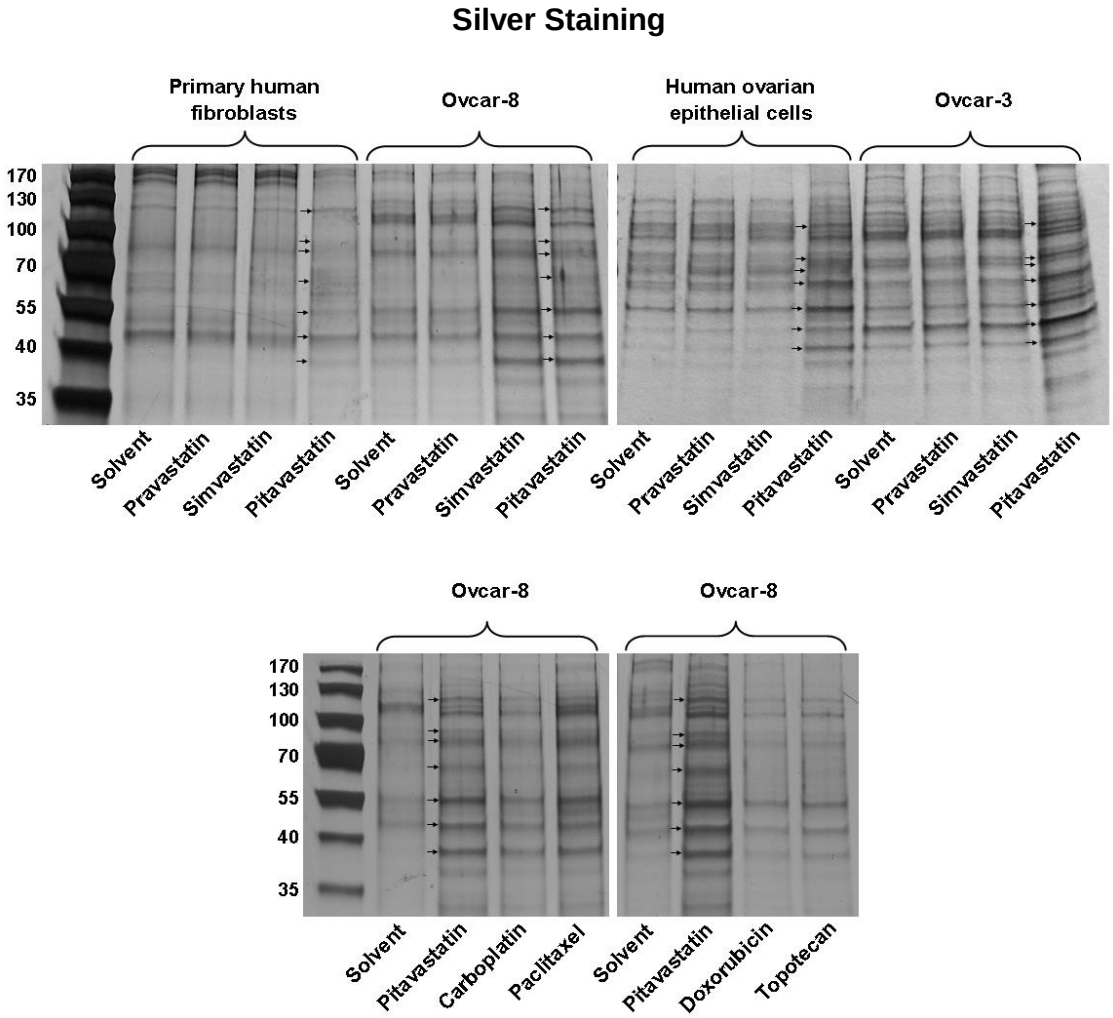

Figure 5.16: The proteins released from normal cells and ovarian cancer cells exposed to statins and chemotherapeutic agents. Ovcar-8 cells and human foreskin fibroblasts (HFF) were exposed to 1 μM pitavastatin (5 x IC_{50}) or 10 μM simvastatin (5 x IC_{50}) or pravastatin; human ovarian epithelial cells (HOE) were exposed to 2 μM pitavastatin (2 x IC_{50}), simvastatin or pravastatin; Ovcar-3 cells were exposed to 8 μM pitavastatin (2 x IC_{50}), simvastatin or pravastatin, or solvent as indicated for 72 hours (n = 3). Ovcar-8 cells were also exposed to 70 μM carboplatin (1 x IC_{50}), 1 μM doxorubicin (5 x IC_{50}), 21 nM paclitaxel (3 x IC_{50}) and 50 nM topotecan (5 x IC_{50}). Proteins in supernatant samples were separated by gel electrophoresis and visualised by silver staining. Protein sizes were estimated using the protein markers (kDa) on the left. Black arrows indicate the protein bands that were excised from a gel stained with Coomassie Brilliant Blue (figure 5.17) for mass spectrometry analysis.

Coomassie Brilliant Blue Staining

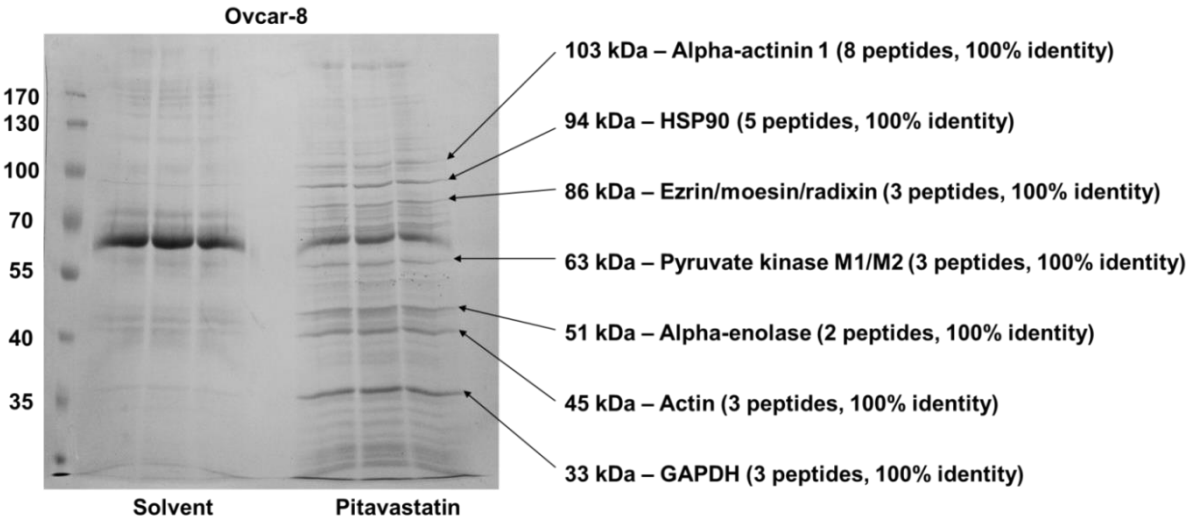

Figure 5.17: The identification of nine proteins released from ovarian cancer cells exposed to pitavastatin. Ovcar-8 cells were exposed to 1 μM pitavastatin (5 x IC_{50}) or solvent for 72 hours. Proteins in supernatant samples were separated by gel electrophoresis and visualised by Coomassie Brilliant Blue staining. The bands indicated by black arrows were excised, and proteins were identified by mass spectroscopy sequencing by Dr Elzbieta Piatkowska and Dr Sarah Hart at Keele University. The peptide sequences identified are detailed in appendix 4. Protein sizes were estimated using the protein markers (kDa) on the left. Heat shock protein 90, HSP90; glyceraldehyde-3-phosphate dehydrogenase, GAPDH.

To confirm the identity of the proteins identified by mass spectrometry, the cell culture medium taken from Ovcar-8 and Ovcar-3 cells exposed to pitavastatin for 72 hours was analysed by western blotting (figure 5.18). Medium from cells exposed to pitavastatin contained an increase in each protein, suggesting that these proteins had

been accurately identified by mass spectrometry, and they may be novel biomarkers of statin-induced cell death (figure 5.18).

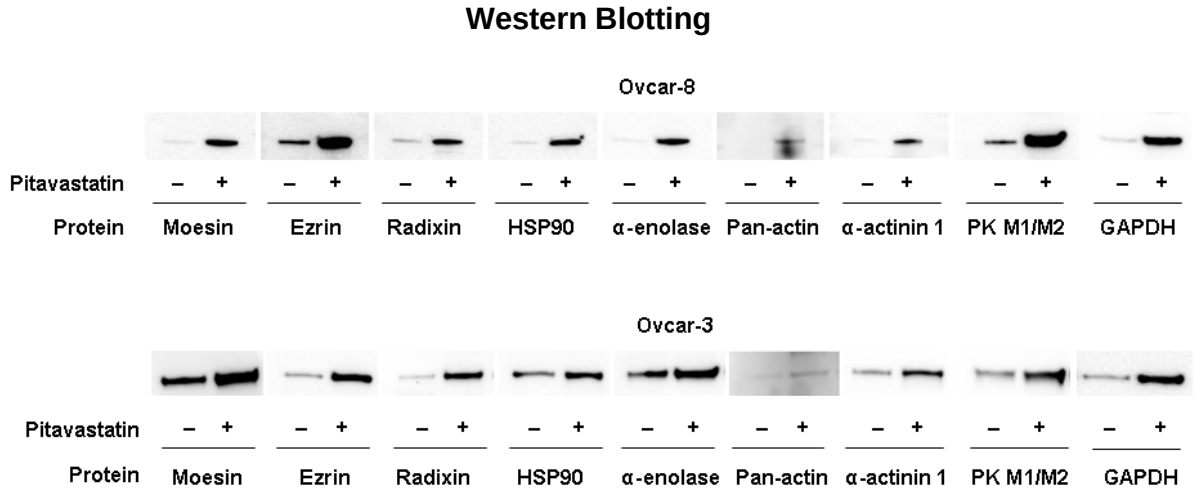

Figure 5.18: Validation of the release of nine proteins from ovarian cancer cells exposed to pitavastatin. Ovcar-8 and Ovcar-3 cells exposed to 1 μM (5 x IC_{50}) or 8 μM (2 x IC_{50}) pitavastatin (+) respectively, or solvent (-) for 72 hours. Proteins in supernatant samples, previously identified by mass spectroscopy sequencing, were increased in cells exposed to pitavastatin (n = 3). Heat shock protein 90, HSP90; pyruvate kinase isoform M1 or M2, PK M1/M2; glyceraldehyde-3-phosphate dehydrogenase, GAPDH.

5.3.8 Pitavastatin modestly inhibits the growth of Ovcar-3 tumour xenografts

To determine whether pitavastatin could inhibit the growth of tumour cells *in vivo*, Ovcar-3 xenografts were established in nude mice (these studies were performed by Charles River Discovery Research Services, North Carolina). The maximum tolerated dose (MTD) of 78.95 mg/kg, orally, every 12 hours was determined in an initial study which evaluated a range of doses of pitavastatin in mice (26.32 – 157.89 mg/kg every

12 hours). Subsequently, mice were treated with either pitavastatin at the MTD or vehicle alone for 33 days. Pitavastatin treatment was well tolerated with less than 5% decrease in mean body weight throughout the experiment. Pitavastatin marginally reduced tumour volume after 25 days compared to tumours treated with vehicle alone, although the overall reduction in tumour volume was not statistically significant (figure 5.19).

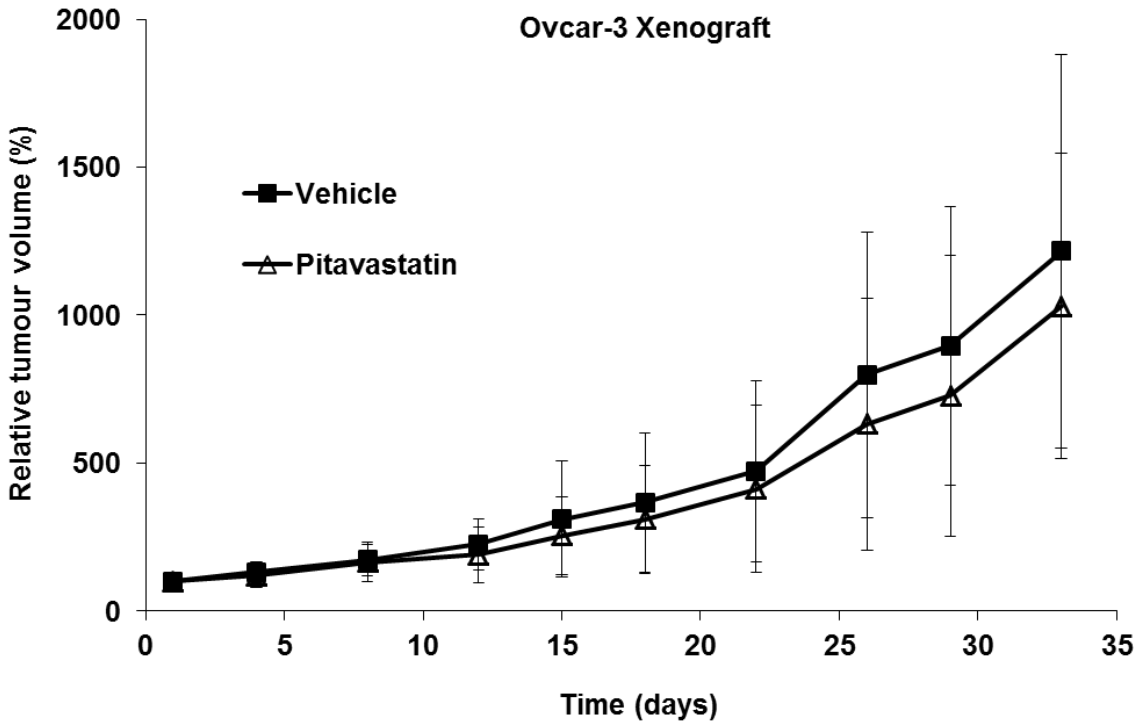

Figure 5.19: The effects of pitavastatin on the growth of Ovcar-3 xenografts in SCID mice. Mice were treated with 78.95 mg/kg pitavastatin or vehicle alone every 12 hours orally for 33 days (10 animals per group). Tumour volume was measured twice a week (mean ± S.E.M., n = 10). This xenograft study was completed by Charles River Discovery Research Services in Morrisville, North Carolina.

Pitavastatin was previously shown to cause apoptosis in ovarian cancer cell lines (figure 5.8). Furthermore, simultaneous induction and inhibition of the autophagy pathway following pitavastatin exposure may contribute to these cytotoxic effects. In order to determine if pitavastatin had any effects on apoptosis or autophagy in the tumour xenografts after 33 days of pitavastatin exposure, six representative tumours were homogenised and the levels of LC3-II, p62, Rab7, and PARP cleavage were determined.

PARP cleavage was possibly increased in two of the tumours treated with pitavastatin, suggesting that pitavastatin may have contributed to an increase in apoptosis in these tumours (figure 5.20). Furthermore, there was an increase in LC3-II or p62 in two pitavastatin-treated tumours, and a reduction in the level of Rab7 in all tumours exposed to pitavastatin (figure 5.20). Taken together, these results are reminiscent of those obtained *in vitro*, and the effects of pitavastatin on both apoptosis and autophagy may have contributed to the modest reduction in tumour volume.

HMGCR has been reported to be upregulated in response to statin treatment, and this may contribute to resistance to the cytotoxic effects of statins [173, 525]. This raised the possibility that an increase in HMGCR in the statin-treated xenograft tumours may have overcome the cytotoxic effects of pitavastatin, resulting in only a modest reduction in tumour growth. Therefore, the level of HMGCR was determined in the six representative tumours. The level of HMGCR did not differ significantly between tumours treated with pitavastatin or vehicle, suggesting that this is not likely to have contributed to resistance to pitavastatin (figure 5.20).

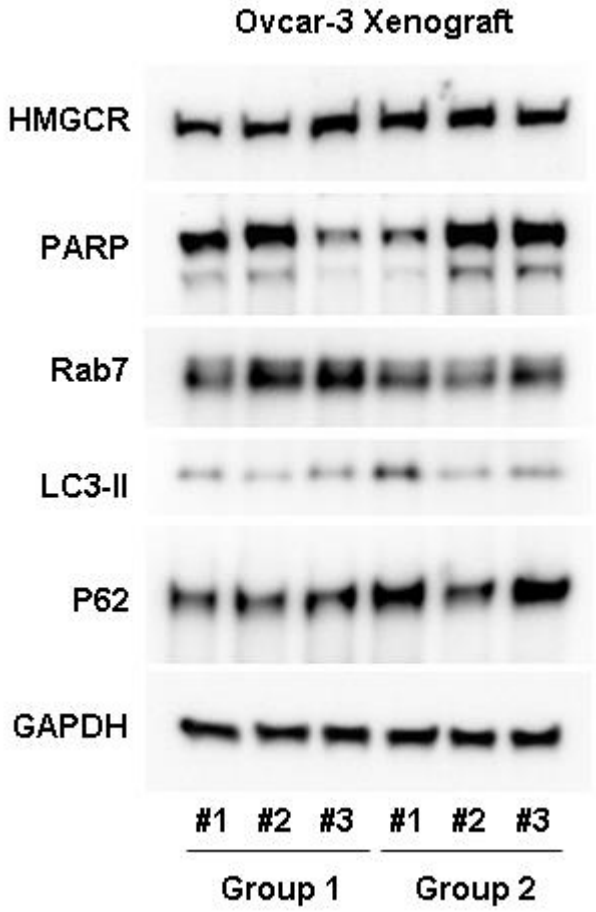

Figure 5.20: The effects of pitavastatin on HMGCR and proteins involved in autophagy and apoptosis in Ovcar-3 xenograft tumours. Six Ovcar-3 tumours from xenograft studies were lysed (group 1 = vehicle, group 2 = pitavastatin). PARP cleavage, HMGCR, Rab7, LC3-II and p62 levels were determined by western blotting. GAPDH was used as a loading control (n = 3).

To further understand why pitavastatin only modestly inhibited tumour growth *in vivo*, the concentration of pitavastatin in each tumour was determined. Solid phase extraction (SPE) was used to extract pitavastatin from homogenised tumours, and the concentration of pitavastatin in each tumour was determined by high-performance liquid chromatography (HPLC). HPLC was completed by Dr Clare Hoskins at Keele University.

Xenograft tumours treated with vehicle contained no pitavastatin, whereas tumours exposed to pitavastatin contained between 32 µM and 114 µM pitavastatin, thereby suggesting that pitavastatin had penetrated the tumours (table 5.1). To further confirm the presence of pitavastatin in the tumours, Ovcar-8 cells were exposed to a range of concentrations of the pitavastatin extracts from each tumour, and the effect on cell growth was determined. Extracts from xenograft tumours treated with vehicle had no effect on the growth of Ovcar-8 cells. However, tumour extracts from pitavastatin-treated tumours were approximately 10-fold less potent than authentic pitavastatin. Furthermore, when the potency of each tumour extract in the bioassay was compared to that of authentic pitavastatin, the pitavastatin concentration in the tumour extracts was approximately 5-fold lower than that measured by HPLC (table 5.1). These data support the presence of pitavastatin in the xenograft tumours treated with pitavastatin, however the reduction in potency compared to authentic pitavastatin suggests that either the pitavastatin concentration in the tumour extracts was less than that measured by HPLC, or there were other factors inhibiting pitavastatin activity.

Ovcar-3 tumour xenograft	Pitavastatin concentration in tumour extract (HPLC) (μM)	Pitavastatin concentration in tumour extract (bioassay) (μM)
Group 1 #1-3	0	0
Group 2 #1	106	17
Group 2 #2	32	8
Group 2 #3	114	22

Table 5.1: Determination of the concentration of pitavastatin in Ovcar-3 xenograft tumours. Pitavastatin was extracted from six Ovcar-3 tumour samples from xenograft studies (group 1 = vehicle, group 2 = pitavastatin) and quantified using HPLC (data was obtained from Dr Clare Hoskins at Keele University). Alternatively, a bioassay was performed in which a range of concentrations of the tumour extracts, as estimated by the HPLC method, were added to Ovcar-8 cells *in vitro* and the potency of the extracts were compared to that of authentic pitavastatin.

An additional factor that could have contributed to the insufficient reduction in tumour growth in xenografts treated with pitavastatin was the presence of geranylgeraniol in the mouse chow. Nomura and colleagues reported that a high-fat diet restored tumour growth in mice deficient in monoacylglycerol lipase, a lipolytic enzyme which promotes tumour growth and invasion [526]. This raised the possibility that exogenous sources of lipids may have blocked the cytotoxic effects of the statins. Lipids were extracted from the Lab Diet mouse chow used in the xenograft study along with two other mouse chows, Special Diets and Open Source Diets, and a selection of foodstuffs (table 5.2).

Foodstuff	Documented fat content in foodstuff	Mass of lipid extract obtained
Tesco pure sunflower oil	100 g in 110 mL	608 mg
Sainsbury's olive oil	92 g in 100 mL	388 mg
Japonica polished rice (Kinuhikari)	Not Available	510 mg
Lab Diet NIH 31 0045117 chow	5 g in 100 g	928 mg
Special Diets Services 801960 BK001(E) chow	Not Available	198 mg
Open Source Diets D11112201 chow	7 g in 100 g	340 mg
Ensure Plus drink	5 g in 100 mL	10 mg
Fresubin 2 kcal drink	8 g in 100 mL	10 mg

Table 5.2: Yields of lipid extracts obtained from foodstuffs. Lipids were extracted from a range of mouse chow diets, sunflower oil, olive oil, rice, and several food replacement drinks. Lipids were extracted from 50 g of each foodstuff. The fat content in each foodstuff is also given where available.

These extracts were added to ovarian cancer cells exposed to pitavastatin to determine if they could suppress the cytotoxic effects of the statins. The extracts on their own had no significant effect on cell growth or apoptosis (figures 5.21 and 5.22). However, when Ovcar-8 and Ovcar-3 cells exposed to pitavastatin were supplemented with the extracts from the mouse chow used in the xenograft study (Lab Diet) and the Special Diets mouse chow, there was a modest but significant inhibition of the anti-growth and pro-apoptotic effects of pitavastatin (figures 5.21 and 5.22). Furthermore, the Open Source Diets mouse chow also prevented the anti-growth

effects of pitavastatin in ovarian cancer cell lines, although only modestly inhibited caspase 3/7 activity (figures 5.21 and 5.22).

These data made it important to determine if other foodstuffs, which would presumably be consumed by patients treated with statins during clinical trials, also contained lipids that may inhibit the cytotoxic activity of pitavastatin. Extracts were also prepared from various foods, and their ability to suppress the cytotoxic effects of pitavastatin was determined. Previous studies have reported the presence of geranylgeraniol, geranylgeranyl diphosphate or geranylgeranyl esters in foodstuffs including Kinuhikari polished rice [456], sunflower oil [527], olive oil [527], and virgin olive oil [528]. Extracts from sunflower oil and Kinuhikari polished rice significantly prevented the anti-growth and pro-apoptotic effects of pitavastatin in Ovcar-8 or Ovcar-3 cell lines (figures 5.21 and 5.22). Notably, sunflower oil extract almost completely inhibited pitavastatin-induced apoptosis in both cell lines (figure 5.22). Extracts from olive oil also modestly inhibited the effects of pitavastatin on cell growth and apoptosis (figures 5.21 and 5.22). However, extracts from olive oil and rice did not appear to prevent the anti-growth effects of pitavastatin in Ovcar-8 and Ovcar-3 cells respectively, despite modestly decreasing pitavastatin-induced apoptosis in these cell lines. This may reflect lower concentrations of lipids in these extracts, which may only partially reverse the effects of pitavastatin.

These studies highlighted the need for a food that patients could consume during a clinical trial of pitavastatin, which would not suppress the drug's pro-apoptotic effect. Lipids were also extracted from two food replacement drinks, Ensure Plus and Fresubin (table 5.2). These food replacement drinks have less fat / mL compared to the sunflower and olive oils (table 5.2). The extracts from Ensure Plus and Fresubin

had no effect on the anti-growth and pro-apoptotic effects of pitavastatin, suggesting that these food replacement drinks could be used as an alternative diet in studies evaluating pitavastatin for the treatment of cancer *in vivo* (figures 5.21 and 5.22).

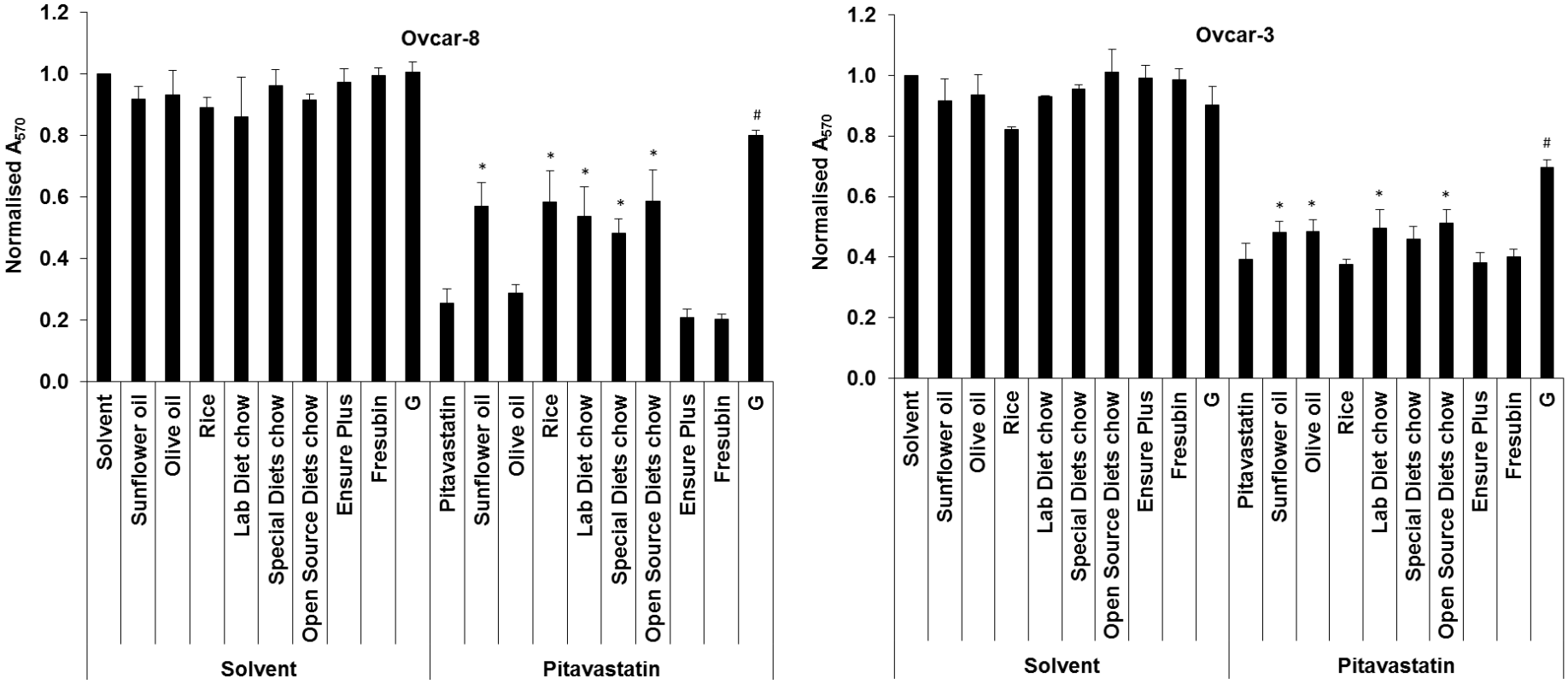

Figure 5.21: The effects of lipids extracted from various foodstuffs on the anti-growth effects of pitavastatin. Ovcar-8 and Ovcar-3 cells were supplemented with lipids extracted from 8 foodstuffs (sunflower oil, olive oil, polished rice, Lab Diet chow, Special Diets chow, Open Source Diets chow, Ensure Plus and Fresubin) or 10 μM geranylgeraniol (G), either in the presence of 0.4 μM (Ovcar-8) or 8 μM (Ovcar-3) pitavastatin (2 x IC_{50}) or solvent for 72 hours. The number of cells surviving (mean ± S.D., n = 3-5) was expressed as a fraction of those surviving in samples treated with solvent alone. The number of cells was significantly increased compared to cells exposed to pitavastatin alone where indicated (*, paired *t*-test, $P<0.05$; $^{\#}$, paired *t*-test, $P<5\times10^{-5}$).

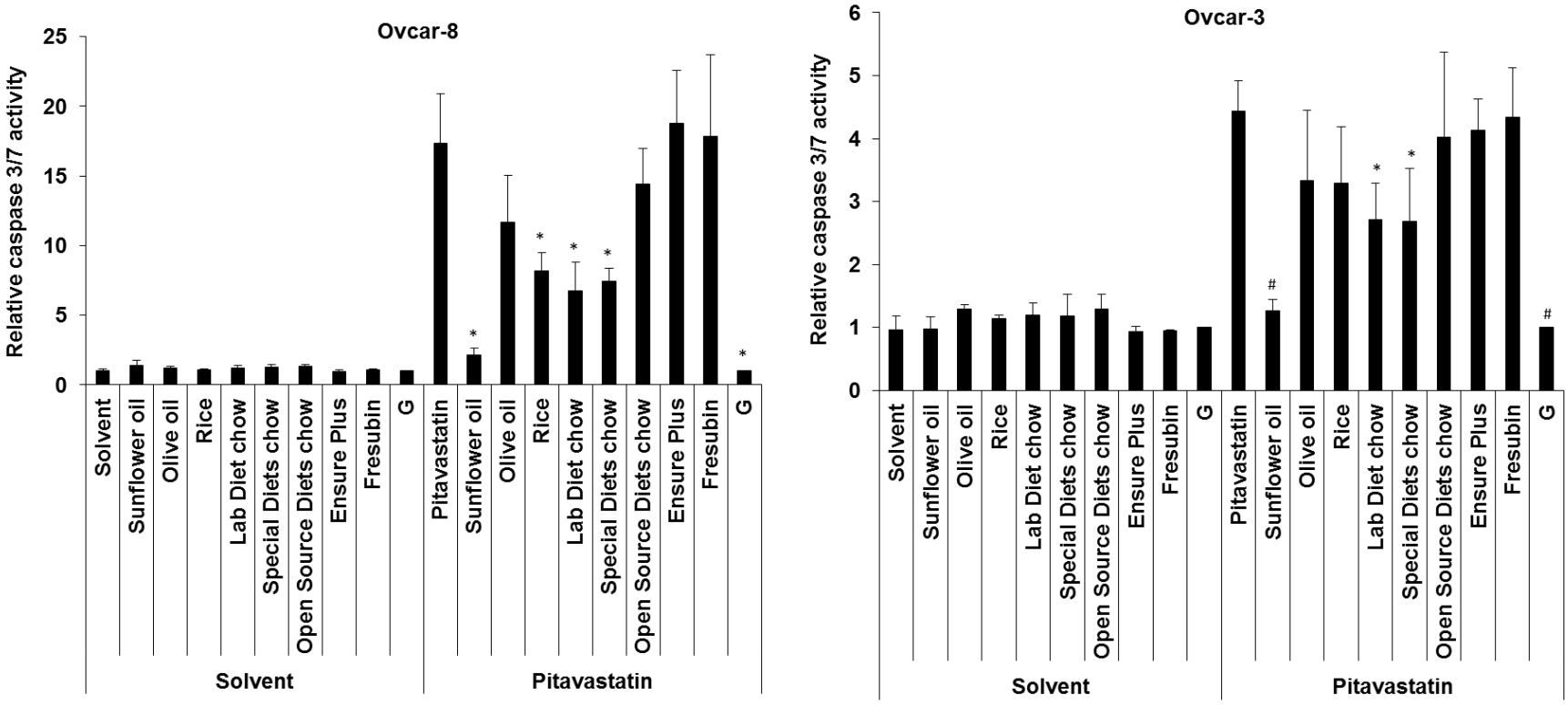

Figure 5.22: The effects of lipids extracted from various foodstuffs on the pro-apoptotic effects of pitavastatin. Ovcar-8 and Ovcar-3 cells were supplemented with lipids extracted from 8 foodstuffs (sunflower oil, olive oil, polished rice, Lab Diet chow, Special Diets chow, Open Source Diets chow, Ensure Plus and Fresubin) or 10 µM geranylgeraniol (G), either in the presence of 0.4 µM (Ovcar-8) or 8 µM (Ovcar-3) pitavastatin (2 x IC_{50}) or solvent for 72 hours. Caspase 3/7 activity was expressed as a fraction (mean ± S.D., n = 3) of the activity measured in cells exposed to geranylgeraniol. Caspase 3/7 activity was significantly decreased compared to cells exposed to pitavastatin alone where indicated (*, paired *t*-test, $P<0.05$; $^{\#}$, paired *t*-test, $P<0.01$).

5.4 Discussion

This chapter aimed to evaluate pitavastatin in ovarian cancer, because this statin has an improved half-life of around 11 hours, and previous results demonstrated that a statin with a longer half-life than simvastatin (2-3 hours) may be required to improve drug exposure (chapter 4).

HMGCR has been labelled as a metabolic oncogene as overexpression was correlated with cell growth, transformation and migration, and a poor prognosis in breast cancer patients [137, 146]. Furthermore, the *TP53* tumour suppressor gene is mutated in most ovarian cancers, and mutant p53 can associate with sterol gene promoters including SREBP, resulting in the expression of genes involved in the mevalonate pathway [148]. In the studies presented here, HMGCR was significantly increased in ovarian cancer cell lines compared to normal ovarian epithelial cells. The cells tested all lack wild-type p53, raising the possibility that the increased expression may be driven by mutant p53/SREBP. The description of HMGCR as a metabolic oncogene in breast cancer suggests that it may have a similar role in ovarian tumorigenesis. In any event, these findings provide a rationale for the evaluation of HMGCR inhibitors, statins, in ovarian cancer. The lipophilic statin, simvastatin was previously shown to have cytotoxic activity in ovarian cancer cell lines (chapter 4). However, simvastatin has a short half-life (2-3 hours), and therefore, repeated dosing is likely to be necessary for continual inhibition of HMGCR and the cytotoxic effects of simvastatin (chapter 4). Pitavastatin has a considerably longer half-life of 11 hours, and therefore, twice daily dosing may be adequate to maintain suppression of HMGCR. The data presented here aimed to evaluate pitavastatin as a therapy for the

treatment of ovarian cancer, and to identify novel biomarkers of statin-induced cell death which could be used to predict response to statins in clinical trials.

Pitavastatin was found to be more potent than simvastatin in a panel of ovarian cancer cell lines. Reminiscent of simvastatin, the inhibition of cell growth by pitavastatin was reversed by simultaneous exposure to geranylgeraniol, suggesting that these effects were mediated through inhibition of HMGCR. Pitavastatin also demonstrated anti-growth activity in paired ovarian cancer cell lines, some of which had developed resistance to chemotherapy, reaffirming that statins could be used in chemotherapy resistant disease. Clinical trials with pitavastatin could be carried out in patients with advanced chemoresistant ovarian cancer, although it may be difficult to show a therapeutic benefit in this subset of patients. Pitavastatin also significantly inhibited the growth of normal human ovarian epithelial cells and human foreskin fibroblasts with a similar potency to that observed in some ovarian cancer cell lines. This suggests that the cytotoxic effects of statins may also affect normal cells, independent of the level of HMGCR. Conversely, other studies reported that statins had no cytotoxic effect on other normal cell lines including mesothelial cells [321], mammary epithelial cells [254], embryonic stem cells [529], and primary tissue cultures established from normal ovarian epithelium [337], suggesting that normal cells exhibit varying sensitivities to statins. Furthermore, despite the potential cytotoxic effects of statins on normal human cells, clinical trials have administered high doses of statins in patients without considerable toxicity [419, 497]. One possible interpretation is that the evaluation of toxicity *in vitro* is a poor predictor of clinical activity. Immortalised “normal” cells *in vitro* proliferate continually, a feature that is not shared by most cells *in vivo*.

The activity of pitavastatin was confirmed in an ovarian cancer spheroid model. Pitavastatin reduced ATP in cancer spheroids, although there was a significant decrease in potency in A2780 and Ovcar-8 spheroids compared to the respective monolayer cultures. Reminiscent of the activity of simvastatin in ovarian cancer spheroids, these differences could reflect limited drug penetration or reduced proliferation of cells in the spheroid core (chapter 4). Furthermore, the different analytical methods used to estimate the IC_{50} in cell monolayers versus spheroids could have contributed to the variation in drug potency.

Further studies on cell monolayers demonstrated that pitavastatin significantly induced cell death in a panel of ovarian cancer cell lines. Notably, after 96 hours of continuous exposure to pitavastatin at 5 times the IC_{50}, more than 75% of A2780, cisA2780, Ovcar-3 and Ovcar-8 cells were dead when assessed by Trypan blue exclusion, suggesting that several days of high concentrations of pitavastatin may be necessary to induce cell death. This has several implications for clinical trials evaluating pitavastatin in ovarian cancer. The maximum tolerated dose (MTD) of pitavastatin in humans is 64 mg daily and this achieves a maximum plasma concentration (C_{max}) of approximately 2.7 µM (calculated based on linear pharmacokinetics and previously reported data from [530-532]). This concentration is representative of the IC_{50} of pitavastatin in most of the ovarian cancer cell lines evaluated. Furthermore, pitavastatin can be administered at the MTD for up to two weeks without significant myotoxicity [533]. Taken together, this suggests that pitavastatin administered at the MTD could achieve plasma concentrations comparable to those required for anti-cancer activity *in vitro*, and these high concentrations can be maintained for several weeks to allow the turnover of proteins which are already prenylated before cell death can occur.

To further justify a clinical trial of pitavastatin in ovarian cancer, an Ovcar-3 xenograft study was conducted with the MTD of pitavastatin in mice (78.95 mg/kg, orally, every 12 hours) administered for 33 days. The MTD was predicted to achieve a C_{max} of approximately 56 µM in the mice (calculated based on linear pharmacokinetics and previously reported data from [161]), which is well above the concentration required for cytotoxicity *in vitro*. Furthermore, based on a half-life of 7 hours in rats, the pitavastatin concentration was estimated to be approximately 17 µM 12 hours after a single administration, suggesting that adequately high concentrations would be maintained over 12 hours, and this should allow continual inhibition of HMGCR. Despite this, pitavastatin only marginally reduced tumour volume compared to mice treated with vehicle alone after 33 days. This was supported by a small increase in PARP cleavage in two representative pitavastatin-treated tumours, suggestive of an induction in apoptosis. Furthermore, pitavastatin also increased the autophagy proteins, LC3-II and p62, in two tumours exposed to pitavastatin and this may contribute to an inhibition of autophagy, which may increase the sensitivity of ovarian cancer cells to apoptosis. The geranylgeranylated GTPase, Rab7 is required for autophagosome maturation and trafficking during autophagy [488], and statins were shown to reduce Rab7 in ovarian cancer cells *in vitro*. Pitavastatin was also modestly decreased Rab7 in three tumours, providing confidence that pitavastatin had reached the tumours. One pitavastatin-treated tumour displayed no increase in PARP cleavage despite an apparent increase in both LC3-II and p62, suggesting that there may have been other factors which prevented pitavastatin-induced apoptosis. Therefore, it was necessary to determine the reasons for the limited activity observed in the Ovcar-3 xenograft study, before pitavastatin could be evaluated in further xenograft studies or clinical trials. HMGCR is upregulated in response to statin exposure and this can contribute to resistance to the effects of statins, presumably by overcoming the

inhibition of HMGCR [173, 525]. The level of HMGCR was similar in both drug- and placebo-treated tumours, suggesting that this was not likely to be a mechanism of resistance to pitavastatin in this study. Alternatively, pitavastatin may not have penetrated the tumours in sufficient concentrations to cause cell death. To assess this, the drug was extracted from the tumours and its concentration measured by HPLC. Pitavastatin concentrations in drug-treated tumours ranged from 32 µM to 114 µM, which was anticipated to be more than adequate to induce apoptosis in ovarian cancer cell lines. To confirm the HPLC results, a bioassay was performed in which the tumour extracts were added to ovarian cancer cells *in vitro* and the potency of the extract was compared to that of authentic pitavastatin. When ovarian cancer cells were exposed to pitavastatin extracted from drug-treated tumours, using the HPLC estimation of pitavastatin concentration, the extracts were approximately 10-fold less potent than authentic pitavastatin. There are several possible explanations for this discrepancy. The concentration of pitavastatin measured by HPLC may have been higher than the actual concentration in the extracts. This is surprising because SPE of pitavastatin followed by detection by HPLC has previously been reported to be a sensitive and accurate method for the quantitative analysis of pitavastatin in biological samples [453, 534]. Another explanation is that the tumour extracts contained compounds related to geranylgeraniol. The reversed phase SPE process includes a nonpolar solid phase composed of silica packing modified with hydrophobic alkyl and aryl groups. This might retain geranylgeraniol, which could suppress the activity of the pitavastatin in the tumour extract, and make it appear less potent. Nonetheless, it was still surprising that pitavastatin had little effect because even if the bioassay was a more accurate measure of pitavastatin than the HPLC method, the concentration of drug in the tumour extracts would have ranged from 8-22 µM, 2-5 fold above the IC_{50} measured *in vitro*. Taken together, these data suggest that a significant amount of

pitavastatin reached the tumour and that a further explanation for the lack of efficacy was necessary.

The possibility that the mice had a dietary source of geranylgeraniol was considered. It was noted that the mouse chow used in the xenograft study contained fat, which may encompass geranylgeranyl-related lipids. Nomura and colleagues reported that mouse chow containing elevated amounts of fatty acids restored tumour growth in mice deficient in monoacylglycerol lipase, a lipolytic enzyme which promotes tumour growth and invasion [526]. Notably, lipids extracted from the mouse chow used in the xenograft study modestly, but nevertheless significantly, inhibited the effects of pitavastatin on Ovcar-8 and Ovcar-3 cell growth and apoptosis, suggesting that the consumption of mouse chow containing these lipids could have suppressed the cytotoxic effects in the xenograft study. Importantly, these findings were also demonstrated for two other brands of mouse chow. Thus, it is plausible that dietary geranylgeraniol contributed to the modest effect of pitavastatin in the xenograft study.

The discovery that lipids in mouse chow could inhibit the cytotoxic effects of pitavastatin raised the concern that lipids in common foodstuffs consumed by patients could suppress the activity of statins in ovarian cancer clinical trials. Geranylgeranyl diphosphate, geranylgeraniol or geranylgeranyl esters have been extracted from several foodstuffs including Kinuhikari polished rice [456], sunflower oil [527], olive oil [527], and virgin olive oil [528]. In most cases, lipid extracts from sunflower oil, olive oil and rice modestly inhibited the effects of pitavastatin on cell growth and apoptosis. Notably, extracts from sunflower oil, which is commonly used in cooking, almost completely attenuated the pro-apoptotic effect of pitavastatin in cells. The lipids in these foodstuffs (e.g. geranylgeraniol) may contribute to the production of

geranylgeranyl diphosphate, resulting in an inhibition of the cytotoxic activity of statins. Collectively, these results have significant implications for future clinical trials evaluating statins as a therapy for cancer, as the consumption of foodstuffs which contain these lipids may prevent the anti-cancer activity of statins, potentially resulting in tumour progression.

As these observations could potentially undermine clinical trials of statins, we therefore identified a food that could be consumed by patients during a clinical trial which may lack geranylgeraniol. Lipids extracted from the food replacement drinks, Ensure Plus and Fresubin, did not prevent the anti-growth and pro-apoptotic effects of pitavastatin in ovarian cancer cells. Taken together, these results suggest that xenograft studies and clinical trials evaluating statins as a cancer treatment should ensure that dietary fat intake is minimised and this can be achieved through the administration of a controlled diet using food replacement drinks.

Further studies aimed to determine the mechanism of statin-induced cytotoxicity in ovarian cancer cells. Previous data suggested that both simvastatin and pitavastatin inhibited cell growth and caused cell death in cells, although the mechanism is complex (chapter 4). Statins have been shown to inhibit the proliferation of many cancer cell lines by G_0/G_1 cell cycle arrest [217-233]. Despite a significant decrease in the fraction of ovarian cancer cells in G_2/M phase(s) of the cell cycle following pitavastatin exposure, there was no corresponding increase in cells in G_1 phase. The significant increase in subG_1, potentially corresponding to an induction of apoptosis in pitavastatin-treated cells, may have masked G_1 phase cell cycle arrest. In contrast to this increase in subG_1, there was no significant increase in Ovcar-8 cell death following exposure to simvastatin for 48 hours (chapter 4). This discrepancy may

reflect differences in the sensitivity of Ovcar-8 and Ovcar-3 cells to statin after 48 hours. This is supported by greater caspase 3/7 activity in Ovcar-3 cells compared to Ovcar-8 cells after 48 hours of pitavastatin treatment. Furthermore, cell cycle analysis involves the permeabilization of cell membranes, which enables propidium iodide to label DNA, and this is likely to enable the earlier identification of apoptotic cells which have a reduced DNA content due to degradation by endonucleases. Trypan blue can only penetrate cells that have lost plasma membrane integrity, a feature occurring in the very late stages of apoptosis (secondary necrosis). Taken together, after 48 hours of statin treatment, DNA fragmentation may be occurring in a significant proportion of cells, whilst the plasma membrane remains intact.

Simvastatin was previously reported to induce apoptosis in ovarian cancer cells through the activation of JNK, which resulted in an induction of Bim expression, and subsequent stimulation of the intrinsic apoptotic pathway [338]. Caspase-9 is cleaved and activated following cytochrome c release from the mitochondria, and therefore, can be used as a marker of intrinsic apoptosis pathway stimulation. Pitavastatin caused a significant increase in the activation of caspase-9, caspase-3, caspase-7 and PARP cleavage in ovarian cancer cell lines, confirming that pitavastatin induced apoptosis though the intrinsic pathway. Previous research also demonstrated that pitavastatin increased levels of the pro-apoptotic protein, Bad, and decreased expression of Bcl-2 mRNA in liver cancer xenograft studies, further supporting activation of the intrinsic apoptosis pathway [512]. Despite this, pitavastatin also increased the level of caspase-8, which is stimulated by the death-inducing signalling complex in the extrinsic apoptosis pathway. This raised the possibility that pitavastatin also induced the activation of the extrinsic pathway, potentially though the upregulation of death receptor ligands, as previously observed for simvastatin in

prostate cancer cells [364]. FLIP inhibits the cytoplasmic adaptor protein and caspase-8 complex, which prevents caspase-8 activation, and therefore, negatively regulates the extrinsic apoptosis pathway. Furthermore, FLIP has also been shown to be implicated in resistance to chemotherapy in ovarian cancer [521, 522]. Despite this, FLIP knockdown did not significantly sensitise ovarian cancer cells to the anti-growth effects of pitavastatin. There are several potential explanations for this. An inadequate knockdown of FLIP may have contributed to the absence of a significant effect on the sensitivity of Ovcar-3 cells to pitavastatin. Conversely, statins have been shown to decrease the expression of FLIP in cancer cells, and this may also explain why any further knockdown of FLIP did not alter sensitivity to pitavastatin [240]. Caspase-8 can also be activated by the execution caspases (caspase-3 and caspase-7) in the intrinsic apoptosis pathway, and therefore, pitavastatin may not directly activate the extrinsic apoptosis pathway, rather caspase-8 activation serves as an amplifier of execution caspases in the intrinsic apoptosis pathway [535]. Furthermore, statins cause an accumulation of both LC3-II and p62, and the association of these proteins has previously been demonstrated to recruit FADD-caspase-8 complexes to autophagosomal membranes, through interactions with Atg5, which facilitates the self-activation of caspase-8 [536]. Taken together, pitavastatin induced apoptosis in ovarian cancer cells most likely through the intrinsic pathway, although direct activation of the extrinsic pathway cannot be excluded.

To further investigate the mechanism by which pitavastatin induced cytotoxicity, the effects of pitavastatin on autophagy were also determined. Simvastatin was previously shown to simultaneously induce and inhibit the autophagy pathway at different points *in vitro*, and this may contribute to cell death (chapter 4). A recent study demonstrated that pitavastatin increased the level of the autophagy protein, LC3-II, in cancer cells

[517]. However, LC3-II can accumulate either when autophagy is stimulated due to an increase in LC3-II synthesis, or when autophagy is inhibited as the turnover of LC3-II is prevented. To address this, p62 was also measured as p62 accumulation is a marker of autophagy inhibition [486]. Pitavastatin caused an accumulation of both LC3-II and p62, consistent with an inhibition of autophagy. Furthermore, in addition to simvastatin (chapter 4), pitavastatin also decreased the level of Rab7, and this was moderately reversed by supplementation with geranylgeraniol, suggesting that pitavastatin may block the later stages of autophagy by inhibiting the geranylgeranylation of Rab7. To assess whether the inhibition of autophagy contributed to apoptosis, the expression of Atg5, an essential autophagy-related protein involved in autophagosome formation, was inhibited by RNA interference. Knockdown of Atg5 and subsequent inhibition of autophagy sensitised ovarian cancer cells to apoptosis induced by pitavastatin, suggesting that autophagy inhibition may contribute to the cytotoxic effects of pitavastatin. This is supported by previous results, where Atg5 knockdown modestly sensitised cells to the anti-growth effects of simvastatin (chapter 4). Blocking autophagy may prevent the turnover of mitochondria (mitophagy), leading to an increase in the production and release of ROS from the mitochondria [295, 523]. ROS have previously been shown to induce apoptosis in statin-treated colon cancer cells [352]. This raised the possibility that inhibition of mitophagy may contribute to pitavastatin-induced apoptosis through an elevation of ROS in ovarian cancer cells. Indeed, when mitochondria were stained with Mitotracker dye, pitavastatin caused a small but significant increase in mitochondrial staining in both Ovcar-3 and Ovcar-8 cells. This could represent either an increase in mitochondrial number or larger mitochondria with more surface area for Mitotracker binding, both of which may be consistent with an inhibition of mitophagy [537, 538]. To confirm an increase in mitochondria, the mitochondrial DNA (mtDNA) content was

determined by measuring mitochondrial NADH dehydrogenase 1 (ND1) DNA. There was an increase in the relative mtDNA content in Ovcar-8 cells exposed to pitavastatin, which corresponded to the increase in mitochondria previously observed, but there was no difference in mtDNA content in Ovcar-3 cells. The reason for this discrepancy is unclear, but it may reflect the presence of larger deformed mitochondria in Ovcar-3 cells exposed to pitavastatin, which may have an accumulation of damaged mtDNA. The *cis*-regulatory element in the non-coding (D-loop) region of mtDNA is involved in the replication of mtDNA, and is more susceptible to oxidative damage compared to other regions of mtDNA [539]. A mutated sequence in the D-loop may affect binding to *trans*-acting factors, resulting in a decrease in mtDNA replication [540]. Pitavastatin caused a significant increase in ROS in Ovcar-3 cells, and elevated ROS in these cells may contribute to mutations in the D-loop region, which may impede mtDNA replication. Exposure of Ovcar-8 cells to pitavastatin did not increase ROS, suggesting that these cells may have additional protective mechanisms against oxidative stress. A previous study also reported that DNA-damaging agents including cisplatin and doxorubicin did not induce an accumulation of ROS in Ovcar-8 cells [541]. In contrast to previous reports, the inhibition of ROS in ovarian cancer cells exposed to pitavastatin did not prevent apoptosis, suggesting that the presence or accumulation of ROS is unlikely to significantly contribute to statin-induced apoptosis in ovarian cancer cells. Notably, the oxidising agent TBHP caused a small increase in caspase 3/7 activity in Ovcar-8 cells, which was partially blocked by the superoxide scavenger NAc, suggesting that other cytotoxic agents may stimulate ROS-induced apoptosis in ovarian cancer cells. Taken together, these results suggest that pitavastatin may inhibit autophagy, by preventing the geranylgeranylation of Rab7, which could result in an accumulation of mitochondria with damaged mtDNA, and an increase in ROS. Despite this, it is likely

that there are other mechanisms, independent of ROS, involved in pitavastatin-induced apoptosis, which may also be mediated through the inhibition of autophagy.

Statins have been previously shown to inhibit cancer cell migration and invasion through the inhibition of geranylgeranyl diphosphate in the mevalonate pathway [238, 257-260]. However, in ovarian cancer cells, pitavastatin did not inhibit migration after 36 hours, suggesting that inhibition of cell migration may not contribute to the anti-growth effects of pitavastatin. This may reflect the relatively short time that cells were exposed to pitavastatin in this assay (36 hours), as prolonged exposure to statins may be required to allow the turnover of prenylated proteins that are required for cell migration (chapter 4). Significant cell detachment was observed at higher drug concentrations or after longer exposure times, potentially masking any effects of pitavastatin on cell migration.

Drug-related biomarkers are a measure of the response of the body to a drug, and can be used to predict drug efficacy earlier than conventional clinical endpoints. Clinical trials evaluating statins for the treatment of cancer have frequently used plasma cholesterol levels and urinary mevalonate excretion as markers of HMGCR inhibition. Urinary mevalonate excretion has been correlated with the rate of cholesterol synthesis, although urinary mevalonate levels can be affected by dietary sources of mevalonate [542, 543]. However, cholesterol levels have not been correlated with the anti-cancer activity of statins, and moreover, inhibition of cholesterol synthesis is not responsible for statin-induced cytotoxicity [518]. It is also unsurprising that well characterised drugs such as statins can inhibit plasma cholesterol levels. Therefore, there is a requirement to identify biomarkers which can be used to directly monitor the cytotoxic response of cancer cells to statin treatment.

Cytokeratin 18, a protein expressed predominantly in epithelial cells [544], is cleaved by caspases 3, 7 and 9 during apoptosis to produce ccCK18, which can be detected in the plasma of breast cancer patients receiving chemotherapeutic drugs [519]. Theoretical calculations have suggested that ccCK18 may be detected in patient serum following apoptosis of only 10-20 million cancer cells [545]. Therefore, ccCK18 may be useful as a biomarker in patients with tumours that undergo apoptosis in response to exposure to pitavastatin. To test this, the release of ccCK18 into the cell culture medium of ovarian cancer cells exposed to pitavastatin was measured. The level of ccCK18 was significantly increased in medium of Ovcar-3 and Ovcar-8 cells exposed to pitavastatin or paclitaxel. However, there was no accumulation of ccCK18 in medium taken from Igrov-1 or Skov-3 cells exposed to pitavastatin concentrations which had previously induced cell death. This could reflect differences in cell death after 96 hours, as cell death was considerably lower in Igrov-1 and Skov-3 cells (35-60% cells dead) compared to Ovcar-3 and Ovcar-8 cells (80-90%). Despite this, the relative activities of caspases 3, 7 and 9 in Ovcar-8 and Igrov-1 cells exposed to pitavastatin for 48 hours were comparable, suggesting that there may be other reasons for the lack of ccCK18 release from Igrov-1 cells. A recent study found that both Ovcar-3 and Ovcar-8 are likely to represent high-grade serous ovarian carcinoma (HGSC), whereas the origin of Igrov-1 and Skov-3 is uncertain [438]. Furthermore, Igrov-1 and Skov-3 have been reported to express lower levels of cytokeratin 18 compared to other ovarian cancer cell lines, suggesting that these cells may have a different origin [546]. Taken together, the small increases in ccCK18 from Igrov-1 and Skov-3 cells exposed to pitavastatin may have been below the detection threshold of the assay (25 pM).

The lack of detectable ccCK18 production in half of the ovarian cancer cell lines evaluated made it important to discover additional biomarkers released from ovarian cancer cells in response to statin exposure. To do this, cells in culture were exposed to pitavastatin or simvastatin, and the proteins released into the cell culture medium were identified. Seven protein bands were found in statin-treated ovarian cancer cells which were present at a higher amount compared to either cancer cells exposed to solvent or pravastatin, or normal cells exposed to solvent or statins. This suggested that these proteins were specifically released from cancer cells in response to pitavastatin or simvastatin. Further mass spectrometry analysis of the isolated proteins revealed that three protein bands corresponded to alpha-enolase, glyceraldehyde-3-phosphate dehydrogenase and pyruvate kinase, all of which are involved in glycolysis. Cancer cells frequently upregulate these glycolytic enzymes, resulting in an increase in aerobic glycolysis termed “the Warburg effect”, and this has been correlated with tumorigenesis and poor prognosis [547]. A further three bands were identified to be the cytoskeletal proteins, alpha-actinin 1, actin, ezrin, radixin and moesin (ERM). Alpha-actinin 1 and all three of the ERM proteins have been shown to be upregulated in cancer, and contribute to tumour progression and invasion [548, 549]. Lastly, heat shock protein 90 (HSP90) was also identified in the cell culture medium of pitavastatin-treated cells. Heat shock protein 90 (HSP90) is involved in maintaining cellular protein homeostasis by regulating the folding, stability, activation, function, and proteolytic turnover of more than 100 proteins [550]. HSP90 is frequently upregulated in tumorigenesis, and contributes to the survival, growth, migration and invasion of cancer cells [550]. Notably, these data were confirmed by a recent proteomic analysis of proteins released from endothelial cells exposed to atorvastatin, which identified these proteins in the secretome and many others involved in glycolysis/gluconeogenesis, cytoskeleton organisation, antigen processing and

presentation, cell communication, focal adhesion and gap junctions [520]. HSP90, alpha-enolase and pyruvate kinase have previously been reported to be released into the extracellular environment by an unknown mechanism, as these proteins do not have an N-terminal peptide sequence for direction to the endoplasmic reticulum and secretion through the classical secretory pathway [520, 551, 552]. In the absence of a signal sequence, these may be abundant proteins that are released by unknown secretory independent pathways, cell autolysis or necrosis. Several studies have reported that statins may induce necrosis in some cancers, and this can result in the loss of cell membrane integrity, leading to the release of the cellular contents into the extracellular matrix [219, 333, 553-555]. Further validation of these potential biomarkers is required to establish which proteins are predominantly released from cancer cell lines compared to normal cells, and whether these proteins can be detected in the plasma following pitavastatin treatment *in vivo*.

Taken together, these results suggest that pitavastatin is the most potent statin that possesses anti-growth and pro-apoptotic activities in a panel of ovarian cancer cell lines. Pitavastatin should be evaluated in clinical trials at high concentrations with an appropriate dosing schedule which will enable continual inhibition of HMGCR. Furthermore, clinical trials should ensure that dietary fat intake is minimised, in order to reduce the potential exposure of cancer cells to exogenous sources of isoprenoids, which may reverse the cytotoxic effects of statins. Clinical trials evaluating statins in cancer should also aim to validate potential drug biomarkers identified *in vitro*, in order to obtain novel biomarkers that can be used to predict response to statin treatment in patients.

CHAPTER 6

PRECLINICAL EVALUATION OF PITAVASTATIN IN COMBINATION WITH OTHER ANTI-CANCER AGENTS

6.1 Introduction

The design of rational drug combinations takes into account the biology of the tumour and the molecular pharmacology of the drugs involved. Strategies are frequently focussed on reversing drug resistance, and can include horizontally targeting parallel signalling pathways or vertically targeting one signalling pathway at several nodes, in order to block any compensatory signalling mechanisms which may confer chemoresistance. Nevertheless, any drug combination which combines flux into a cell death signal is a valid approach to combination therapy.

Chapters 4 and 5 have evaluated the anti-cancer activity of simvastatin and pitavastatin in ovarian cancer cells, demonstrating that both high concentrations and continuous exposure to these statins was required to induce cell death. Pitavastatin has been evaluated in clinical trials at doses between 16 mg and 64 mg daily for the treatment of high cholesterol [162]. Dose-limiting toxicities observed after 2-4 weeks of treatment were reversed within 2 weeks of discontinuing therapy [162]. The concentrations of pitavastatin required to cause ovarian cancer cell death (0.2 – 7.6 μM depending on cell line) are similar to the predicted plasma concentration in patients following administration of 64 mg pitavastatin (2.7 μM, assuming linear pharmacokinetics and using data from [530-532]). Whilst pitavastatin can be administered as a single agent at high doses for up to 2 weeks, it may be possible to further reduce the concentration required to cause cancer cell death by combination with other agents that also cause apoptosis, including ABT-737, obatoclax, pictilisib and metformin (figure 6.1).

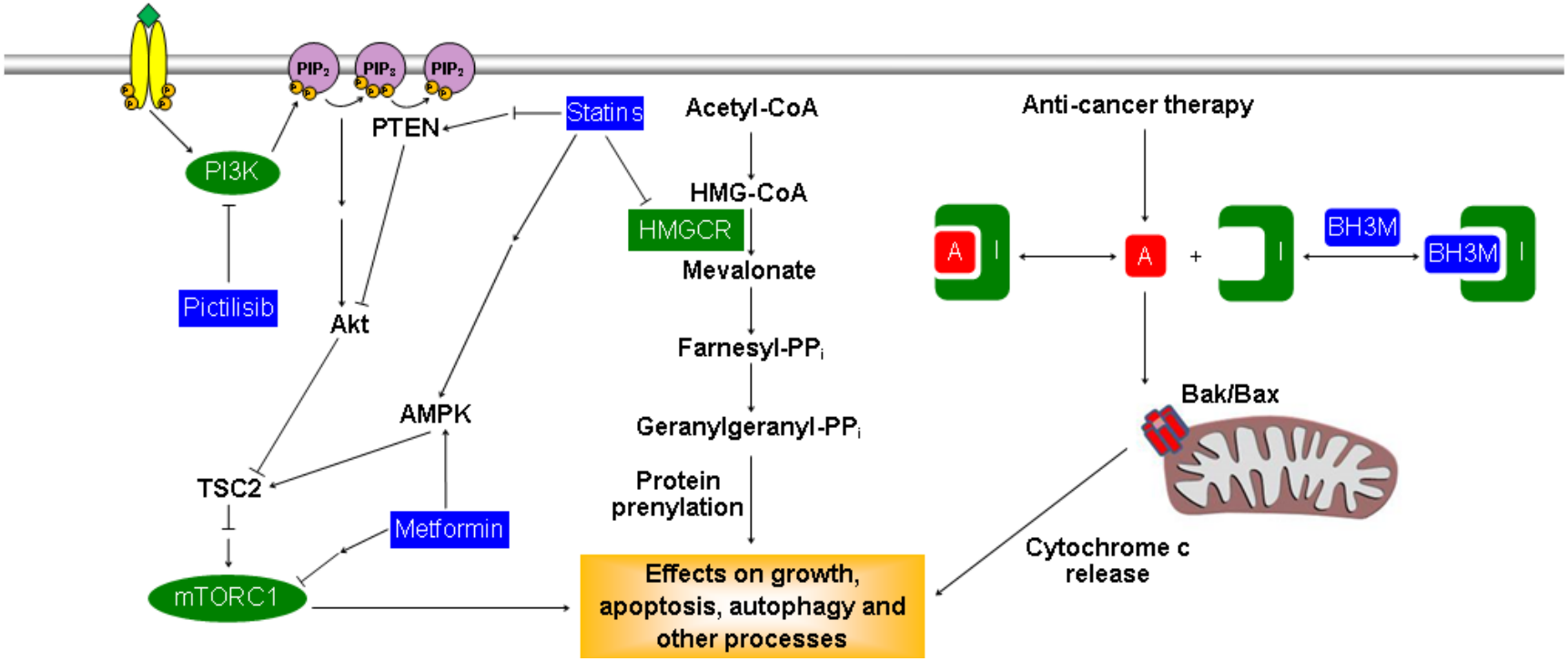

Figure 6.1: Modulation of the PI3K/Akt/mTOR and intrinsic apoptotic pathways by various drugs. Statins inhibit 3-hydroxy-3-methylglutaryl coenzyme A reductase (HMGCR), which prevents the geranylgeranylation of many proteins that regulate diverse intracellular processes, including the PI3K/Akt/mTOR pathway. Both pictilisib and metformin also inhibit components in the PI3K/Akt/mTOR pathway. BH3 mimetics ('BH3M') occupy Bcl-2 family inhibitors ('I'), preventing them from sequestering apoptosis activators ('A'), and sensitising cells to apoptosis. TCS2, tuberous sclerosis complex 2; AMPK, AMP-activated protein kinase; PI3K, phosphatidylinositol 3-kinase; PTEN, phosphatase and tensin homolog; PIP_2, phosphatidylinositol 4,5-bisphosphate; PIP_3, phosphatidylinositol (3,4,5)-trisphosphate; mTORC1, mammalian target of rapamycin complex 1.

6.1.1 BH3 mimetics: ABT-737 and obatoclax

Pro-apoptotic signals increase the expression of pro-apoptotic molecules including apoptosis activators (e.g. Bim, Bid and Puma) and sensitisers (e.g. Bad, Bmf and Noxa), which contain a single BH3 domain. The activators can be sequestered by apoptosis inhibitors (e.g. Bcl-2, Bcl-X_L and Mcl-1) through the hydrophobic BH3-binding groove of the inhibitor binding to the BH3 domain of the activator, thereby preventing apoptosis. Sensitisers or BH3 mimetics (e.g. ABT-737 and obatoclax) can competitively inhibit anti-apoptotic molecules and prevent them from binding to the activators, thereby allowing pro-apoptotic signalling to continue (figure 6.1) [556]. Preliminary reports suggested that obatoclax in combination with cisplatin or TNF-related apoptosis-inducing ligand (TRAIL) increased apoptosis in ovarian cancer cell lines [557]. Furthermore, ABT-737 and the orally bioavailable analogue ABT-263 inhibit Bcl-X_L, Bcl-2 and Bcl-w, and have been shown to enhance the cell death induced by carboplatin or paclitaxel in ovarian cancer cells [450, 558]. One mechanism of these synergistic interactions is thought to be through modulation of the Noxa/Mcl-1 axis. The anti-apoptotic proteins Bcl-X_L and Mcl-1 co-operate to inhibit apoptosis in ovarian cancer cells [559]. Platinum-based compounds decrease Mcl-1 expression and increase the expression of the pro-apoptotic proteins, Noxa and Bim, which increases the sensitivity of chemoresistant cells to ABT-737 [559]. A number of drugs which inhibit Mcl-1 including NVP-BEZ235 are currently being evaluated in combination with ABT-737 for the treatment of ovarian cancer [560]. Statins have also been shown to decrease Mcl-1 in leukemia cells [217], gastric cancer cells [561] and hepatocellular carcinoma [562], and induce the expression of the apoptotic activator Bim in ovarian cancer cell lines [338] and glioblastoma cells [349]. These observations suggest that statins may also demonstrate synergy with ABT-737.

6.1.2 Phosphatidylinositol 3-kinase inhibitors: pictilisib

The phosphatidylinositol 3-kinase (PI3K) pathway plays an important role in cell survival, proliferation, migration and metabolism, and has recently been reported to be frequently activated in advanced epithelial ovarian cancers [56, 563]. Pictilisib is an orally active PI3K inhibitor which is more than 100 times more potent against class I PI3K compared to class II, III and IV family members (figure 6.1) [564]. Pictilisib has previously been shown to inhibit the growth of ovarian cancer cell lines [565], and Igrov-1 ovarian cancer xenografts by 80% [566]. Furthermore, pictilisib enhanced the anti-cancer effects of doxorubicin in ovarian cancer models, resulting in synergy that may be predicted by the dependence of cancer cells on the PI3K pathway for survival [565]. Statins have also been shown to interfere with PI3K signalling by inhibiting NFκB, resulting in an increase in the transcription of phosphatase and tensin homolog (PTEN) and a reduction in Akt phosphorylation [567]. Therefore, statins in combination with PI3K inhibitors could synergistically inhibit PI3K signalling, leading to an increase in cell death.

6.1.3 Biguanides: metformin

The biguanide metformin, currently indicated for diabetes and polycystic ovary disease, has also been shown to have antineoplastic activity both *in vitro* [568] and *in vivo* [569]. Retrospective studies have demonstrated that patients treated with metformin for diabetes may have a significantly reduced risk of developing gastrointestinal cancer [570]. In ovarian cancer, millimolar concentrations of metformin supressed cell growth *in vitro* [571, 572] and *in vivo* [573]. Furthermore, an increase in apoptosis was accompanied by an induction of Bax and Bad expression, and the

down regulation of Bcl-2 and Bcl-X_L expression [574]. Metformin inhibits complex I in the mitochondrial respiratory chain, leading to the inhibition of mammalian target of rapamycin (mTOR) signalling through AMP-activated protein kinase (AMPK) dependent and independent pathways (figure 6.1) [575, 576]. This can result in a decrease in both protein synthesis and cell growth. The PI3K inhibitor LY294002 in combination with metformin synergistically inhibited ovarian cancer growth and induced apoptosis, through the simultaneous repression of the PI3K/Akt/mTOR pathway [577]. Statins have also been shown to induce the activation of AMPK, with subsequent inhibition of mTOR [317], and therefore, may demonstrate promising anti-cancer activity in combination with metformin.

6.2 Aims

The work described in this chapter aimed to investigate the anti-cancer activity of pitavastatin in combination with ABT-737, obatoclax, pictilisib or metformin in a panel of ovarian cancer cell lines in order to identify successful combinations, which could potentially be further evaluated in ovarian cancer clinical trials.

6.3 Results

6.3.1 Single agent activity in ovarian cancer cell lines

To investigate the activity of drug combinations with pitavastatin, the potencies of pitavastatin, ABT-737, obatoclax, pictilisib and metformin were first determined in a

panel of four ovarian cancer cell lines. Pitavastatin (IC_{50} = 0.26 – 5.8 μM), ABT-737 (IC_{50} = 2.1 – 4.0 μM), obatoclax (IC_{50} = 0.15 – 0.36 μM) and pictilisib (IC_{50} = 0.072 – 0.88 μM) inhibited the growth of ovarian cancer cell lines (table 6.1). Conversely, metformin did not measurably inhibit the growth of the same panel of cell lines (IC_{50} > 100 μM) (table 6.2).

	Pitavastatin IC_{50} (μM)	ABT-737 IC_{50} (μM)	Obatoclax IC_{50} (μM)	Pictilisib IC_{50} (μM)
A2780	0.82 ± 0.2	4.0 ± 1.1	0.15 ± 0.04	0.29 ± 0.04
Ovcar-3	5.8 ± 1	2.1 ± 0.7	0.23 ± 0.07	0.35 ± 0.1
Ovcar-8	0.26 ± 0.06	2.6 ± 0.8	0.22 ± 0.05	0.88 ± 0.4
Igrov-1	2.9 ± 1	3.2 ± 0.9	0.36 ± 0.2	0.072 ± 0.01

Table 6.1: The potency of pitavastatin, ABT-737, obatoclax and pictilisib as single agents in ovarian cancer cell lines were measured in cell growth assays for 72 hours, and surviving cells were estimated by staining with sulforhodamine B (mean ± S.D., n = 3-9).

	Single agent		Combination with pitavastatin
	Metformin IC_{50} (μM)	Pitavastatin IC_{50} (μM)	Metformin CI
A2780	>100	0.82 ± 0.2	1.0 ± 0.2
Ovcar-3	>100	5.8 ± 1	0.93 ± 0.2
Ovcar-8	>100	0.26 ± 0.06	1.2 ± 0.02*
Igrov-1	>100	2.9 ± 1	1.1 ± 0.3

*P<0.01

Table 6.2: The potency of pitavastatin and metformin as single agents in ovarian cancer cell lines were measured in cell growth assays (columns 1-2, mean ± S.D., n = 3-9). To measure the activity of pitavastatin in combination with metformin, cells were exposed to a range of concentrations of pitavastatin and a fixed concentration of metformin (15 μM). Combination indices (CI) (mean ± S.D., n = 3-9) are quoted at a fraction affected of 0.5 and differed significantly from unity where indicated (*, paired *t*-test, P<0.01).

6.3.2 Combinations of pitavastatin and ABT-737, obatoclax, pictilisib or metformin are additive or antagonistic in ovarian cancer cells

Concentrations of ABT-737 above 20 μM have previously been anticipated to inhibit cell growth independently of Bcl-X_L [450]. Therefore, experiments were completed using a low fixed concentration of ABT-737 to inhibit cell growth by <10%, in combination with a range of concentrations of pitavastatin. ABT-737 was additive in combination with pitavastatin in Igrov-1 cells, and was additive (fraction affected, 0.75) or mildly antagonistic (fraction affected, 0.5) when combined with pitavastatin in Ovcar-3 and Ovcar-8 cells (figure 6.2). ABT-737 in combination with pitavastatin was significantly antagonistic in A2780 cells (fraction affected, 0.5; figure 6.2).

Cells were exposed to a range of concentrations of either obatoclax or pictilisib and pitavastatin combined at a ratio of their single agent IC_{50} values. The combination of obatoclax and pitavastatin was additive in Ovcar-3 and A2780 cells (figure 6.2). However, in Ovcar-8 and Igrov-1 cells, there was significant antagonism (fraction affected, 0.5), which was slightly reduced at higher drug concentrations (fraction affected, 0.75; figure 6.2). Pictilisib and pitavastatin were additive in most cell lines tested, even at higher drug concentrations (fraction affected, 0.75), with significant antagonism observed only in A2780 and Igrov-1 cells (fraction affected, 0.5, figure 6.2).

Metformin exhibited limited activity in single agent studies (table 6.2), and therefore, a fixed concentration of 15 μM metformin was added to cells in combination studies. This concentration reflects the maximum concentration of metformin that is achieved in the plasma of patients following administration of the maximum daily dose (2550

mg) for the treatment of diabetes [447]. Metformin at 15 μM had no effect on ovarian cancer cell growth in these studies, and the combination of pitavastatin and metformin resulted in additivity or mild antagonism in four cell lines (table 6.2).

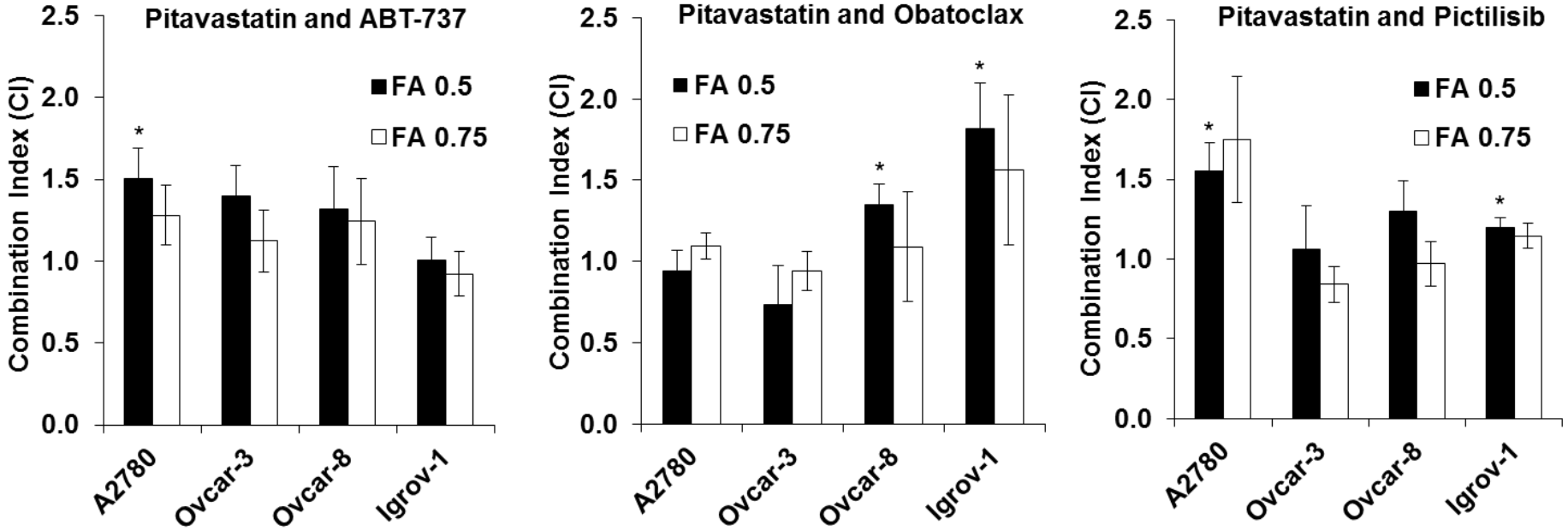

Figure 6.2: Pitavastatin in combination with ABT-737, obatoclax or pictilisib. To measure the activity of drug combinations in cell growth assays, cells were exposed to a range of concentrations of pitavastatin and either a fixed concentration of ABT-737 (A2780, 3 µM; Ovcar 3 and Ovcar-8, 1 µM; Igrov-1, 0.6 µM) or a range of concentrations of either obatoclax or pictilisib, combined with pitavastatin at the ratio of their single agent IC_{50}s. Combination indices (CI) (mean ± S.D., n = 3-9) are quoted at a fraction affected (FA) of 0.5 and 0.75, and differed significantly from unity where indicated (*, paired *t*-test, $P<0.05$).

6.3.3 Pitavastatin in combination with ABT-737 or pictilisib increases cell death in Igrov-1 or Ovcar-3 cells

Igrov-1 and Ovcar-3 cells were exposed to pitavastatin in combination with ABT-737, obatoclax or pictilisib for 72 hours and visualised by light microscopy. An increase in cell death was observed in Ovcar-3 cells exposed to pitavastatin and pictilisib, and Igrov-1 cells exposed to pitavastatin and ABT-737 compared to the single agents alone (figure 6.3). Although this is not necessarily indicative of synergy, these observations prompted further investigation.

To quantify the cell death observed by microscopy, the cells were collected by trypsinisation, stained with Trypan blue and counted. To determine whether a synergistic interaction occurred, the number of dead cells observed was compared to that expected from the Bliss independence criterion. The percentage of dead cells was significantly higher in Ovcar-3 cells exposed to pictilisib and pitavastatin, and in Igrov-1 cells treated with pitavastatin and ABT-737, than that expected (figure 6.4). In other combinations, the percentage of dead cells was not significantly different to that predicted by Bliss independence (figure 6.4).

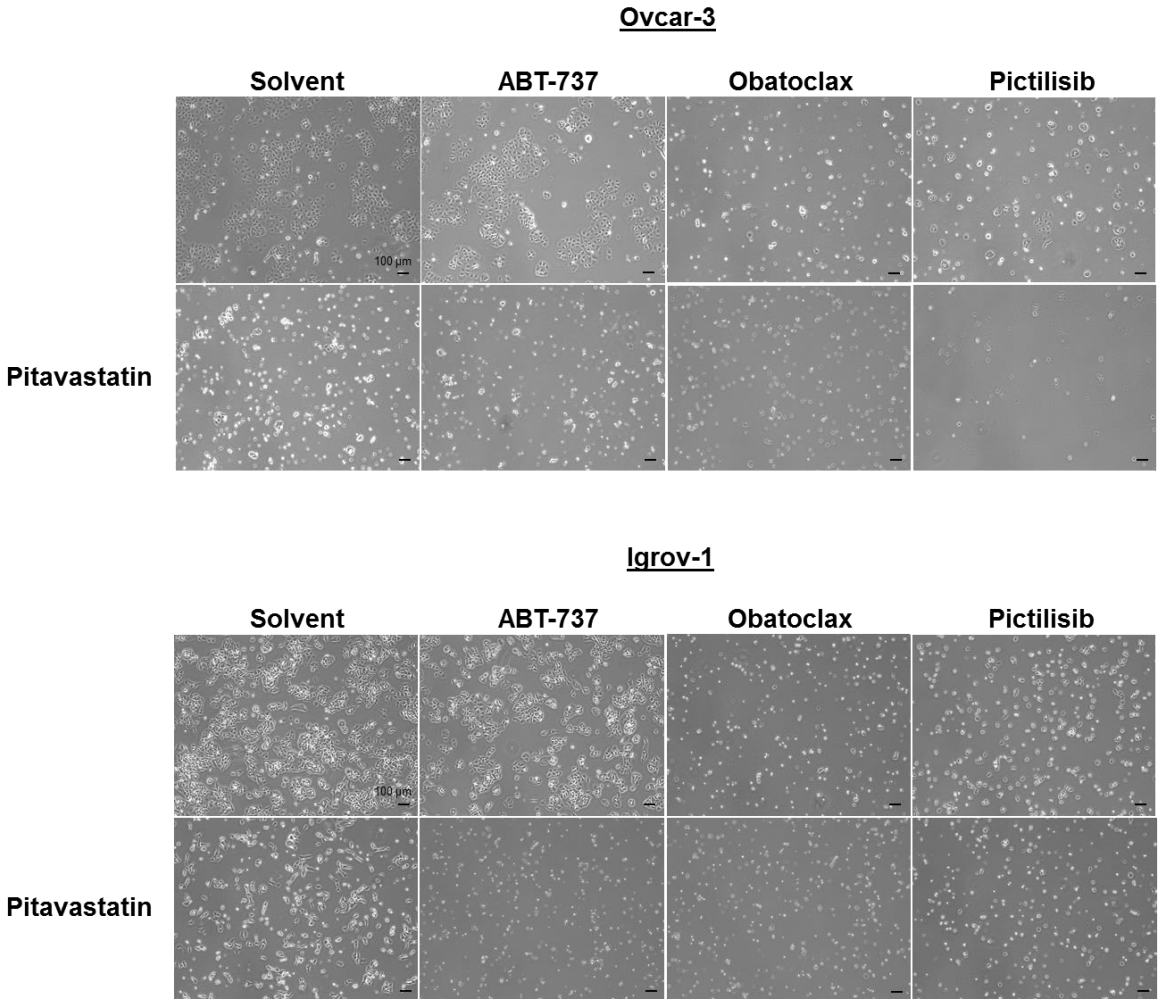

Figure 6.3: Phase contrast microscopy images of ovarian cancer cells exposed to pitavastatin in combination with ABT-737, obatoclax or pictilisib. Cells were exposed to either solvent (DMSO), 6 µM (Igrov-1) and 12 µM (Ovcar-3) pitavastatin (3 x IC_{50}), 0.6 µM (Igrov-1) and 1 µM (Ovcar-3) ABT-737, 2 µM (Ovcar-3) and 3 µM (Igrov-1) obatoclax (10 x IC_{50}), or 0.7 µM (Igrov-1) and 2 µM (Ovcar-3) pictilisib (10 x IC_{50}). The cells were assessed by microscopy after 72 hours. The results are representative of three experiments.

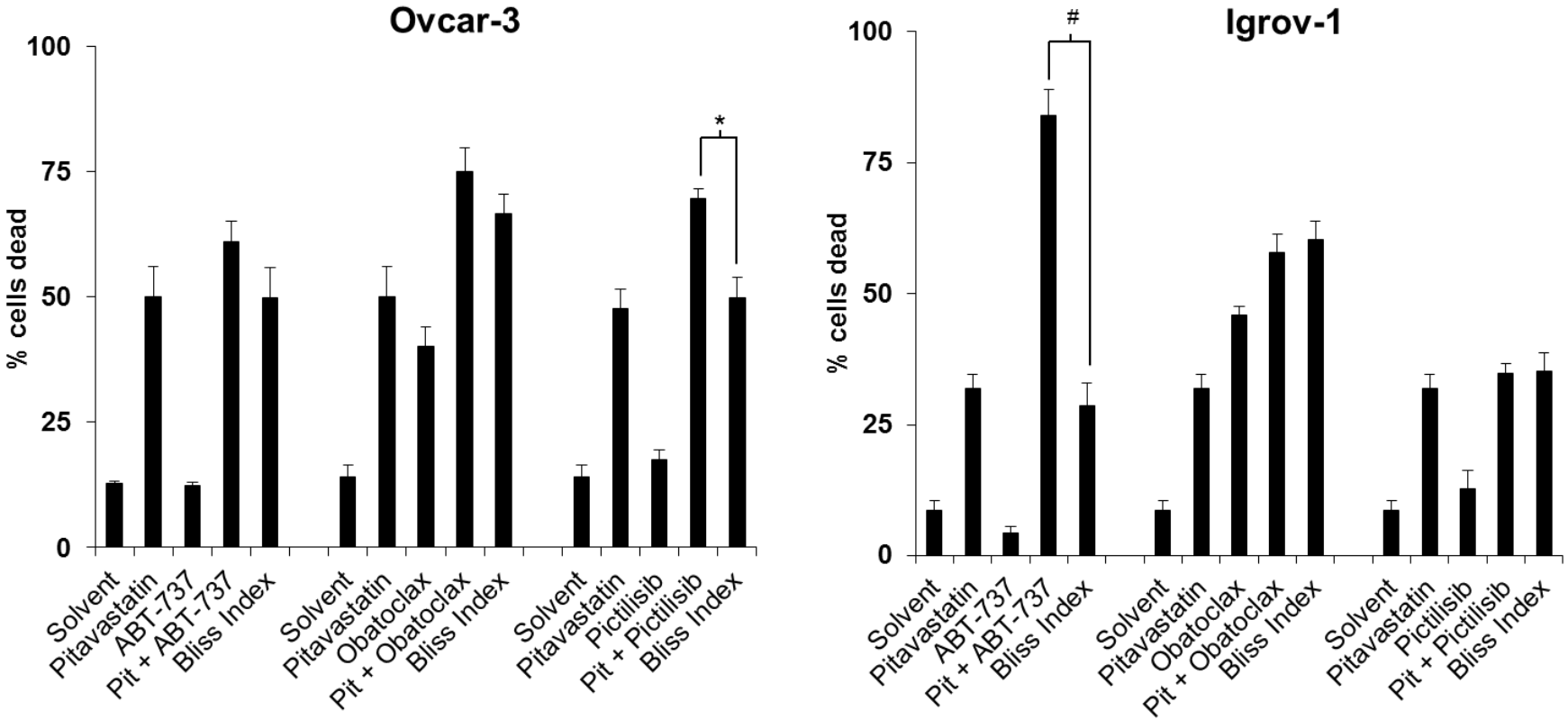

Figure 6.4: The effects of pitavastatin in combination with ABT-737, obatoclax or pictilisib on cell death. The number of dead Ovcar-3 and Igrov-1 cells was determined by Trypan blue staining after exposure for 72 hours to either solvent (DMSO), 6 µM (Igrov-1) and 12 µM (Ovcar-3) pitavastatin (3 x IC_{50}), 0.6 µM (Igrov-1) and 1 µM (Ovcar-3) ABT-737, 2 µM (Ovcar-3) and 3 µM (Igrov-1) obatoclax (10 x IC_{50}), or 0.7 µM (Igrov-1) and 2 µM (Ovcar-3) pictilisib (10 x IC_{50}). The number of dead cells (mean ± S.D., n = 3) was significantly different from Bliss independence calculated for each drug combination where indicated (*, paired *t*-test, $P<0.05$; $^{\#}$, paired *t*-test, $P<0.0005$).

6.3.4 Apoptosis contributes to the mechanism of cell death in combinations of pitavastatin and ABT-737 or pictilisib

To determine whether the increase in cell death observed following exposure to pitavastatin in combination with ABT-737, pictilisib or obatoclax was due to apoptosis, caspases 3 and 7 were measured in Ovcar-3 and Igrov-1 cells. Reminiscent of the results observed in the Trypan blue assay, there was a modest, but significant, increase in caspase 3/7 activity in Ovcar-3 and Igrov-1 cells exposed to pitavastatin and pictilisib or ABT-737 respectively, compared to that predicted by Bliss independence (figure 6.5). This was also supported by a slight increase in poly (ADP) ribose polymerase (PARP) cleavage in Igrov-1 cells exposed to pitavastatin and ABT-737 compared to pitavastatin alone (figure 6.6). These results are consistent with those obtained in the Trypan blue assays, however significant synergy was not observed in the cell growth assays.

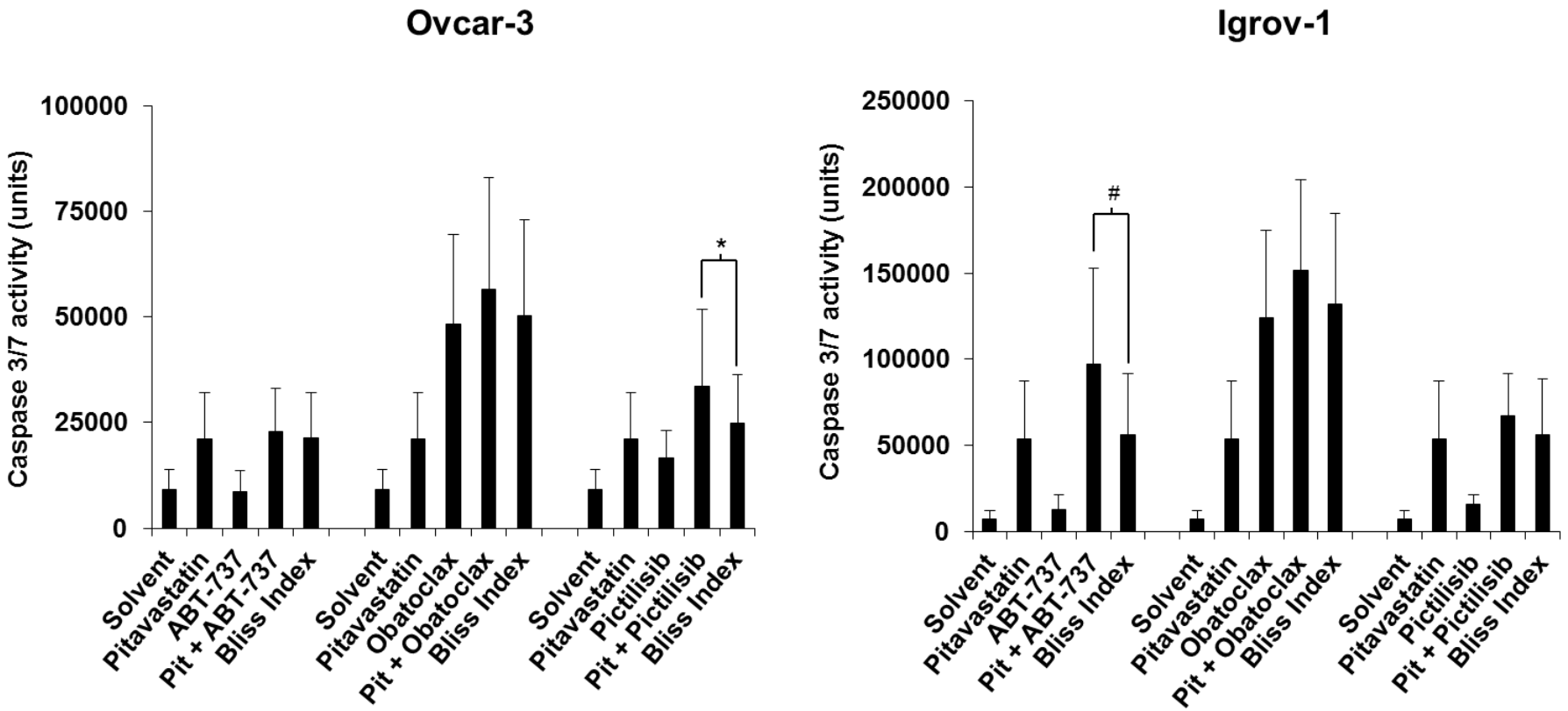

Figure 6.5: The effects of pitavastatin in combination with ABT-737, obatoclax or pictilisib on apoptosis. Caspase 3/7 activity in Ovcar-3 and Igrov-1 cells was measured following exposure to either solvent (DMSO), 6 µM (Igrov-1) and 12 µM (Ovcar-3) pitavastatin (3 x IC_{50}), 0.6 µM (Igrov-1) and 1 µM (Ovcar-3) ABT-737, 2 µM (Ovcar-3) and 3 µM (Igrov-1) obatoclax (10 x IC_{50}), or 0.7 µM (Igrov-1) and 2 µM (Ovcar-3) pictilisib (10 x IC_{50}) for 48 hours. Caspase 3/7 activity (mean ± S.D., n = 3) was significantly different from Bliss independence calculated for each drug combination where indicated (*, paired *t*-test, $P<0.01$; $^{\#}$, paired *t*-test, $P<0.001$).

The mechanism by which ABT-737 potentiated the apoptosis induced by pitavastatin was further evaluated by determining the levels of several Bcl-2 family members. Pitavastatin increased the level of the pro-apoptotic protein, Bim, and decreased the level of Bcl-X_L (figure 6.6). In contrast, exposure to ABT-737 resulted in an increase in Mcl-1. Whilst there were no significant changes in Bcl-X_L and Mcl-1 levels in cells exposed to pitavastatin and ABT-737 compared to pitavastatin alone, the level of Bim was modestly decreased in cells exposed to the drug combination (figure 6.6).

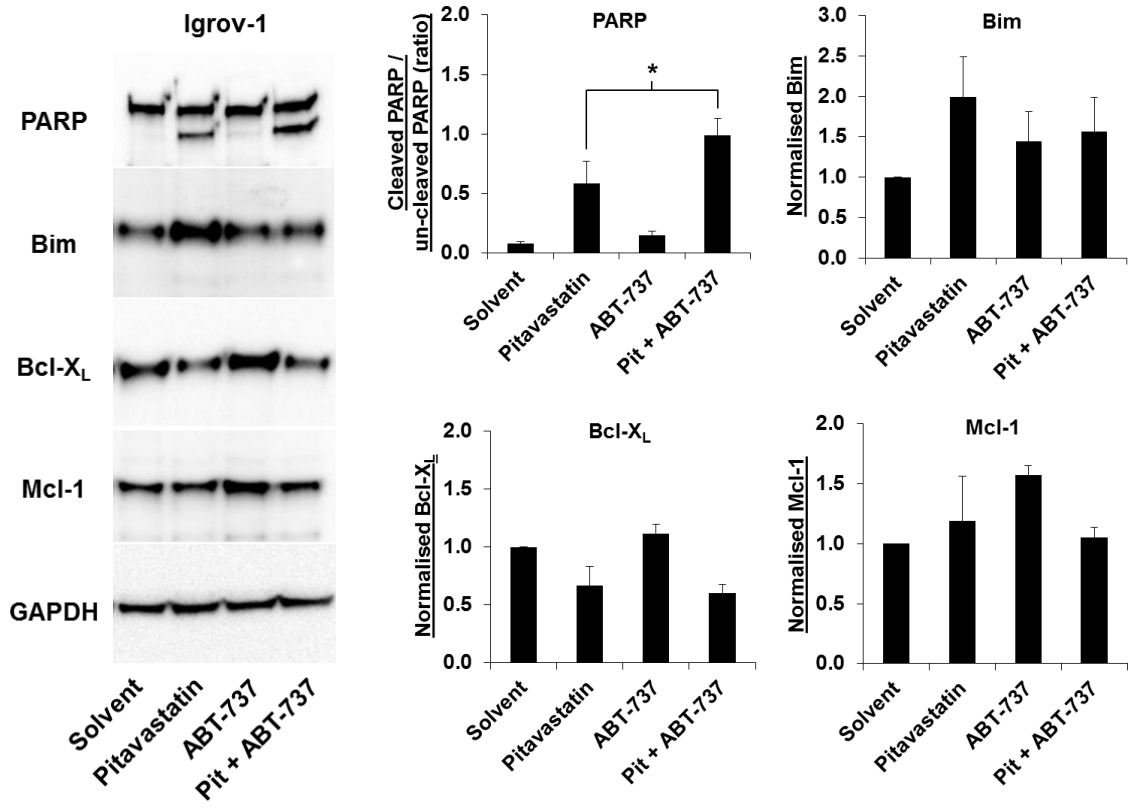

Figure 6.6: The effects of pitavastatin in combination with ABT-737 on proteins involved in the apoptosis pathway. Igrov-1 cells were exposed to solvent or 6 μM pitavastatin (pit, 3 x IC_{50}) or 0.6 μM ABT-737 as single agents, or in combination, for 48 hours. The levels of PARP, Bim, Bcl-X_L and Mcl-1 were measured by western blotting (n = 3). PARP cleavage was significantly increased in cells exposed to pitavastatin and ABT-737 compared to cells exposed to pitavastatin alone (*, paired *t*-test, $P<0.05$). GAPDH was used as a loading control.

6.4 Discussion

Statins have been previously evaluated in combination with various chemotherapeutic agents including cisplatin and doxorubicin, resulting in an additive or synergistic reduction in ovarian cancer cell proliferation [337, 484]. The exposure of cells to high concentrations of simvastatin prior to carboplatin resulted in profound antagonism (chapter 4), and this led to the investigation of compounds which inhibit the same pathways as statins, or sensitise ovarian cancer cells to apoptotic cell death.

ABT-737 or pictilisib in combination with pitavastatin additively inhibited cell growth, and modestly, but significantly, increased apoptosis induced by pitavastatin in Ovcar-3 and Igrov-1 cells. The PI3K pathway contributes to proliferative and anti-apoptotic effects on tumour cells, and is deregulated in 45% of high-grade serous ovarian cancers [56]. Ovcar-3, Ovcar-8, Igrov-1 and A2780 cells have PI3K/Akt pathway alterations consistent with activation of PI3K/Akt signalling, suggesting that these cell lines may be particularly sensitive to PI3K pathway inhibition [578, 579]. This was confirmed by the submicromolar IC_{50} values obtained for pictilisib in all cell lines. Statins have also been shown to inhibit PI3K signalling by inhibiting NF-κB, which results in an increase in the expression of *PTEN* and a reduction in Akt phosphorylation [567, 580]. Dual inhibition of PI3K/Akt/mTOR signalling with a combination of pictilisib and pitavastatin modestly increased apoptosis in Ovcar-3 cells, whilst demonstrating antagonism in A2780 and Igrov-1 cells. In contrast to the other cell lines, A2780 and Igrov-1 have *PTEN* mutations with low or undetectable levels of PTEN protein [578], which may render these cells resistant to further inhibition of PI3K signalling through PTEN modulation by statins.

The activity of ABT-737 has previously been attributed to inhibition of the pro-apoptotic mediators, Bcl-2, Bcl-X_L or Bcl-w, of which Bcl-X_L is overexpressed in ovarian cancer [450, 581]. Statins have been shown to induce apoptosis through a number of pathways, including suppression of Akt/Erk activation [350, 567], increased phosphorylation of the p38 MAPK pathway [350], and attenuation of Mcl-1, probably through the inhibition of NF-κB [582]. Igrov-1 cells were sensitive to the addition of ABT-737, and are therefore likely to have been "primed" for cell death as previously described [583]. In "primed" cells, ABT-737 prevents Bcl-X_L from sequestering pre-existing pro-apoptotic mediators, thereby enabling apoptosis to occur more readily. In contrast to previous reports, pitavastatin did not decrease Mcl-1 levels, but instead reduced the levels of Bcl-X_L and increased Bim. This, together with ABT-737 preventing the interaction of Bim with Bcl-2, Bcl-X_L or Bcl-w, may have contributed to the small, but significant, increase in apoptotic cell death in the combination. Additivity and mild antagonism was observed in the other cell lines exposed to this drug combination, and these differences could be related to the expression of apoptosis inhibitors. Mcl-1 expression may indicate cellular resistance to ABT-737 due to the poor affinity of ABT-737 for Mcl-1 [584]. Previous research demonstrated that expression of Bcl-X_L was markedly lower in A2780 cells, together with increased Mcl-1 levels compared to other ovarian cancer cell lines [450], and this could account for the antagonism observed in this cell line.

Obatoclax is a pan-Bcl-2 inhibitor which also inhibits Mcl-1, and therefore, may overcome the resistance mechanisms which limit ABT-737 activity. Despite this, obatoclax in combination with pitavastatin was additive at best in A2780 and Ovcar-3 cells, with significant antagonism observed in Ovcar-8 and Igrov-1 cells. Interestingly, the latter cell lines express lower Mcl-1 protein levels compared to A2780 and Ovcar-3

cells [450], and this could explain the reduction in sensitivity to obatoclax in Ovcar-8 and Igrov-1 cells in single agent studies, and the antagonism in combination studies. Obatoclax is also thought to have off-target effects in ovarian cancer cells, which may contribute to the antagonism observed in combination studies [585]. Taken together, these results suggest that the combination of obatoclax and pitavastatin may be of limited value in a heterogeneous tumour environment in a clinical setting.

Pitavastatin in combination with a fixed dose of metformin was mostly additive in ovarian cancer cell lines. Metformin has previously been reported to induce autophagy [586], a process involved in the degradation of cellular organelles and proteins during nutrient starvation and metabolic stress. Statins have also been shown to induce autophagy, and in combination with metformin, may exceed the capacity of the cell, leading to the degradation of cytoplasmic contents and death. Despite this, autophagy is no longer widely believed to contribute to cell death, and therefore, autophagy is unlikely to be the only mechanism of cell death. The anti-cancer activity of metformin was limited as cells were exposed to low concentrations of 15 μM, and concentrations of around 5-10 mM have been previously required to inhibit the proliferation of ovarian cancer cell lines [576]. These millimolar concentrations of metformin are not clinically achievable using the maximum tolerated dose (MTD) of metformin (2550 mg) [447], although one study has suggested that metformin may accumulate in mitochondria, and therefore, may reach higher concentrations in cancer cells [587]. However, until metformin is proven to accumulate in cancer tissue, it seems unlikely that metformin will confer a clinical benefit at the MTD in ovarian cancer.

To summarise, pictilisib or ABT-737 in combination with pitavastatin could be used in a subset of ovarian tumours in a clinical setting, and this may have several

implications. The concentration of pitavastatin required for ovarian cancer cell death could be reduced in drug combinations compared to the concentration required as a single agent. These lower concentrations are likely to be clinically achievable since the MTD of pitavastatin in humans (64 mg daily) gives a plasma concentration of 2.7 μM (calculated based on linear pharmacokinetics and previously reported data from [530-532]), and this alone is representative of the IC_{50} of pitavastatin in several cell lines. Reducing the dose of pitavastatin would minimise the dose-limiting side effects including myalgia, myoglobinurea and elevated creatine phosphokinase levels, which may be experienced at high doses of statins [533]. Furthermore, consideration should be given to identifying which patient groups may be sensitive to these combination treatments. Mcl-1 has been shown to confer resistance to ABT-737, and therefore measurement of Mcl-1 could be used to exclude patients from ABT-737 and pitavastatin treatment [584]. One disadvantage of this is that short-term exposure to ABT-737 can increase Mcl-1, and therefore, measurement prior to drug exposure may not give an accurate indication of drug response. Therefore, patients may require brief drug exposure prior to the collection of tumour tissue to predict sensitivity of the cancer to the combination therapy [584]. Additionally, the sensitivity of activator/apoptosis inhibitor complexes to ABT-737 in cells and that predicted from *in vitro* binding studies is often conflicting [588, 589], and therefore, translation to the clinical setting may also be difficult. “BH3 profiling” is one method that can be employed to overcome this. This is a measurement of the sensitivity of cancer cells to ABT-737 by determining the effects of the drug or related peptide on mitochondria isolated from the cancer cells [590]. This allows the identification of apoptosis inhibitors required for cancer cell survival, which negates the requirement to have prior knowledge of the expression or interactions of Bcl-2 family members. Furthermore, this assay could be used clinically in the future [590]. For PI3K inhibitor and

pitavastatin combinations, measurement of PTEN expression may indicate which patients may respond to this combination. A genomic analysis of ovarian cancer cell lines found that good predictors for the presence or loss of PTEN protein were PTEN copy number neutral (diploid) or homozygous deletion, rather than a hemizygous loss of the *PTEN* gene [578]. Furthermore, in a clinical assessment of PTEN loss, immunohistochemistry (IHC) detected most of the endometrioid tumours with PTEN protein loss [591]. A PTEN IHC assay (PREZEON) detected PTEN protein loss resulting from PTEN mutations (verified by copy number analysis in a range of human tumour cell lines), and this assay has already been implemented in a clinical laboratory [592]. These promising drug combinations warrant further preclinical investigations, including ovarian cancer xenograft studies, before clinical trials can be justified.

CHAPTER 7

CONCLUSION AND FURTHER STUDIES

Treatment for advanced ovarian cancer is currently comprised of surgery followed by adjuvant chemotherapy consisting of 3-weekly cycles of carboplatin and paclitaxel. Although the majority of patients respond to initial chemotherapy, drug resistance often emerges with few remaining treatment options, and only around 40% of patients survive 5 years after initial diagnosis with advanced ovarian cancer. Therefore, new treatments for ovarian cancer are urgently required.

There is currently considerable enthusiasm for re-developing drugs to treat conditions for which they were not originally established. For example, rapamycin was initially approved as an immunosuppressant for the prevention of transplant rejection. However, analogues of rapamycin have since been developed for the treatment of renal carcinoma. The use of statins to treat ovarian cancer fits this evolving paradigm. Mevastatin was the first 3-hydroxy-3-methylglutaryl coenzyme A reductase (HMGCR) inhibitor isolated from the culture broth of *Penicillium citrinum* by Akira Endo [593], and was subsequently shown to have anti-growth activity in Chinese hamster ovary cells and human malignant lymphoma cells [594]. Around a decade later, the cytotoxic activity of statins was confirmed in ovarian cancer cell lines [595]. This early study highlighted that the concentration of lovastatin required to inhibit the growth of ovarian cancer cell lines was achievable in the plasma of cancer patients exposed to high doses of lovastatin [595, 596]. The research presented here also found that the concentrations of both simvastatin and pitavastatin required for cytotoxicity *in vitro* were similar to the plasma concentrations achieved in patients following administration of the maximum tolerated dose. Furthermore, continual blockade of HMGCR for several days was required for cell death, suggesting that statins with short half-lives of 2-3 hours (e.g. simvastatin or lovastatin) may require frequent administration. Pitavastatin has a longer half-life of around 11 hours and was demonstrated to be the

most potent statin in ovarian cancer cell lines, and therefore, offers the best prospect to evaluate the clinical efficacy of statins in ovarian cancer. In addition to the choice of statin and dosing frequency, further consideration should be given to the patient's diet, as lipids present in many commonly consumed foodstuffs may reverse the cytotoxic effects of statins. Nomura and colleagues recently reported that a high-fat diet rescued the anti-cancer effects of monoacylglycerol lipase inhibition in a xenograft model, suggesting that exogenous lipids may contribute to cell survival pathways [526]. Further research could determine the effect of diets with varying fat content on the cytotoxic activity of statins in xenograft studies. Collectively, these data are in contrast to most ongoing clinical trials, which are evaluating statins at standard doses (40-80 mg once daily) used for the treatment of high cholesterol in patients presumably receiving a normal diet, and suggest that these clinical trials are unlikely to succeed. With the exception of hepatocellular cancer, clinical trials that have previously evaluated standard doses of statins in combination with chemotherapy for cancer treatment have not reported any survival benefit compared to standard chemotherapy regimens [409-411, 415].

Research investigating which patients should receive statins for the treatment of cancer is currently underway. Previous studies have reported that increased HMGCR contributed to cancer cell growth and migration [137, 146]. However, HMGCR level did not significantly correlate with the sensitivity of ovarian or breast cancer cells to statins, suggesting that there are likely to be other molecular features which determine sensitivity to statins [597]. Goard and colleagues recently identified a 10-gene signature that could be used to predict fluvastatin sensitivity in a panel of breast cancer cell lines [597]. A similar approach could be employed in ovarian cancer cell lines to determine a statin-sensitivity signature, and this could be used to identify

patients with ovarian cancers that are more likely to respond to statin treatment in clinical trials. Importantly, statins retained potency in ovarian cancer cell lines relatively resistant to chemotherapy, suggesting that statins could be used in chemoresistant disease. One possibility is that patients with disease that has failed to respond to carboplatin or paclitaxel treatment could receive high doses of pitavastatin in a clinical trial setting. An initial phase I clinical trial to identify a therapeutic window could evaluate escalating doses of pitavastatin (8-32 mg), administered orally twice daily for 1-2 weeks. Each dose level should be tested in a new group of patients to minimise the risk of toxicity (e.g. myopathy). Adverse effects should be determined by clinical assessment, and laboratory analysis including a full blood count, liver enzymes, creatine phosphokinase and renal function. Furthermore, efficacy should be assessed by computed tomography (CT) scans and measurement of the serum biomarker CA125. The results of the phase I trial could be used to inform a phase II study, which should incorporate two arms, pitavastatin versus placebo drug, and assess overall survival as the primary endpoint.

There is currently a requirement for the development of accurate, non-invasive biomarkers which can be used to predict response to statin therapy in cancer patients. A recent proteomic analysis of proteins released from endothelial cells exposed to atorvastatin identified approximately 83 differentially expressed proteins in the statin-treated “cell secretome” [520]. This research confirmed that nine of these proteins were also predominately detected in the medium of ovarian cancer cells exposed to statins, although the mechanism by which they were released is unknown. The gel approach to identifying proteins can have several drawbacks as it can be difficult to analyse proteins with very low (<15 kDa) or high (>100 kDa) molecular weights, and there may be multiple proteins in one band [520]. Further studies could incorporate a

gel-free proteomic approach involving a liquid chromatography/mass spectrometry-based method to identify proteins exclusively released by ovarian cancer cells but not normal cells in response to statin exposure. Cellular necrosis could contribute to the mechanism of protein release from cells exposed to statins, and therefore, this potential mechanism of cell death should also be investigated.

Combination of Statins with Other Chemotherapeutic Agents for the Treatment of Ovarian Cancer

Novel therapeutic agents are frequently evaluated in combination with existing chemotherapy in oncology. However, simvastatin did not demonstrate synergy with either carboplatin or paclitaxel in ovarian cancer cell lines [492]. Statins can also be used in combination with targeted therapeutic agents. Pitavastatin in combination with pictilisib or ABT-737 modestly increased cell death in several ovarian cancer cell lines, and therefore, these drug combinations may be superior over single agent therapy in a subset of ovarian tumours. The identification of appropriate biomarkers will help to determine which tumours may be sensitive to combination treatment. The remainder of this discussion will focus on the potential of statins in combination with current chemotherapeutic agents or targeted therapeutic agents.

Statins and Platinum-Containing Compounds

The platinum-containing compound, carboplatin, is included in the first line chemotherapeutic regimen for the treatment of ovarian cancer (chapter 1), and therefore, is a candidate for combination therapy. Previous research evaluating combinations of statins and cisplatin have reported that statins enhance the cytotoxic

effects of cisplatin by increasing apoptosis and S or G_2/M phase cell cycle arrest in colon, ovarian and squamous cell cancers [337, 357, 466, 484]. Furthermore, in non-small cell lung cancer cells, atorvastatin and carboplatin synergistically reduced cell viability and increased apoptosis [598]. This was confirmed in xenograft studies, where the combination reduced tumour size and increased survival time compared to the single agents alone [598]. Despite this, the simultaneous combination of simvastatin and carboplatin demonstrated additive or mild antagonistic interactions in seven ovarian cancer cell lines [492]. Furthermore, in dose scheduling experiments, significant antagonism was observed when ovarian cancer cells were exposed to high concentrations of simvastatin before carboplatin treatment (chapter 4). Therefore, it is unlikely that this combination will produce any clinical benefits compared to the single agents alone. Instead, these results suggest that high doses of statin should not be administered immediately prior to carboplatin treatment, as this may result in the antagonism of existing chemotherapy. Statins could be used after carboplatin treatment as "consolidation therapy" or in cancer which is resistant to carboplatin.

Statins and Paclitaxel

Paclitaxel can also be administrated in combination with carboplatin, as first line adjuvant chemotherapy in ovarian cancer (chapter 1). Statins in combination with paclitaxel have achieved variable results in cell-based studies. In leukemia cells, simvastatin or lovastatin in combination with paclitaxel resulted in a synergistic increase in cytotoxicity and G_2/M phase cell cycle arrest [599, 600]. However, similar combinations were antagonistic in anaplastic thyroid cancer cells [601], and ovarian cancer cells [492]. Further research could evaluate the activity of statins combined with paclitaxel in dose scheduling experiments, as this has previously been shown to influence whether synergy is observed [450, 602]. However, statins induce G_0/G_1

phase cell cycle arrest and this could prevent G_2/M arrest induced by paclitaxel, thereby contributing to antagonism. Indeed, carboplatin was demonstrated to antagonise the cytotoxic effects of paclitaxel in several dose schedules, by preventing breast cancer cells from progressing to M phase of the cell cycle [602]. Therefore, as statins induce G_0/G_1 phase cell cycle arrest, it may be preferable to administer paclitaxel prior to the statin.

Statins and Doxorubicin

Doxorubicin is used for the treatment of recurrent ovarian cancer; however chronic cardiotoxicity is a major factor limiting its prolonged use. Statins have been reported to potentiate the cytotoxic effects of doxorubicin in osteosarcoma cells [603], malignant melanoma cells [604, 605], ovarian cancer cells [485], and in p53-deficient cancer cells [606]. Furthermore, the synergistic interaction between lovastatin and doxorubicin has also been confirmed in animal studies, where the combination reduced tumour volume, increased apoptosis, and reduced the number of metastases compared to the single agents alone [604, 605, 607]. Statins have been proposed to reverse doxorubicin resistance in cancer cells by directly inhibiting the multidrug resistance protein, P-glycoprotein (P-gp) [485, 608]. P-gp resides in the cell membrane where it functions to remove toxins or drugs from the cell. In the presence of statins, cells accumulate doxorubicin in the nucleus resulting in a reduction in topoisomerase II activity, and an increase in double-strand DNA breaks [608, 609]. These results suggest that the combination of statins and doxorubicin should be further evaluated in dose scheduling experiments and ovarian cancer xenograft studies.

Statins and Bevacizumab

Vascular endothelial growth factor (VEGF) is an important mediator of angiogenesis, and is upregulated in ovarian cancer [610]. Bevacizumab is a humanised monoclonal antibody which inhibits circulating VEGF. Similarly, at high concentrations, statins have also been shown to have anti-angiogenic activity, including the attenuation of VEGF. These converging effects on angiogenesis provide a rationale for the use of statins in combination with bevacizumab to inhibit angiogenesis in ovarian cancer. Statins were first combined with bevacizumab and radiotherapy in a case study of a young woman presenting with an embryonal rhabdomyosarcoma of the retromaxillary space, which was refractory to two chemotherapy regimens [611]. The tumour growth was well controlled by this treatment and this enabled surgical removal of the tumour [611]. More recently, statins in combination with bevacizumab significantly reduced the growth and metastasis of colon cancer xenografts compared to bevacizumab alone [248]. Interestingly, statins were administered at doses equivalent to those used in patients with hypercholesterolaemia. Furthermore, the combination of bevacizumab and simvastatin (0.2 μM) also reduced cell viability, migration and invasion of human umbilical vein endothelial cells *in vitro* by attenuating the release of angiogenic mediators including angiopoietin2, binding immunoglobulin protein and HSP90α from colon cancer cells [248]. Taken together, these results suggest that statins at clinically achievable concentrations in combination with bevacizumab may be beneficial for the treatment of ovarian cancer.

Statins and Bisphosphonates

Nitrogen-containing bisphosphonates, including pamidronate, alendronate, ibandronate, risedronate and zoledronic acid, inhibit farnesyl diphosphate synthase in the mevalonate pathway, which prevents the synthesis of farnesyl diphosphate and

geranylgeranyl diphosphate. Therefore, bisphosphonates, like statins, also interfere with the prenylation of signalling molecules involved in many cellular processes. Furthermore, inhibition of farnesyl diphosphate synthase results in the accumulation of isopentenyl diphosphate, which can be metabolised to the intracellular ATP analogue, ApppI, and this may directly induce apoptosis [612, 613]. Bisphosphonates have been shown to inhibit the growth and migration of ovarian cancer cells *in vitro* [614, 615] and *in vivo* [616]. Furthermore, zoledronic acid in combination with simvastatin or fluvastatin was synergistic in breast [617] and myeloma [618] cancer cells, and ovarian tumours [619]. Interestingly, ovarian tumour cells were less sensitive to zoledronic acid following pre-exposure to fluvastatin [619], suggesting that statins may be more effective when given after zoledronic acid. This supports the alternative ApppI mechanism, as the accumulation of isopentenyl diphosphate may be required for zoledronic acid-induced cell death. Subsequent addition of statins may further prevent the synthesis of isoprenoids, thereby contributing to an inhibition of the prenylation of essential GTPases. Clinical trials combining statins and zoledronic acid for the treatment of cancers including multiple myeloma are ongoing [425]. Taken together, these results give further support to combined strategies aimed at inhibiting the mevalonate pathway for the treatment of ovarian cancer. Future studies could aim to confirm the synergy between statins and zoledronic acid in xenograft models, prior to ovarian cancer clinical trials.

Statins and Geranylgeranyltransferase Inhibitors

The post-translational prenylation of proteins requires prenyltransferase enzymes, including farnesyltransferase (FT) and geranylgeranyltransferase (GGT), which catalyse the addition of the isoprenoid onto a C-terminal CaaX motif [181]. Prenylation facilitates the correct cellular localisation and interactions of proteins involved in many

processes including cell proliferation, angiogenesis, migration and invasion. Farnesyltransferase inhibitors (FTI) were developed to inhibit the prenylation, membrane localisation, and function of the Ras oncogene, which is frequently activated in cancer. However, FTIs lacked significant cytotoxicity in clinical trials, and this was later attributed to the discovery that GGTs alternatively prenylated Ras when FT was blocked [620]. Consequently, FTIs were used in combination with geranylgeranyltransferase inhibitors (GGTI), however this dual prenyltransferase inhibitor therapy resulted in unacceptable toxicity in preclinical models [621]. Another approach to prevent the geranylgeranylation of proteins involved in tumorigenesis involves simultaneously inhibiting the prenylation pathway at two points, one to reduce the production of geranylgeranyl diphosphate using statins, and the other to competitively inhibit the binding of geranylgeranyl diphosphate to the GGT using GGTIs. These two compounds may exhibit synergistic activity in combination because statins deplete the cellular pool of geranylgeranyl diphosphate, which may allow the isoprenoid-competitive GGTI to target the GGT more efficiently. The combination of GGTI-2Z and lovastatin resulted in synergistic anti-proliferative effects in malignant peripheral nerve sheath tumour cells [322]. Furthermore, there was no significant toxicity in normal immortalized Schwann cells [322]. Ageberg and colleagues reported that both GGTI-298 and the combined Rab geranylgeranyltransferase and farnesyltransferase inhibitor, BMS1, inhibited the growth of lymphoma cells [500]. Interestingly, the addition of geranylgeraniol did not reverse the cytotoxic activity of either GGTI-298 or BMS1, suggesting that these compounds may specifically inhibit Rab GGT [500]. Additional studies have also shown that inhibition of Rab GGT and subsequent prevention of Rab prenylation cannot be reversed by geranylgeraniol [622, 623]. This can be explained by the mechanism of action of the inhibitors, although it is also possible that both GGTI-298 and BMS1 may have anti-cancer

effects independent of prenylation [500]. These results raise the possibility that statins could be used in combination with Rab GGTIs for the treatment of ovarian cancer. This may have several implications. Statins have been demonstrated to reduce the levels of Rab GTPases involved in autophagy, which may contribute to an inhibition of the autophagy pathway and potentiation of cell death (chapters 4 and 5; [327]). Rab GGTIs have also been shown to reduce the prenylation of Rab GTPases including Rab6 [622, 623]. Therefore, Rab GGTIs in combination with statins may synergistically inhibit autophagy and this may sensitise cancer cells to apoptotic cell death. Furthermore, it would also be important to determine what effect the addition of geranylgeraniol had on the cytotoxic activity of this drug combination, since this lipid may be present in the diet of patients receiving treatment for ovarian cancer (chapter 5). Isoprenoids including geranylgeraniol reversed the cytotoxic effects of statins *in vitro*, raising the possibility that isoprenoids ingested from the diet may also inhibit the anti-cancer activity of statins in clinical trials. The activity of Rab GGTIs is not prevented by geranylgeraniol and therefore, Rab GGTIs in combination with statins could maintain cytotoxic activity in the presence of exogenous isoprenoids from the diet.

Conclusion

Pitavastatin should be evaluated as a single agent in clinical trials of ovarian cancer, in patients with disease that is chemoresistant or after chemotherapy as “consolidation therapy”, using high doses with twice daily administration, as determined by a phase I study. Administration of pitavastatin at these doses is required for at least 4 days to allow inhibition of HMGCR and cell death, although this duration may be longer *in vivo*, and the maximum tolerated dose can be administered for up to two weeks

without significant toxicity. The validation of biomarkers of statin-induced cancer cell death will help to identify a biological response to statin treatment. Clinical trials should ensure that dietary fat intake is minimised, and this can be achieved by substituting a standard diet with food replacement drinks. These findings go a considerable way toward informing future clinical trials of statins in ovarian cancer.

REFERENCES

[1] Siegel, R., Ward, E., Brawley, O., Jemal, A. Cancer statistics, 2011: the impact of eliminating socioeconomic and racial disparities on premature cancer deaths. CA: a cancer journal for clinicians. 2011;61(4):212-36.

[2] Cancer Research UK. Ovarian cancer statistics. 2014 [accessed 1st July, 2014]; Available: http://www.cancerresearchuk.org/cancer-info/cancerstats/types/ovary/.

[3] National Institute for Health and Care Excellence. Ovarian cancer: The recognition and initial management of ovarian cancer (CG122). 2011 [accessed 1st July, 2014]; Available from: http://www.nice.org.uk/guidance/CG122/.

[4] Freedman, J. Ovarian Cancer: Current and Emerging Trends in Detection and Treatment. New York: The Rosen Publishing Group; 2009.

[5] Prat, J. Staging classification for cancer of the ovary, fallopian tube, and peritoneum. International journal of gynaecology and obstetrics: the official organ of the International Federation of Gynaecology and Obstetrics. 2014;124(1):1-5.

[6] National Cancer Intelligence Network. Overview of Ovarian Cancer in England: Incidence, Mortality and Survival. 2012 [accessed 1st July, 2014]; Available from: http://www.ncin.org.uk/cancer_type_and_topic_specific_work/cancer_type_specific_work/gynaecological_cancer/gynaecological_cancer_hub/resources/ovarian_cancer.

[7] National Cancer Intelligence Network. Cancer Incidence and Survival By Major Ethnic Group, England, 2002-2006. 2009 [accessed 1st July, 2014]; Available from: http://publications.cancerresearchuk.org/downloads/product/CSINCSURVBYETHNICITY.pdf.

[8] Edmondson, R. J., Monaghan, J. M. The epidemiology of ovarian cancer. International journal of gynecological cancer : official journal of the International Gynecological Cancer Society. 2001;11(6):423-9.

[9] Tate, A. R., Nicholson, A., Cassell, J. A. Are GPs under-investigating older patients presenting with symptoms of ovarian cancer? Observational study using General Practice Research Database. British journal of cancer. 2010;102(6):947-51.

[10] Ford, D., Easton, D. F., Bishop, D. T., Narod, S. A., Goldgar, D. E. Risks of cancer in BRCA1-mutation carriers. Breast Cancer Linkage Consortium. Lancet. 1994;343(8899):692-5.

[11] Bergfeldt, K., Rydh, B., Granath, F., Gronberg, H., Thalib, L., Adami, H. O., et al. Risk of ovarian cancer in breast-cancer patients with a family history of breast or ovarian cancer: a population-based cohort study. Lancet. 2002;360(9337):891-4.

[12] Doufekas, K., Olaitan, A. Clinical epidemiology of epithelial ovarian cancer in the UK. International journal of women's health. 2014;6:537-45.

[13] King, S. M., Hilliard, T. S., Wu, L. Y., Jaffe, R. C., Fazleabas, A. T., Burdette, J. E. The impact of ovulation on fallopian tube epithelial cells: evaluating three hypotheses connecting ovulation and serous ovarian cancer. Endocrine-related cancer. 2011;18(5):627-42.

[14] Whittemore, A. S., Harris, R., Itnyre, J. Characteristics relating to ovarian cancer risk: collaborative analysis of 12 US case-control studies. II. Invasive epithelial ovarian cancers in white women. Collaborative Ovarian Cancer Group. American journal of epidemiology. 1992;136(10):1184-203.

[15] Hankinson, S. E., Colditz, G. A., Hunter, D. J., Willett, W. C., Stampfer, M. J., Rosner, B., et al. A prospective study of reproductive factors and risk of epithelial ovarian cancer. Cancer. 1995;76(2):284-90.

[16] Tsilidis, K. K., Allen, N. E., Key, T. J., Dossus, L., Lukanova, A., Bakken, K., et al. Oral contraceptive use and reproductive factors and risk of ovarian cancer in the European Prospective Investigation into Cancer and Nutrition. British journal of cancer. 2011;105(9):1436-42.

[17] Tworoger, S. S., Fairfield, K. M., Colditz, G. A., Rosner, B. A., Hankinson, S. E. Association of oral contraceptive use, other contraceptive methods, and infertility with ovarian cancer risk. American journal of epidemiology. 2007;166(8):894-901.

[18] Vessey, M. P., Painter, R. Endometrial and ovarian cancer and oral contraceptives--findings in a large cohort study. British journal of cancer. 1995;71(6):1340-2.

[19] McLaughlin, J. R., Risch, H. A., Lubinski, J., Moller, P., Ghadirian, P., Lynch, H., et al. Reproductive risk factors for ovarian cancer in carriers of BRCA1 or BRCA2 mutations: a case-control study. The lancet oncology. 2007;8(1):26-34.

[20] Garg, P. P., Kerlikowske, K., Subak, L., Grady, D. Hormone replacement therapy and the risk of epithelial ovarian carcinoma: a meta-analysis. Obstetrics and gynecology. 1998;92(3):472-9.

[21] Beral, V., Bull, D., Green, J., Reeves, G. Ovarian cancer and hormone replacement therapy in the Million Women Study. Lancet. 2007;369(9574):1703-10.

[22] Cramer, D. W. Perineal talc exposure and subsequent epithelial ovarian cancer: a case-control study. Obstetrics and gynecology. 1999;94(1):160-1.

[23] Karageorgi, S., Gates, M. A., Hankinson, S. E., De Vivo, I. Perineal use of talcum powder and endometrial cancer risk. Cancer epidemiology, biomarkers & prevention : a publication of the American Association for Cancer Research, cosponsored by the American Society of Preventive Oncology. 2010;19(5):1269-75.

[24] Huncharek, M., Muscat, J. Perineal talc use and ovarian cancer risk: a case study of scientific standards in environmental epidemiology. European journal of cancer prevention : the official journal of the European Cancer Prevention Organisation. 2011;20(6):501-7.

[25] Modugno, F., Ness, R. B., Allen, G. O., Schildkraut, J. M., Davis, F. G., Goodman, M. T. Oral contraceptive use, reproductive history, and risk of epithelial ovarian cancer in women with and without endometriosis. American journal of obstetrics and gynecology. 2004;191(3):733-40.

[26] Borgfeldt, C., Andolf, E. Cancer risk after hospital discharge diagnosis of benign ovarian cysts and endometriosis. Acta obstetricia et gynecologica Scandinavica. 2004;83(4):395-400.

[27] Heaps, J. M., Nieberg, R. K., Berek, J. S. Malignant neoplasms arising in endometriosis. Obstetrics and gynecology. 1990;75(6):1023-8.

[28] Fathalla, M. F. Incessant ovulation--a factor in ovarian neoplasia? Lancet. 1971;2(7716):163.

[29] Erickson, B. K., Conner, M. G., Landen, C. N., Jr. The role of the fallopian tube in the origin of ovarian cancer. American journal of obstetrics and gynecology. 2013;209(5):409-14.

[30] Piek, J. M., van Diest, P. J., Zweemer, R. P., Jansen, J. W., Poort-Keesom, R. J., Menko, F. H., et al. Dysplastic changes in prophylactically removed Fallopian tubes of women predisposed to developing ovarian cancer. The Journal of pathology. 2001;195(4):451-6.

[31] Gross, A. L., Kurman, R. J., Vang, R., Shih Ie, M., Visvanathan, K. Precursor lesions of high-grade serous ovarian carcinoma: morphological and molecular characteristics. Journal of oncology. 2010;2010:126295.

[32] Crum, C. P., Drapkin, R., Kindelberger, D., Medeiros, F., Miron, A., Lee, Y. Lessons from BRCA: the tubal fimbria emerges as an origin for pelvic serous cancer. Clinical medicine & research. 2007;5(1):35-44.

[33] Callahan, M. J., Crum, C. P., Medeiros, F., Kindelberger, D. W., Elvin, J. A., Garber, J. E., et al. Primary fallopian tube malignancies in BRCA-positive women undergoing surgery for ovarian cancer risk reduction. Journal of clinical oncology : official journal of the American Society of Clinical Oncology. 2007;25(25):3985-90.

[34] Piek, J. M., Verheijen, R. H., Kenemans, P., Massuger, L. F., Bulten, H., van Diest, P. J. BRCA1/2-related ovarian cancers are of tubal origin: a hypothesis. Gynecologic oncology. 2003;90(2):491.

[35] Tone, A. A., Begley, H., Sharma, M., Murphy, J., Rosen, B., Brown, T. J., et al. Gene expression profiles of luteal phase fallopian tube epithelium from BRCA mutation carriers resemble high-grade serous carcinoma. Clinical cancer research : an official journal of the American Association for Cancer Research. 2008;14(13):4067-78.

[36] Kindelberger, D. W., Lee, Y., Miron, A., Hirsch, M. S., Feltmate, C., Medeiros, F., et al. Intraepithelial carcinoma of the fimbria and pelvic serous carcinoma: Evidence for a causal relationship. The American journal of surgical pathology. 2007;31(2):161-9.

[37] Przybycin, C. G., Kurman, R. J., Ronnett, B. M., Shih Ie, M., Vang, R. Are all pelvic (nonuterine) serous carcinomas of tubal origin? The American journal of surgical pathology. 2010;34(10):1407-16.

[38] Kim, J., Coffey, D. M., Creighton, C. J., Yu, Z., Hawkins, S. M., Matzuk, M. M. High-grade serous ovarian cancer arises from fallopian tube in a mouse model. Proceedings of the National Academy of Sciences of the United States of America. 2012;109(10):3921-6.

[39] Kurman, R. J. Origin and molecular pathogenesis of ovarian high-grade serous carcinoma. Annals of oncology : official journal of the European Society for Medical Oncology / ESMO. 2013;24 Suppl 10:x16-21.

[40] Horiuchi, A., Itoh, K., Shimizu, M., Nakai, I., Yamazaki, T., Kimura, K., et al. Toward understanding the natural history of ovarian carcinoma development: a clinicopathological approach. Gynecologic oncology. 2003;88(3):309-17.

[41] Bast, R. C., Jr., Hennessy, B., Mills, G. B. The biology of ovarian cancer: new opportunities for translation. Nature reviews Cancer. 2009;9(6):415-28.

[42] Seidman, J. D., Horkayne-Szakaly, I., Haiba, M., Boice, C. R., Kurman, R. J., Ronnett, B. M. The histologic type and stage distribution of ovarian carcinomas of surface epithelial origin. International journal of gynecological pathology : official journal of the International Society of Gynecological Pathologists. 2004;23(1):41-4.

[43] Prat, J. Ovarian carcinomas: five distinct diseases with different origins, genetic alterations, and clinicopathological features. Virchows Archiv : an international journal of pathology. 2012;460(3):237-49.

[44] Karst, A. M., Drapkin, R. Ovarian cancer pathogenesis: a model in evolution. Journal of oncology. 2010;2010:932371.

[45] Nezhat, F. D., M. S.; Hanson, V.; Pejovic, T.; Nezhat, C. The relationship of endometriosis and ovarian malignancy: a review. Fertility and Sterility. 2008. p. 1559-70.

[46] Palacios, J., Gamallo, C. Mutations in the beta-catenin gene (CTNNB1) in endometrioid ovarian carcinomas. Cancer research. 1998;58(7):1344-7.

[47] Kobayashi, H., Kajiwara, H., Kanayama, S., Yamada, Y., Furukawa, N., Noguchi, T., et al. Molecular pathogenesis of endometriosis-associated clear cell carcinoma of the ovary (review). Oncology reports. 2009;22(2):233-40.

[48] Takano, M., Tsuda, H., Sugiyama, T. Clear cell carcinoma of the ovary: is there a role of histology-specific treatment? Journal of experimental & clinical cancer research : CR. 2012;31:53.

[49] Yamaguchi, K., Mandai, M., Oura, T., Matsumura, N., Hamanishi, J., Baba, T., et al. Identification of an ovarian clear cell carcinoma gene signature that reflects inherent disease biology and the carcinogenic processes. Oncogene. 2010;29(12):1741-52.

[50] Woodruff, J. D., Bie, L. S., Sherman, R. J. Mucinous tumors of the ovary. Obstetrics and gynecology. 1960;16:699-712.

[51] Nomura, K., Aizawa, S. A histogenetic consideration of ovarian mucinous tumors based on an analysis of lesions associated with teratomas or Brenner tumors. Pathology international. 1997;47(12):862-5.

[52] Jha, P., Ranson, M. K., Nguyen, S. N., Yach, D. Estimates of global and regional smoking prevalence in 1995, by age and sex. American journal of public health. 2002;92(6):1002-6.

[53] Jordan, S. J., Whiteman, D. C., Purdie, D. M., Green, A. C., Webb, P. M. Does smoking increase risk of ovarian cancer? A systematic review. Gynecologic oncology. 2006;103(3):1122-9.

[54] Cho, K. R., Shih Ie, M. Ovarian cancer. Annual review of pathology. 2009;4:287-313.

[55] Kurman, R. J., Shih Ie, M. Pathogenesis of ovarian cancer: lessons from morphology and molecular biology and their clinical implications. International journal of gynecological pathology : official journal of the International Society of Gynecological Pathologists. 2008;27(2):151-60.

[56] Cancer Genome Atlas Research Network. Integrated genomic analyses of ovarian carcinoma. Nature. 2011;474(7353):609-15.

[57] Olivier, M., Hollstein, M., Hainaut, P. TP53 mutations in human cancers: origins, consequences, and clinical use. Cold Spring Harbor perspectives in biology. 2010;2(1):a001008.

[58] Kang, H. J., Chun, S. M., Kim, K. R., Sohn, I., Sung, C. O. Clinical relevance of gain-of-function mutations of p53 in high-grade serous ovarian carcinoma. PloS one. 2013;8(8):e72609.

[59] Oren, M., Rotter, V. Mutant p53 gain-of-function in cancer. Cold Spring Harbor perspectives in biology. 2010;2(2):a001107.

[60] Ding, L., Getz, G., Wheeler, D. A., Mardis, E. R., McLellan, M. D., Cibulskis, K., et al. Somatic mutations affect key pathways in lung adenocarcinoma. Nature. 2008;455(7216):1069-75.

[61] Aldred, M. A., Trembath, R. C. Activating and inactivating mutations in the human GNAS1 gene. Human mutation. 2000;16(3):183-9.

[62] Lowe, K. A., Andersen, M. R., Urban, N., Paley, P., Dresher, C. W., Goff, B. A. The temporal stability of the Symptom Index among women at high-risk for ovarian cancer. Gynecologic oncology. 2009;114(2):225-30.

[63] Andersen, M. R., Goff, B. A., Lowe, K. A., Scholler, N., Bergan, L., Dresher, C. W., et al. Combining a symptoms index with CA 125 to improve detection of ovarian cancer. Cancer. 2008;113(3):484-9.

[64] Goff, B. A., Mandel, L. S., Drescher, C. W., Urban, N., Gough, S., Schurman, K. M., et al. Development of an ovarian cancer symptom index: possibilities for earlier detection. Cancer. 2007;109(2):221-7.

[65] Hamilton, W., Peters, T. J., Bankhead, C., Sharp, D. Risk of ovarian cancer in women with symptoms in primary care: population based case-control study. BMJ. 2009;339:b2998.

[66] Castle, P. E. Gynecological cancer: More evidence supporting human papillomavirus testing. Nature reviews Clinical oncology. 2012;9(3):131-2.

[67] Moyer, V. A. Screening for ovarian cancer: U.S. Preventive Services Task Force reaffirmation recommendation statement. Annals of internal medicine. 2012;157(12):900-4.

[68] Jacobs, I., Bast, R. C., Jr. The CA 125 tumour-associated antigen: a review of the literature. Human reproduction. 1989;4(1):1-12.

[69] Felder, M., Kapur, A., Gonzalez-Bosquet, J., Horibata, S., Heintz, J., Albrecht, R., et al. MUC16 (CA125): tumor biomarker to cancer therapy, a work in progress. Molecular cancer. 2014;13:129.

[70] O'Brien, T. J., Beard, J. B., Underwood, L. J., Dennis, R. A., Santin, A. D., York, L. The CA 125 gene: an extracellular superstructure dominated by repeat sequences. Tumour biology : the journal of the International Society for Oncodevelopmental Biology and Medicine. 2001;22(6):348-66.

[71] Medeiros, L. R., Rosa, D. D., da Rosa, M. I., Bozzetti, M. C. Accuracy of CA 125 in the diagnosis of ovarian tumors: a quantitative systematic review. European journal of obstetrics, gynecology, and reproductive biology. 2009;142(2):99-105.

[72] Meden, H., Fattahi-Meibodi, A. CA 125 in benign gynecological conditions. The International journal of biological markers. 1998;13(4):231-7.

[73] Kobayashi, H., Yamada, Y., Sado, T., Sakata, M., Yoshida, S., Kawaguchi, R., et al. A randomized study of screening for ovarian cancer: a multicenter study in Japan. International journal of gynecological cancer : official journal of the International Gynecological Cancer Society. 2008;18(3):414-20.

[74] Skates, S. J., Xu, F. J., Yu, Y. H., Sjovall, K., Einhorn, N., Chang, Y., et al. Toward an optimal algorithm for ovarian cancer screening with longitudinal tumor markers. Cancer. 1995;76(10 Suppl):2004-10.

[75] Jacobs, I. R., A.; Skates, S. et al. Performance characteristics of multimodal screening with serum CA125 in the United Kingdom Collaborative Trial of Ovarian Cancer Screening (UKCTOCS). National Cancer Research Institute Cancer Conference; Liverpool. 2012.

[76] van Nagell, J. R., Jr., DePriest, P. D., Ueland, F. R., DeSimone, C. P., Cooper, A. L., McDonald, J. M., et al. Ovarian cancer screening with annual transvaginal sonography: findings of 25,000 women screened. Cancer. 2007;109(9):1887-96.

[77] van Nagell, J. R., Jr., Miller, R. W., DeSimone, C. P., Ueland, F. R., Podzielinski, I., Goodrich, S. T., et al. Long-term survival of women with epithelial ovarian cancer detected by ultrasonographic screening. Obstetrics and gynecology. 2011;118(6):1212-21.

[78] Hermsen, B. B., Olivier, R. I., Verheijen, R. H., van Beurden, M., de Hullu, J. A., Massuger, L. F., et al. No efficacy of annual gynaecological screening in BRCA1/2 mutation carriers; an observational follow-up study. British journal of cancer. 2007;96(9):1335-42.

[79] Stirling, D., Evans, D. G., Pichert, G., Shenton, A., Kirk, E. N., Rimmer, S., et al. Screening for familial ovarian cancer: failure of current protocols to detect ovarian cancer at an early stage according to the international Federation of gynecology and obstetrics system. Journal of clinical oncology : official journal of the American Society of Clinical Oncology. 2005;23(24):5588-96.

[80] Moore, L. E., Pfeiffer, R. M., Zhang, Z., Lu, K. H., Fung, E. T., Bast, R. C., Jr. Proteomic biomarkers in combination with CA 125 for detection of epithelial ovarian cancer using prediagnostic serum samples from the Prostate, Lung, Colorectal, and Ovarian (PLCO) Cancer Screening Trial. Cancer. 2012;118(1):91-100.

[81] Anderson, G. L., McIntosh, M., Wu, L., Barnett, M., Goodman, G., Thorpe, J. D., et al. Assessing lead time of selected ovarian cancer biomarkers: a nested case-control study. Journal of the National Cancer Institute. 2010;102(1):26-38.

[82] Timms, J. F., Menon, U., Devetyarov, D., Tiss, A., Camuzeaux, S., McCurrie, K., et al. Early detection of ovarian cancer in samples pre-diagnosis using CA125 and MALDI-MS peaks. Cancer genomics & proteomics. 2011;8(6):289-305.

[83] Forshew, T., Murtaza, M., Parkinson, C., Gale, D., Tsui, D. W., Kaper, F., et al. Noninvasive identification and monitoring of cancer mutations by targeted deep sequencing of plasma DNA. Science translational medicine. 2012;4(136):136ra68.

[84] Kinde, I., Bettegowda, C., Wang, Y., Wu, J., Agrawal, N., Shih Ie, M., et al. Evaluation of DNA from the Papanicolaou test to detect ovarian and endometrial cancers. Science translational medicine. 2013;5(167):167ra4.

[85] Fleischer, A. C., Lyshchik, A., Andreotti, R. F., Hwang, M., Jones, H. W., 3rd, Fishman, D. A. Advances in sonographic detection of ovarian cancer: depiction of tumor neovascularity with microbubbles. AJR American journal of roentgenology. 2010;194(2):343-8.

[86] McAlpine, J. N., El Hallani, S., Lam, S. F., Kalloger, S. E., Luk, M., Huntsman, D. G., et al. Autofluorescence imaging can identify preinvasive or clinically occult lesions in fallopian tube epithelium: a promising step towards screening and early detection. Gynecologic oncology. 2011;120(3):385-92.

[87] Zeppernick, F., Meinhold-Heerlein, I. The new FIGO staging system for ovarian, fallopian tube, and primary peritoneal cancer. Archives of gynecology and obstetrics. 2014;290(5):839-42.

[88] Bast, R. C., Jr. Molecular approaches to personalizing management of ovarian cancer. Annals of oncology : official journal of the European Society for Medical Oncology / ESMO. 2011;22 Suppl 8:viii5-viii15.

[89] Vaughan, S., Coward, J. I., Bast, R. C., Jr., Berchuck, A., Berek, J. S., Brenton, J. D., et al. Rethinking ovarian cancer: recommendations for improving outcomes. Nature reviews Cancer. 2011;11(10):719-25.

[90] National Institute for Health and Care Excellence. Paclitaxel, pegylated liposomal doxorubicin hydrochloride and topotecan for second-line or subsequent treatment of advanced ovarian cancer: Review of Technology Appraisal Guidance 28, 45 and 55 (TA91). 2005 [accessed 12th August, 2014]; Available from: http://www.nice.org.uk/guidance/TA91.

[91] Jamieson, E. R., Lippard, S. J. Structure, Recognition, and Processing of Cisplatin-DNA Adducts. Chemical reviews. 1999;99(9):2467-98.

[92] Folkman, J. Tumor angiogenesis: therapeutic implications. The New England journal of medicine. 1971;285(21):1182-6.

[93] Duhoux, F. P., Machiels, J. P. Antivascular therapy for epithelial ovarian cancer. Journal of oncology. 2010;2010:372547.

[94] Burger, R. A., Sill, M. W., Monk, B. J., Greer, B. E., Sorosky, J. I. Phase II trial of bevacizumab in persistent or recurrent epithelial ovarian cancer or primary peritoneal cancer: a Gynecologic Oncology Group Study. Journal of clinical oncology : official journal of the American Society of Clinical Oncology. 2007;25(33):5165-71.

[95] Cannistra, S. A., Matulonis, U. A., Penson, R. T., Hambleton, J., Dupont, J., Mackey, H., et al. Phase II study of bevacizumab in patients with platinum-resistant ovarian cancer or peritoneal serous cancer. Journal of clinical oncology : official journal of the American Society of Clinical Oncology. 2007;25(33):5180-6.

[96] Burger, R. A. B., M. F.; Bookmanet, M. A. et al. Phase III trial of bevacizumab (BEV) in the primary treatment of advanced epithelial ovarian cancer (EOC), primary peritoneal cancer (PPC), or fallopian tube cancer (FTC): A Gynecologic Oncology Group study. Journal of Clinical Oncology. 2010;28(18):946s.

[97] Perren, T. S., A. M.; Pfistere, J. et al. ICON7: A phase III randomized gynaecologic cancer Intergroup trial of concurrent bevacizumab and chemotherapy followed by maintenance bevacizumab. versus chemotherapy alone in women with newly diagnosed epithelial ovarian (EOC), primary peritoneal (PPC) or fallopian tube cancer (FTC). Annals of Oncology. 2010;21(8).

[98] Aghajanian, C. F., N. J.; Rutherford, T. et al. OCEANS: A randomized, double-blinded, placebo-controlled phase III trial of chemotherapy with or without bevacizumab (BEV) in patients with platinum-sensitive recurrent epithelial ovarian (EOC), primary peritoneal (PPC), or fallopian tube cancer (FTC). Journal of Clinical Oncology (ASCO Annual Meeting Abstracts). 2011;29:LBA5007.

[99] Pujade-Lauraine, E., Hilpert, F., Weber, B., Reuss, A., Poveda, A., Kristensen, G., et al. Bevacizumab combined with chemotherapy for platinum-resistant recurrent ovarian cancer: The AURELIA open-label randomized phase III trial. Journal of clinical oncology : official journal of the American Society of Clinical Oncology. 2014;32(13):1302-8.

[100] Stockler, M. R., Hilpert, F., Friedlander, M., King, M. T., Wenzel, L., Lee, C. K., et al. Patient-reported outcome results from the open-label phase III AURELIA trial evaluating bevacizumab-containing therapy for platinum-resistant ovarian cancer. Journal of clinical oncology : official journal of the American Society of Clinical Oncology. 2014;32(13):1309-16.

[101] National Institute for Health and Care Excellence. Bevacizumab in combination with paclitaxel and carboplatin for first-line treatment of advanced ovarian cancer (TA284). 2013 [accessed 12th August, 2014]; Available from: https://www.nice.org.uk/guidance/TA284.

[102] National Institute for Health and Care Excellence. Bevacizumab in combination with gemcitabine and carboplatin for treating the first recurrence of platinum-sensitive advanced ovarian cancer (TA285). 2013 [accessed 12th August, 2014]; Available from: https://www.nice.org.uk/guidance/TA285.

[103] Reed, E. Platinum-DNA adduct, nucleotide excision repair and platinum based anti-cancer chemotherapy. Cancer treatment reviews. 1998;24(5):331-44.

[104] Selvakumaran, M., Pisarcik, D. A., Bao, R., Yeung, A. T., Hamilton, T. C. Enhanced cisplatin cytotoxicity by disturbing the nucleotide excision repair pathway in ovarian cancer cell lines. Cancer research. 2003;63(6):1311-6.

[105] Murphy, M. A., Wentzensen, N. Frequency of mismatch repair deficiency in ovarian cancer: a systematic review This article is a US Government work and, as such, is in the public domain of the United States of America. International journal of cancer Journal international du cancer. 2011;129(8):1914-22.

[106] Gifford, G., Paul, J., Vasey, P. A., Kaye, S. B., Brown, R. The acquisition of hMLH1 methylation in plasma DNA after chemotherapy predicts poor survival for ovarian cancer patients. Clinical cancer research : an official journal of the American Association for Cancer Research. 2004;10(13):4420-6.

[107] Watanabe, Y., Koi, M., Hemmi, H., Hoshai, H., Noda, K. A change in microsatellite instability caused by cisplatin-based chemotherapy of ovarian cancer. British journal of cancer. 2001;85(7):1064-9.

[108] Ashworth, A. A synthetic lethal therapeutic approach: poly(ADP) ribose polymerase inhibitors for the treatment of cancers deficient in DNA double-strand break repair. Journal of clinical oncology : official journal of the American Society of Clinical Oncology. 2008;26(22):3785-90.

[109] Rouleau, M., Patel, A., Hendzel, M. J., Kaufmann, S. H., Poirier, G. G. PARP inhibition: PARP1 and beyond. Nature reviews Cancer. 2010;10(4):293-301.

[110] Sakai, W., Swisher, E. M., Karlan, B. Y., Agarwal, M. K., Higgins, J., Friedman, C., et al. Secondary mutations as a mechanism of cisplatin resistance in BRCA2-mutated cancers. Nature. 2008;451(7182):1116-20.

[111] Swisher, E. M., Sakai, W., Karlan, B. Y., Wurz, K., Urban, N., Taniguchi, T. Secondary BRCA1 mutations in BRCA1-mutated ovarian carcinomas with platinum resistance. Cancer research. 2008;68(8):2581-6.

[112] Bryant, H. E., Schultz, N., Thomas, H. D., Parker, K. M., Flower, D., Lopez, E., et al. Specific killing of BRCA2-deficient tumours with inhibitors of poly(ADP-ribose) polymerase. Nature. 2005;434(7035):913-7.

[113] Farmer, H., McCabe, N., Lord, C. J., Tutt, A. N., Johnson, D. A., Richardson, T. B., et al. Targeting the DNA repair defect in BRCA mutant cells as a therapeutic strategy. Nature. 2005;434(7035):917-21.

[114] Ledermann, J., Harter, P., Gourley, C., Friedlander, M., Vergote, I., Rustin, G., et al. Olaparib maintenance therapy in patients with platinum-sensitive relapsed serous ovarian cancer: a preplanned retrospective analysis of outcomes by BRCA status in a randomised phase 2 trial. The Lancet Oncology. 2014;15(8):852-61.

[115] Rivkin, S. E. Phase Ib/II with expansion of patients at the MTD study of olaparib plus weekly (metronomic) carboplatin and paclitaxel in relapsed ovarian cancer patients. Journal of Clinical Oncology. 2014;32:5s.

[116] Audeh, M. W., Carmichael, J., Penson, R. T., Friedlander, M., Powell, B., Bell-McGuinn, K. M., et al. Oral poly(ADP-ribose) polymerase inhibitor olaparib in patients with BRCA1 or BRCA2 mutations and recurrent ovarian cancer: a proof-of-concept trial. Lancet. 2010;376(9737):245-51.

[117] Fong, P. C., Yap, T. A., Boss, D. S., Carden, C. P., Mergui-Roelvink, M., Gourley, C., et al. Poly(ADP)-ribose polymerase inhibition: frequent durable responses in BRCA carrier ovarian cancer correlating with platinum-free interval. Journal of clinical oncology : official journal of the American Society of Clinical Oncology. 2010;28(15):2512-9.

[118] Kaye, S. B., Lubinski, J., Matulonis, U., Ang, J. E., Gourley, C., Karlan, B. Y., et al. Phase II, open-label, randomized, multicenter study comparing the efficacy and safety of olaparib, a poly (ADP-ribose) polymerase inhibitor, and pegylated liposomal doxorubicin in patients with BRCA1 or BRCA2 mutations and recurrent ovarian cancer. Journal of clinical oncology : official journal of the American Society of Clinical Oncology. 2012;30(4):372-9.

[119] Ledermann, J., Harter, P., Gourley, C., Friedlander, M., Vergote, I., Rustin, G., et al. Olaparib maintenance therapy in platinum-sensitive relapsed ovarian cancer. The New England journal of medicine. 2012;366(15):1382-92.

[120] Liu, J. F., Tolaney, S. M., Birrer, M., Fleming, G. F., Buss, M. K., Dahlberg, S. E., et al. A Phase 1 trial of the poly(ADP-ribose) polymerase inhibitor olaparib (AZD2281) in combination with the anti-angiogenic cediranib (AZD2171) in recurrent epithelial ovarian or triple-negative breast cancer. European journal of cancer. 2013;49(14):2972-8.

[121] Lee, J. M., Ledermann, J. A., Kohn, E. C. PARP Inhibitors for BRCA1/2 mutation-associated and BRCA-like malignancies. Annals of oncology : official journal of the European Society for Medical Oncology / ESMO. 2014;25(1):32-40.

[122] Lee, J. M., Hays, J. L., Annunziata, C. M., Noonan, A. M., Minasian, L., Zujewski, J. A., et al. Phase I/Ib study of olaparib and carboplatin in BRCA1 or BRCA2 mutation-associated breast or ovarian cancer with biomarker analyses. Journal of the National Cancer Institute. 2014;106(6):dju089.

[123] Tapia, G., Diaz-Padilla, I. Molecular Mechanisms of Platinum Resistance in Ovarian Cancer In: Díaz-Padilla, I., editor. Ovarian Cancer - A Clinical and Translational Update: InTech; 2013.

[124] Holzer, A. K., Katano, K., Klomp, L. W., Howell, S. B. Cisplatin rapidly down-regulates its own influx transporter hCTR1 in cultured human ovarian carcinoma cells. Clinical cancer research : an official journal of the American Association for Cancer Research. 2004;10(19):6744-9.

[125] Samimi, G., Katano, K., Holzer, A. K., Safaei, R., Howell, S. B. Modulation of the cellular pharmacology of cisplatin and its analogs by the copper exporters ATP7A and ATP7B. Molecular pharmacology. 2004;66(1):25-32.

[126] Nakayama, K., Kanzaki, A., Ogawa, K., Miyazaki, K., Neamati, N., Takebayashi, Y. Copper-transporting P-type adenosine triphosphatase (ATP7B) as a cisplatin based chemoresistance marker in ovarian carcinoma: comparative analysis with expression of MDR1, MRP1, MRP2, LRP and BCRP. International journal of cancer Journal international du cancer. 2002;101(5):488-95.

[127] Fracasso, P. M., Brady, M. F., Moore, D. H., Walker, J. L., Rose, P. G., Letvak, L., et al. Phase II study of paclitaxel and valspodar (PSC 833) in refractory ovarian carcinoma: a gynecologic oncology group study. Journal of clinical oncology : official journal of the American Society of Clinical Oncology. 2001;19(12):2975-82.

[128] Kelland, L. The resurgence of platinum-based cancer chemotherapy. Nature reviews Cancer. 2007;7(8):573-84.

[129] Yang, X., Xing, H., Gao, Q., Chen, G., Lu, Y., Wang, S., et al. Regulation of HtrA2/Omi by X-linked inhibitor of apoptosis protein in chemoresistance in human ovarian cancer cells. Gynecologic oncology. 2005;97(2):413-21.

[130] Williams, J., Lucas, P. C., Griffith, K. A., Choi, M., Fogoros, S., Hu, Y. Y., et al. Expression of Bcl-xL in ovarian carcinoma is associated with chemoresistance and recurrent disease. Gynecologic oncology. 2005;96(2):287-95.

[131] Yang, X., Zheng, F., Xing, H., Gao, Q., Wei, W., Lu, Y., et al. Resistance to chemotherapy-induced apoptosis via decreased caspase-3 activity and overexpression of antiapoptotic proteins in ovarian cancer. Journal of cancer research and clinical oncology. 2004;130(7):423-8.

[132] Siperstein, M. D., Fagan, V. M. Deletion of the Cholesterol-Negative Feedback System in Liver Tumors. Cancer research. 1964;24:1108-15.

[133] Siperstein, M. D. Role of cholesterogenesis and isoprenoid synthesis in DNA replication and cell growth. Journal of lipid research. 1984;25(13):1462-8.

[134] Larsson, O. HMG-CoA reductase inhibitors: role in normal and malignant cells. Critical reviews in oncology/hematology. 1996;22(3):197-212.

[135] Li, H. Y., Appelbaum, F. R., Willman, C. L., Zager, R. A., Banker, D. E. Cholesterol-modulating agents kill acute myeloid leukemia cells and sensitize them to therapeutics by blocking adaptive cholesterol responses. Blood. 2003;101(9):3628-34.

[136] Mo, H., Elson, C. E. Studies of the isoprenoid-mediated inhibition of mevalonate synthesis applied to cancer chemotherapy and chemoprevention. Experimental biology and medicine. 2004;229(7):567-85.

[137] Clendening, J. W., Pandyra, A., Boutros, P. C., El Ghamrasni, S., Khosravi, F., Trentin, G. A., et al. Dysregulation of the mevalonate pathway promotes transformation. Proceedings of the National Academy of Sciences of the United States of America. 2010;107(34):15051-6.

[138] Ginestier, C., Monville, F., Wicinski, J., Cabaud, O., Cervera, N., Josselin, E., et al. Mevalonate metabolism regulates Basal breast cancer stem cells and is a potential therapeutic target. Stem cells. 2012;30(7):1327-37.

[139] Chen, H. W., Kandutsch, A. A., Heiniger, H. J. The role of cholesterol in malignancy. Progress in experimental tumor research. 1978;22:275-316.

[140] Gregg, R. G., Sabine, J. R., Wilce, P. A. Regulation of 3-hydroxy-3-methylglutaryl-coenzyme A reductase in rat liver and Morris hepatomas 5123C, 9618A and 5123t.c. The Biochemical journal. 1982;204(2):457-62.

[141] Yachnin, S., Mannickarottu, V. Increased 3-hydroxy-3-methylglutaryl coenzyme A reductase activity and cholesterol biosynthesis in freshly isolated hairy cell leukemia cells. Blood. 1984;63(3):690-3.

[142] Yachnin, S., Toub, D. B., Mannickarottu, V. Divergence in cholesterol biosynthetic rates and 3-hydroxy-3-methylglutaryl-CoA reductase activity as a consequence of granulocyte versus monocyte-macrophage differentiation in HL-60 cells. Proceedings of the National Academy of Sciences of the United States of America. 1984;81(3):894-7.

[143] Erickson, S. K., Cooper, A. D., Barnard, G. F., Havel, C. M., Watson, J. A., Feingold, K. R., et al. Regulation of cholesterol metabolism in a slow-growing hepatoma in vivo. Biochimica et biophysica acta. 1988;960(2):131-8.

[144] Azrolan, N. I., Coleman, P. S. A discoordinate increase in the cellular amount of 3-hydroxy-3-methylglutaryl-CoA reductase results in the loss of rate-limiting control over cholesterogenesis in a tumour cell-free system. The Biochemical journal. 1989;258(2):421-5.

[145] Llaverias, G., Danilo, C., Mercier, I., Daumer, K., Capozza, F., Williams, T. M., et al. Role of cholesterol in the development and progression of breast cancer. The American journal of pathology. 2011;178(1):402-12.

[146] Zhong, C., Fan, L., Yao, F., Shi, J., Fang, W., Zhao, H. HMGCR is necessary for the tumorigenecity of esophageal squamous cell carcinoma and is regulated by Myc. Tumour biology : the journal of the International Society for Oncodevelopmental Biology and Medicine. 2014;35(5):4123-9.

[147] Krycer, J. R., Phan, L., Brown, A. J. A key regulator of cholesterol homoeostasis, SREBP-2, can be targeted in prostate cancer cells with natural products. The Biochemical journal. 2012;446(2):191-201.

[148] Freed-Pastor, W. A., Mizuno, H., Zhao, X., Langerod, A., Moon, S. H., Rodriguez-Barrueco, R., et al. Mutant p53 disrupts mammary tissue architecture via the mevalonate pathway. Cell. 2012;148(1-2):244-58.

[149] Cruz, P. M., Mo, H., McConathy, W. J., Sabnis, N., Lacko, A. G. The role of cholesterol metabolism and cholesterol transport in carcinogenesis: a review of scientific findings, relevant to future cancer therapeutics. Frontiers in pharmacology. 2013;4:119.

[150] Bengtsson, E., Nerjovaj, P., Wangefjord, S., Nodin, B., Eberhard, J., Uhlen, M., et al. HMG-CoA reductase expression in primary colorectal cancer correlates with favourable clinicopathological characteristics and an improved clinical outcome. Diagnostic pathology. 2014;9:78.

[151] Borgquist, S., Djerbi, S., Ponten, F., Anagnostaki, L., Goldman, M., Gaber, A., et al. HMG-CoA reductase expression in breast cancer is associated with a less aggressive phenotype and influenced by anthropometric factors. International journal of cancer Journal international du cancer. 2008;123(5):1146-53.

[152] Brennan, D. J., Brandstedt, J., Rexhepaj, E., Foley, M., Ponten, F., Uhlen, M., et al. Tumour-specific HMG-CoAR is an independent predictor of recurrence free survival in epithelial ovarian cancer. BMC cancer. 2010;10:125.

[153] Fiorenza, A. M., Branchi, A., Sommariva, D. Serum lipoprotein profile in patients with cancer. A comparison with non-cancer subjects. International journal of clinical & laboratory research. 2000;30(3):141-5.

[154] Delimaris, I., Faviou, E., Antonakos, G., Stathopoulou, E., Zachari, A., Dionyssiou-Asteriou, A. Oxidized LDL, serum oxidizability and serum lipid levels in patients with breast or ovarian cancer. Clinical biochemistry. 2007;40(15):1129-34.

[155] Scoles, D. R., Xu, X., Wang, H., Tran, H., Taylor-Harding, B., Li, A., et al. Liver X receptor agonist inhibits proliferation of ovarian carcinoma cells stimulated by oxidized low density lipoprotein. Gynecologic oncology. 2010;116(1):109-16.

[156] Scallen, T. J., Sanghvi, A. Regulation of three key enzymes in cholesterol metabolism by phosphorylation/dephosphorylation. Proceedings of the National Academy of Sciences of the United States of America. 1983;80(9):2477-80.

[157] Endo, A., Kuroda, M., Tsujita, Y. ML-236A, ML-236B, and ML-236C, new inhibitors of cholesterogenesis produced by Penicillium citrinium. The Journal of antibiotics. 1976;29(12):1346-8.

[158] Alberts, A. W., Chen, J., Kuron, G., Hunt, V., Huff, J., Hoffman, C., et al. Mevinolin: a highly potent competitive inhibitor of hydroxymethylglutaryl-coenzyme A reductase and a cholesterol-lowering agent. Proceedings of the National Academy of Sciences of the United States of America. 1980;77(7):3957-61.

[159] Hoffman, W. F., Alberts, A. W., Anderson, P. S., Chen, J. S., Smith, R. L., Willard, A. K. 3-Hydroxy-3-methylglutaryl-coenzyme A reductase inhibitors. 4. Side chain ester derivatives of mevinolin. Journal of medicinal chemistry. 1986;29(5):849-52.

[160] Endo, A. The discovery and development of HMG-CoA reductase inhibitors. Journal of lipid research. 1992;33(11):1569-82.

[161] Reinoso, R. F., Sanchez Navarro, A., Garcia, M. J., Prous, J. R. Preclinical pharmacokinetics of statins. Methods and findings in experimental and clinical pharmacology. 2002;24(9):593-613.

[162] Mukhtar, R. Y., Reid, J., Reckless, J. P. Pitavastatin. International journal of clinical practice. 2005;59(2):239-52.

[163] Istvan, E. S., Deisenhofer, J. Structural mechanism for statin inhibition of HMG-CoA reductase. Science. 2001;292(5519):1160-4.

[164] Stierand, K., Rarey, M. From modeling to medicinal chemistry: automatic generation of two-dimensional complex diagrams. ChemMedChem. 2007;2(6):853-60.

[165] Olsson, A. G., Pears, J., McKellar, J., Mizan, J., Raza, A. Effect of rosuvastatin on low-density lipoprotein cholesterol in patients with hypercholesterolemia. The American journal of cardiology. 2001;88(5):504-8.

[166] Saito, Y., Yamada, N., Teramoto, T., Itakura, H., Hata, Y., Nakaya, N., et al. A randomized, double-blind trial comparing the efficacy and safety of pitavastatin versus pravastatin in patients with primary hypercholesterolemia. Atherosclerosis. 2002;162(2):373-9.

[167] Jones, P. H., Davidson, M. H., Stein, E. A., Bays, H. E., McKenney, J. M., Miller, E., et al. Comparison of the efficacy and safety of rosuvastatin versus atorvastatin, simvastatin, and pravastatin across doses (STELLAR* Trial). The American journal of cardiology. 2003;92(2):152-60.

[168] Hanna, E. B., Hennebry, T. A. Periprocedural myocardial infarction: review and classification. Clinical cardiology. 2010;33(8):476-83.

[169] Toth, P. P. Drug treatment of hyperlipidaemia: a guide to the rational use of lipid-lowering drugs. Drugs. 2010;70(11):1363-79.

[170] Prinz, V., Endres, M. Statins and stroke: prevention and beyond. Current opinion in neurology. 2011;24(1):75-80.

[171] Perez-Sala, D. Protein isoprenylation in biology and disease: general overview and perspectives from studies with genetically engineered animals. Frontiers in bioscience : a journal and virtual library. 2007;12:4456-72.

[172] Sebti, S. M. Protein farnesylation: implications for normal physiology, malignant transformation, and cancer therapy. Cancer cell. 2005;7(4):297-300.

[173] Garcia-Ruiz, C., Morales, A., Fernandez-Checa, J. C. Statins and protein prenylation in cancer cell biology and therapy. Anti-cancer agents in medicinal chemistry. 2012;12(4):303-15.

[174] Zhang, F. L., Casey, P. J. Protein prenylation: molecular mechanisms and functional consequences. Annual review of biochemistry. 1996;65:241-69.

[175] Winter-Vann, A. M., Casey, P. J. Post-prenylation-processing enzymes as new targets in oncogenesis. Nature reviews Cancer. 2005;5(5):405-12.

[176] Roberts, P. J., Mitin, N., Keller, P. J., Chenette, E. J., Madigan, J. P., Currin, R. O., et al. Rho Family GTPase modification and dependence on CAAX motif-signaled posttranslational modification. The Journal of biological chemistry. 2008;283(37):25150-63.

[177] Zverina, E. A., Lamphear, C. L., Wright, E. N., Fierke, C. A. Recent advances in protein prenyltransferases: substrate identification, regulation, and disease interventions. Current opinion in chemical biology. 2012;16(5-6):544-52.

[178] Rocks, O., Gerauer, M., Vartak, N., Koch, S., Huang, Z. P., Pechlivanis, M., et al. The palmitoylation machinery is a spatially organizing system for peripheral membrane proteins. Cell. 2010;141(3):458-71.

[179] Thurnher, M., Gruenbacher, G., Nussbaumer, O. Regulation of mevalonate metabolism in cancer and immune cells. Biochimica et biophysica acta. 2013;1831(6):1009-15.

[180] Calero, M., Chen, C. Z., Zhu, W., Winand, N., Havas, K. A., Gilbert, P. M., et al. Dual prenylation is required for Rab protein localization and function. Molecular biology of the cell. 2003;14(5):1852-67.

[181] Konstantinopoulos, P. A., Karamouzis, M. V., Papavassiliou, A. G. Post-translational modifications and regulation of the RAS superfamily of GTPases as anticancer targets. Nature reviews Drug discovery. 2007;6(7):541-55.

[182] Gysin, S., Salt, M., Young, A., McCormick, F. Therapeutic strategies for targeting ras proteins. Genes & cancer. 2011;2(3):359-72.

[183] Lin, C. a. A., M. Protein Prenylation and Hematological Maligancies. In: Novak, E. a. R., E., editor. Physiopathogenesis of Hematological Cancer: Bentham Science Publishers; 2012. p. 103-21.

[184] Joyce, P. L., Cox, A. D. Rac1 and Rac3 are targets for geranylgeranyltransferase I inhibitor-mediated inhibition of signaling, transformation, and membrane ruffling. Cancer research. 2003;63(22):7959-67.

[185] Nishimura, A., Linder, M. E. Identification of a novel prenyl and palmitoyl modification at the CaaX motif of Cdc42 that regulates RhoGDI binding. Molecular and cellular biology. 2013;33(7):1417-29.

[186] Chen, M., Knifley, T., Subramanian, T., Spielmann, H. P., O'Connor, K. L. Use of synthetic isoprenoids to target protein prenylation and Rho GTPases in breast cancer invasion. PloS one. 2014;9(2):e89892.

[187] Karlsson, R., Pedersen, E. D., Wang, Z., Brakebusch, C. Rho GTPase function in tumorigenesis. Biochimica et biophysica acta. 2009;1796(2):91-8.

[188] Qiu, R. G., Chen, J., McCormick, F., Symons, M. A role for Rho in Ras transformation. Proceedings of the National Academy of Sciences of the United States of America. 1995;92(25):11781-5.

[189] Olson, M. F., Ashworth, A., Hall, A. An essential role for Rho, Rac, and Cdc42 GTPases in cell cycle progression through G1. Science. 1995;269(5228):1270-2.

[190] Bryan, B. A., D'Amore, P. A. What tangled webs they weave: Rho-GTPase control of angiogenesis. Cellular and molecular life sciences : CMLS. 2007;64(16):2053-65.

[191] Aspenstrom, P., Fransson, A., Saras, J. Rho GTPases have diverse effects on the organization of the actin filament system. The Biochemical journal. 2004;377(Pt 2):327-37.

[192] Wheeler, A. P., Ridley, A. J. Why three Rho proteins? RhoA, RhoB, RhoC, and cell motility. Experimental cell research. 2004;301(1):43-9.

[193] Horiuchi, A., Imai, T., Wang, C., Ohira, S., Feng, Y., Nikaido, T., et al. Up-regulation of small GTPases, RhoA and RhoC, is associated with tumor progression in ovarian carcinoma. Laboratory investigation; a journal of technical methods and pathology. 2003;83(6):861-70.

[194] Heard, J. J., Fong, V., Bathaie, S. Z., Tamanoi, F. Recent progress in the study of the Rheb family GTPases. Cellular signalling. 2014;26(9):1950-7.

[195] Hanker, A. B., Mitin, N., Wilder, R. S., Henske, E. P., Tamanoi, F., Cox, A. D., et al. Differential requirement of CAAX-mediated posttranslational processing for Rheb localization and signaling. Oncogene. 2010;29(3):380-91.

[196] Aspuria, P. J., Tamanoi, F. The Rheb family of GTP-binding proteins. Cellular signalling. 2004;16(10):1105-12.

[197] Lu, Z. H., Shvartsman, M. B., Lee, A. Y., Shao, J. M., Murray, M. M., Kladney, R. D., et al. Mammalian target of rapamycin activator RHEB is frequently overexpressed in human carcinomas and is critical and sufficient for skin epithelial carcinogenesis. Cancer research. 2010;70(8):3287-98.

[198] Recchi, C., Seabra, M. C. Novel functions for Rab GTPases in multiple aspects of tumour progression. Biochemical Society transactions. 2012;40(6):1398-403.

[199] Cheng, K. W., Lahad, J. P., Kuo, W. L., Lapuk, A., Yamada, K., Auersperg, N., et al. The RAB25 small GTPase determines aggressiveness of ovarian and breast cancers. Nature medicine. 2004;10(11):1251-6.

[200] Caswell, P. T., Spence, H. J., Parsons, M., White, D. P., Clark, K., Cheng, K. W., et al. Rab25 associates with alpha5beta1 integrin to promote invasive migration in 3D microenvironments. Developmental cell. 2007;13(4):496-510.

[201] Gentry, L. R., Martin, T. D., Reiner, D. J., Der, C. J. Ral small GTPase signaling and oncogenesis: More than just 15minutes of fame. Biochimica et biophysica acta. 2014;1843(12):2976-88.

[202] Falsetti, S. C., Wang, D. A., Peng, H., Carrico, D., Cox, A. D., Der, C. J., et al. Geranylgeranyltransferase I inhibitors target RalB to inhibit anchorage-dependent growth and induce apoptosis and RalA to inhibit anchorage-independent growth. Molecular and cellular biology. 2007;27(22):8003-14.

[203] Chien, Y., White, M. A. RAL GTPases are linchpin modulators of human tumour-cell proliferation and survival. EMBO reports. 2003;4(8):800-6.

[204] Wang, K., Terai, K., Peng, W., Rouyanian, A., Liu, J., Roby, K. F., et al. The role of RalA in biology and therapy of ovarian cancer. Oncotarget. 2013. Dec 10. [Epub ahead of print].

[205] Si, X., Zeng, Q., Ng, C. H., Hong, W., Pallen, C. J. Interaction of farnesylated PRL-2, a protein-tyrosine phosphatase, with the beta-subunit of geranylgeranyltransferase II. The Journal of biological chemistry. 2001;276(35):32875-82.

[206] Guzinska-Ustymowicz, K., Pryczynicz, A. PRL-3, an emerging marker of carcinogenesis, is strongly associated with poor prognosis. Anti-cancer agents in medicinal chemistry. 2011;11(1):99-108.

[207] Reich, R., Hadar, S., Davidson, B. Expression and clinical role of protein of regenerating liver (PRL) phosphatases in ovarian carcinoma. International journal of molecular sciences. 2011;12(2):1133-45.

[208] Dittmer, T. A., Misteli, T. The lamin protein family. Genome biology. 2011;12(5):222.

[209] Goldberg, M. W., Huttenlauch, I., Hutchison, C. J., Stick, R. Filaments made from A- and B-type lamins differ in structure and organization. Journal of cell science. 2008;121(Pt 2):215-25.

[210] Alaiya, A. A., Franzen, B., Fujioka, K., Moberger, B., Schedvins, K., Silfversvard, C., et al. Phenotypic analysis of ovarian carcinoma: polypeptide expression in benign, borderline and malignant tumors. International journal of cancer Journal international du cancer. 1997;73(5):678-83.

[211] Wang, Y., Wu, R., Cho, K. R., Thomas, D. G., Gossner, G., Liu, J. R., et al. Differential protein mapping of ovarian serous adenocarcinomas: identification of potential markers for distinct tumor stage. Journal of proteome research. 2009;8(3):1452-63.

[212] Ho, C. Y., Lammerding, J. Lamins at a glance. Journal of cell science. 2012;125(Pt 9):2087-93.

[213] Schafer-Hales, K., Iaconelli, J., Snyder, J. P., Prussia, A., Nettles, J. H., El-Naggar, A., et al. Farnesyl transferase inhibitors impair chromosomal maintenance in cell lines and human tumors by compromising CENP-E and CENP-F function. Molecular cancer therapeutics. 2007;6(4):1317-28.

[214] Hussein, D., Taylor, S. S. Farnesylation of Cenp-F is required for G2/M progression and degradation after mitosis. Journal of cell science. 2002;115(Pt 17):3403-14.

[215] Giacinti, C., Giordano, A. RB and cell cycle progression. Oncogene. 2006;25(38):5220-7.

[216] Busino, L., Chiesa, M., Draetta, G. F., Donzelli, M. Cdc25A phosphatase: combinatorial phosphorylation, ubiquitylation and proteolysis. Oncogene. 2004;23(11):2050-6.

[217] Zolnierczyk, J. D., Borowiak, A., Hikisz, P., Cebula-Obrzut, B., Blonski, J. Z., Smolewski, P., et al. Promising anti-leukemic activity of atorvastatin. Oncology reports. 2013;29(5):2065-71.

[218] Kamigaki, M., Sasaki, T., Serikawa, M., Inoue, M., Kobayashi, K., Itsuki, H., et al. Statins induce apoptosis and inhibit proliferation in cholangiocarcinoma cells. International journal of oncology. 2011;39(3):561-8.

[219] Sanchez, C. A., Rodriguez, E., Varela, E., Zapata, E., Paez, A., Masso, F. A., et al. Statin-induced inhibition of MCF-7 breast cancer cell proliferation is related to cell cycle arrest and apoptotic and necrotic cell death mediated by an enhanced oxidative stress. Cancer investigation. 2008;26(7):698-707.

[220] Moreau, A. S., Jia, X., Patterson, C. J., Roccaro, A. M., Xu, L., Sacco, A., et al. The HMG-CoA inhibitor, simvastatin, triggers in vitro anti-tumour effect and decreases IgM secretion in Waldenstrom macroglobulinaemia. British journal of haematology. 2008;142(5):775-85.

[221] Sutter, A. P., Maaser, K., Hopfner, M., Huether, A., Schuppan, D., Scherubl, H. Cell cycle arrest and apoptosis induction in hepatocellular carcinoma cells by HMG-CoA reductase inhibitors. Synergistic antiproliferative action with ligands of the peripheral benzodiazepine receptor. Journal of hepatology. 2005;43(5):808-16.

[222] Shibata, M. A., Ito, Y., Morimoto, J., Otsuki, Y. Lovastatin inhibits tumor growth and lung metastasis in mouse mammary carcinoma model: a p53-independent mitochondrial-mediated apoptotic mechanism. Carcinogenesis. 2004;25(10):1887-98.

[223] Shibata, M. A., Kavanaugh, C., Shibata, E., Abe, H., Nguyen, P., Otsuki, Y., et al. Comparative effects of lovastatin on mammary and prostate oncogenesis in transgenic mouse models. Carcinogenesis. 2003;24(3):453-9.

[224] Denoyelle, C., Vasse, M., Korner, M., Mishal, Z., Ganne, F., Vannier, J. P., et al. Cerivastatin, an inhibitor of HMG-CoA reductase, inhibits the signaling pathways involved in the invasiveness and metastatic properties of highly invasive breast cancer cell lines: an in vitro study. Carcinogenesis. 2001;22(8):1139-48.

[225] Macaulay, R. J., Wang, W., Dimitroulakos, J., Becker, L. E., Yeger, H. Lovastatin-induced apoptosis of human medulloblastoma cell lines in vitro. Journal of neuro-oncology. 1999;42(1):1-11.

[226] Zhong, W. B., Hsu, S. P., Ho, P. Y., Liang, Y. C., Chang, T. C., Lee, W. S. Lovastatin inhibits proliferation of anaplastic thyroid cancer cells through up-regulation of p27 by interfering with the Rho/ROCK-mediated pathway. Biochemical pharmacology. 2011;82(11):1663-72.

[227] Zeybek, N. D., Gulcelik, N. E., Kaymaz, F. F., Sarisozen, C., Vural, I., Bodur, E., et al. Rosuvastatin induces apoptosis in cultured human papillary thyroid cancer cells. The Journal of endocrinology. 2011;210(1):105-15.

[228] Favero, G. M., M, F. O., Oliveira, K. A., Bohatch, M. S., Jr., Borelli, P., Barros, F. E., et al. Simvastatin impairs murine melanoma growth. Lipids in health and disease. 2010;9:142.

[229] Relja, B., Meder, F., Wilhelm, K., Henrich, D., Marzi, I., Lehnert, M. Simvastatin inhibits cell growth and induces apoptosis and G0/G1 cell cycle arrest in hepatic cancer cells. International journal of molecular medicine. 2010;26(5):735-41.

[230] Saito, A., Saito, N., Mol, W., Furukawa, H., Tsutsumida, A., Oyama, A., et al. Simvastatin inhibits growth via apoptosis and the induction of cell cycle arrest in human melanoma cells. Melanoma research. 2008;18(2):85-94.

[231] Park, W. H., Lee, Y. Y., Kim, E. S., Seol, J. G., Jung, C. W., Lee, C. C., et al. Lovastatin-induced inhibition of HL-60 cell proliferation via cell cycle arrest and apoptosis. Anticancer research. 1999;19(4B):3133-40.

[232] Hoque, A., Chen, H., Xu, X. C. Statin induces apoptosis and cell growth arrest in prostate cancer cells. Cancer epidemiology, biomarkers & prevention : a publication of the American Association for Cancer Research, cosponsored by the American Society of Preventive Oncology. 2008;17(1):88-94.

[233] Rao, S., Lowe, M., Herliczek, T. W., Keyomarsi, K. Lovastatin mediated G1 arrest in normal and tumor breast cells is through inhibition of CDK2 activity and redistribution of p21 and p27, independent of p53. Oncogene. 1998;17(18):2393-402.

[234] Park, C., Lee, I., Kang, W. K. Lovastatin-induced E2F-1 modulation and its effect on prostate cancer cell death. Carcinogenesis. 2001;22(10):1727-31.

[235] Tu, Y. S., Kang, X. L., Zhou, J. G., Lv, X. F., Tang, Y. B., Guan, Y. Y. Involvement of Chk1-Cdc25A-cyclin A/CDK2 pathway in simvastatin induced S-phase cell cycle arrest and apoptosis in multiple myeloma cells. European journal of pharmacology. 2011;670(2-3):356-64.

[236] Fuchs, D., Berges, C., Opelz, G., Daniel, V., Naujokat, C. HMG-CoA reductase inhibitor simvastatin overcomes bortezomib-induced apoptosis resistance by disrupting a geranylgeranyl pyrophosphate-dependent survival pathway. Biochemical and biophysical research communications. 2008;374(2):309-14.

[237] Denoyelle, C., Albanese, P., Uzan, G., Hong, L., Vannier, J. P., Soria, J., et al. Molecular mechanism of the anti-cancer activity of cerivastatin, an inhibitor of HMG-CoA reductase, on aggressive human breast cancer cells. Cellular signalling. 2003;15(3):327-38.

[238] Collisson, E. A., Kleer, C., Wu, M., De, A., Gambhir, S. S., Merajver, S. D., et al. Atorvastatin prevents RhoC isoprenylation, invasion, and metastasis in human melanoma cells. Molecular cancer therapeutics. 2003;2(10):941-8.

[239] Maksimova, E., Yie, T. A., Rom, W. N. In vitro mechanisms of lovastatin on lung cancer cell lines as a potential chemopreventive agent. Lung. 2008;186(1):45-54.

[240] Ahn, K. S., Sethi, G., Aggarwal, B. B. Simvastatin potentiates TNF-alpha-induced apoptosis through the down-regulation of NF-kappaB-dependent antiapoptotic gene products: role of IkappaBalpha kinase and TGF-beta-activated kinase-1. Journal of immunology. 2007;178(4):2507-16.

[241] Campbell, M. J., Esserman, L. J., Zhou, Y., Shoemaker, M., Lobo, M., Borman, E., et al. Breast cancer growth prevention by statins. Cancer research. 2006;66(17):8707-14.

[242] Gazzerro, P., Proto, M. C., Gangemi, G., Malfitano, A. M., Ciaglia, E., Pisanti, S., et al. Pharmacological actions of statins: a critical appraisal in the management of cancer. Pharmacological reviews. 2012;64(1):102-46.

[243] Frick, M., Dulak, J., Cisowski, J., Jozkowicz, A., Zwick, R., Alber, H., et al. Statins differentially regulate vascular endothelial growth factor synthesis in endothelial and vascular smooth muscle cells. Atherosclerosis. 2003;170(2):229-36.

[244] Chen, J., Liu, B., Yuan, J., Yang, J., Zhang, J., An, Y., et al. Atorvastatin reduces vascular endothelial growth factor (VEGF) expression in human non-small cell lung carcinomas (NSCLCs) via inhibition of reactive oxygen species (ROS) production. Molecular oncology. 2012;6(1):62-72.

[245] Weis, M., Heeschen, C., Glassford, A. J., Cooke, J. P. Statins have biphasic effects on angiogenesis. Circulation. 2002;105(6):739-45.

[246] Feleszko, W., Balkowiec, E. Z., Sieberth, E., Marczak, M., Dabrowska, A., Giermasz, A., et al. Lovastatin and tumor necrosis factor-alpha exhibit potentiated antitumor effects against Ha-ras-transformed murine tumor via inhibition of tumor-induced angiogenesis. International journal of cancer Journal international du cancer. 1999;81(4):560-7.

[247] Dulak, J., Jozkowicz, A. Anti-angiogenic and anti-inflammatory effects of statins: relevance to anti-cancer therapy. Current cancer drug targets. 2005;5(8):579-94.

[248] Lee, S. J., Lee, I., Lee, J., Park, C., Kang, W. K. Statins, 3-hydroxy-3-methylglutaryl coenzyme A reductase inhibitors, potentiate the anti-angiogenic effects of bevacizumab by suppressing angiopoietin2, BiP, and Hsp90alpha in human colorectal cancer. British journal of cancer. 2014;111(3):497-505.

[249] Zhao, Y., Zheng, H. C., Chen, S., Gou, W. F., Xiao, L. J., Niu, Z. F. The role of RhoC in ovarian epithelial carcinoma: a marker for carcinogenesis, progression, prognosis, and target therapy. Gynecologic oncology. 2013;130(3):570-8.

[250] Muck, A. O., Seeger, H., Wallwiener, D. Class-specific pro-apoptotic effect of statins on human vascular endothelial cells. Zeitschrift fur Kardiologie. 2004;93(5):398-402.

[251] Kaneta, S., Satoh, K., Kano, S., Kanda, M., Ichihara, K. All hydrophobic HMG-CoA reductase inhibitors induce apoptotic death in rat pulmonary vein endothelial cells. Atherosclerosis. 2003;170(2):237-43.

[252] Kureishi, Y., Luo, Z., Shiojima, I., Bialik, A., Fulton, D., Lefer, D. J., et al. The HMG-CoA reductase inhibitor simvastatin activates the protein kinase Akt and promotes angiogenesis in normocholesterolemic animals. Nature medicine. 2000;6(9):1004-10.

[253] Brouet, A., Sonveaux, P., Dessy, C., Moniotte, S., Balligand, J. L., Feron, O. Hsp90 and caveolin are key targets for the proangiogenic nitric oxide-mediated effects of statins. Circulation research. 2001;89(10):866-73.

[254] Kotamraju, S., Williams, C. L., Kalyanaraman, B. Statin-induced breast cancer cell death: role of inducible nitric oxide and arginase-dependent pathways. Cancer research. 2007;67(15):7386-94.

[255] Wai Wong, C., Dye, D. E., Coombe, D. R. The role of immunoglobulin superfamily cell adhesion molecules in cancer metastasis. International journal of cell biology. 2012;2012:340296.

[256] Parri, M., Chiarugi, P. Rac and Rho GTPases in cancer cell motility control. Cell communication and signaling : CCS. 2010;8:23.

[257] Brown, M., Hart, C., Tawadros, T., Ramani, V., Sangar, V., Lau, M., et al. The differential effects of statins on the metastatic behaviour of prostate cancer. British journal of cancer. 2012;106(10):1689-96.

[258] Sokalska, A., Cress, A., Bruner-Tran, K. L., Osteen, K. G., Taylor, H. S., Ortega, I., et al. Simvastatin decreases invasiveness of human endometrial stromal cells. Biology of reproduction. 2012;87(1):2, 1-6.

[259] Kusama, T., Mukai, M., Iwasaki, T., Tatsuta, M., Matsumoto, Y., Akedo, H., et al. Inhibition of epidermal growth factor-induced RhoA translocation and invasion of human pancreatic cancer cells by 3-hydroxy-3-methylglutaryl-coenzyme a reductase inhibitors. Cancer research. 2001;61(12):4885-91.

[260] Zhong, W. B., Liang, Y. C., Wang, C. Y., Chang, T. C., Lee, W. S. Lovastatin suppresses invasiveness of anaplastic thyroid cancer cells by inhibiting Rho geranylgeranylation and RhoA/ROCK signaling. Endocrine-related cancer. 2005;12(3):615-29.

[261] Horiuchi, A., Kikuchi, N., Osada, R., Wang, C., Hayashi, A., Nikaido, T., et al. Overexpression of RhoA enhances peritoneal dissemination: RhoA suppression with Lovastatin may be useful for ovarian cancer. Cancer science. 2008;99(12):2532-9.

[262] Wang, I. K., Lin-Shiau, S. Y., Lin, J. K. Suppression of invasion and MMP-9 expression in NIH 3T3 and v-H-Ras 3T3 fibroblasts by lovastatin through inhibition of ras isoprenylation. Oncology. 2000;59(3):245-54.

[263] Glynn, S. A., O'Sullivan, D., Eustace, A. J., Clynes, M., O'Donovan, N. The 3-hydroxy-3-methylglutaryl-coenzyme A reductase inhibitors, simvastatin, lovastatin and mevastatin inhibit proliferation and invasion of melanoma cells. BMC cancer. 2008;8:9.

[264] Nubel, T., Dippold, W., Kleinert, H., Kaina, B., Fritz, G. Lovastatin inhibits Rho-regulated expression of E-selectin by TNFalpha and attenuates tumor cell adhesion. FASEB journal : official publication of the Federation of American Societies for Experimental Biology. 2004;18(1):140-2.

[265] Takeda, I., Maruya, S., Shirasaki, T., Mizukami, H., Takahata, T., Myers, J. N., et al. Simvastatin inactivates beta1-integrin and extracellular signal-related kinase signaling and inhibits cell proliferation in head and neck squamous cell carcinoma cells. Cancer science. 2007;98(6):890-9.

[266] Matsuura, M., Suzuki, T., Saito, T. Osteopontin is a new target molecule for ovarian clear cell carcinoma therapy. Cancer science. 2010;101(8):1828-33.

[267] Matsuura, M., Suzuki, T., Suzuki, M., Tanaka, R., Ito, E., Saito, T. Statin-mediated reduction of osteopontin expression induces apoptosis and cell growth arrest in ovarian clear cell carcinoma. Oncology reports. 2011;25(1):41-7.

[268] Wagner, B. J., Lob, S., Lindau, D., Horzer, H., Guckel, B., Klein, G., et al. Simvastatin reduces tumor cell adhesion to human peritoneal mesothelial cells by decreased expression of VCAM-1 and beta1 integrin. International journal of oncology. 2011;39(6):1593-600.

[269] De Duve, C. The lysosome. Scientific American. 1963;208:64-72.

[270] De Duve, C., Wattiaux, R. Functions of lysosomes. Annual review of physiology. 1966;28:435-92.

[271] Klionsky, D. J., Emr, S. D. Autophagy as a regulated pathway of cellular degradation. Science. 2000;290(5497):1717-21.

[272] Rubinsztein, D. C. The roles of intracellular protein-degradation pathways in neurodegeneration. Nature. 2006;443(7113):780-6.

[273] Alavian, S. M., Ande, S. R., Coombs, K. M., Yeganeh, B., Davoodpour, P., Hashemi, M., et al. Virus-triggered autophagy in viral hepatitis - possible novel strategies for drug development. Journal of viral hepatitis. 2011;18(12):821-30.

[274] Itakura, E., Mizushima, N. Characterization of autophagosome formation site by a hierarchical analysis of mammalian Atg proteins. Autophagy. 2010;6(6):764-76.

[275] Proikas-Cezanne, T., Waddell, S., Gaugel, A., Frickey, T., Lupas, A., Nordheim, A. WIPI-1alpha (WIPI49), a member of the novel 7-bladed WIPI protein family, is aberrantly expressed in human cancer and is linked to starvation-induced autophagy. Oncogene. 2004;23(58):9314-25.

[276] Pattingre, S., Espert, L., Biard-Piechaczyk, M., Codogno, P. Regulation of macroautophagy by mTOR and Beclin 1 complexes. Biochimie. 2008;90(2):313-23.

[277] Mehrpour, M., Esclatine, A., Beau, I., Codogno, P. Overview of macroautophagy regulation in mammalian cells. Cell research. 2010;20(7):748-62.

[278] Hirota, Y., Tanaka, Y. A small GTPase, human Rab32, is required for the formation of autophagic vacuoles under basal conditions. Cellular and molecular life sciences : CMLS. 2009;66(17):2913-32.

[279] Itoh, T., Fujita, N., Kanno, E., Yamamoto, A., Yoshimori, T., Fukuda, M. Golgi-resident small GTPase Rab33B interacts with Atg16L and modulates autophagosome formation. Molecular biology of the cell. 2008;19(7):2916-25.

[280] Tanida, I. Autophagy basics. Microbiology and immunology. 2011;55(1):1-11.

[281] Matsushita, M., Suzuki, N. N., Obara, K., Fujioka, Y., Ohsumi, Y., Inagaki, F. Structure of Atg5.Atg16, a complex essential for autophagy. The Journal of biological chemistry. 2007;282(9):6763-72.

[282] Mizushima, N., Yamamoto, A., Hatano, M., Kobayashi, Y., Kabeya, Y., Suzuki, K., et al. Dissection of autophagosome formation using Apg5-deficient mouse embryonic stem cells. The Journal of cell biology. 2001;152(4):657-68.

[283] Pankiv, S., Clausen, T. H., Lamark, T., Brech, A., Bruun, J. A., Outzen, H., et al. p62/SQSTM1 binds directly to Atg8/LC3 to facilitate degradation of ubiquitinated protein aggregates by autophagy. The Journal of biological chemistry. 2007;282(33):24131-45.

[284] Itakura, E., Mizushima, N. p62 Targeting to the autophagosome formation site requires self-oligomerization but not LC3 binding. The Journal of cell biology. 2011;192(1):17-27.

[285] Mathew, R., Karp, C. M., Beaudoin, B., Vuong, N., Chen, G., Chen, H. Y., et al. Autophagy suppresses tumorigenesis through elimination of p62. Cell. 2009;137(6):1062-75.

[286] Matsunaga, K., Saitoh, T., Tabata, K., Omori, H., Satoh, T., Kurotori, N., et al. Two Beclin 1-binding proteins, Atg14L and Rubicon, reciprocally regulate autophagy at different stages. Nature cell biology. 2009;11(4):385-96.

[287] Zhong, Y., Wang, Q. J., Li, X., Yan, Y., Backer, J. M., Chait, B. T., et al. Distinct regulation of autophagic activity by Atg14L and Rubicon associated with Beclin 1-phosphatidylinositol-3-kinase complex. Nature cell biology. 2009;11(4):468-76.

[288] Wurmser, A. E., Sato, T. K., Emr, S. D. New component of the vacuolar class C-Vps complex couples nucleotide exchange on the Ypt7 GTPase to SNARE-dependent docking and fusion. The Journal of cell biology. 2000;151(3):551-62.

[289] Gutierrez, M. G., Munafo, D. B., Beron, W., Colombo, M. I. Rab7 is required for the normal progression of the autophagic pathway in mammalian cells. Journal of cell science. 2004;117(Pt 13):2687-97.

[290] Jager, S., Bucci, C., Tanida, I., Ueno, T., Kominami, E., Saftig, P., et al. Role for Rab7 in maturation of late autophagic vacuoles. Journal of cell science. 2004;117(Pt 20):4837-48.

[291] Sun, Q., Zhang, J., Fan, W., Wong, K. N., Ding, X., Chen, S., et al. The RUN domain of rubicon is important for hVps34 binding, lipid kinase inhibition, and autophagy suppression. The Journal of biological chemistry. 2011;286(1):185-91.

[292] Fader, C. M., Sanchez, D. G., Mestre, M. B., Colombo, M. I. TI-VAMP/VAMP7 and VAMP3/cellubrevin: two v-SNARE proteins involved in specific steps of the autophagy/multivesicular body pathways. Biochimica et biophysica acta. 2009;1793(12):1901-16.

[293] Raiborg, C., Stenmark, H. The ESCRT machinery in endosomal sorting of ubiquitylated membrane proteins. Nature. 2009;458(7237):445-52.

[294] Jahreiss, L., Menzies, F. M., Rubinsztein, D. C. The itinerary of autophagosomes: from peripheral formation to kiss-and-run fusion with lysosomes. Traffic. 2008;9(4):574-87.

[295] Lee, J., Giordano, S., Zhang, J. Autophagy, mitochondria and oxidative stress: cross-talk and redox signalling. The Biochemical journal. 2012;441(2):523-40.

[296] Lloyd, J. B. Metabolite efflux and influx across the lysosome membrane. Sub-cellular biochemistry. 1996;27:361-86.

[297] Yu, L., McPhee, C. K., Zheng, L., Mardones, G. A., Rong, Y., Peng, J., et al. Termination of autophagy and reformation of lysosomes regulated by mTOR. Nature. 2010;465(7300):942-6.

[298] Chen, S., Rehman, S. K., Zhang, W., Wen, A., Yao, L., Zhang, J. Autophagy is a therapeutic target in anticancer drug resistance. Biochimica et biophysica acta. 2010;1806(2):220-9.

[299] Lum, J. J., Bauer, D. E., Kong, M., Harris, M. H., Li, C., Lindsten, T., et al. Growth factor regulation of autophagy and cell survival in the absence of apoptosis. Cell. 2005;120(2):237-48.

[300] Spowart, J. E., Townsend, K. N., Huwait, H., Eshragh, S., West, N. R., Ries, J. N., et al. The Autophagy Protein LC3A Correlates with Hypoxia and is a Prognostic Marker of Patient Survival in Clear Cell Ovarian Cancer. The Journal of pathology. 2012;228(4):437-47.

[301] Badgwell, D. B., Lu, Z., Le, K., Gao, F., Yang, M., Suh, G. K., et al. The tumor-suppressor gene ARHI (DIRAS3) suppresses ovarian cancer cell migration through inhibition of the Stat3 and FAK/Rho signaling pathways. Oncogene. 2012;31(1):68-79.

[302] Luo, R. Z., Fang, X., Marquez, R., Liu, S. Y., Mills, G. B., Liao, W. S., et al. ARHI is a Ras-related small G-protein with a novel N-terminal extension that inhibits growth of ovarian and breast cancers. Oncogene. 2003;22(19):2897-909.

[303] Zhu, H., Wu, H., Liu, X., Li, B., Chen, Y., Ren, X., et al. Regulation of autophagy by a beclin 1-targeted microRNA, miR-30a, in cancer cells. Autophagy. 2009;5(6):816-23.

[304] Coward, J., Kulbe, H., Chakravarty, P., Leader, D., Vassileva, V., Leinster, D. A., et al. Interleukin-6 as a therapeutic target in human ovarian cancer. Clinical cancer research : an official journal of the American Association for Cancer Research. 2011;17(18):6083-96.

[305] Lane, D., Matte, I., Rancourt, C., Piche, A. Prognostic significance of IL-6 and IL-8 ascites levels in ovarian cancer patients. BMC cancer. 2011;11:210.

[306] Zhang, N., Qi, Y., Wadham, C., Wang, L., Warren, A., Di, W., et al. FTY720 induces necrotic cell death and autophagy in ovarian cancer cells: a protective role of autophagy. Autophagy. 2010;6(8):1157-67.

[307] Zhang, Y., Cheng, Y., Ren, X., Zhang, L., Yap, K. L., Wu, H., et al. NAC1 modulates sensitivity of ovarian cancer cells to cisplatin by altering the HMGB1-mediated autophagic response. Oncogene. 2012;31(8):1055-64.

[308] Kanzawa, T., Zhang, L., Xiao, L., Germano, I. M., Kondo, Y., Kondo, S. Arsenic trioxide induces autophagic cell death in malignant glioma cells by upregulation of mitochondrial cell death protein BNIP3. Oncogene. 2005;24(6):980-91.

[309] Shao, Y., Gao, Z., Marks, P. A., Jiang, X. Apoptotic and autophagic cell death induced by histone deacetylase inhibitors. Proceedings of the National Academy of Sciences of the United States of America. 2004;101(52):18030-5.

[310] Le, X. F., Mao, W., Lu, Z., Carter, B. Z., Bast, R. C., Jr. Dasatinib induces autophagic cell death in human ovarian cancer. Cancer. 2010;116(21):4980-90.

[311] Chen, M. Y., Liao, W. S., Lu, Z., Bornmann, W. G., Hennessey, V., Washington, M. N., et al. Decitabine and suberoylanilide hydroxamic acid (SAHA) inhibit growth of ovarian cancer cell lines and xenografts while inducing expression of imprinted tumor suppressor genes, apoptosis, G2/M arrest, and autophagy. Cancer. 2011;117(19):4424-38.

[312] Liu, N., Tai, S., Ding, B., Thor, R. K., Bhuta, S., Sun, Y., et al. Arsenic trioxide synergizes with everolimus (Rad001) to induce cytotoxicity of ovarian cancer cells through increased autophagy and apoptosis. Endocrine-related cancer. 2012;19(5):711-23.

[313] Liang, X. H., Jackson, S., Seaman, M., Brown, K., Kempkes, B., Hibshoosh, H., et al. Induction of autophagy and inhibition of tumorigenesis by beclin 1. Nature. 1999;402(6762):672-6.

[314] Shen, Y., Li, D. D., Wang, L. L., Deng, R., Zhu, X. F. Decreased expression of autophagy-related proteins in malignant epithelial ovarian cancer. Autophagy. 2008;4(8):1067-8.

[315] Orfanelli, T., Jeong, J. M., Doulaveris, G., Holcomb, K., Witkin, S. S. Involvement of autophagy in cervical, endometrial and ovarian cancer. International journal of cancer Journal international du cancer. 2014;135(3):519-28.

[316] Bunkholt Elstrand, M., Dong, H. P., Odegaard, E., Holth, A., Elloul, S., Reich, R., et al. Mammalian target of rapamycin is a biomarker of poor survival in metastatic serous ovarian carcinoma. Human pathology. 2010;41(6):794-804.

[317] Misirkic, M., Janjetovic, K., Vucicevic, L., Tovilovic, G., Ristic, B., Vilimanovich, U., et al. Inhibition of AMPK-dependent autophagy enhances in vitro antiglioma effect of simvastatin. Pharmacological research : the official journal of the Italian Pharmacological Society. 2012;65(1):111-9.

[318] Parikh, A., Childress, C., Deitrick, K., Lin, Q., Rukstalis, D., Yang, W. Statin-induced autophagy by inhibition of geranylgeranyl biosynthesis in prostate cancer PC3 cells. The Prostate. 2010;70(9):971-81.

[319] Yang, P. M., Liu, Y. L., Lin, Y. C., Shun, C. T., Wu, M. S., Chen, C. C. Inhibition of autophagy enhances anticancer effects of atorvastatin in digestive malignancies. Cancer research. 2010;70(19):7699-709.

[320] Araki, M., Maeda, M., Motojima, K. Hydrophobic statins induce autophagy and cell death in human rhabdomyosarcoma cells by depleting geranylgeranyl diphosphate. European journal of pharmacology. 2012;674(2-3):95-103.

[321] Shi, Y., Felley-Bosco, E., Marti, T. M., Stahel, R. A. Differential effects of lovastatin on cisplatin responses in normal human mesothelial cells versus cancer cells: implication for therapy. PloS one. 2012;7(9):e45354.

[322] Sane, K. M., Mynderse, M., Lalonde, D. T., Dean, I. S., Wojtkowiak, J. W., Fouad, F., et al. A novel geranylgeranyl transferase inhibitor in combination with lovastatin inhibits proliferation and induces autophagy in STS-26T MPNST cells. The Journal of pharmacology and experimental therapeutics. 2010;333(1):23-33.

[323] Zhang, Q., Yang, Y. J., Wang, H., Dong, Q. T., Wang, T. J., Qian, H. Y., et al. Autophagy activation: a novel mechanism of atorvastatin to protect mesenchymal stem cells from hypoxia and serum deprivation via AMP-activated protein kinase/mammalian target of rapamycin pathway. Stem cells and development. 2012;21(8):1321-32.

[324] Toepfer, N., Childress, C., Parikh, A., Rukstalis, D., Yang, W. Atorvastatin induces autophagy in prostate cancer PC3 cells through activation of LC3 transcription. Cancer biology & therapy. 2011;12(8):691-9.

[325] Lai, E. H., Hong, C. Y., Kok, S. H., Hou, K. L., Chao, L. H., Lin, L. D., et al. Simvastatin alleviates the progression of periapical lesions by modulating autophagy and apoptosis in osteoblasts. Journal of endodontics. 2012;38(6):757-63.

[326] Ghavami, S., Mutawe, M. M., Sharma, P., Yeganeh, B., McNeill, K. D., Klonisch, T., et al. Mevalonate cascade regulation of airway mesenchymal cell autophagy and apoptosis: a dual role for p53. PloS one. 2011;6(1):e16523.

[327] Wojtkowiak, J. W., Sane, K. M., Kleinman, M., Sloane, B. F., Reiners, J. J., Jr., Mattingly, R. R. Aborted autophagy and nonapoptotic death induced by farnesyl transferase inhibitor and lovastatin. The Journal of pharmacology and experimental therapeutics. 2011;337(1):65-74.

[328] Kerr, J. F., Wyllie, A. H., Currie, A. R. Apoptosis: a basic biological phenomenon with wide-ranging implications in tissue kinetics. British journal of cancer. 1972;26(4):239-57.

[329] Elmore, S. Apoptosis: a review of programmed cell death. Toxicologic pathology. 2007;35(4):495-516.

[330] Koyuturk, M., Ersoz, M., Altiok, N. Simvastatin induces apoptosis in human breast cancer cells: p53 and estrogen receptor independent pathway requiring signalling through JNK. Cancer letters. 2007;250(2):220-8.

[331] Hwang, K. E., Na, K. S., Park, D. S., Choi, K. H., Kim, B. R., Shim, H., et al. Apoptotic induction by simvastatin in human lung cancer A549 cells via Akt signaling dependent down-regulation of survivin. Investigational new drugs. 2011;29(5):945-52.

[332] Pelaia, G., Gallelli, L., Renda, T., Fratto, D., Falcone, D., Caraglia, M., et al. Effects of statins and farnesyl transferase inhibitors on ERK phosphorylation, apoptosis and cell viability in non-small lung cancer cells. Cell proliferation. 2012;45(6):557-65.

[333] Oliveira, K. A., Zecchin, K. G., Alberici, L. C., Castilho, R. F., Vercesi, A. E. Simvastatin inducing PC3 prostate cancer cell necrosis mediated by calcineurin and mitochondrial dysfunction. Journal of bioenergetics and biomembranes. 2008;40(4):307-14.

[334] Zhang, W., Wu, J., Zhou, L., Xie, H. Y., Zheng, S. S. Fluvastatin, a lipophilic statin, induces apoptosis in human hepatocellular carcinoma cells through mitochondria-operated pathway. Indian journal of experimental biology. 2010;48(12):1167-74.

[335] Kaneko, R., Tsuji, N., Asanuma, K., Tanabe, H., Kobayashi, D., Watanabe, N. Survivin down-regulation plays a crucial role in 3-hydroxy-3-methylglutaryl coenzyme A reductase inhibitor-induced apoptosis in cancer. The Journal of biological chemistry. 2007;282(27):19273-81.

[336] Qi, X. F., Kim, D. H., Yoon, Y. S., Kim, S. K., Cai, D. Q., Teng, Y. C., et al. Involvement of oxidative stress in simvastatin-induced apoptosis of murine CT26 colon carcinoma cells. Toxicology letters. 2010;199(3):277-87.

[337] Kato, S., Smalley, S., Sadarangani, A., Chen-Lin, K., Oliva, B., Branes, J., et al. Lipophilic but not hydrophilic statins selectively induce cell death in gynaecological cancers expressing high levels of HMGCoA reductase. Journal of cellular and molecular medicine. 2010;14(5):1180-93.

[338] Liu, H., Liang, S. L., Kumar, S., Weyman, C. M., Liu, W., Zhou, A. Statins induce apoptosis in ovarian cancer cells through activation of JNK and enhancement of Bim expression. Cancer chemotherapy and pharmacology. 2009;63(6):997-1005.

[339] Kang, M., Jeong, C. W., Ku, J. H., Kwak, C., Kim, H. H. Inhibition of autophagy potentiates atorvastatin-induced apoptotic cell death in human bladder cancer cells in vitro. International journal of molecular sciences. 2014;15(5):8106-21.

[340] Laezza, C., Fiorentino, L., Pisanti, S., Gazzerro, P., Caraglia, M., Portella, G., et al. Lovastatin induces apoptosis of k-ras-transformed thyroid cells via inhibition of ras farnesylation and by modulating redox state. Journal of molecular medicine. 2008;86(12):1341-51.

[341] Zhong, W. B., Wang, C. Y., Chang, T. C., Lee, W. S. Lovastatin induces apoptosis of anaplastic thyroid cancer cells via inhibition of protein geranylgeranylation and de novo protein synthesis. Endocrinology. 2003;144(9):3852-9.

[342] Koyuturk, M., Ersoz, M., Altiok, N. Simvastatin induces proliferation inhibition and apoptosis in C6 glioma cells via c-jun N-terminal kinase. Neuroscience letters. 2004;370(2-3):212-7.

[343] Rattan, R., Giri, S., Singh, A. K., Singh, I. Rho/ROCK pathway as a target of tumor therapy. Journal of neuroscience research. 2006;83(2):243-55.

[344] Yanae, M., Tsubaki, M., Satou, T., Itoh, T., Imano, M., Yamazoe, Y., et al. Statin-induced apoptosis via the suppression of ERK1/2 and Akt activation by inhibition of the geranylgeranyl-pyrophosphate biosynthesis in glioblastoma. Journal of experimental & clinical cancer research : CR. 2011;30:74.

[345] Tomiyama, N., Matzno, S., Kitada, C., Nishiguchi, E., Okamura, N., Matsuyama, K. The possibility of simvastatin as a chemotherapeutic agent for all-trans retinoic acid-resistant promyelocytic leukemia. Biological & pharmaceutical bulletin. 2008;31(3):369-74.

[346] Fromigué, O., Hay, E., Modrowski, D., Bouvet, S., Jacquel, A., Auberger, P., et al. RhoA GTPase inactivation by statins induces osteosarcoma cell apoptosis by inhibiting p42/p44-MAPKs-Bcl-2 signaling independently of BMP-2 and cell differentiation. Cell death and differentiation. 2006;13(11):1845-56.

[347] Niknejad, N., Morley, M., Dimitroulakos, J. Activation of the integrated stress response regulates lovastatin-induced apoptosis. The Journal of biological chemistry. 2007;282(41):29748-56.

[348] Dimitroulakos, J., Marhin, W. H., Tokunaga, J., Irish, J., Gullane, P., Penn, L. Z., et al. Microarray and biochemical analysis of lovastatin-induced apoptosis of squamous cell carcinomas. Neoplasia. 2002;4(4):337-46.

[349] Jiang, Z., Zheng, X., Lytle, R. A., Higashikubo, R., Rich, K. M. Lovastatin-induced up-regulation of the BH3-only protein, Bim, and cell death in glioblastoma cells. Journal of neurochemistry. 2004;89(1):168-78.

[350] Qi, X. F., Zheng, L., Lee, K. J., Kim, D. H., Kim, C. S., Cai, D. Q., et al. HMG-CoA reductase inhibitors induce apoptosis of lymphoma cells by promoting ROS generation and regulating Akt, Erk and p38 signals via suppression of mevalonate pathway. Cell death & disease. 2013;4:e518.

[351] Cafforio, P., Dammacco, F., Gernone, A., Silvestris, F. Statins activate the mitochondrial pathway of apoptosis in human lymphoblasts and myeloma cells. Carcinogenesis. 2005;26(5):883-91.

[352] Zhu, Y., Casey, P. J., Kumar, A. P., Pervaiz, S. Deciphering the signaling networks underlying simvastatin-induced apoptosis in human cancer cells: evidence for non-canonical activation of RhoA and Rac1 GTPases. Cell death & disease. 2013;4:e568.

[353] Sassano, A., Katsoulidis, E., Antico, G., Altman, J. K., Redig, A. J., Minucci, S., et al. Suppressive effects of statins on acute promyelocytic leukemia cells. Cancer research. 2007;67(9):4524-32.

[354] Joneson, T., Bar-Sagi, D. Suppression of Ras-induced apoptosis by the Rac GTPase. Molecular and cellular biology. 1999;19(9):5892-901.

[355] Mayo, M. W., Baldwin, A. S. The transcription factor NF-kappaB: control of oncogenesis and cancer therapy resistance. Biochimica et biophysica acta. 2000;1470(2):M55-62.

[356] Sulciner, D. J., Irani, K., Yu, Z. X., Ferrans, V. J., Goldschmidt-Clermont, P., Finkel, T. rac1 regulates a cytokine-stimulated, redox-dependent pathway necessary for NF-kappaB activation. Molecular and cellular biology. 1996;16(12):7115-21.

[357] Agarwal, B., Bhendwal, S., Halmos, B., Moss, S. F., Ramey, W. G., Holt, P. R. Lovastatin augments apoptosis induced by chemotherapeutic agents in colon cancer cells. Clinical cancer research : an official journal of the American Association for Cancer Research. 1999;5(8):2223-9.

[358] Cho, S. J., Kim, J. S., Kim, J. M., Lee, J. Y., Jung, H. C., Song, I. S. Simvastatin induces apoptosis in human colon cancer cells and in tumor xenografts, and attenuates colitis-associated colon cancer in mice. International journal of cancer Journal international du cancer. 2008;123(4):951-7.

[359] Dimitroulakos, J., Thai, S., Wasfy, G. H., Hedley, D. W., Minden, M. D., Penn, L. Z. Lovastatin induces a pronounced differentiation response in acute myeloid leukemias. Leukemia & lymphoma. 2000;40(1-2):167-78.

[360] Murga, C., Zohar, M., Teramoto, H., Gutkind, J. S. Rac1 and RhoG promote cell survival by the activation of PI3K and Akt, independently of their ability to stimulate JNK and NF-kappaB. Oncogene. 2002;21(2):207-16.

[361] Ghavami, S., Mutawe, M. M., Hauff, K., Stelmack, G. L., Schaafsma, D., Sharma, P., et al. Statin-triggered cell death in primary human lung mesenchymal cells involves p53-PUMA and release of Smac and Omi but not cytochrome c. Biochimica et biophysica acta. 2010;1803(4):452-67.

[362] Lee, S. K., Kim, Y. C., Song, S. B., Kim, Y. S. Stabilization and translocation of p53 to mitochondria is linked to Bax translocation to mitochondria in simvastatin-induced apoptosis. Biochemical and biophysical research communications. 2010;391(4):1592-7.

[363] Chapman-Shimshoni, D., Yuklea, M., Radnay, J., Shapiro, H., Lishner, M. Simvastatin induces apoptosis of B-CLL cells by activation of mitochondrial caspase 9. Experimental hematology. 2003;31(9):779-83.

[364] Goc, A., Kochuparambil, S. T., Al-Husein, B., Al-Azayzih, A., Mohammad, S., Somanath, P. R. Simultaneous modulation of the intrinsic and extrinsic pathways by simvastatin in mediating prostate cancer cell apoptosis. BMC cancer. 2012;12:409.

[365] Minichsdorfer, C., Hohenegger, M. Autocrine amplification loop in statin-induced apoptosis of human melanoma cells. British journal of pharmacology. 2009;157(7):1278-90.

[366] MacDonald, J. S., Gerson, R. J., Kornbrust, D. J., Kloss, M. W., Prahalada, S., Berry, P. H., et al. Preclinical evaluation of lovastatin. The American journal of cardiology. 1988;62(15):16J-27J.

[367] Kubatka, P., Kruzliak, P., Rotrekl, V., Jelinkova, S., Mladosievicova, B. Statins in oncological research: From experimental studies to clinical practice. Critical reviews in oncology/hematology. 2014;92(3):296-311.

[368] Tatsuta, M., Iishi, H., Baba, M., Iseki, K., Yano, H., Uehara, H., et al. Suppression by pravastatin, an inhibitor of p21ras isoprenylation, of hepatocarcinogenesis induced by N-nitrosomorpholine in Sprague-Dawley rats. British journal of cancer. 1998;77(4):581-7.

[369] Narisawa, T., Fukaura, Y., Terada, K., Umezawa, A., Tanida, N., Yazawa, K., et al. Prevention of 1,2-dimethylhydrazine-induced colon tumorigenesis by HMG-CoA reductase inhibitors, pravastatin and simvastatin, in ICR mice. Carcinogenesis. 1994;15(9):2045-8.

[370] Wang, C. Y., Shui, H. A., Chang, T. C. In vivo evidence of duality effects for lovastatin in a nude mouse cancer model. International journal of cancer Journal international du cancer. 2010;126(2):578-82.

[371] Kubatka, P., Kajo, K., Zihlavnikova, K., Adamicova, K., Vybohova, D., Pec, M., et al. Immunohistochemical and histomorphological analysis of rat mammary tumors after simvastatin treatment. Neoplasma. 2012;59(5):516-23.

[372] Kubatka, P., Stollarova, N., Skarda, J., Zihlavnikova, K., Kajo, K., Kapinova, A., et al. Preventive effects of fluvastatin in rat mammary carcinogenesis. European journal of cancer prevention : the official journal of the European Cancer Prevention Organisation. 2013;22(4):352-7.

[373] Kubatka, P. Ž., K., Solár, P., Kajo, K., Valentová, V., Péč, M., Bojková, B., Kassayová, M., Stollárová, N., Ahlers, I. Antitumor effects of atorvastatin in the chemoprevention of rat mammary carcinogenesis. Biologia. 2011;66(4):727-34.

[374] Bjerre, L. M., LeLorier, J. Do statins cause cancer? A meta-analysis of large randomized clinical trials. The American journal of medicine. 2001;110(9):716-23.

[375] Bonovas, S., Filioussi, K., Tsavaris, N., Sitaras, N. M. Statins and cancer risk: a literature-based meta-analysis and meta-regression analysis of 35 randomized controlled trials. Journal of clinical oncology : official journal of the American Society of Clinical Oncology. 2006;24(30):4808-17.

[376] Browning, D. R., Martin, R. M. Statins and risk of cancer: a systematic review and metaanalysis. International journal of cancer Journal international du cancer. 2007;120(4):833-43.

[377] Dale, K. M., Coleman, C. I., Henyan, N. N., Kluger, J., White, C. M. Statins and cancer risk: a meta-analysis. JAMA. 2006;295(1):74-80.

[378] Kuoppala, J., Lamminpaa, A., Pukkala, E. Statins and cancer: A systematic review and meta-analysis. European journal of cancer. 2008;44(15):2122-32.

[379] Strandberg, T. E., Pyorala, K., Cook, T. J., Wilhelmsen, L., Faergeman, O., Thorgeirsson, G., et al. Mortality and incidence of cancer during 10-year follow-up of the Scandinavian Simvastatin Survival Study (4S). Lancet. 2004;364(9436):771-7.

[380] Bonovas, S., Filioussi, K., Tsavaris, N., Sitaras, N. M. Use of statins and breast cancer: a meta-analysis of seven randomized clinical trials and nine observational studies. Journal of clinical oncology : official journal of the American Society of Clinical Oncology. 2005;23(34):8606-12.

[381] Undela, K., Srikanth, V., Bansal, D. Statin use and risk of breast cancer: a meta-analysis of observational studies. Breast cancer research and treatment. 2012;135(1):261-9.

[382] Deng, Z., Zhang, S., Yi, L., Chen, S. Can statins reduce risk of lung cancer, especially among elderly people? A meta-analysis. Chinese journal of cancer research = Chung-kuo yen cheng yen chiu. 2013;25(6):679-88.

[383] Tan, M., Song, X., Zhang, G., Peng, A., Li, X., Li, M., et al. Statins and the risk of lung cancer: a meta-analysis. PloS one. 2013;8(2):e57349.

[384] Bonovas, S., Filioussi, K., Flordellis, C. S., Sitaras, N. M. Statins and the risk of colorectal cancer: a meta-analysis of 18 studies involving more than 1.5 million patients. Journal of clinical oncology : official journal of the American Society of Clinical Oncology. 2007;25(23):3462-8.

[385] Bonovas, S., Nikolopoulos, G., Filioussi, K., Peponi, E., Bagos, P., Sitaras, N. M. Can statin therapy reduce the risk of melanoma? A meta-analysis of randomized controlled trials. European journal of epidemiology. 2010;25(1):29-35.

[386] Li, X., Wu, X. B., Chen, Q. Statin use is not associated with reduced risk of skin cancer: a meta-analysis. British journal of cancer. 2014;110(3):802-7.

[387] Zhang, X. L., Geng, J., Zhang, X. P., Peng, B., Che, J. P., Yan, Y., et al. Statin use and risk of bladder cancer: a meta-analysis. Cancer causes & control : CCC. 2013;24(4):769-76.

[388] Zhang, X. L., Liu, M., Qian, J., Zheng, J. H., Zhang, X. P., Guo, C. C., et al. Statin use and risk of kidney cancer: a meta-analysis of observational studies and randomized trials. British journal of clinical pharmacology. 2014;77(3):458-65.

[389] Bonovas, S., Filioussi, K., Sitaras, N. M. Statins are not associated with a reduced risk of pancreatic cancer at the population level, when taken at low doses for managing hypercholesterolemia: evidence from a meta-analysis of 12 studies. The American journal of gastroenterology. 2008;103(10):2646-51.

[390] Cui, X., Xie, Y., Chen, M., Li, J., Liao, X., Shen, J., et al. Statin use and risk of pancreatic cancer: a meta-analysis. Cancer causes & control : CCC. 2012;23(7):1099-111.

[391] Pradelli, D., Soranna, D., Scotti, L., Zambon, A., Catapano, A., Mancia, G., et al. Statins and primary liver cancer: a meta-analysis of observational studies. European journal of cancer prevention : the official journal of the European Cancer Prevention Organisation. 2013;22(3):229-34.

[392] Shi, M., Zheng, H., Nie, B., Gong, W., Cui, X. Statin use and risk of liver cancer: an update meta-analysis. BMJ open. 2014;4(9):e005399.

[393] Singh, S., Singh, P. P., Singh, A. G., Murad, M. H., Sanchez, W. Statins are associated with a reduced risk of hepatocellular cancer: a systematic review and meta-analysis. Gastroenterology. 2013;144(2):323-32.

[394] Zhang, H. G., C.; Fang, L.; Yao, S. Statin use and risk of liver cancer: A meta-analysis of 7 studies involving more than 4.7 million patients. World Journal of Meta-Analysis. 2013;1(3):130-7.

[395] Ma, Z. W., W.; Jin, G.; Chu, P., Li, H. Effect of statins on gastric cancer incidence: A meta-Analysis of case control studies. Journal of Cancer Research and Therapeutics. 2014;10(4):859-65.

[396] Yi, X., Jia, W., Jin, Y., Zhen, S. Statin use is associated with reduced risk of haematological malignancies: evidence from a meta-analysis. PloS one. 2014;9(1):e87019.

[397] Bonovas, S., Filioussi, K., Sitaras, N. M. Statin use and the risk of prostate cancer: A metaanalysis of 6 randomized clinical trials and 13 observational studies. International journal of cancer Journal international du cancer. 2008;123(4):899-904.

[398] Bansal, D., Undela, K., D'Cruz, S., Schifano, F. Statin use and risk of prostate cancer: a meta-analysis of observational studies. PloS one. 2012;7(10):e46691.

[399] Park, H. S., Schoenfeld, J. D., Mailhot, R. B., Shive, M., Hartman, R. I., Ogembo, R., et al. Statins and prostate cancer recurrence following radical prostatectomy or radiotherapy: a systematic review and meta-analysis. Annals of oncology : official journal of the European Society for Medical Oncology / ESMO. 2013;24(6):1427-34.

[400] Kaye, J. A., Jick, H. Statin use and cancer risk in the General Practice Research Database. British journal of cancer. 2004;90(3):635-7.

[401] Yu, O., Boudreau, D. M., Buist, D. S., Miglioretti, D. L. Statin use and female reproductive organ cancer risk in a large population-based setting. Cancer causes & control : CCC. 2009;20(5):609-16.

[402] Elmore, R. G., Ioffe, Y., Scoles, D. R., Karlan, B. Y., Li, A. J. Impact of statin therapy on survival in epithelial ovarian cancer. Gynecologic oncology. 2008;111(1):102-5.

[403] Lavie, O., Pinchev, M., Rennert, H. S., Segev, Y., Rennert, G. The effect of statins on risk and survival of gynecological malignancies. Gynecologic oncology. 2013;130(3):615-9.

[404] Habis, M., Wroblewski, K., Bradaric, M., Ismail, N., Yamada, S. D., Litchfield, L., et al. Statin therapy is associated with improved survival in patients with non-serous-papillary epithelial ovarian cancer: a retrospective cohort analysis. PloS one. 2014;9(8):e104521.

[405] Liu, Y., Qin, A., Li, T., Qin, X., Li, S. Effect of statin on risk of gynecologic cancers: a meta-analysis of observational studies and randomized controlled trials. Gynecologic oncology. 2014;133(3):647-55.

[406] Lee, J., Jung, K. H., Park, Y. S., Ahn, J. B., Shin, S. J., Im, S. A., et al. Simvastatin plus irinotecan, 5-fluorouracil, and leucovorin (FOLFIRI) as first-line chemotherapy in metastatic colorectal patients: a multicenter phase II study. Cancer chemotherapy and pharmacology. 2009;64(4):657-63.

[407] Kornblau, S. M., Banker, D. E., Stirewalt, D., Shen, D., Lemker, E., Verstovsek, S., et al. Blockade of adaptive defensive changes in cholesterol uptake and synthesis in AML by the addition of pravastatin to idarubicin + high-dose Ara-C: a phase 1 study. Blood. 2007;109(7):2999-3006.

[408] Chen, T. L., Estey, E. H., Othus, M., Gardner, K. M., Markle, L. J., Walter, R. B. Cyclosporine modulation of multidrug resistance in combination with pravastatin, mitoxantrone and etoposide for adult patients with relapsed/refractory acute myeloid leukemia: a phase 1/2 study. Leukemia & lymphoma. 2013;54(11):2534-6.

[409] Han, J. Y., Lee, S. H., Yoo, N. J., Hyung, L. S., Moon, Y. J., Yun, T., et al. A randomized phase II study of gefitinib plus simvastatin versus gefitinib alone in previously treated patients with advanced non-small cell lung cancer. Clinical cancer research : an official journal of the American Association for Cancer Research. 2011;17(6):1553-60.

[410] Han, J. Y., Lim, K. Y., Yu, S. Y., Yun, T., Kim, H. T., Lee, J. S. A phase 2 study of irinotecan, cisplatin, and simvastatin for untreated extensive-disease small cell lung cancer. Cancer. 2011;117(10):2178-85.

[411] Hong, J. Y., Nam, E. M., Lee, J., Park, J. O., Lee, S. C., Song, S. Y., et al. Randomized double-blinded, placebo-controlled phase II trial of simvastatin and gemcitabine in advanced pancreatic cancer patients. Cancer chemotherapy and pharmacology. 2014;73(1):125-30.

[412] Kawata, S., Yamasaki, E., Nagase, T., Inui, Y., Ito, N., Matsuda, Y., et al. Effect of pravastatin on survival in patients with advanced hepatocellular carcinoma. A randomized controlled trial. British journal of cancer. 2001;84(7):886-91.

[413] Graf, H., Jungst, C., Straub, G., Dogan, S., Hoffmann, R. T., Jakobs, T., et al. Chemoembolization combined with pravastatin improves survival in patients with hepatocellular carcinoma. Digestion. 2008;78(1):34-8.

[414] Lersch, C., Schmelz, R., Erdmann, J., Hollweck, R., Schulte-Frohlinde, E., Eckel, F., et al. Treatment of HCC with pravastatin, octreotide, or gemcitabine--a critical evaluation. Hepato-gastroenterology. 2004;51(58):1099-103.

[415] Konings, I. R., van der Gaast, A., van der Wijk, L. J., de Jongh, F. E., Eskens, F. A., Sleijfer, S. The addition of pravastatin to chemotherapy in advanced gastric carcinoma: a randomised phase II trial. European journal of cancer. 2010;46(18):3200-4.

[416] Knox, J. J., Siu, L. L., Chen, E., Dimitroulakos, J., Kamel-Reid, S., Moore, M. J., et al. A Phase I trial of prolonged administration of lovastatin in patients with recurrent or metastatic squamous cell carcinoma of the head and neck or of the cervix. European journal of cancer. 2005;41(4):523-30.

[417] Kim, W. S., Kim, M. M., Choi, H. J., Yoon, S. S., Lee, M. H., Park, K., et al. Phase II study of high-dose lovastatin in patients with advanced gastric adenocarcinoma. Investigational new drugs. 2001;19(1):81-3.

[418] van der Spek, E., Bloem, A. C., Sinnige, H. A., Lokhorst, H. M. High dose simvastatin does not reverse resistance to vincristine, adriamycin, and dexamethasone (VAD) in myeloma. Haematologica. 2007;92(12):e130-1.

[419] van der Spek, E., Bloem, A. C., van de Donk, N. W., Bogers, L. H., van der Griend, R., Kramer, M. H., et al. Dose-finding study of high-dose simvastatin combined with standard chemotherapy in patients with relapsed or refractory myeloma or lymphoma. Haematologica. 2006;91(4):542-5.

[420] Hus, M., Grzasko, N., Szostek, M., Pluta, A., Helbig, G., Woszczyk, D., et al. Thalidomide, dexamethasone and lovastatin with autologous stem cell transplantation as a salvage immunomodulatory therapy in patients with relapsed and refractory multiple myeloma. Annals of hematology. 2011;90(10):1161-6.

[421] Garwood, E. R., Kumar, A. S., Baehner, F. L., Moore, D. H., Au, A., Hylton, N., et al. Fluvastatin reduces proliferation and increases apoptosis in women with high grade breast cancer. Breast cancer research and treatment. 2010;119(1):137-44.

[422] Lopez-Aguilar, E., Sepulveda-Vildosola, A. C., Betanzos-Cabrera, Y., Rocha-Moreno, Y. G., Gascon-Lastiri, G., Rivera-Marquez, H., et al. Phase II study of metronomic chemotherapy with thalidomide, carboplatin-vincristine-fluvastatin in the treatment of brain stem tumors in children. Archives of medical research. 2008;39(7):655-62.

[423] Manoukian, G. E., Tannir, N. M., Jonasch, E., Qiao, W., Haygood, T. M., Tu, S. M. Pilot trial of bone-targeted therapy combining zoledronate with fluvastatin or atorvastatin for patients with metastatic renal cell carcinoma. Clinical genitourinary cancer. 2011;9(2):81-8.

[424] Shitara, Y., Sugiyama, Y. Pharmacokinetic and pharmacodynamic alterations of 3-hydroxy-3-methylglutaryl coenzyme A (HMG-CoA) reductase inhibitors: drug-drug interactions and interindividual differences in transporter and metabolic enzyme functions. Pharmacology & therapeutics. 2006;112(1):71-105.

[425] National Institutes of Health. ClinicalTrials.gov. United States of America. 2014 [accessed 13th October, 2014]; Available from: https://clinicaltrials.gov/.

[426] Konstantinopoulos, P. A., Matulonis, U. A. Current status and evolution of preclinical drug development models of epithelial ovarian cancer. Frontiers in oncology. 2013;3:296.

[427] Sandberg, R., Ernberg, I. Assessment of tumor characteristic gene expression in cell lines using a tissue similarity index (TSI). Proceedings of the National Academy of Sciences of the United States of America. 2005;102(6):2052-7.

[428] Zietarska, M., Maugard, C. M., Filali-Mouhim, A., Alam-Fahmy, M., Tonin, P. N., Provencher, D. M., et al. Molecular description of a 3D in vitro model for the study of epithelial ovarian cancer (EOC). Molecular carcinogenesis. 2007;46(10):872-85.

[429] Ahmed, N., Stenvers, K. L. Getting to know ovarian cancer ascites: opportunities for targeted therapy-based translational research. Frontiers in oncology. 2013;3:256.

[430] Kobayashi, H., Man, S., Graham, C. H., Kapitain, S. J., Teicher, B. A., Kerbel, R. S. Acquired multicellular-mediated resistance to alkylating agents in cancer. Proceedings of the National Academy of Sciences of the United States of America. 1993;90(8):3294-8.

[431] Achilli, T. M., Meyer, J., Morgan, J. R. Advances in the formation, use and understanding of multi-cellular spheroids. Expert opinion on biological therapy. 2012;12(10):1347-60.

[432] Carlsson, J., Acker, H. Relations between pH, oxygen partial pressure and growth in cultured cell spheroids. International journal of cancer Journal international du cancer. 1988;42(5):715-20.

[433] Friedrich, J., Seidel, C., Ebner, R., Kunz-Schughart, L. A. Spheroid-based drug screen: considerations and practical approach. Nature protocols. 2009;4(3):309-24.

[434] Hamilton, T. C., Young, R. C., Louie, K. G., Behrens, B. C., McKoy, W. M., Grotzinger, K. R., et al. Characterization of a xenograft model of human ovarian carcinoma which produces ascites and intraabdominal carcinomatosis in mice. Cancer research. 1984;44(11):5286-90.

[435] Kelland, L. R., Jones, M., Abel, G., Valenti, M., Gwynne, J., Harrap, K. R. Human ovarian-carcinoma cell lines and companion xenografts: a disease-oriented approach to new platinum anticancer drug discovery. Cancer chemotherapy and pharmacology. 1992;30(1):43-50.

[436] Hu, L., Hofmann, J., Holash, J., Yancopoulos, G. D., Sood, A. K., Jaffe, R. B. Vascular endothelial growth factor trap combined with paclitaxel strikingly inhibits tumor and ascites, prolonging survival in a human ovarian cancer model. Clinical cancer research : an official journal of the American Association for Cancer Research. 2005;11(19 Pt 1):6966-71.

[437] Lengyel, E., Burdette, J. E., Kenny, H. A., Matei, D., Pilrose, J., Haluska, P., et al. Epithelial ovarian cancer experimental models. Oncogene. 2014;33(28):3619-33.

[438] Domcke, S., Sinha, R., Levine, D. A., Sander, C., Schultz, N. Evaluating cell lines as tumour models by comparison of genomic profiles. Nature communications. 2013;4:2126.

[439] Eva, A., Robbins, K. C., Andersen, P. R., Srinivasan, A., Tronick, S. R., Reddy, E. P., et al. Cellular genes analogous to retroviral onc genes are transcribed in human tumour cells. Nature. 1982;295(5845):116-9.

[440] Godwin, A. K., Meister, A., O'Dwyer, P. J., Huang, C. S., Hamilton, T. C., Anderson, M. E. High resistance to cisplatin in human ovarian cancer cell lines is associated with marked increase of glutathione synthesis. Proceedings of the National Academy of Sciences of the United States of America. 1992;89(7):3070-4.

[441] Hamilton, T. C., Young, R. C., McKoy, W. M., Grotzinger, K. R., Green, J. A., Chu, E. W., et al. Characterization of a human ovarian carcinoma cell line (NIH:OVCAR-3) with androgen and estrogen receptors. Cancer research. 1983;43(11):5379-89.

[442] Hamilton, T. C., Young, R. C., Ozols, R. F. Experimental model systems of ovarian cancer: applications to the design and evaluation of new treatment approaches. Seminars in oncology. 1984;11(3):285-98.

[443] Bénard, J., Da Silva, J., De Blois, M. C., Boyer, P., Duvillard, P., Chiric, E., et al. Characterization of a human ovarian adenocarcinoma line, IGROV1, in tissue culture and in nude mice. Cancer research. 1985;45(10):4970-9.

[444] Buick, R. N., Pullano, R., Trent, J. M. Comparative properties of five human ovarian adenocarcinoma cell lines. Cancer research. 1985;45(8):3668-76.

[445] Fogh, J., Fogh, J. M., Orfeo, T. One hundred and twenty-seven cultured human tumor cell lines producing tumors in nude mice. Journal of the National Cancer Institute. 1977;59(1):221-6.

[446] Langdon, S. P., Lawrie, S. S., Hay, F. G., Hawkes, M. M., McDonald, A., Hayward, I. P., et al. Characterization and properties of nine human ovarian adenocarcinoma cell lines. Cancer research. 1988;48(21):6166-72.

[447] Dowling, R. J., Niraula, S., Stambolic, V., Goodwin, P. J. Metformin in cancer: translational challenges. Journal of molecular endocrinology. 2012;48(3):R31-43.

[448] Chou, T. C., Talalay, P. Quantitative analysis of dose-effect relationships: the combined effects of multiple drugs or enzyme inhibitors. Advances in enzyme regulation. 1984;22:27-55.

[449] Goldoni, M., Johansson, C. A mathematical approach to study combined effects of toxicants in vitro: evaluation of the Bliss independence criterion and the Loewe additivity model. Toxicology in vitro : an international journal published in association with BIBRA. 2007;21(5):759-69.

[450] Witham, J., Valenti, M. R., De-Haven-Brandon, A. K., Vidot, S., Eccles, S. A., Kaye, S. B., et al. The Bcl-2/Bcl-XL family inhibitor ABT-737 sensitizes ovarian cancer cells to carboplatin. Clinical cancer research : an official journal of the American Association for Cancer Research. 2007;13(23):7191-8.

[451] Cui, H., Huang, P., Wang, Z., Zhang, Y., Zhang, Z., Xu, W., et al. Association of decreased mitochondrial DNA content with the progression of colorectal cancer. BMC cancer. 2013;13:110.

[452] Peviva. M30 CytoDeath™ ELISA: Apoptosis detection in cell cultures. Stockholm: Peviva; 2014 [accessed 30th June, 2014]; Available from: http://www.peviva.com/m30-cytodeath-elisa.aspx.

[453] Di, B., Su, M. X., Yu, F., Qu, L. J., Zhao, L. P., Cheng, M. C., et al. Solid-phase extraction and liquid chromatography/tandem mass spectrometry assay for the determination of pitavastatin in human plasma and urine for application to Phase I clinical pharmacokinetic studies. Journal of chromatography B, Analytical technologies in the biomedical and life sciences. 2008;868(1-2):95-101.

[454] Folch, J., Lees, M., Sloane Stanley, G. H. A simple method for the isolation and purification of total lipides from animal tissues. The Journal of biological chemistry. 1957;226(1):497-509.

[455] Bligh, E. G., Dyer, W. J. A rapid method of total lipid extraction and purification. Canadian journal of biochemistry and physiology. 1959;37(8):911-7.

[456] Muraguchi, T. O., K.; Mitake, M.; Ogawa, H.; Shidoji, Y. Polished rice as natural sources of cancer-preventing geranylgeranoic acid. Journal of clinical biochemistry and nutrition. 2011;49(1):8-15.

[457] Tobert, J. A. Lovastatin and beyond: the history of the HMG-CoA reductase inhibitors. Nature reviews Drug discovery. 2003;2(7):517-26.

[458] Kolovou, G. D., Katerina, A., Ioannis, V., Cokkinos, D. V. Simvastatin: two decades in a circle. Cardiovascular therapeutics. 2008;26(2):166-78.

[459] Grodos, D., Tonglet, R. Scandinavian simvastatin study (4S). Lancet. 1994;344(8939-8940):1768.

[460] Kanugula, A. K., Gollavilli, P. N., Vasamsetti, S. B., Karnewar, S., Gopoju, R., Ummanni, R., et al. Statin-induced inhibition of breast cancer proliferation and invasion involves attenuation of iron transport: Intermediacy of nitric oxide and antioxidant defence mechanisms. The FEBS journal. 2014;281(16):3719-38.

[461] Yu, X., Pan, Y., Ma, H., Li, W. Simvastatin inhibits proliferation and induces apoptosis in human lung cancer cells. Oncology research. 2013;20(8):351-7.

[462] Gbelcová, H., Lenicek, M., Zelenka, J., Knejzlik, Z., Dvorakova, G., Zadinova, M., et al. Differences in antitumor effects of various statins on human pancreatic cancer. International journal of cancer Journal international du cancer. 2008;122(6):1214-21.

[463] Sekine, Y., Furuya, Y., Nishii, M., Koike, H., Matsui, H., Suzuki, K. Simvastatin inhibits the proliferation of human prostate cancer PC-3 cells via down-regulation of the insulin-like growth factor 1 receptor. Biochemical and biophysical research communications. 2008;372(2):356-61.

[464] Fang, Z., Tang, Y., Fang, J., Zhou, Z., Xing, Z., Guo, Z., et al. Simvastatin inhibits renal cancer cell growth and metastasis via AKT/mTOR, ERK and JAK2/STAT3 pathway. PloS one. 2013;8(5):e62823.

[465] Wu, H., Jiang, H., Lu, D., Xiong, Y., Qu, C., Zhou, D., et al. Effect of simvastatin on glioma cell proliferation, migration, and apoptosis. Neurosurgery. 2009;65(6):1087-97.

[466] Stoehr, M., Mozet, C., Boehm, A., Aigner, A., Dietz, A., Wichmann, G. Simvastatin suppresses head and neck squamous cell carcinoma ex vivo and enhances the cytostatic effects of chemotherapeutics. Cancer chemotherapy and pharmacology. 2014;73(4):827-37.

[467] von Tresckow, B., von Strandmann, E. P., Sasse, S., Tawadros, S., Engert, A., Hansen, H. P. Simvastatin-dependent apoptosis in Hodgkin's lymphoma cells and growth impairment of human Hodgkin's tumors in vivo. Haematologica. 2007;92(5):682-5.

[468] Otsuki, T., Sakaguchi, H., Hatayama, T., Fujii, T., Tsujioka, T., Sugihara, T., et al. Effects of an HMG-CoA reductase inhibitor, simvastatin, on human myeloma cells. Oncology reports. 2004;11(5):1053-8.

[469] Konturek, P. C., Burnat, G., Hahn, E. G. Inhibition of Barret's adenocarcinoma cell growth by simvastatin: involvement of COX-2 and apoptosis-related proteins. Journal of physiology and pharmacology : an official journal of the Polish Physiological Society. 2007;58 Suppl 3:141-8.

[470] Crescencio, M. E., Rodriguez, E., Paez, A., Masso, F. A., Montano, L. F., Lopez-Marure, R. Statins inhibit the proliferation and induce cell death of human papilloma virus positive and negative cervical cancer cells. International journal of biomedical science : IJBS. 2009;5(4):411-20.

[471] Osmak, M. Statins and cancer: current and future prospects. Cancer letters. 2012;324(1):1-12.

[472] Aberg, M., Wickstrom, M., Siegbahn, A. Simvastatin induces apoptosis in human breast cancer cells in a NFkappaB-dependent manner and abolishes the anti-apoptotic signaling of TF/FVIIa and TF/FVIIa/FXa. Thrombosis research. 2008;122(2):191-202.

[473] Gopalan, A., Yu, W., Sanders, B. G., Kline, K. Simvastatin inhibition of mevalonate pathway induces apoptosis in human breast cancer cells via activation of JNK/CHOP/DR5 signaling pathway. Cancer letters. 2013;329(1):9-16.

[474] Park, Y. H., Seo, S. Y., Lee, E., Ku, J. H., Kim, H. H., Kwak, C. Simvastatin induces apoptosis in castrate resistant prostate cancer cells by deregulating nuclear factor-kappaB pathway. The Journal of urology. 2013;189(4):1547-52.

[475] Ogunwobi, O. O., Beales, I. L. Statins inhibit proliferation and induce apoptosis in Barrett's esophageal adenocarcinoma cells. The American journal of gastroenterology. 2008;103(4):825-37.

[476] Chang, H. L., Chen, C. Y., Hsu, Y. F., Kuo, W. S., Ou, G., Chiu, P. T., et al. Simvastatin induced HCT116 colorectal cancer cell apoptosis through p38MAPK-p53-survivin signaling cascade. Biochimica et biophysica acta. 2013;1830(8):4053-64.

[477] Schointuch, M. N., Gilliam, T. P., Stine, J. E., Han, X., Zhou, C., Gehrig, P. A., et al. Simvastatin, an HMG-CoA reductase inhibitor, exhibits anti-metastatic and anti-tumorigenic effects in endometrial cancer. Gynecologic oncology. 2014;134(2):346-55.

[478] Kah, J., Wustenberg, A., Keller, A. D., Sirma, H., Montalbano, R., Ocker, M., et al. Selective induction of apoptosis by HMG-CoA reductase inhibitors in hepatoma cells and dependence on p53 expression. Oncology reports. 2012;28(3):1077-83.

[479] Miller, T., Yang, F., Wise, C. E., Meng, F., Priester, S., Munshi, M. K., et al. Simvastatin stimulates apoptosis in cholangiocarcinoma by inhibition of Rac1 activity. Digestive and liver disease : official journal of the Italian Society of Gastroenterology and the Italian Association for the Study of the Liver. 2011;43(5):395-403.

[480] Yu, H., Su, J., Xu, Y., Kang, J., Li, H., Zhang, L., et al. p62/SQSTM1 involved in cisplatin resistance in human ovarian cancer cells by clearing ubiquitinated proteins. European journal of cancer. 2011;47(10):1585-94.

[481] Araki, M., Motojima, K. Hydrophobic statins induce autophagy in cultured human rhabdomyosarcoma cells. Biochemical and biophysical research communications. 2008;367(2):462-7.

[482] Ahmed, T. A., Hayslip, J., Leggas, M. Pharmacokinetics of high-dose simvastatin in refractory and relapsed chronic lymphocytic leukemia patients. Cancer chemotherapy and pharmacology. 2013;72(6):1369-74.

[483] Ahmed, T. High dose simvastatin as a potential anticancer therapy in leukemia patients. Kentucky: University of Kentucky; PhD Thesis; 2013.

[484] Taylor-Harding, B., Orsulic, S., Karlan, B. Y., Li, A. J. Fluvastatin and cisplatin demonstrate synergistic cytotoxicity in epithelial ovarian cancer cells. Gynecologic oncology. 2010;119(3):549-56.

[485] Martirosyan, A., Clendening, J. W., Goard, C. A., Penn, L. Z. Lovastatin induces apoptosis of ovarian cancer cells and synergizes with doxorubicin: potential therapeutic relevance. BMC cancer. 2010;10:103.

[486] Bjørkøy, G., Lamark, T., Pankiv, S., Overvatn, A., Brech, A., Johansen, T. Monitoring autophagic degradation of p62/SQSTM1. Methods in enzymology. 2009;452:181-97.

[487] Mizushima, N., Yoshimori, T., Levine, B. Methods in mammalian autophagy research. Cell. 2010;140(3):313-26.

[488] Ganley, I. G., Wong, P. M., Gammoh, N., Jiang, X. Distinct autophagosomal-lysosomal fusion mechanism revealed by thapsigargin-induced autophagy arrest. Molecular cell. 2011;42(6):731-43.

[489] Pankiv, S., Alemu, E. A., Brech, A., Bruun, J. A., Lamark, T., Overvatn, A., et al. FYCO1 is a Rab7 effector that binds to LC3 and PI3P to mediate microtubule plus end-directed vesicle transport. The Journal of cell biology. 2010;188(2):253-69.

[490] Wang, T., Ming, Z., Xiaochun, W., Hong, W. Rab7: role of its protein interaction cascades in endo-lysosomal traffic. Cellular signalling. 2011;23(3):516-21.

[491] Laezza, C., Bucci, C., Santillo, M., Bruni, C. B., Bifulco, M. Control of Rab5 and Rab7 expression by the isoprenoid pathway. Biochemical and biophysical research communications. 1998;248(3):469-72.

[492] Robinson, E., Nandi, M., Wilkinson, L. L., Arrowsmith, D. M., Curtis, A. D., Richardson, A. Preclinical evaluation of statins as a treatment for ovarian cancer. Gynecologic oncology. 2013;129(2):417-24.

[493] Tang, H. L., Yuen, K. L., Tang, H. M., Fung, M. C. Reversibility of apoptosis in cancer cells. British journal of cancer. 2009;100(1):118-22.

[494] Tang, H. L., Tang, H. M., Mak, K. H., Hu, S., Wang, S. S., Wong, K. M., et al. Cell survival, DNA damage, and oncogenic transformation after a transient and reversible apoptotic response. Molecular biology of the cell. 2012;23(12):2240-52.

[495] Ichim, G., Lopez, J., Ahmed, S. U., Muthalagu, N., Giampazolias, E., Delgado, M. E., et al. Limited mitochondrial permeabilization causes DNA damage and genomic instability in the absence of cell death. Molecular cell. 2015;57(5):860-72.

[496] Kajinami, K., Mabuchi, H., Saito, Y. NK-104: a novel synthetic HMG-CoA reductase inhibitor. Expert opinion on investigational drugs. 2000;9(11):2653-61.

[497] Sondergaard, T. E., Pedersen, P. T., Andersen, T. L., Soe, K., Lund, T., Ostergaard, B., et al. A phase II clinical trial does not show that high dose simvastatin has beneficial effect on markers of bone turnover in multiple myeloma. Hematological oncology. 2009;27(1):17-22.

[498] Takatori, E., Shoji, T., Sawai, T., Kurose, A., Sugiyama, T. Analysis of the antitumor activity of gemcitabine and carboplatin against ovarian clear-cell carcinoma using the DNA damage marker gammaH2AX. OncoTargets and therapy. 2013;6:901-7.

[499] Jain, A., Lamark, T., Sjottem, E., Larsen, K. B., Awuh, J. A., Overvatn, A., et al. p62/SQSTM1 is a target gene for transcription factor NRF2 and creates a positive feedback loop by inducing antioxidant response element-driven gene transcription. The Journal of biological chemistry. 2010;285(29):22576-91.

[500] Ageberg, M., Rydstrom, K., Linden, O., Linderoth, J., Jerkeman, M., Drott, K. Inhibition of geranylgeranylation mediates sensitivity to CHOP-induced cell death of DLBCL cell lines. Experimental cell research. 2011;317(8):1179-91.

[501] Wasko, B. M., Dudakovic, A., Hohl, R. J. Bisphosphonates induce autophagy by depleting geranylgeranyl diphosphate. The Journal of pharmacology and experimental therapeutics. 2011;337(2):540-6.

[502] Iwaizumi, M., Tseng-Rogenski, S., Carethers, J. M. DNA mismatch repair proficiency executing 5-fluorouracil cytotoxicity in colorectal cancer cells. Cancer biology & therapy. 2011;12(8):756-64.

[503] Li, X., Yan, J., Wang, L., Xiao, F., Yang, Y., Guo, X., et al. Beclin1 inhibition promotes autophagy and decreases gemcitabine-induced apoptosis in Miapaca2 pancreatic cancer cells. Cancer cell international. 2013;13(1):26.

[504] Wang, W., Fan, H., Zhou, Y., Duan, P., Zhao, G., Wu, G. Knockdown of autophagy-related gene BECLIN1 promotes cell growth and inhibits apoptosis in the A549 human lung cancer cell line. Molecular medicine reports. 2013;7(5):1501-5.

[505] Kajinami, K., Takekoshi, N., Saito, Y. Pitavastatin: efficacy and safety profiles of a novel synthetic HMG-CoA reductase inhibitor. Cardiovascular drug reviews. 2003;21(3):199-215.

[506] Chapman, M. J., McTaggart, F. Optimizing the pharmacology of statins: characteristics of rosuvastatin. Atherosclerosis Supplements. 2002;2(4):33-6.

[507] Hsiang, B., Zhu, Y., Wang, Z., Wu, Y., Sasseville, V., Yang, W. P., et al. A novel human hepatic organic anion transporting polypeptide (OATP2). Identification of a liver-specific human organic anion transporting polypeptide and identification of rat and human hydroxymethylglutaryl-CoA reductase inhibitor transporters. The Journal of biological chemistry. 1999;274(52):37161-8.

[508] Ose, L., Budinski, D., Hounslow, N., Arneson, V. Comparison of pitavastatin with simvastatin in primary hypercholesterolaemia or combined dyslipidaemia. Current medical research and opinion. 2009;25(11):2755-64.

[509] Hayashi, T., Yokote, K., Saito, Y., Iguchi, A. Pitavastatin: efficacy and safety in intensive lipid lowering. Expert opinion on pharmacotherapy. 2007;8(14):2315-27.

[510] Wang, J., Kitajima, I. Pitavastatin inactivates NF-kappaB and decreases IL-6 production through Rho kinase pathway in MCF-7 cells. Oncology reports. 2007;17(5):1149-54.

[511] Wang, J., Tokoro, T., Higa, S., Kitajima, I. Anti-inflammatory effect of pitavastatin on NF-kappaB activated by TNF-alpha in hepatocellular carcinoma cells. Biological & pharmaceutical bulletin. 2006;29(4):634-9.

[512] Shimizu, M., Yasuda, Y., Sakai, H., Kubota, M., Terakura, D., Baba, A., et al. Pitavastatin suppresses diethylnitrosamine-induced liver preneoplasms in male C57BL/KsJ-db/db obese mice. BMC cancer. 2011;11:281.

[513] Yasuda, Y., Shimizu, M., Shirakami, Y., Sakai, H., Kubota, M., Hata, K., et al. Pitavastatin inhibits azoxymethane-induced colonic preneoplastic lesions in C57BL/KsJ-db/db obese mice. Cancer science. 2010;101(7):1701-7.

[514] Yasui, Y., Suzuki, R., Miyamoto, S., Tsukamoto, T., Sugie, S., Kohno, H., et al. A lipophilic statin, pitavastatin, suppresses inflammation-associated mouse colon carcinogenesis. International journal of cancer Journal international du cancer. 2007;121(10):2331-9.

[515] Teraoka, N., Mutoh, M., Takasu, S., Ueno, T., Yamamoto, M., Sugimura, T., et al. Inhibition of intestinal polyp formation by pitavastatin, a HMG-CoA reductase inhibitor. Cancer prevention research. 2011;4(3):445-53.

[516] Jiang, P., Mukthavaram, R., Chao, Y., Nomura, N., Bharati, I. S., Fogal, V., et al. In vitro and in vivo anticancer effects of mevalonate pathway modulation on human cancer cells. British journal of cancer. 2014;111(8):1562-71.

[517] Jiang, P., Mukthavaram, R., Chao, Y., Bharati, I. S., Fogal, V., Pastorino, S., et al. Novel anti-glioblastoma agents and therapeutic combinations identified from a collection of FDA approved drugs. Journal of translational medicine. 2014;12:13.

[518] Holstein, S. A., Knapp, H. R., Clamon, G. H., Murry, D. J., Hohl, R. J. Pharmacodynamic effects of high dose lovastatin in subjects with advanced malignancies. Cancer chemotherapy and pharmacology. 2006;57(2):155-64.

[519] Ulukaya, E., Karaagac, E., Ari, F., Oral, A. Y., Adim, S. B., Tokullugil, A. H., et al. Chemotherapy increases caspase-cleaved cytokeratin 18 in the serum of breast cancer patients. Radiology and oncology. 2011;45(2):116-22.

[520] Brioschi, M., Lento, S., Tremoli, E., Banfi, C. Proteomic analysis of endothelial cell secretome: a means of studying the pleiotropic effects of Hmg-CoA reductase inhibitors. Journal of proteomics. 2013;78:346-61.

[521] Abedini, M. R., Qiu, Q., Yan, X., Tsang, B. K. Possible role of FLICE-like inhibitory protein (FLIP) in chemoresistant ovarian cancer cells in vitro. Oncogene. 2004;23(42):6997-7004.

[522] Vidot, S., Witham, J., Agarwal, R., Greenhough, S., Bamrah, H. S., Tigyi, G. J., et al. Autotaxin delays apoptosis induced by carboplatin in ovarian cancer cells. Cellular signalling. 2010;22(6):926-35.

[523] Sena, L. A., Chandel, N. S. Physiological roles of mitochondrial reactive oxygen species. Molecular cell. 2012;48(2):158-67.

[524] Tal, M. C., Sasai, M., Lee, H. K., Yordy, B., Shadel, G. S., Iwasaki, A. Absence of autophagy results in reactive oxygen species-dependent amplification of RLR signaling. Proceedings of the National Academy of Sciences of the United States of America. 2009;106(8):2770-5.

[525] Goldstein, J. L., Brown, M. S. Regulation of the mevalonate pathway. Nature. 1990;343(6257):425-30.

[526] Nomura, D. K., Long, J. Z., Niessen, S., Hoover, H. S., Ng, S. W., Cravatt, B. F. Monoacylglycerol lipase regulates a fatty acid network that promotes cancer pathogenesis. Cell. 2010;140(1):49-61.

[527] Reiter, B. L., E. Analysis of the Wax Ester Fraction of Olive Oil and Sunflower Oil by Gas Chromatography and Gas Chromatography–Mass Spectrometry. Journal of the American Oil Chemists' Society. 2001;78:881-8.

[528] Ranalli, A. M., G.; Patumi, M.; Fontanazza, G. The compositional quality and sensory properties of virgin olive oil from a new olive cultivar - I-77. Food Chemistry. 2000;69:37-46.

[529] Gauthaman, K., Manasi, N., Bongso, A. Statins inhibit the growth of variant human embryonic stem cells and cancer cells in vitro but not normal human embryonic stem cells. British journal of pharmacology. 2009;157(6):962-73.

[530] Ando, H., Tsuruoka, S., Yanagihara, H., Sugimoto, K., Miyata, M., Yamazoe, Y., et al. Effects of grapefruit juice on the pharmacokinetics of pitavastatin and atorvastatin. British journal of clinical pharmacology. 2005;60(5):494-7.

[531] Chung, J. Y., Cho, J. Y., Yu, K. S., Kim, J. R., Oh, D. S., Jung, H. R., et al. Effect of OATP1B1 (SLCO1B1) variant alleles on the pharmacokinetics of pitavastatin in healthy volunteers. Clinical pharmacology and therapeutics. 2005;78(4):342-50.

[532] Hui, C. K., Cheung, B. M., Lau, G. K. Pharmacokinetics of pitavastatin in subjects with Child-Pugh A and B cirrhosis. British journal of clinical pharmacology. 2005;59(3):291-7.

[533] Flores, N. A. Pitavastatin Nissan/Kowa Yakuhin/Novartis/Sankyo. Current opinion in investigational drugs. 2002;3(9):1334-41.

[534] Kumar, N. S. N., N.; Nirmal, J.; Sonali, N; Bagyalakshmi, J. HPLC Determination of Pitavastatin Calcium in Pharmaceutical Dosage Forms. Pharmaceutica Analytica Acta. 2011;2(2):1-4.

[535] Engels, I. H., Stepczynska, A., Stroh, C., Lauber, K., Berg, C., Schwenzer, R., et al. Caspase-8/FLICE functions as an executioner caspase in anticancer drug-induced apoptosis. Oncogene. 2000;19(40):4563-73.

[536] Young, M. M., Takahashi, Y., Khan, O., Park, S., Hori, T., Yun, J., et al. Autophagosomal membrane serves as platform for intracellular death-inducing signaling complex (iDISC)-mediated caspase-8 activation and apoptosis. The Journal of biological chemistry. 2012;287(15):12455-68.

[537] Komatsu, M., Waguri, S., Ueno, T., Iwata, J., Murata, S., Tanida, I., et al. Impairment of starvation-induced and constitutive autophagy in Atg7-deficient mice. The Journal of cell biology. 2005;169(3):425-34.

[538] Pua, H. H., Guo, J., Komatsu, M., He, Y. W. Autophagy is essential for mitochondrial clearance in mature T lymphocytes. Journal of immunology. 2009;182(7):4046-55.

[539] Mambo, E., Gao, X., Cohen, Y., Guo, Z., Talalay, P., Sidransky, D. Electrophile and oxidant damage of mitochondrial DNA leading to rapid evolution of homoplasmic mutations. Proceedings of the National Academy of Sciences of the United States of America. 2003;100(4):1838-43.

[540] Lee, H. C., Wei, Y. H. Mitochondrial biogenesis and mitochondrial DNA maintenance of mammalian cells under oxidative stress. The international journal of biochemistry & cell biology. 2005;37(4):822-34.

[541] Ozaki, K., Kishikawa, F., Tanaka, M., Sakamoto, T., Tanimura, S., Kohno, M. Histone deacetylase inhibitors enhance the chemosensitivity of tumor cells with cross-resistance to a wide range of DNA-damaging drugs. Cancer science. 2008;99(2):376-84.

[542] Lindenthal, B., Simatupang, A., Dotti, M. T., Federico, A., Lutjohann, D., von Bergmann, K. Urinary excretion of mevalonic acid as an indicator of cholesterol synthesis. Journal of lipid research. 1996;37(10):2193-201.

[543] Lindenthal, B., von Bergmann, K. Urinary excretion and serum concentration of mevalonic acid during acute intake of alcohol. Metabolism: clinical and experimental. 2000;49(1):62-6.

[544] Abe, M., Oshima, R. G. A single human keratin 18 gene is expressed in diverse epithelial cells of transgenic mice. The Journal of cell biology. 1990;111(3):1197-206.

[545] Linder, S., Havelka, A. M., Ueno, T., Shoshan, M. C. Determining tumor apoptosis and necrosis in patient serum using cytokeratin 18 as a biomarker. Cancer letters. 2004;214(1):1-9.

[546] Nishizuka, S., Charboneau, L., Young, L., Major, S., Reinhold, W. C., Waltham, M., et al. Proteomic profiling of the NCI-60 cancer cell lines using new high-density reverse-phase lysate microarrays. Proceedings of the National Academy of Sciences of the United States of America. 2003;100(24):14229-34.

[547] Colell, A., Green, D. R., Ricci, J. E. Novel roles for GAPDH in cell death and carcinogenesis. Cell death and differentiation. 2009;16(12):1573-81.

[548] Clucas, J., Valderrama, F. ERM proteins in cancer progression. Journal of cell science. 2014;127(Pt 2):267-75.

[549] Quick, Q., Skalli, O. Alpha-actinin 1 and alpha-actinin 4: contrasting roles in the survival, motility, and RhoA signaling of astrocytoma cells. Experimental cell research. 2010;316(7):1137-47.

[550] Sidera, K., Patsavoudi, E. HSP90 inhibitors: current development and potential in cancer therapy. Recent patents on anti-cancer drug discovery. 2014;9(1):1-20.

[551] Capello, M., Ferri-Borgogno, S., Cappello, P., Novelli, F. alpha-Enolase: a promising therapeutic and diagnostic tumor target. The FEBS journal. 2011;278(7):1064-74.

[552] Chaker, S., Kashat, L., Voisin, S., Kaur, J., Kak, I., MacMillan, C., et al. Secretome proteins as candidate biomarkers for aggressive thyroid carcinomas. Proteomics. 2013;13(5):771-87.

[553] Bababeygy, S. R., Polevaya, N. V., Youssef, S., Sun, A., Xiong, A., Prugpichailers, T., et al. HMG-CoA reductase inhibition causes increased necrosis and apoptosis in an in vivo mouse glioblastoma multiforme model. Anticancer research. 2009;29(12):4901-8.

[554] Costa, R. A., Fernandes, M. P., de Souza-Pinto, N. C., Vercesi, A. E. Protective effects of l-carnitine and piracetam against mitochondrial permeability transition and PC3 cell necrosis induced by simvastatin. European journal of pharmacology. 2013;701(1-3):82-6.

[555] Kroemer, G., Martin, S. J. Caspase-independent cell death. Nature medicine. 2005;11(7):725-30.

[556] Labi, V., Grespi, F., Baumgartner, F., Villunger, A. Targeting the Bcl-2-regulated apoptosis pathway by BH3 mimetics: a breakthrough in anticancer therapy? Cell death and differentiation. 2008;15(6):977-87.

[557] Martinez-Paniagua, M. A. R.-G., L. A.; Anguiano-Hernandez, Y. M.; Gonzalez-Torres, C.; Vega, M. I. Abstract 1735: Obatoclax enhances CDDP and trail-induced apoptosis in epithelial ovarian adenocarcinoma cells. AACR 104th Annual Meeting 2013; Washington, DC: Cancer Research; 2013. p. 1735.

[558] Stamelos, V. A., Robinson, E., Redman, C. W., Richardson, A. Navitoclax augments the activity of carboplatin and paclitaxel combinations in ovarian cancer cells. Gynecologic oncology. 2013;128(2):377-82.

[559] Simonin, K., N'Diaye, M., Lheureux, S., Loussouarn, C., Dutoit, S., Briand, M., et al. Platinum compounds sensitize ovarian carcinoma cells to ABT-737 by modulation of the Mcl-1/Noxa axis. Apoptosis : an international journal on programmed cell death. 2013;18(4):492-508.

[560] Jebahi, A., Villedieu, M., Petigny-Lechartier, C., Brotin, E., Louis, M. H., Abeilard, E., et al. PI3K/mTOR dual inhibitor NVP-BEZ235 decreases Mcl-1 expression and sensitizes ovarian carcinoma cells to Bcl-xL-targeting strategies, provided that Bim expression is induced. Cancer letters. 2014;348(1-2):38-49.

[561] Follet, J., Corcos, L., Baffet, G., Ezan, F., Morel, F., Simon, B., et al. The association of statins and taxanes: an efficient combination trigger of cancer cell apoptosis. British journal of cancer. 2012;106(4):685-92.

[562] Gao, J., Jia, W. D., Li, J. S., Wang, W., Xu, G. L., Ma, J. L., et al. Combined inhibitory effects of celecoxib and fluvastatin on the growth of human hepatocellular carcinoma xenografts in nude mice. The Journal of international medical research. 2010;38(4):1413-27.

[563] Engelman, J. A., Luo, J., Cantley, L. C. The evolution of phosphatidylinositol 3-kinases as regulators of growth and metabolism. Nature reviews Genetics. 2006;7(8):606-19.

[564] Workman, P., Clarke, P. A., Raynaud, F. I., van Montfort, R. L. Drugging the PI3 kinome: from chemical tools to drugs in the clinic. Cancer research. 2010;70(6):2146-57.

[565] Wallin, J. J., Guan, J., Prior, W. W., Edgar, K. A., Kassees, R., Sampath, D., et al. Nuclear phospho-Akt increase predicts synergy of PI3K inhibition and doxorubicin in breast and ovarian cancer. Science translational medicine. 2010;2(48):48ra66.

[566] Raynaud, F. I., Eccles, S. A., Patel, S., Alix, S., Box, G., Chuckowree, I., et al. Biological properties of potent inhibitors of class I phosphatidylinositide 3-kinases: from PI-103 through PI-540, PI-620 to the oral agent GDC-0941. Molecular cancer therapeutics. 2009;8(7):1725-38.

[567] Ghosh-Choudhury, N., Mandal, C. C., Ghosh Choudhury, G. Simvastatin induces derepression of PTEN expression via NFkappaB to inhibit breast cancer cell growth. Cellular signalling. 2010;22(5):749-58.

[568] Zakikhani, M., Dowling, R., Fantus, I. G., Sonenberg, N., Pollak, M. Metformin is an AMP kinase-dependent growth inhibitor for breast cancer cells. Cancer research. 2006;66(21):10269-73.

[569] Anisimov, V. N., Egormin, P. A., Bershtein, L. M., Zabezhinskii, M. A., Piskunova, T. S., Popovich, I. G., et al. Metformin decelerates aging and development of mammary tumors in HER-2/neu transgenic mice. Bulletin of experimental biology and medicine. 2005;139(6):721-3.

[570] Lee, M. S., Hsu, C. C., Wahlqvist, M. L., Tsai, H. N., Chang, Y. H., Huang, Y. C. Type 2 diabetes increases and metformin reduces total, colorectal, liver and pancreatic cancer incidences in Taiwanese: a representative population prospective cohort study of 800,000 individuals. BMC cancer. 2011;11:20.

[571] Shank, J. J., Yang, K., Ghannam, J., Cabrera, L., Johnston, C. J., Reynolds, R. K., et al. Metformin targets ovarian cancer stem cells in vitro and in vivo. Gynecologic oncology. 2012;127(2):390-7.

[572] Wu, B., Li, S., Sheng, L., Zhu, J., Gu, L., Shen, H., et al. Metformin inhibits the development and metastasis of ovarian cancer. Oncology reports. 2012;28(3):903-8.

[573] Rattan, R., Graham, R. P., Maguire, J. L., Giri, S., Shridhar, V. Metformin suppresses ovarian cancer growth and metastasis with enhancement of cisplatin cytotoxicity in vivo. Neoplasia. 2011;13(5):483-91.

[574] Yasmeen, A., Beauchamp, M. C., Piura, E., Segal, E., Pollak, M., Gotlieb, W. H. Induction of apoptosis by metformin in epithelial ovarian cancer: involvement of the Bcl-2 family proteins. Gynecologic oncology. 2011;121(3):492-8.

[575] Brunmair, B., Staniek, K., Gras, F., Scharf, N., Althaym, A., Clara, R., et al. Thiazolidinediones, like metformin, inhibit respiratory complex I: a common mechanism contributing to their antidiabetic actions? Diabetes. 2004;53(4):1052-9.

[576] Rattan, R., Giri, S., Hartmann, L. C., Shridhar, V. Metformin attenuates ovarian cancer cell growth in an AMP-kinase dispensable manner. Journal of cellular and molecular medicine. 2011;15(1):166-78.

[577] Li, C., Liu, V. W., Chan, D. W., Yao, K. M., Ngan, H. Y. LY294002 and metformin cooperatively enhance the inhibition of growth and the induction of apoptosis of ovarian cancer cells. International journal of gynecological cancer : official journal of the International Gynecological Cancer Society. 2012;22(1):15-22.

[578] Hanrahan, A. J., Schultz, N., Westfal, M. L., Sakr, R. A., Giri, D. D., Scarperi, S., et al. Genomic complexity and AKT dependence in serous ovarian cancer. Cancer discovery. 2012;2(1):56-67.

[579] Huang, J., Zhang, L., Greshock, J., Colligon, T. A., Wang, Y., Ward, R., et al. Frequent genetic abnormalities of the PI3K/AKT pathway in primary ovarian cancer predict patient outcome. Genes, chromosomes & cancer. 2011;50(8):606-18.

[580] Miraglia, E., Hogberg, J., Stenius, U. Statins exhibit anticancer effects through modifications of the pAkt signaling pathway. International journal of oncology. 2012;40(3):867-75.

[581] Robinson, E., Fisher, N., Stamelos, V., Redman, C., Richardson, A. New strategies for the treatment of ovarian cancer. Biochemical Society transactions. 2014;42(1):125-9.

[582] Liu, H., Yang, J., Yuan, Y., Xia, Z., Chen, M., Xie, L., et al. Regulation of Mcl-1 by constitutive activation of NF-kappaB contributes to cell viability in human esophageal squamous cell carcinoma cells. BMC cancer. 2014;14:98.

[583] Certo, M., Del Gaizo Moore, V., Nishino, M., Wei, G., Korsmeyer, S., Armstrong, S. A., et al. Mitochondria primed by death signals determine cellular addiction to antiapoptotic BCL-2 family members. Cancer cell. 2006;9(5):351-65.

[584] Stamelos, V. A., Redman, C. W., Richardson, A. Understanding sensitivity to BH3 mimetics: ABT-737 as a case study to foresee the complexities of personalized medicine. Journal of molecular signaling. 2012;7(1):12.

[585] Stamelos, V. Investigation of the BH3-mimetics navitoclax and obatoclax as potential therapeutics for ovarian cancer. Staffordshire: Keele University; PhD Thesis; 2014.

[586] Tomic, T., Botton, T., Cerezo, M., Robert, G., Luciano, F., Puissant, A., et al. Metformin inhibits melanoma development through autophagy and apoptosis mechanisms. Cell death & disease. 2011;2:e199.

[587] Bridges, H. R., Jones, A. J., Pollak, M. N., Hirst, J. Effects of metformin and other biguanides on oxidative phosphorylation in mitochondria. The Biochemical journal. 2014;462(3):475-87.

[588] Aranovich, A., Liu, Q., Collins, T., Geng, F., Dixit, S., Leber, B., et al. Differences in the mechanisms of proapoptotic BH3 proteins binding to Bcl-XL and Bcl-2 quantified in live MCF-7 cells. Molecular cell. 2012;45(6):754-63.

[589] Merino, D., Khaw, S. L., Glaser, S. P., Anderson, D. J., Belmont, L. D., Wong, C., et al. Bcl-2, Bcl-x(L), and Bcl-w are not equivalent targets of ABT-737 and navitoclax (ABT-263) in lymphoid and leukemic cells. Blood. 2012;119(24):5807-16.

[590] Del Gaizo Moore, V., Letai, A. BH3 profiling--measuring integrated function of the mitochondrial apoptotic pathway to predict cell fate decisions. Cancer letters. 2013;332(2):202-5.

[591] Djordjevic, B., Hennessy, B. T., Li, J., Barkoh, B. A., Luthra, R., Mills, G. B., et al. Clinical assessment of PTEN loss in endometrial carcinoma: immunohistochemistry outperforms gene sequencing. Modern pathology : an official journal of the United States and Canadian Academy of Pathology, Inc. 2012;25(5):699-708.

[592] Sangale, Z., Prass, C., Carlson, A., Tikishvili, E., Degrado, J., Lanchbury, J., et al. A robust immunohistochemical assay for detecting PTEN expression in human tumors. Applied immunohistochemistry & molecular morphology : AIMM / official publication of the Society for Applied Immunohistochemistry. 2011;19(2):173-83.

[593] Endo, A. A historical perspective on the discovery of statins. Proceedings of the Japan Academy Series B, Physical and biological sciences. 2010;86(5):484-93.

[594] Goldstein, J. L., Helgeson, J. A., Brown, M. S. Inhibition of cholesterol synthesis with compactin renders growth of cultured cells dependent on the low density lipoprotein receptor. The Journal of biological chemistry. 1979;254(12):5403-9.

[595] Melichar, B., Ferrandina, G., Verschraegen, C. F., Loercher, A., Abbruzzese, J. L., Freedman, R. S. Growth inhibitory effects of aromatic fatty acids on ovarian tumor cell lines. Clinical cancer research : an official journal of the American Association for Cancer Research. 1998;4(12):3069-76.

[596] Thibault, A., Samid, D., Tompkins, A. C., Figg, W. D., Cooper, M. R., Hohl, R. J., et al. Phase I study of lovastatin, an inhibitor of the mevalonate pathway, in patients with cancer. Clinical cancer research : an official journal of the American Association for Cancer Research. 1996;2(3):483-91.

[597] Goard, C. A., Chan-Seng-Yue, M., Mullen, P. J., Quiroga, A. D., Wasylishen, A. R., Clendening, J. W., et al. Identifying molecular features that distinguish fluvastatin-sensitive breast tumor cells. Breast cancer research and treatment. 2014;143(2):301-12.

[598] Chen, J., Lan, T., Hou, J., Zhang, J., An, Y., Tie, L., et al. Atorvastatin sensitizes human non-small cell lung carcinomas to carboplatin via suppression of AKT activation and upregulation of TIMP-1. The international journal of biochemistry & cell biology. 2012;44(5):759-69.

[599] Ahn, K. S., Sethi, G., Aggarwal, B. B. Reversal of chemoresistance and enhancement of apoptosis by statins through down-regulation of the NF-kappaB pathway. Biochemical pharmacology. 2008;75(4):907-13.

[600] Holstein, S. A., Hohl, R. J. Synergistic interaction of lovastatin and paclitaxel in human cancer cells. Molecular cancer therapeutics. 2001;1(2):141-9.

[601] Chung, Y. S., Cho, S., Ryou, H. J., Jee, H. G., Choi, J. Y., Yoon, K., et al. Is there a treatment advantage when paclitaxel and lovastatin are combined to dose anaplastic thyroid carcinoma cell lines? Thyroid : official journal of the American Thyroid Association. 2011;21(7):735-44.

[602] Xiong, X., Sui, M., Fan, W., Kraft, A. S. Cell cycle dependent antagonistic interactions between paclitaxel and carboplatin in combination therapy. Cancer biology & therapy. 2007;6(7):1067-73.

[603] Fromigue, O., Hamidouche, Z., Marie, P. J. Statin-induced inhibition of 3-hydroxy-3-methyl glutaryl coenzyme a reductase sensitizes human osteosarcoma cells to anticancer drugs. The Journal of pharmacology and experimental therapeutics. 2008;325(2):595-600.

[604] Feleszko, W., Mlynarczuk, I., Balkowiec-Iskra, E. Z., Czajka, A., Switaj, T., Stoklosa, T., et al. Lovastatin potentiates antitumor activity and attenuates cardiotoxicity of doxorubicin in three tumor models in mice. Clinical cancer research : an official journal of the American Association for Cancer Research. 2000;6(5):2044-52.

[605] Feleszko, W., Mlynarczuk, I., Olszewska, D., Jalili, A., Grzela, T., Lasek, W., et al. Lovastatin potentiates antitumor activity of doxorubicin in murine melanoma via an apoptosis-dependent mechanism. International journal of cancer Journal international du cancer. 2002;100(1):111-8.

[606] Roudier, E., Mistafa, O., Stenius, U. Statins induce mammalian target of rapamycin (mTOR)-mediated inhibition of Akt signaling and sensitize p53-deficient cells to cytostatic drugs. Molecular cancer therapeutics. 2006;5(11):2706-15.

[607] Rozados, V. R., Hinrichsen, L. I., Binda, M. M., Gervasoni, S. I., Matar, P., Bonfil, R. D., et al. Lovastatin enhances the antitumoral and apoptotic activity of doxorubicin in murine tumor models. Oncology reports. 2008;19(5):1205-11.

[608] Werner, M., Atil, B., Sieczkowski, E., Chiba, P., Hohenegger, M. Simvastatin-induced compartmentalisation of doxorubicin sharpens up nuclear topoisomerase II inhibition in human rhabdomyosarcoma cells. Naunyn-Schmiedeberg's archives of pharmacology. 2013;386(7):605-17.

[609] Sieczkowski, E., Lehner, C., Ambros, P. F., Hohenegger, M. Double impact on p-glycoprotein by statins enhances doxorubicin cytotoxicity in human neuroblastoma cells. International journal of cancer Journal international du cancer. 2010;126(9):2025-35.

[610] Folkman, J. A new link in ovarian cancer angiogenesis: lysophosphatidic acid and vascular endothelial growth factor expression. Journal of the National Cancer Institute. 2001;93(10):734-5.

[611] Linden, O., Greiff, L., Wahlberg, P., Vinge, E., Kjellen, E. Chemorefractory rhabdomyosarcoma treated with radiotherapy, bevacizumab, statins and surgery and maintenance with bevacizumab and chemotherapy. Onkologie. 2008;31(7):391-3.

[612] Green, J. R. Bisphosphonates: preclinical review. The oncologist. 2004;9 Suppl 4:3-13.

[613] Monkkonen, H., Auriola, S., Lehenkari, P., Kellinsalmi, M., Hassinen, I. E., Vepsalainen, J., et al. A new endogenous ATP analog (AppppI) inhibits the mitochondrial adenine nucleotide translocase (ANT) and is responsible for the apoptosis induced by nitrogen-containing bisphosphonates. British journal of pharmacology. 2006;147(4):437-45.

[614] Sawada, K., Morishige, K., Tahara, M., Kawagishi, R., Ikebuchi, Y., Tasaka, K., et al. Alendronate inhibits lysophosphatidic acid-induced migration of human ovarian cancer cells by attenuating the activation of rho. Cancer research. 2002;62(21):6015-20.

[615] Hirata, J., Kikuchi, Y., Kudoh, K., Kita, T., Seto, H. Inhibitory effects of bisphosphonates on the proliferation of human ovarian cancer cell lines and the mechanism. Medicinal chemistry. 2006;2(3):223-6.

[616] Hashimoto, K., Morishige, K., Sawada, K., Tahara, M., Kawagishi, R., Ikebuchi, Y., et al. Alendronate inhibits intraperitoneal dissemination in in vivo ovarian cancer model. Cancer research. 2005;65(2):540-5.

[617] Budman, D. R., Calabro, A. Zoledronic acid (Zometa) enhances the cytotoxic effect of gemcitabine and fluvastatin: in vitro isobologram studies with conventional and nonconventional cytotoxic agents. Oncology. 2006;70(2):147-53.

[618] Schmidmaier, R., Simsek, M., Baumann, P., Emmerich, B., Meinhardt, G. Synergistic antimyeloma effects of zoledronate and simvastatin. Anti-cancer drugs. 2006;17(6):621-9.

[619] Knight, L. A., Kurbacher, C. M., Glaysher, S., Fernando, A., Reichelt, R., Dexel, S., et al. Activity of mevalonate pathway inhibitors against breast and ovarian cancers in the ATP-based tumour chemosensitivity assay. BMC cancer. 2009;9:38.

[620] Downward, J. Targeting RAS signalling pathways in cancer therapy. Nature reviews Cancer. 2003;3(1):11-22.

[621] Lobell, R. B., Omer, C. A., Abrams, M. T., Bhimnathwala, H. G., Brucker, M. J., Buser, C. A., et al. Evaluation of farnesyl:protein transferase and geranylgeranyl:protein transferase inhibitor combinations in preclinical models. Cancer research. 2001;61(24):8758-68.

[622] Coxon, F. P., Helfrich, M. H., Larijani, B., Muzylak, M., Dunford, J. E., Marshall, D., et al. Identification of a novel phosphonocarboxylate inhibitor of Rab geranylgeranyl transferase that specifically prevents Rab prenylation in osteoclasts and macrophages. The Journal of biological chemistry. 2001;276(51):48213-22.

[623] Roelofs, A. J., Hulley, P. A., Meijer, A., Ebetino, F. H., Russell, R. G., Shipman, C. M. Selective inhibition of Rab prenylation by a phosphonocarboxylate analogue of risedronate induces apoptosis, but not S-phase arrest, in human myeloma cells. International journal of cancer Journal international du cancer. 2006;119(6):1254-61.

APPENDICES

Appendix 1: siRNA transfection

SMARTpool (Dharmacon) or individual siRNA (Dharmacon) were reconstituted in siRNA buffer (Dharmacon) to 20 µM solutions. The siRNA used are detailed in the table below.

Name	**Concentration**	**Target Sequence**
Rab7 SMARTpool	20 nM	N/A
Atg5 SMARTpool	20 nM	N/A
Beclin 1 SMARTpool	20 nM	N/A
FLIP SMARTpool	0.3 nM	N/A
FLIP #4	25 nM	AAUAACUUCAGGCUCCAUAUU
FLIP #18	3 nM	UAAAGAACAUCCACAGAAUUU

Appendix 2: Primer sequences and amplicon sizes

The primers used for qPCR were reconstituted in DNase/RNase-free distilled water to a concentration of 100 µM. The final primer concentration in the reaction mix was 100 nM. Primers were obtained from Sigma-Aldrich.

Primer Name	**Forward (5' → 3')**	**Reverse (5' → 3')**	**Amplicon Size (bp)**
ND1	TAATGCTTACCGAACGAA	TTATGGCGTCAGCGAAGG	104
β-actin	GCAAAGTTCCCAAGCACA	AAGCAAGCAGCGGAGCAG	105

Appendix 3: Antibodies used for protein immunodetection

The primary and secondary antibodies used for protein immunodetection were prepared in TBST (or PBS for immunofluorescence) containing 5% skimmed milk powder or 5% BSA at the following dilutions.

Antibody	**Dilution**	**Product Code and Supplier**
anti-LC3 primary antibody	1/2000 (western blotting) or 1/100 (immunofluorescence)	LC3-2G6, Nanotools
anti-Rab7 primary antibody	1/1000 (western blotting) or 1/100 (immunofluorescence)	9367, Cell Signaling Technology
anti-SQSTM1/p62 primary antibody	1/1000	AB56416, Abcam
anti-GAPDH primary antibody	1/5000	MAB374, Millipore
anti-PARP primary antibody	1/1000	9542, Cell Signaling Technology
anti-Bim primary antibody	1/1000	2819, Cell Signaling Technology
anti-Bcl-X_L primary antibody	1/1000	2762, Cell Signaling Technology
anti-Mcl-1 (D35A5) primary antibody	1/1000	5453, Cell Signaling Technology
anti-α-Actinin primary antibody	1/1000	3134, Cell Signaling Technology
anti-HSP90 primary antibody	1/1000	4874, Cell Signaling Technology
anti-Enolase-1 primary antibody	1/1000	3810, Cell Signaling Technology
anti-Pan-Actin primary antibody	1/1000	4968, Cell Signaling Technology

anti-Ezrin primary antibody	1/1000	3145, Cell Signaling Technology
anti-Moesin (Q480) primary antibody	1/1000	3150, Cell Signaling Technology
anti-Radixin (C4G7) primary antibody	1/1000	2636, Cell Signaling Technology
anti-Atg5 primary antibody	1/1000	2630, Cell Signaling Technology
anti-Beclin 1 (D40C5) primary antibody	1/1000	3495, Cell Signaling Technology
anti-FLIP (D16A8) primary antibody	1/1000	8510, Cell Signaling Technology
anti-PMK1/2 (C103A3) primary antibody	1/1000	3190, Cell Signaling Technology
anti-HMGCR [EPR1685(N)] primary antibody	1/1000	AB174830, Abcam
anti-mouse IgG secondary antibody linked to HRP	1/2000	7076, Cell Signaling Technology
anti-rabbit IgG secondary antibody linked to HRP	1/2000	7074, Cell Signaling Technology
anti-mouse Cy2 antibody	1/1000	AB6944, Abcam
anti-rabbit Alexa Fluor 568 antibody	1/1000	A10042, Life Technologies

Appendix 4: Peptide sequences identified from mass spectrometry analysis of proteins in cell culture medium from Ovcar-8 cells exposed to pitavastatin

Protein Name	Matched Peptides (Bold Red)
Alpha-actinin 1	1 MDHYDSQQTN DYMQPEEDWD RDLLLDPAWE KQQRKTFTAW CNSHLRKAGT 51 QIENIEEDFR DGLKLMLLLE VISGERLAKP ERGKMRVHKI SNVNKALDFI 101 ASKGVKLVSI GAEEIVDGNV KMTLGMIWTI ILRFAIQDIS VEETSAKEGL 151 LLWCQRKTAP YKNVNIQNFH ISWKDGLGFC ALIHRHRPEL IDYGKLRKDD 201 PLTNLNTAFD VAEKYLDIPK MLDAEDIVGT ARPDEKAIMT YVSSFYHAFS 251 GAQKAETAAN RICKVLAVNQ ENEQLMEDYE KLASDLLEWI RRTIPWLENR 301 VPENTMHAMQ QKLEDFRDYR RLHKPPKVQE KCQLEINFNT LQTKLRLSNR 351 PAFMPSEGRM VSDINNAWGC LEQVEKGYEE WLLNEIRRLE RLDHLAEKFR 401 QKASIHEAWT DGKEAMLRQK DYETATLSEI KALLKKHEAF ESDLAAHQDR 451 VEQIAAIAQE LNELDYYDSP SVNARCQKIC DQWDNLGALT QKRREALERT 501 EKLLETIDQL YLEYAKRAAP FNNWMEGAME DLQDTFIVHT IEEIQGLTTA 551 HEQFKATLPD ADKERLAILG IHNEVSKIVQ TYHVNMAGTN PYTTITPQEI 601 NGKWDHVRQL VPRRDQALTE EHARQQHNER LRKQFGAQAN VIGPWIQTKM 651 EEIGRISIEM HGTLEDQLSH LRQYEKSIVN YKPKIDQLEG DHQLIQEALI 701 FDNKHTNYTM EHIRVGWEQL LTTIARTINE VENQILTRDA KGISQEQMNE 751 FRASFNHFDR DHSGTLGPEE FKACLISLGY DIGNDPQGEA EFARIMSIVD 801 PNRLGVVTFQ AFIDFMSRET ADTDTADQVM ASFKILAGDK NYITMDELRR 851 ELPPDQAEYC IARMAPYTGP DSVPGALDYM SFSTALYGES DL
Heat shock protein 90	1 PEETQTQDQP MEEEEVETFA FQAEIAQLMS LIINTFYSNK EIFLRELISN 51 SSDALDKIRY ETLTDPSKLD SGKELHINLI PNKQDRTLTI VDTGIGMTKA 101 DLINNLGTIA KSGTKAFMEA LQAGADISMI GQFGVGFYSA YLVAEKVTVI 151 TKHNDDEQYA WESSAGGSFT VRTDTGEPMG RGTKVILHLK EDQTEYLEER 201 RIKEIVKKHS QFIGYPITLF VEKERDKEVS DDEAEEKEDK EEEKEKEEKE 251 SEDKPEIEDV GSDEEEEKKD GDKKKKKKIK EKYIDQEELN KTKPIWTRNP 301 DDITNEEYGE FYKSLTNDWE DHLAVKHFSV EGQLEFRALL FVPRRAPFDL 351 FENRKKKNNI KLYVRRVFIM DNCEELIPEY LNFIRGVVDS EDLPLNISRE 401 MLQQSKILKV IRKNLVKKCL ELFTELAEDK ENYKKFYEQF SKNIKLGIHE 451 DSQNRKKLSE LLRYYTSASG DEMVSLKDYC TRMKENQKHI YYITGETKDQ 501 VANSAFVERL RKHGLEVIYM IEPIDEYCVQ QLKEFEGKTL VSVTKEGLEL 551 PEDEEEKKKQ EEKKTKFENL CKIMKDILEK KVEKVVVSNR LVTSPCCIVT 601 STYGWTANME RIMKAQALRD NSTMGYMAAK KHLEINPDHS IIETLRQKAE 651 ADKNDKSVKD LVILLYETAL LSSGFSLEDP QTHANRIYRM IKLGLGIDED 701 DPTADDTSAA VTEEMPPLEG DDDTSRMEEV D
Ezrin	1 PKPINVRVTI MDAELEFAIQ PNTTGKQLFD QVVKTIGLRE VWYFGLQYVD 51 NKGFPTWLKL DKKVSAQEVR KESPLQFKFR AKFYPEDVAE ELIQDITQKL 101 FFLQVKEGIL SDEIYCPPET AVLLGSYAVQ AKFGDYNKEL HKAGYLGSER 151 LIPQRVMDQH KLTRDQWEDR IQVWHAEHRG MLKDSAMLEY LKIAQDLEMY 201 GINYFEIKNK KGTDLWLGVD ALGLNIYEKD DKLTPKIGFP WSEIRNISFN 251 DKKFVIKPID KKAPDFVFYA PRLRINKRIL QLCMGNHELY MRRRKPDTIE 301 VQQMKAQARE EKHQKQLERQ QLETEKKRRE TVEREKEQMM REKEELMLRL 351 QDYEEKTRKA EKELSDQIQR ALKLEEERKR AQEEAGRLEA DRLAALRAKE 401 ELERQAADQI KSQEQLATEL AEYTAKIALL EEARRRKENE VEEWQLRAKE 451 AQDDLVKTRE ELHLVMTAPP PPPVYEPVNY HVHEGPQEEG TELSAELSSE 501 GILDDRNEEK RITEAEKNER VQRQLMTLTS ELSQARDENK RTHNDIIHNE 551 NMRQGRDKYK TLRQIRQGNT KQRIDEFEAM
Pyruvate kinase M1/M2	1 SKPHSEAGTA FIQTQQLHAA MADTFLEHMC RLDIDSPPIT ARNTGIICTI 51 GPASRSVETL KEMIKSGMNV ARLNFSHGTH EYHAETIKNV RTATESFASD 101 PILYRPVAVA LDTKGPEIRT GLIKGSGTAE VELKKGATLK ITLDNAYMEK 151 CDENILWLDY KNICKVVEVG SKIYVDDGLI SLQVKQKGAD FLVTEVENGG 201 SLGSKKGVNL PGAAVDLPAV SEKDIQDLKF GVEQDVDMVF ASFIRKASDV 251 HEVRKVLGEK GKNIKIISKI ENHEGVRRFD EILEASDGIM VARGDLGIEI 301 PAEKVFLAQK MMIGRCNRAG KPVICATQML ESMIKKPRPT RAEGSDVANA 351 VLDGADCIML SGETAKGDYP LEAVRMQHLI AREAEAAIYH LQLFEELRRL 401 APITSDPTEA TAVGAVEASF KCCSGAIIVL TKSGRSAHQV ARYRPRAPII 451 AVTRNPQTAR QAHLYRGIFP VLCKDPVQEA WAEDVDLRVN FAMNVGKARG 501 FFKKGDVVIV LTGWRPGSGF TNTMRVVPVP
Alpha-enolase	1 SILKIHAREI FDSRGNPTVE VDLFTSKGLF RAAVPSGAST GIYEALELRD 51 NDKTRYMGKG VSKAVEHINK TIAPALVSKK LNVTEQEKID KLMIEMDGTE 101 NKSKFGANAI LGVSLAVCKA GAVEKGVPLY RHIADLAGNS EVILPVPAFN 151 VINGGSHAGN KLAMQEFMIL PVGAANFREA MRIGAEVYHN LKNVIKEKYG 201 KDATNVGDEG GFAPNILENK EGLELLKTAI GKAGYTDKVV IGMDVAASEF 251 FRSGKYDLDF KSPDDPSRYI SPDQLADLYK SFIKDYPVVS IEDPFDQDDW 301 GAWQKFTASA GIQVVGDDLT VTNPKRIAKA VNEKSCNCLL LKVNQIGSVT 351 ESLQACKLAQ ANGWGVMVSH RSGETEDTFI ADLVVGLCTG QIKTGAPCRS 401 ERLAKYNQLL RIEEELGSKA KFAGRNFRNP LAK

Actin	1 MDDDIAALVV DNGSGMCKAG FAGDDAPRAV FPSIVGRPRH QGVMVGMGQK 51 DSYVGDEAQS KRGILTLKYP IEHGIVTNWD DMEKIWHHTF YNELRVAPEE 101 HPVLLTEAPL NPKANREKMT QIMFETFNTP AMYVAIQAVL SLYASGRTTG 151 IVMDSGDGVT HTVPIYEGYA LPHAILRLDL AGRDLTDYLM KILTERGYSF 201 TTTAEREIVR DIKEKLCYVA LDFEQEMATA ASSSSLEKSY ELPDGQVITI 251 GNERFRCPEA LFQPSFLGME SCGIHETTFN SIMKCDVDIR KDLYANTVLS 301 GGTTMYPGIA DRMQKEITAL APSTMKIKII APPERKYSVW IGGSILASLS 351 TFQQMWISKQ EYDESGPSIV HRKCF
Glyceraldehyde-3-phosphate dehydrogenase	1 GKVKVGVNGF GRIGRLVTRA AFNSGKVDIV AINDPFIDLN YMVYMFQYDS 51 THGKFHGTVK AENGKLVING NPITIFQERD PSKIKWGDAG AEYVVESTGV 101 FTTMEKAGAH LQGGAKRVII SAPSADAPMF VMGVNHEKYD NSLKIISNAS 151 CTTNCLAPLA KVIHDNFGIV EGLMTTVHAI TATQKTVDGP SGKLWRDGRG 201 ALQNIIPAST GAAKAVGKVI PELNGKLTGM AFRVPTANVS VVDLTCRLEK 251 PAKYDDIKKV VKQASEGPLK GILGYTEHQV VSSDFNSDTH SSTFDAGAGI 301 ALNDHFVKLI SWYDNEFGYS NRVVDLMAHM ASKE